

STAT

**Page Denied**

STAT

# TRANSLATION

HEAT PROCESSES IN THE ATMOSPHERE

By L. R. Rakipova

September 1959

216 Pages

PREPARED BY  
LIAISON OFFICE  
TECHNICAL INFORMATION CENTER  
MCLTD  
WRIGHT-PATTERSON AIR FORCE BASE, OHIO

STAT

**Tepolvoy Rezhim Atmosfery**

**Publishing Office**

**Gidrometeorologicheskoe Izdatel'stvo**

**Leningrad - 1957**

**183 Pages**

STAT

## SYNOPSIS

This book summarizes the results of the experimental and theoretical investigations of the laws governing the heat processes of the atmosphere, sheds light on the principal results of the theoretical research on determining the temperature field of the atmosphere, expounds the theory of the zonal thermal field of the atmosphere, quotes and analyzes the calculations of the horizontal macro-transfer of heat, non-turbulent and turbulent, for the principal climates, and discusses the present state of the problem of the thermal regime of the stratosphere and the relationship between the upper layers of the atmosphere and the troposphere.

The readers not interested in the mathematical aspects of the problems discussed, may ignore them without detracting from their comprehension of the physical aspects of these problems.

This monograph is intended for scientific research workers, physicists and meteorologists, climatologists, and for the postgraduate and graduate students of advanced courses in higher schools of hydrometeorology and university departments of geography and physics.

STAT



TABLE OF CONTENTS

	<u>Page</u>
Preface .....	1
Introduction .....	4
<b>Chapter I. Fundamental Problems of the Heat Processes</b>	
in the Atmosphere .....	10
The Heat Processes in the Stratosphere .....	10
Temperature Distribution in the Troposphere .....	76
Climatological Studies of the Heat Balance of the Atmosphere. The Earth's Albedo .....	101
<b>Chapter II. The Zonal Thermal Field of the Atmosphere</b> .....	110
The Setting-Up and the Solution of the Problem of the Zonal and Nonzonal Distribution of Temperature in the Atmosphere .....	110
Selecting the Quantitative Values of the Parameters .....	134
The Calculation of the Zonal Distribution of Temperatures and of the Components of the Heat Balance of the Atmosphere. Analysis of the Obtained Results .....	150
<b>Chapter III. Heat Advection in the Atmosphere</b>	
Integral Characteristics of Heat Advection .....	171
Calculating the Components of Nonturbulent Advection. Evaluating the Horizontal Turbulent Heat Transfer .....	177
Bibliography .....	217

## PREFACE

Historically, the development of dynamic meteorology has become so complex that in studies of atmospheric processes the principal consideration is the dynamics of these processes, i. e., the problem of the relationship between the various forces acting in the atmosphere and the motions they have induced. The direction and velocity of atmospheric motions, which are quantitatively obtained by resolving corresponding equations of hydrodynamics, are of interest primarily because they are related to weather changes, - and the forecasting of these changes is of immediate practical importance. But sufficient attention has not been given to the energetics of atmospheric processes, i. e., the study of the original causes of the genesis of air currents. And yet, it is perfectly obvious that such research must be of fundamental importance not only according to its physical nature but also because of its practical applicability to weather forecasting: it is difficult to predict successfully the course of phenomena whose causes have not been adequately investigated.

The kinetic energy of atmospheric motions arises owing to the internal and potential energies of the air masses. As for the question of the storing-up of these forms of energy, this is a question of the conversion of the radiant energy of the sun into these forms, i. e., a question of temperature distribution in the earth's atmosphere. Therefore, the problem of the theoretical explanation of the formation of the temperature field of the atmosphere is of cardinal importance: it entails the possibility of finding a physical explanation of the causes of atmospheric motions. In the existing theoretical studies of the general atmospheric circulation, the factor of temperature distribution is considered as a known factor (or an adiabatic state of the processes is presupposed), and thus the question of the causes of circulation is not ultimately resolved.

The problem of the temperature field of the atmosphere is closely related to the questions of the formation of the earth's climate. The contrasts between the air

STAT

temperatures in the lower and higher latitudes, and over the continents and the oceans, are the original causes of the presence of numerous variations in climate from marine to continental - on the terrestrial sphere. The disintegration of fronts (frontolysis) and the formation of cyclones and anticyclones also are closely related to the energetics of atmospheric processes. Therefore, the understanding of both the stable processes creating the climates of various regions and the unstable processes resulting in weather changes, is predicated on the investigation of the non-turbulent and turbulent horizontal heat transfers developing between the sources and outlets of heat in a moving atmosphere. However, in modern climatology and synoptic meteorology very little attention has been paid to investigating the advective and turbulent transports of heat, - which are among the principal causes of the formation of the physical foundation of climate and weather; moreover, the few studies that have been made are either of a qualitative nature or they suffer from quantitative inaccuracies and vagueness.

Studies of the stratosphere and the problem of the relationship between the upper layers of the atmosphere and the troposphere are of great importance to atmospheric physics. Even now, much remains to be explained with regard to the structure of the stratosphere and, in particular, its heat processes. The mechanism of the relationships between various layers of the atmosphere, generally speaking, has not been investigated in dynamic meteorology. In the meantime, investigations of this group of related problems which are ultimately bound to provide the physical foundations for the effect on atmospheric processes of such cosmic energy sources as ultraviolet and corpuscular radiation in the active areas of the sun, are very promising in view of their great significance and also because they lie on the boundary between two sciences - geophysics and astrophysics. As for the practical importance of these investigations, it is self-evident: they should be instrumental in improving the accuracy of weather forecasting.

The present monograph communicates the results of the author's studies of some principal problems of the heat processes in the atmosphere.

Primarily, this monograph provides a theory of the zonal atmospheric temperature

distribution that differs from the existing theories by its greater completeness; it cites a solution of the problem of the azonal temperature distribution (Chapter 2).

Also, this monograph describes methods of calculating the atmospheric heat transfer by means of non-turbulent macro-advection and of horizontal turbulent mixing, which make it possible to obtain sufficiently accurate and detailed characteristics of the corresponding heat transport processes. Calculations are made for the principal climates of the earth (Chapter 3).

Further, it describes studies of the heat processes in the stratosphere; the hypothesis underlying these studies makes possible a closer approach to the solution of the problem of the "intermixed" atmosphere (up to an altitude of 80 kilometers). Lastly, this monograph provides one of the possible hydrothermodynamic schemes of the relationship among the various layers of the atmosphere, designed so as to take account of the physical mechanism of the effect of solar activity on the dynamic processes in the troposphere (Chapter 1).

Owing to the great complexity of the problems under study, it was not found possible to obtain all the results through the purely theoretical approach; consequently, some of them were obtained by processing empirical data.

The manuscript of this book was perused, with important revisions, by K. Ya. Kondrat'yev, M.E. Shvets, and M. I. Yudin, to whom the author expresses his deep appreciation.

## INTRODUCTION

The temperature of the earth's atmosphere is one of the chief meteorological elements and one on which an immense mass of observational data has been accumulated.

The study of heat processes in the atmosphere is of primary importance for formulating a theory of climate, of the general circulation of the atmosphere and for developing methods of weather forecasting. However, there does not as yet exist a sufficiently complete quantitative theory explaining the observed temperature distribution in the atmosphere. This is because of the great complexity of the whole of the physical processes determining the thermal state of the atmosphere, and because of the mathematical complications arising in the resolving of the corresponding problems of dynamic meteorology.

The qualitative picture of heat processes in the atmosphere is represented as follows:

It is known that the air becomes warmed up principally as a result of the radiational and turbulent transfer of heat from the earth's surface. The atmosphere is extremely transparent to short-wave solar radiation, and it absorbs to a great extent the long-wave radiation emitted by the earth's surface. The long-wave radiation emitted by the earth's surface depends basically on the solar energy entering the earth's atmosphere in quantities varying with the latitude and the season of the year. The substances absorbing the long-wave radiation are chiefly water vapor, carbon dioxide, and ozone. Therefore, the distribution of the atmosphere's elements in space may exert an influence on the temperature distribution in the atmosphere.

Turbulent mixing results in a reduction in the temperature gradients in both the horizontal and the vertical directions. The vertical turbulent flux distributing the heat between the earth's surface and the atmosphere depends essentially on the physical features of the terrain below. The horizontal turbulent macro-exchange reduces the equatorial temperature and increases the polar temperature, in which connection the magnitude of its effect is greater in the proximity of the poles, because with an

STAT

increase in latitude there is a corresponding decrease in the area of the latitude-degree interval (quadrant). The horizontal turbulent fluxes are particularly essential in the polar areas in winter, when they, together with advection, become the principal source of heat.

The phase transformations of water, accompanied by the absorption and liberation of the latent heat of condensation, also affect the atmospheric temperature. This pertains primarily to the evaporation of water from the earth's surface and the condensation of the water vapor in the atmosphere, accompanied by the formation of clouds and the subsequent falling of precipitation. The influence of the evaporation from the earth's surface on the temperature of the air is concentrated principally in the lower layers. The influence of the condensation of atmospheric water vapor manifests itself at higher altitudes, i. e., at the cloud-formation level.

In addition, the character of the underlying terrain and the distribution of cloudiness, which determine the reflectivity of the earth's surface and of the atmosphere - the albedo - limit the quantity of the solar energy being absorbed by the earth's surface.

Clouds not only reflect solar radiation, by removing a portion of it back into space from the atmosphere, and not only constitute areas of the liberation (or absorption) of the latent heat of condensation, but also absorb long-wave radiation and are transparent to short-wave radiation in a manner differing from that of the free atmosphere.

The wind, which produces a non-turbulent transfer of heat from individual atmospheric regions into others, also exerts an essential influence on the thermal regime of the atmosphere.

All these factors do not operate independently; they are interrelated by the general processes of the variations in the quantities of heat and of motion with respect to both space and time, as expressed by the corresponding laws of conservation applied to the conditions of the earth's atmosphere.

Therefore, the problem of determining atmospheric temperature in the most general form is reduced to deriving the following set of equations of thermo- and hydrodynamics:

STAT

Equation of motion

$$\frac{dv}{dt} = F - \frac{1}{\rho} \nabla p - 2[\omega \cdot v] + \frac{\mu}{\rho} \Delta v. \quad (1)$$

Equation of continuity

$$\frac{dp}{dt} + \text{div } \rho v = 0. \quad (2)$$

Equation of state

$$p = \rho RT. \quad (3)$$

Equation of heat influx

$$\varepsilon = \rho c_p \frac{dT}{dt} - A \frac{dp}{dt}. \quad (4)$$

where  $V$  is the velocity vector,  $F$  is the vector of mass forces,  $\omega$  is the vector of angular velocity of the earth's rotation,  $\mu$  is the coefficient of turbulent viscosity,  $p$  is air pressure,  $T$  is air temperature,  $R$  is the gas constant,  $A$  is the thermal work equivalent,  $\varepsilon$  is the influx of heat to a unit of air volume per time unit,  $t$  is time and  $c_p$  is the specific heat at constant pressure.

The heat influx in the atmosphere is effected by radiative and turbulent processes, and also by the phase transformations of water vapor. Equations (1) to (4) form a closed set of equations with respect to the four unknowns  $T$ ,  $\rho$ ,  $p$ , and  $V$  only in the case if no new unknown functions are introduced into this set when determining the heat influx  $\varepsilon$ , for example; for adiabatic motions, when  $\varepsilon = 0$ , or in cases when  $\varepsilon$  may be considered as a set function of coordinates, time or also of the sought-for functions. Therefore, in particular, for processes in which the heat flux is effected solely through heat conductivity, the above set of equations proves to be closed, because here  $\varepsilon = \varepsilon(T, p)$ .

Generally speaking, however, the introduction of the  $\varepsilon$  function necessitates a search for new relationships making it possible to close the set of equations [21]. For instance, if it is necessary to investigate the radiative heat fluxes relating to the absorption and emission of radiant energy by air particles, this is coupled to the necessity of introducing new unknown functions, and the construction of equations

for determining these new functions entails difficulties of both a mathematical and a physical nature.

In effect, in this case

$$\varepsilon = -\operatorname{div} R. \quad (4')$$

Here  $R$  is the radiant energy flux: the quantity of radiant energy in all possible directions passing during a time unit through a cross-sectional-area unit (at a given direction of the normal to the latter).

By definition

$$R = \int_0^{\infty} d\nu \int I_{\nu}(r) \cos(n, r) d\omega,$$

where  $I_{\nu}$  is intensity of radiation of frequency  $\nu$ , which, unlike  $R$ , depends on direction  $r$ .

To determine  $I_{\nu}$ , use is made of the equation of radiant energy transfer, which is a relation regulating the change in  $I_{\nu}$  along a ray of given direction  $r$  in a medium characterized by absorption coefficient  $\alpha_{\nu}$  and scattering coefficient  $\sigma_{\nu}$ ;

$$\frac{1}{\rho} \frac{\partial I_{\nu}}{\partial r} = \eta_{\nu} + \frac{\sigma_{\nu}}{4\pi} \int I_{\nu}(r') \Upsilon_{\nu}(r') d\omega' - (\alpha_{\nu} + \sigma_{\nu}) I_{\nu}. \quad (5)$$

Here,  $\eta_{\nu}$  is the radiation coefficient - the quantity of radiant energy of frequency  $\nu$  being emitted by a mass unit during a time unit per solid-angle unit (assuming that the mass portion emits identical quantities of energy in all directions).

$\frac{1}{4\pi} \Upsilon_{\nu}(P, r, r')$  is the function determining the scattering law - the variation in  $I_{\nu}(r, P)$  owing to the redistribution of energy among the various directions  $r'$  from point  $P$ .

From the total quantity of the scattered energy of a  $r'$  - directed ray equal to  $\sigma_{\nu} I_{\nu}(P, r') \rho dr'$ , the  $\frac{\sigma_{\nu} I_{\nu} \rho dr'}{4\pi} \Upsilon_{\nu}(P, r, r')$  portion deviates along the  $r$ -direction. The  $\Upsilon_{\nu}$  - function should satisfy the condition

$$\frac{1}{4\pi} \int \Upsilon_{\nu}(P, r, r') d\omega' = 1,$$

where  $d\omega'$  is the solid-angle component corresponding to the  $r'$  - direction, and  $\rho$  is

STAT



the density of the radiation-absorbing substance. If  $\eta_s = 1$ , scattering is homogeneous.

The sense of eq. (5) thus consists in the circumstance that the intensity of radiation  $I_r$  along a ray  $\underline{r}$  varies owing to the processes of radiation, absorption and scattering. The  $\nu$  frequency-integration of this equation entails considerable mathematical difficulties owing to the complexity of the absorption spectra of the atmospheric-air constituents.

The  $\alpha_r$ ,  $\sigma_r$ , and  $\gamma_r$  functions are usually given, in which connection it is assumed that  $\alpha_r$  and  $\sigma_r$  do not depend on  $\underline{r}$  (isotropic radiation). Consequently, the relationship (5) contains two unknown functions,  $I_r$  and  $\eta_r$ , the determination of which requires the finding of yet another relationship. This relationship can be found after making the assumption that thermal conditions in the atmosphere correspond to a state of "local thermodynamic equilibrium". This state is closely related to the concept of the thermodynamic equilibrium. Thermodynamic equilibrium exists when a medium has a temperature that is identical at all points and is the same as the temperature of the walls confining the medium. The radiation field of a system existing in such an equilibrium displays the simplest properties:  $I_r$  is of an identical value in all points of the medium (refraction index equals 1) and is not affected by direction of the ray (isotropic radiation). Such a medium is subject to Kirchhoff's law:

$$\frac{\eta_r}{\alpha_r} = B_r, \quad (6)$$

or

$$\frac{\eta_r}{\sigma_r} = I_r, \quad (7)$$

because at thermodynamic equilibrium

$$I_r = B_r,$$

where  $B_r$  is intensity of radiation of an absolutely black body.

Inasmuch as the thermal state of the earth's atmosphere does not satisfy the conditions of thermodynamic equilibrium, and its temperature varies from point to

STAT

point and  $I_e \neq B_e$ , Kirchhoff's law in form (7) is not applicable to the calculation of the radiative characteristics of that atmosphere.

As introduced by the astrophysicists, the term "local thermodynamic equilibrium" characterizes such a state of the medium in which the relationship (6) is satisfied at every point in the medium but the classically conceived (eq. 7) thermodynamic equilibrium is absent.

Temperature may vary from point to point in the medium, but every such point should be characterized by a definite temperature: every particle of the medium exists, as it were, in a thermodynamic equilibrium at its characteristic temperature. A number of important astrophysical problems has been resolved on the basis of such an interpretation of Kirchhoff's law. In meteorology also, the concept of "local thermodynamic equilibrium" is utilized as a satisfactory approximation of the conditions in the lower layers of the atmosphere. In the upper layers, where the processes of radiant energy absorption play a considerably smaller role than the processes of scattering, the local thermodynamic equilibrium will not occur.

If expression (6) be  $\nu$ -integrated, in using Planck's formula for  $B_\nu$  when  $\alpha_\nu = 1$ , the following well-known relation is obtained:

$$E = \sigma T^4, \quad (8)$$

which is termed the Stefan-Boltzmann law. Here  $E$  is the radiation flux of an absolutely black body.

Thus, the added consideration in a problem of the radiative flux of heat  $R$  would require the introduction of two complementary equations, (5) and (6), in order to close the set of equations (1)-(4).

Given the distribution of absorbing substances in the atmosphere, then, in resolving the set of equations (1)-(4), (5), and (6), at definite initial and boundary conditions, we will obtain the quantitative characteristic of the thermal and dynamic processes in the atmosphere that have been qualitatively described above.

STAT

## CHAPTER I

## FUNDAMENTAL PROBLEMS OF THE HEAT PROCESSES IN

## THE ATMOSPHERE

## The Heat Processes in the Stratosphere

The road toward the derivation of the complete closed set of the afore-written nonlinear differential equations is impeded by as yet insurmountable complications of a physical and mathematical nature.

Therefore, in its application to the determination of temperature and to all other problems of dynamic meteorology, the above complete set of equations is subjected to various types of simplification in accordance with this or that stylization of the problem being resolved. Here the sense of these simplifications consists in that, out of the aggregate of factors determining atmospheric temperature, various investigators select only some such factors, and the essence of the results they obtain consists in the evaluation of the influence of the isolated factors on the temperature regime of the atmosphere.

From this viewpoint, research projects conducted up to the present are of a very great importance.

The first studies in this direction (Humphreys, Gold, Emden) assisted in clarifying the question of the heat-process regime in the principal layers of the atmosphere. Subsequently, it became clear which components of heat influx  $\epsilon$  determine the temperature stratification of the troposphere and stratosphere. That is to say, the most probable hypothesis became that, as a first approximation, the temperature of the stratosphere is established as a result of a radiative equilibrium at which eqs. (4) and (4') are reduced to

$$\epsilon = -\operatorname{div} R = 0 \quad (9)$$

This condition means that the atmosphere is stationary, that it lacks any sources of heat and is not acted upon by any process of heat transfer other than the radiational,

STAT

and that the temperature at any point in the atmosphere remains unchanged. In other words, this means that, for every parcel of the air mass, the sum of heating (owing to the absorption of radiation) and cooling (owing to emission of radiation) equals zero. On reintegrating eq. (9) throughout the entire volume of the atmosphere we obtain

$$R = \text{const.} \quad (10)$$

At all points in the atmosphere the radiational flux maintains an identical value equal to its value at any boundary of the atmosphere, e. g., at the upper such boundary

$$R_s = R_{1, s=\infty} = (S_0 - B_s) \quad (11)$$

where  $S_0$  is incoming solar radiation,  $B_s$  is the outgoing terrestrial radiation, and  $R_s$  is the radiation balance of the earth-atmosphere system.

Eqs. (9), (10) and (11) represent different treatments of the radiational equilibrium condition.

Having resolved the thus stylized problem, Emden succeeded in obtaining for the stratosphere the correct value of the mean annual temperature in the middle latitudes and in obtaining the corresponding isothermal vertical profile. And indeed, the vertical temperature lapse rates in the stratosphere are approximately of an order less than those of the troposphere. Hence, it was possible to conclude in due time that the thermal regime of the stratosphere corresponds to conditions (9), (10) and (11).

It can be very easily ascertained that the absorption of radiation by the atmosphere causes an increase in the temperature at the earth's surface and a decrease in the temperature at the upper boundary of the atmosphere. In effect, if the earth did not have an atmosphere or if it had an atmosphere totally incapable of absorbing radiation, there would have to exist an equilibrium, on an average, for all latitudes and during a lengthy period of time, between the incoming solar radiation and the thermal radiation being emitted by the earth's surface. In this case, the temperature

STAT

of the earth's surface would equal 242° K. This value is too low compared with the observed 287°-K temperature of the earth's surface and too high compared with the temperature of the stratosphere.

Let us survey in greater detail Emden's problem, which constituted the first attempt at a theoretical explanation of the heat processes in the atmosphere.

Emden adapted transfer equation (5) to very simplified conditions. Water vapor was the only absorbing substance he took into account, as a grey body with absorption coefficient  $\alpha_1$  for long-wave radiation  $\lambda > 3\mu$  and  $\alpha_2$  for short-wave solar radiation  $\lambda < 3\mu$ ; in which connection the radiation fluxes are propagated only in the vertical direction. Consequently, the selectivity of radiation absorption and the diffusivity of radiation propagation were ignored. The processes of radiation scattering were also not considered.

Thereupon: 1.  $\cos(\tau, n) = 1$

$$R = A - B + S,$$

where A and B are downward-and-upward-directed long-wave radiation fluxes, respectively:

$$2. \quad \eta = S\eta, \quad d_1 = \alpha_1 E;$$

$$3. \quad \rho \, dz = dm,$$

where m is the quantity of water vapor with  $\rho$  density in an atmospheric column of a unit cross-section and of height z;

$$4. \quad \alpha_2 = 0.$$

Let us obtain from (5) the transfer equation for flux A

$$\frac{dA}{dm} = -\alpha_1 E + \alpha_1 A, \quad (12)$$

for flux B

$$\frac{dB}{dm} = \alpha_1 E - \alpha_1 B. \quad (13)$$

Eq. (4) is thus written for the radiative-equilibrium condition:

$$s = -\operatorname{div} R = -\frac{dS}{dm} + \frac{dB}{dm} - \frac{dA}{dm} = 0. \quad (14)$$

STAT

Here  $S$  represents the solar radiation flux.

The substitution of eqs. (12) and (13) into (14) gives [67]

$$\frac{dS}{dm} + \alpha_1(A+B) = 2\alpha_1 E. \quad (15)$$

Eq. (15) shows that the radiation of every mass unit is compensated by the absorption of solar radiation  $S$ , and of long-wave  $A$  and  $B$  radiation.

The integration of (14) yields

$$-S + B - A = -R_s, \quad (16)$$

where  $-R_s$  is the difference (independent of  $m$ ) between incoming downward and upward radiation. The combination of (12) and (13) in taking (14) into account and the substitution into (16) yield:

$$2 \frac{dA}{dm} = -\frac{dS}{dm} - \alpha_1 S + \alpha_1 R_s. \quad (17)$$

Let us integrate (17) under the condition that counter-radiation is absent at the upper boundary of the atmosphere when  $m = M$ , i. e.,  $A(M) = 0$ .

Thereupon, we obtain

$$A(m) = \frac{1}{2} \left[ S(M) - S(m) + \alpha_1 \int_m^M S dm - \alpha_1 R_s (M - m) \right]. \quad (18)$$

Substituting (18) into (12) let us find the temperature distribution by altitude  $T(m)$ :

$$\sigma T^4(m) = \frac{1}{2} \left[ S(M) + \alpha_1 \int_m^M S dm + \frac{1}{\alpha_1} \frac{dS}{dm} - \alpha_1 R_s (M - m) - R_s \right].$$

Whence the temperature at the upper boundary of the atmosphere is

$$T(M) = \sqrt[4]{\frac{1}{2\sigma} \left[ S(M) + \frac{1}{\alpha_1} \frac{dS}{dm} - R_s \right]}. \quad (19)$$

The average  $S(M)$  for all latitudes may be determined by the solar constant  $I_0$ , reduced by the correction for the reflection of solar radiation from the atmosphere, clouds and the earth's surface, into outer space, because the reflected part exerts

STAT

no thermal effect on the atmosphere. The mean quantity of solar energy on an average falling onto a unit area, per unit of time at the upper boundary of the atmosphere is as follows:

$$S(M) = \frac{I_0}{4} (1 - \Gamma). \quad (20)$$

The  $\Gamma$  value is termed the energetics albedo of the earth, or the albedo of the earth-atmosphere system.

The incoming and outgoing radiation should be considered mutually equal as averaged for the earth as a whole over long time intervals, because the atmosphere does not cool from year to year, as it retains a constant mean temperature. consequently, for these conditions,  $R_s = 0$ . Inasmuch as the solar radiation arriving at some  $m$ -level is represented by the expression

$$S(m) = S(M) e^{-\alpha_2(M-m)}, \quad (21)$$

where  $\alpha_2$  is the "grey" absorption coefficient for short-wave radiation, we obtain the following expression for boundary temperature

$$T(M) = \sqrt[4]{\frac{1}{25} S(M) \left(1 + \frac{\alpha_2}{\alpha_1}\right)}. \quad (22)$$

On substituting the numerical values of  $I_0 = 1.91$  calories/square centimeter/minute and  $\alpha_1 = 2.3$  square centimeters/gram, and  $\alpha_2 = 0.1053$  square centimeters/gram, Emden obtained a value equal to  $-68.5^\circ$  for the temperature of the stratosphere at the condition of radiative equilibrium, which agrees satisfactorily with the actual, latitudinal mean annual temperature of the stratosphere ( $-65^\circ$ ). Let us note that the computed temperatures obtained from the radiative equilibrium condition are termed radiational temperatures. The gradients obtained by Emden for the troposphere were superadiabatic, but the boundary temperature (22) was obtained upward from a level of as little as 10 kilometers, i. e., an approximate isothermal state is established above the tropopause.

Hence, it could be concluded that the troposphere obviously is not in a radiational

STAT

equilibrium, while for the stratosphere Emden's calculations provide a good approximation despite their pronounced simplifications in setting up the problem.

It should be noted that formula (22) provides a very weak relationship between stratospheric temperature  $T(M)$  and radiation absorption by water vapor, because for it the ratio  $\frac{a_2}{a_1} = 0.046$  is small compared with unity. But above 20 kilometers, where the principal absorbing medium is no longer water vapor but ozone (for which the  $\frac{a_2}{a_1}$  ratio is much higher than for water vapor), formula (22) yields higher temperatures than in the lower stratosphere. Such a temperature rise is indeed observed in reality and, consequently, Emden's theory provides a valid explanation thereof.

For the latitudinal course of temperature the calculations based on (22) give results incompatible with the actually observed distribution. Owing to the pole-ward decrease in  $S(M)$  from the equator,  $T(M)$  has the following values:

$S(M)$ cal/cm <sup>2</sup> min	0	30	60	90
$T(M)$ °K	0.363	0.315	0.182	0
$T_{actual}$	223	216	188	0
	198	206	222	227

In reality, the actual temperature of the stratosphere  $T_{actual}$  increases pole-ward from the equator [85].

Mügge [75] showed that this contradiction can be eliminated if it be assumed that  $R_g$  is positive in the tropics and negative in the polar areas. Thereupon, inasmuch as then the  $\frac{1}{2\sigma} R_g$  term will be included under the root symbol, formula (22) will give the correct latitudinal course of  $T(M)$ . Such an assumption with respect to  $R_g$  corresponds with reality, because it signifies that in the tropics the influx of solar radiation exceeds the terrestrial irradiation, while in polar areas, conversely, irradiation predominates. However, it is impossible to introduce greater accuracy into the calculations of  $T(M)$  according to (22) owing to a certain given latitudinal distribution of  $R_g$ , because the quantitative calculations of the outgoing terrestrial

STAT



radiation already presuppose as known the temperature distribution throughout the entire atmosphere including its upper boundary. Therefore, Mücke proceeded differently. Inasmuch as the latitudinal profile of zonal temperatures has an extremely simple geometrical form, it could be expected that it would be possible to obtain a quite satisfactory approximation of that profile by means of a relationship containing only two to-be-determined parameters. For the temperature of the stratosphere Mücke selected the following approximation function:

$$T(M) = d + q \sin \varphi. \quad (23)$$

In order to determine the parameters  $q$  and  $d$  it is necessary to find two conditions. In order to obtain the first condition, Mücke set the temperature of the stratosphere at a certain latitude, viz., he assumed  $T(M) = 220^\circ$  (Centigrade) for latitude  $\varphi = 52^\circ N$ , in accordance with repeated observations. Then having substituted the corresponding value of  $\sin \varphi = 0.789$  into eq. (23), we obtain

$$d = 220 - 0.789q. \quad (24)$$

The second condition was obtained by Mücke from the following considerations: If  $-R_s(\varphi)$  is the quantity of heat conveyed to or from an air column with a transverse cross-section of one square centimeter by advective fluxes inside the troposphere at latitude  $\varphi$ , then the quantity of heat transported by advective fluxes through a circle bounded by the equator and latitude  $\varphi$ , will be

$$\bar{R}_s = 2\alpha_0^2 \pi \int_0^\varphi R_s \cos \varphi d\varphi.$$

(where  $\alpha_0$  is the radius of the earth). This total flux, transported across latitudinal parallels, should revert to zero at the pole. Whence

$$\int_0^\varphi R_s \cos \varphi d\varphi = 0. \quad (25)$$

Having substituted here the  $R_s$  expression according to Emden, Mücke obtained after integration the second condition for determining  $q$  and  $d$ . He approximated the incoming solar radiation by a latitudinal function in the following form:

$$S(M) = \frac{I_0}{\pi} (1 - \Gamma) \cos \varphi. \quad (26)$$

The calculations gave:  $q = 38$  and  $d = 190$ . Thereupon, Midge succeeded in constructing the latitudinal distributions of  $T(M)$  according to (23) and of  $R_s$  from (19) (Figs. 1 and 2).

As it can be seen from Fig. 1, the computed  $T(M)$  values approximate the actual ones. Essentially, here  $T(M)$  is determined independently of  $R_s$ . The inclusion of  $R_s$  for determining the  $q$  and  $d$  parameter is purely formal and therefore unnecessary.

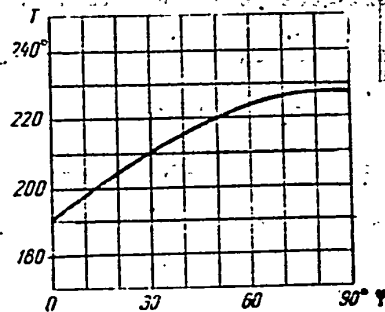


Fig. 1. Relationship Between Stratospheric Temperature and Geographic Latitude

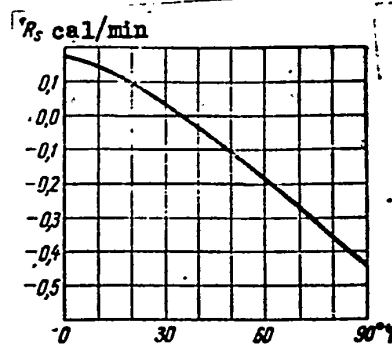


Fig. 2. Quantity of Radiative Heat  $R_s$  Transported To An Atmospheric Column With a Cross-Section of One Square Centimeter

Actually, eq. (25) denotes a radiational equilibrium condition satisfied for the earth as a whole, on the average. Inasmuch as this condition determines the temperature of the stratosphere in the moderate latitudes (30 to 40°), the method of determining  $T(M)$  is thus, according to Midge, reduced to determining the curve of (23) in the STAT

where  $T(0)$  is the temperature of the earth's surface, and  $B_1$  and  $B_2$  are the fluxes in the transparent and nontransparent intervals of the spectrum, respectively.

After combining (28) with (29) and substituting  $B_2$  from (30) we obtain

$$\frac{2dA}{dm} = -\frac{dS}{dm} - \alpha_1 S + \alpha_1 (B_1 + R_s)$$

and

$$A(m) = \frac{1}{2} \left\{ S(M) - S(m) + \alpha_1 \int_m^M S dm - \alpha_1 (B_1 + R_s)(M - m) \right\}$$

From (29)

$$E(m) = \frac{1}{2f} \left\{ S(M) + \alpha_1 \int_m^M S dm + \frac{1}{\alpha_1} \frac{dS}{dm} - \alpha_1 (B_1 + R_s)(M - m) - (B_1 + R_s) \right\} \quad (31)$$

From condition

$$B_1 = (1 - f) [B_1 + B_2(0)]$$

and by means of (30) we obtain

$$B_1 = (1 - f) [A(0) + S(0) - R_s],$$

or

$$B_1 = \frac{1 - f}{2 + (1 - f)\alpha_1 M} \left[ \left(1 + \frac{\alpha_1}{\alpha_2}\right) S(M) + \left(1 - \frac{\alpha_1}{\alpha_2}\right) S(0) - (\alpha_1 M + 2) R_s \right]$$

From this equation and from (27) we immediately obtain  $T(0)$  and  $T(M)$  from (31):

$$2f\sigma T^4(M) = \left(1 + \frac{\alpha_2}{\alpha_1}\right) S(M) - (B_1 + R_s).$$

After substituting the above-indicated quantitative values for  $\alpha_1$ ,  $f$  when  $R_s = 0$ , it can be found that the temperature of the earth's surface is  $T(0) = 365^\circ$ , while the temperature at the upper boundary of the atmosphere is  $T(M) = 129^\circ$ .

A similar value of  $T(M)$ , just as far removed from the actually observed values, was obtained by Möller's calculations [70], in which he divided the long-wave absorption spectrum of water vapor into two regions,  $\alpha_1 = 100 \text{ cm}^{-1}$  and  $\alpha_2 = 1 \text{ cm}^{-1}$ , with

STAT

$0 < \varphi < \frac{\pi}{2}$  interval according to two points (which can be carried out satisfactorily owing to the simplicity of the latitudinal profile of the actual stratospheric temperatures). Such a determination of  $T(M)$  is inherently formal and has no physical foundations that could explain the obtained results. As for the  $R_3$  flux, it is obtained as a consequence of (23) and therefore it can not be used to explain the latitudinal course of  $T(M)$ .

It is to be noted that according to Emden's formulas,  $T(M)$  depends on absorption coefficients  $\alpha_1$  and  $\alpha_2$ , for water vapor and is independent of the quantity and of the vertical distribution of that vapor.

The assumption of the "grey" absorption of radiation in the atmosphere appears to be too crude an approximation of the actual spectrum of water vapor.

However, attempts at a more accurate consideration of the selectivity of radiation absorption by water vapor have demonstrated clearly that in the stratosphere not only the horizontal but also the vertical temperature distribution does not correspond with a radiational equilibrium with respect to water vapor. This can be ascertained by recalculating the  $T(M)$  temperatures by means of the simplest approximation of the water-vapor absorption spectrum as proposed by Albrecht [67]; at 9 to 12 microns water vapor is considered transparent, while in the remaining part of its spectrum the absorption is so great that a quantity of water vapor corresponding to 0.03 centimeters of water attenuates the incident radiation by 95 percent. This leads to an  $\alpha_1$  absorption coefficient with a value of  $\alpha_1 = 100 \text{ cm}^{-1}$  (per volume unit). The part of radiation comprised within the 9-12  $\mu$  interval is assumed equal to  $1 - f = 0.16$  in relation to total radiation  $\sigma T^4$ .

Thereupon, the equations of radiative equilibrium will have the following form:

$$B_1 = (1-f)\sigma T^4(0), \quad (27)$$

$$\frac{dB_2}{dM} = -\alpha_1 B_2 + \alpha_1 f E, \quad (28)$$

$$\frac{dA}{dM} = \alpha_1 A - \alpha_1 f E, \quad (29)$$

$$-S + B_1 + B_2 - A = -R_r, \quad (30)$$

where  $T(0)$  is the temperature of the earth's surface, and  $B_1$  and  $B_2$  are the fluxes in the transparent and nontransparent intervals of the spectrum, respectively.

After combining (28) with (29) and substituting  $B_2$  from (30) we obtain

$$\frac{2dA}{dm} = -\frac{dS}{dm} - \alpha_1 S + \alpha_1 (B_1 + R_s)$$

and

$$A(m) = \frac{1}{2} \left\{ S(M) - S(m) + \alpha_1 \int_m^M S dm - \alpha_1 (B_1 + R_s)(M - m) \right\}$$

From (29)

$$E(m) = \frac{1}{2f} \left\{ S(M) + \alpha_1 \int_m^M S dm + \frac{1}{\alpha_1} \frac{dS}{dm} - \alpha_1 (B_1 + R_s)(M - m) - (B_1 + R_s) \right\} \quad (31)$$

From condition

$$B_1 = (1 - f) [B_1 + B_2(0)]$$

and by means of (30) we obtain

$$B_1 = (1 - f) [A(0) + S(0) - R_s],$$

or

$$B_1 = \frac{1 - f}{2 + (1 - f)\alpha_1 M} \left[ \left(1 + \frac{\alpha_1}{\alpha_2}\right) S(M) + \left(1 - \frac{\alpha_1}{\alpha_2}\right) S(0) - (\alpha_1 M + 2)R_s \right].$$

From this equation and from (27) we immediately obtain  $T(0)$  and  $T(M)$  from (31):

$$2f_2 T^4(M) = \left(1 + \frac{\alpha_2}{\alpha_1}\right) S(M) - (B_1 + R_s).$$

After substituting the above-indicated quantitative values for  $\alpha_1$ ,  $f$  when  $R_s = 0$ , it can be found that the temperature of the earth's surface is  $T(0) = 365^\circ$ , while the temperature at the upper boundary of the atmosphere is  $T(M) = 129^\circ$ .

A similar value of  $T(M)$ , just as far removed from the actually observed values, was obtained by Möller's calculations [70], in which he divided the long-wave absorption spectrum of water vapor into two regions,  $\alpha_1 = 100 \text{ cm}^{-1}$  and  $\alpha_2 = 1 \text{ cm}^{-1}$ , with

STAT

the relative energy regions of  $f_1 = 0.552$  and  $f_2 = 0.448$ , respectively, and derived the set of four differential equations of form (12) and (13) in relation to  $B_1$ ,  $B_2$ ,  $A_1$ , and  $A_2$ . It was found that  $T(0) = 313^\circ$  and  $T(M) = 136^\circ$ , in which connection there is no isothermal state in the stratosphere (at the 10-kilometer altitude,  $T = 173^\circ$ , so that thenceforth to the boundary of the atmosphere the temperature decreases by 37 degrees).

Accordingly, the computed  $T(M)$  values do not agree with the observed values of temperature in the stratosphere. Therefore, Links and Moller [57] came to the conclusion that it is impossible to determine approximately the radiative equilibrium in the stratosphere without taking account of the  $CO_2$  and  $O_3$  absorption. This was already noted by Lindemann (in 1919) but only superficially, because at that time sufficient data on radiation absorption in the atmosphere was not available.

Investigations of the processes of cooling and heating in the atmosphere, as corroborated by observations, indicate that the thermal effectiveness of water vapor is insignificant at altitudes above 14 kilometers, while carbon dioxide at high altitudes exerts a strong radiational effect. Therefore, it may be conjectured that the combined radiation by carbon dioxide and water vapor exerts a pronounced effect on the formation of the stratosphere. Above altitudes of 20 kilometers, ozone begins to participate in the radiative processes.

The amount of water vapor in the stratosphere is very low, according to measurements by Dobson [52], Barrett [47] and others. For several kilometers above the tropopause the dew point continues to decrease at the same rate as in the troposphere. The relative humidity at the altitude of 2 kilometers above the troposphere becomes less than one percent, and the total amount of water vapor decreases to  $10^{-10}$  grams/cubic centimeter. According to the spectographic aeroplane measurements made over England, it may be tentatively concluded that at altitudes above 10 kilometers the water vapor present amounts to approximately  $1.4 \cdot 10^{-3}$  grams/cubic centimeter.

As for  $CO_2$ , it has a very intense absorption band at approximately  $15\mu$ . In the very weak part of the band, at approximately  $10\mu$ , only one percent of the radiation

is absorbed by a layer the thickness of which is equivalent to the volume of  $\text{CO}_2$  in the entire atmosphere. The strong part of the band, at  $4\mu$ , lies on the threshold of the long-wave spectrum:

The absorption in the  $15\text{-}\mu$  band is known. Moller [71] calculated in his diagram the  $\text{CO}_2$  radiation emitted by the isothermal stratosphere, and found its maximum effect to lie at the 26-kilometer altitude with a cooling of 1.5 to 2.0° (C) per day. It is obvious that actually the maximum cooling level is located somewhat lower, because the calculations assumed too high a value of the volume concentration of  $\text{CO}_2$  (0.03 percent). The radiational effect of ozone was also not considered here. Some investigators assume that, in the lower stratosphere, the retarding (lag) effect of  $\text{CO}_2$  on the outgoing radiation should cause a warming-up effect. Linke and Moller [69] showed that in the moderate latitudes carbon dioxide will exert a heating effect in the tropopause, and this conclusion was reached also by Goody.

Ozone has a sufficiently intense absorption band at approximately  $14\mu$ , situated nearly in the same location as the  $\text{CO}_2$  band. The fine structure of the  $\text{O}_3$  band, which probably differs from the fine structure of the  $\text{CO}_2$  band, is not known and cannot, therefore, be considered in the calculations. Inasmuch as one half of the ozone total is present at altitudes above 20 kilometers, the  $\text{CO}_2$ -outgoing radiation is thus shielded to a considerable extent, so that the radiation losses of the atmosphere in this wave-length interval occur at higher levels. The experimental studies of the ozone spectrum are still unsatisfactory. In addition to the  $14\text{-}\mu$  band there is another intense band at approximately  $9.6\mu$ , situated precisely in the transparency interval of the absorption spectrum of water vapor.

Owing to extensive research the ozone content in the atmosphere and the vertical distribution of ozone are well known. Recently, this vertical distribution was optically measured by means of rockets [59]. The resulting data on ozone distribution was obtained for two days. The ultraviolet spectrum of the sun was photographed by means of small automatic spectographs. No ozone was found at altitudes above 45 kilometers, and the maximum concentration of ozone was found at altitudes between 15 and 24

kilometers.

The previously deduced (Govan, Penndorf) conclusions about the radiation phenomena relating to ozone were based on incorrect laboratory measurements of absorption coefficients by Hettner. Therefore, their conclusions concerning the thermal effect of ozone at various altitudes can not be considered correct. Recently, Oder [72] carried out new calculations. Inasmuch as he used mean absorption coefficients for the individual bands in his calculations, which distorts the transparency function, his results do not pretend to be quantitatively accurate.

However, the conclusions he inferred are very interesting. At an altitude of approximately 40 kilometers, radiation by ozone causes a cooling of the atmosphere at the rate of about  $5^{\circ}$  an hour. It is not very easy to explain what processes in the upper layers compensate this considerable cooling. At lower altitudes,  $O_3$  induces, for the same reasons as  $CO_2$ , a warming effect.

In the atmosphere there is still quite a number of other polyatomic gases with infrared absorption bands ( $N_2O$ ,  $NO_2$ ,  $CH_4$ , and others) but in such inconsiderable quantities that they can not play any major role in the absorption and emission of radiation.

It should be noted that the research in the radiational processes in the stratosphere is a considerably more difficult problem than the analogous research in the troposphere. First of all, the absorbing medium here is at a very low pressure, and therefore it is always difficult to establish the limits to which the absorption coefficients measured under laboratory conditions may be utilized. The relationship between absorption and temperature is indefinite, the extent to which the condition of local thermodynamic equilibrium holds true is unknown, and the concentration of absorbing media is insufficiently known. Radiation can no longer be considered as an individual thermal process independent of the general physical phenomena. In the troposphere the individual constituents of the air do not change their molecular composition during absorption or emission of radiation. True enough, their overall state may vary. For example, owing to radiational cooling, water vapor may be



brought to condensation. But, in the stratosphere, oxygen  $O_2$  and ozone  $O_3$  are subject to stronger variations. During absorption of solar ultraviolet radiation,  $O_3$  is formed from  $O_2$ , and ozone again is dissociated under the influence of longer waves in the ultraviolet part of the spectrum. Therefore, radiation processes in the stratosphere can not be isolated from physical-chemical processes.

The first investigators who ever attempted to resolve the question, what thermal effect in the lower stratosphere will cause absorption of radiation by various substances, were Dobson, Brewer and Cwiling [52]. They came to the conclusion that water vapor and carbon dioxide cool the stratosphere, while ozone warms it. This is caused by the differences in the effective radiational temperatures for  $H_2O$ ,  $CO_2$ , and  $O_3$  in the lower stratosphere: 200, 200 and 260° respectively (which, with equal volume of all three gases, results in a probable mean temperature of 220° in the stratosphere). If an equilibrium is maintained, the warming by ozone should counter-balance the cooling caused by the other gases, and therefore the stratosphere should react to change in ozone concentration, in the sense that an increase in ozone concentration should result in a rise in temperature. This simple argument was used by the above-named authors as the basis for their explanation of the principal features of the thermal regime of the stratosphere. The ozone concentration is greater over the Arctic regions than over the tropics, and therefore the temperature of the stratosphere is higher in the polar areas. Inasmuch as ozone concentration increases with altitude, positive temperature lapse rates form in the stratosphere. In the course of the seasons of the year the maximum ozone concentration over moderate latitudes occurs during the spring months, which explains the striking phase changes in the seasonal variations of stratospheric temperature: the highest temperatures appear in the months preceding the summer solstices.

The work by Dobson et al [52] in its time aroused considerable interest, because the "ozone hypothesis" displayed great simplicity and thus showed itself to be a tempting approach to the explanation of the temperature peculiarities of the stratosphere. However, the principal assumptions from which Dobson proceeded in his

research were inaccurate.

Subsequent investigations revealed a warming rather than cooling effect of  $\text{CO}_2$  in the lower stratosphere over the moderate latitudes, as noted before (by Linke, Goody, and Moller). Goody [58] came to the conclusion that the radiational equilibrium in the stratosphere always depends on the contrast between two absorbers, and that the absorbing media in the tropics and at moderate latitudes are different. He found that at middle and high latitudes such an equilibrium exists principally between the warming effect of  $\text{CO}_2$  and the cooling effect of  $\text{H}_2\text{O}$ . In the tropical stratosphere the influence of water vapor is small owing to its extremely low concentration; as for  $\text{CO}_2$ , it exerts there, at higher altitudes, a cooling effect. Therefore, an equilibrium between the effects of  $\text{CO}_2$  and  $\text{O}_3$  exists in the tropics. The warming effect of  $\text{O}_3$  is identical for all latitudes and is relatively small over middle latitudes where its amount is in a ratio of 0.05 to 0.1 to the contributions of  $\text{H}_2\text{O}$  and  $\text{CO}_2$  in the radiation balance (see Table 1).

Table 1

Radiative Influxes at the Tropopause Level

$z$	$^{\circ}\text{O}_2$	$^{\circ}\text{CO}_2$	$^{\circ}\text{H}_2\text{O}$	$z$
0	$0.1 \cdot 10^{-2}$	$-1.5 \cdot 10^{-3}$	$1 \cdot 10^{-3}$	$-0.5 \cdot 10^{-3}$
10	0.1	0	-0.5	0.5
20	0.1	3.3	-2.2	2.1
30	0.1	5.0	-7.8	-1.8
40	0.1	7.5	-10.5	-2.0
50	0.1	10.0	-14.0	-3.0
60	0.1	11.0	-17.5	-5.5
70	0.1	12.0	-18.0	-5.0
80	0.1	13.3	-18.0	-3.7

Goody assumed the following thermal model of the atmosphere: the convective layer extends so high up that the temperature lapse rates in the radiative layer are less than the adiabatic lapse rates. The condition of equilibrium between both layers is the absence of a discontinuity in temperature at their common boundary, but the temperature lapse rate has a discontinuity (6 degrees per kilometer in the

STAT

troposphere and an isothermal state in the stratosphere).

In investigating the correspondence between this model and the actual conditions, Goody attempted to survey how the variations of different factors will influence the thermal equilibrium of the tropopause in which it is neither cooled nor warmed. By calculating the absorption in the individual bands of the three absorbing substances, he investigated the relationship between the radiation balance and the pressure and temperature in the tropopause, assuming that the absorption bands do not overlap.

The consideration of deviations from Beer's law in every  $j$ th band is based on the use of Callender's transparency function instead of the exponential function. Following Dobson, the calculations have been confined to  $O_3$ ,  $CO_2$ , and  $H_2O$  alone. True enough, nitric oxide may exert the same effect as ozone, but quantitatively it is smaller. The absence of data on nitric oxide distribution necessitates the overlooking of its possible effect. The only more or less definite circumstance with a comparison of the effective radiational temperatures of nitric oxide ( $+5^\circ$ ) and ozone ( $-10^\circ$ ) is that nitric oxide is found principally in the troposphere [47].

Two functions are examined with regard to every  $j$ th band:

$$T_j = \int [A_\lambda(t) - E_\lambda(t)] \rho(t) \alpha_\lambda(t) d\lambda \quad (32)$$

for the troposphere ( $t$ ), and

$$S_j = \int [B_\lambda(s) - E_\lambda(s)] \rho(s) \alpha_\lambda(s) d\lambda \quad (33)$$

for the stratosphere ( $s$ ).

Here  $T_j$  is a function of conditions in the troposphere only, and it gives the quantity of radiation energy being exchanged between the lower surface of the infinitely thin layer directly beneath the tropopause and the troposphere; while  $S_j$  correspondingly is the function of conditions in the stratosphere only and gives the energy which is exchanged between the upper surface of the layer immediately above the tropopause and the stratosphere.

If  $E_\nu(t) = E_\nu(s)$  when  $s = t$ , then the equation

STAT

$$\sum_j (T_j + S_j) - \sum_j \epsilon_j = \frac{\partial}{\partial z} (A - B) = 0, \quad (34)$$

will, analogously to eq. (15), yield the radiational equilibrium condition (in relation to long-wave radiation only) in the lower stratosphere with continuity of temperature through the tropopause. The calculation of the  $S_j$  function is based on employing the discontinuity of temperature lapse rates when  $t = z$ .  $T_j$  is essentially positive, because the troposphere as a whole has a higher temperature than the tropopause.  $S_j$  is always negative and depends, proceeding as before from the assumption of the existence of an isothermal state in the stratosphere, on the ratio of gas density in the tropopause to its total volume per square centimeter in the stratosphere. Therefore, it may be expected that the  $S_j$ -conditioned major cooling effects must be associated with gases the density of which rapidly decreases with altitude in the stratosphere.

Goody assumed that  $\text{CO}_2$  is thoroughly intermixed in the atmosphere at all altitudes. This makes it possible to express its density, and consequently, also the thermal effects it involves, by the temperature and pressure of the atmosphere. The density of water vapor in the atmosphere is related to the air temperature assuming that relative humidity is constant. Ozone concentration in the stratosphere may be expressed as a function of latitude and season.

Consequently,  $\sum_j \epsilon_j$  is a complex function of latitude, season, and atmospheric temperature and pressure. In calculating this function, the numerical values of the parameters in (32) and (33) were chosen according to the actual data. On the basis of his calculations, the author considers (34) as correct for the stratosphere.

As for the radiational influxes relating to individual absorbers,  $\epsilon_{\text{H}_2\text{O}} < 0$ , and the greater the cooling caused by water vapor is, the higher the temperature is;  $\epsilon_{\text{CO}_2} > 0$  and increases with increase in temperature and pressure (with a pressure of  $> 0.1$  atmospheres,  $\epsilon_{\text{CO}_2} < 0$ ); while  $\epsilon_{\text{O}_3} > 0$  has an identical value at all latitudes. Fig. 3 portrays the components through which the radiative equilibrium STAT

satisfied at various latitudes. The broken lines in Fig. 3 connect points with observed temperature and pressure values at the tropopause level for latitudes 0, 40 and 80°. The upper broken-line curve in Fig. 3 indicates the magnitude of the energy influx per cubic centimeter necessary to warm up the stratosphere at various latitudes by 0.1°-(C) per day.

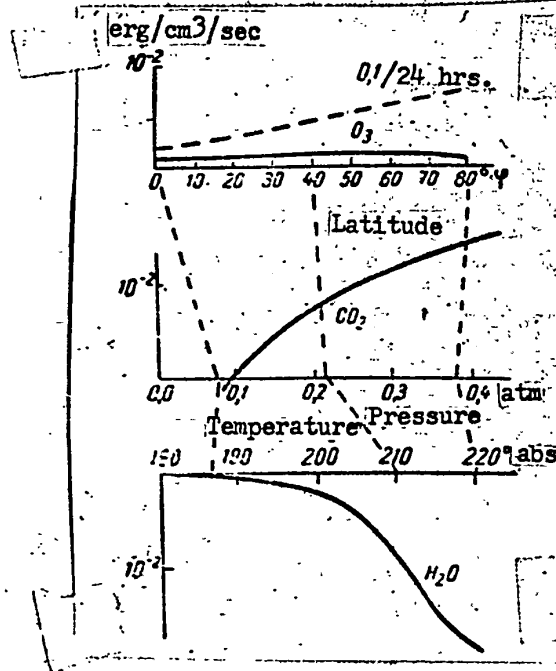


Fig. 3. Radiation Balances of  $H_2O$ ,  $CO_2$  and  $O_3$  in the Tropopause

The thus obtained relationships make it possible to explain easily the latitudinal course of temperature in the stratosphere.

Let in Fig. 4 the  $T_1(0)$ ,  $t_1$ ,  $T_1(S)$  curve be the equilibrium temperature distribution associated with the temperature at the earth's surface  $T_1(0)$ . And let us examine the distribution resulting at a higher surface temperature  $T_2(0)$ . Let us assume that this new tropopause has reached the  $t'_2$  altitude and that the temperature distribution is indicated by the  $T_2(0)$ ,  $t'_2$ ,  $T_1(S)$  curve. Now let us compare the radiation balances at altitudes  $t_1$  and  $t'_2$ . Here the temperature is the same for both,  $T_1(S)$ , and the cooling due to water vapor also must be the same, but the pressure at  $t'_2$  will be lower than at  $t_1$ , and the warming-up effect of  $CO_2$  will be lower at  $t'_2$ . Inasmuch as the radiational heat influx is balanced at  $t_1$ , the atmosphere will be

STAT

cooled at  $t'_2$ . Therefore,  $T_2(z) < T_1(z)$  must correspond to the new equilibrium temperature distribution with  $T_2(0) > T_1(0)$ .

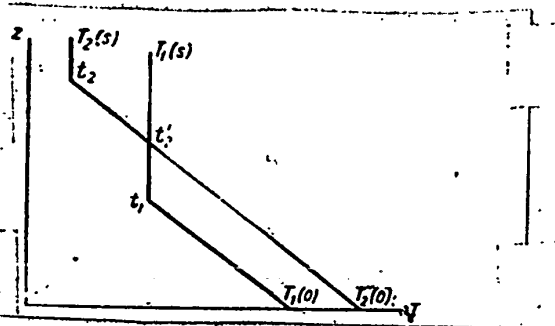


Fig. 4. Relationship Between Stratospheric and Tropospheric Temperatures

In this way, Goody explains the temperature distribution in the stratosphere not by the influence of ozone but rather by the combination of the cooling effect of water vapor with the warming effect of carbon dioxide.

As to the seasonal variations of temperature in the stratosphere owing to the influence of ozone, Goody's numerical calculations were corroborated by the values proposed in Dobson's work [52], amounting, as they do, to  $\pm 2^\circ$ .

Calculations of vertical temperature lapse rates in the stratosphere have shown that the isothermal distribution of temperature in the stratosphere requires the participation of more than one absorbing gas in the radiative equilibrium. Let us quote the computed  $\frac{\partial T(s)}{\partial z}$  values corresponding to temperature of the stratosphere  $T(s)$  in the moderate and high latitudes:

$T(s)$ °K	200	210	220
$\frac{\partial T(s)}{\partial z}$ °K/kilometer	-1.7	-2.1	-3.1

Although the results thus obtained are extremely interesting and contain much that is new, it is impossible not to mention the limitations of the quantitative basis of the above-executed calculations. It suffices to indicate that the transparency function determined empirically by Callender [50] for the 15- $\mu$  band of  $\text{CO}_2$  extended to all absorption bands of the gases under investigation (which made it possible to integrate the  $T_j$  expression for  $\text{H}_2\text{O}$  and  $\text{CO}_2$ ). Thereupon, it was assumed that the

STAT

cooled at  $t'_2$ . Therefore,  $T_2(z) < T_1(z)$  must correspond to the new equilibrium temperature distribution with  $T_2(0) > T_1(0)$ .

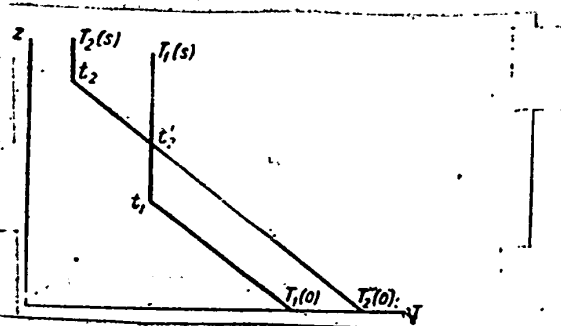


Fig. 4. Relationship Between Stratospheric and Tropospheric Temperatures

In this way, Goody explains the temperature distribution in the stratosphere not by the influence of ozone but rather by the combination of the cooling effect of water vapor with the warming effect of carbon dioxide.

As to the seasonal variations of temperature in the stratosphere owing to the influence of ozone, Goody's numerical calculations were corroborated by the values proposed in Dobson's work [52], amounting, as they do, to  $\pm 2^\circ$ .

Calculations of vertical temperature lapse rates in the stratosphere have shown that the isothermal distribution of temperature in the stratosphere requires the participation of more than one absorbing gas in the radiative equilibrium. Let us quote the computed  $\frac{\partial T(z)}{\partial z}$  values corresponding to temperature of the stratosphere  $T(z)$  in the moderate and high latitudes:

$T(z)$ OK	200	210	220
$\frac{\partial T(z)}{\partial z}$ OK/kilometer	-1.7	-2.1	-3.1

Although the results thus obtained are extremely interesting and contain much that is new, it is impossible not to mention the limitations of the quantitative basis of the above-executed calculations. It suffices to indicate that the transparency function determined empirically by Callender [50] for the 15- $\mu$  band of  $\text{CO}_2$  extended all absorption bands of the gases under investigation (which made it possible to integrate the  $T_j$  expression for  $\text{H}_2\text{O}$  and  $\text{CO}_2$ ). Thereupon, it was assumed that the

STAT

$\alpha_j$  absorption coefficients for  $H_2O$  and  $O_3$  are proportional to  $\sqrt{p}$ , and for  $CO_2$ , to  $p$ . There exist few arguments pro or con of such an assumption (the slight cooling in the tropics entailed by this assumption, owing to the influence of  $CO_2$ , vanishes if it is assumed that  $\alpha_j$  is fluctuating like  $\sqrt{p}$ ).

As a consequence of the above assumptions and of the insufficient accuracy of the quantitative values of the parameters, there is some doubt as to the conclusions obtained. In effect, if the data in Fig. 3 are used for calculating the influx of long-wave radiation  $\xi$  for every latitude, the thus obtained values are insufficiently low compared with the individual components of  $\xi$  (Table 1). But a radiational equilibrium condition requires the zero equality of the total radiative heat influx.

It is difficult to determine on the basis of [58] whether this is the result of the inaccuracy of the calculations or whether this is a reflection of the true state of affairs, i. e., the non-correspondence between the state of the stratosphere and the radiative equilibrium condition. The values obtained for the temperature lapse rates in the stratosphere are not so small as to justify the assumption, made by the author, that the stratosphere might be considered isothermal. Let us note that the available data on the temperature in the lower stratosphere (up to 16 kilometers) at various latitudes does not corroborate the generally accepted assumptions about its isothermal condition. The isotherm charts for the altitudinal levels of 10, 13, 16, and 19 kilometers [85] give after averaging for the warmer (April-September) and colder (October-March) 6-month periods the temperature distribution in the lower stratosphere cited in Table 2.

Lastly, as noted by Møller [72], the selection of the tropopause for such calculations is not quite fortunate owing to the peculiarities of radiation processes at the point of discontinuity in the temperature lapse rate.

Flass and Strong [79] have also attempted to evaluate the participation of the principal absorbing media in the radiation balance of the stratosphere. For this purpose, they isolated the following bands for the single most sensitive portion of the spectrum of each of the following gases:  $15\mu$  band, for  $CO_2$ ; the infrared

STAT



portion of  $\lambda > 25 \mu$ , for  $H_2O$ , and  $9.6 \mu$  for  $O_3$ . The stratosphere is here assumed to be isothermal, since it is relatively easy to make the calculations for these conditions.

Table 2  
Temperature Distribution in the Lower Stratosphere

z km	T°						
	10	20	30	40	50	60	70
Warmer 6-months (Apr.-Sept.)							
10	239	237	235	230	226	224	223
13	215	215	215	215	219	223	226
16	197	200	204	210	218	224	228
19	200	202	207	212	218	225	228
Colder 6-months (Oct.-Mar.)							
10	239	235	229	223	220	219	219
13	215	214	213	214	216	219	221
16	198	199	204	209	215	220	222
19	198	200	204	209	215	219	221

In assuming the temperature of the earth's surface equal to  $300^\circ$ , they found that the heat coming into the stratosphere from the earth's surface amounts to 40 microcalories/square centimeter/second in the  $15 \mu$  band of  $CO_2$ ; in this connection it is assumed that the entire atmosphere is isothermal at  $220^\circ$ . Moreover, the heat coming into the stratosphere in this band comes also from the lower, warmer layers of the troposphere. The corresponding total flux is estimated at 60 microcalories/square centimeter/second. The heat losses to outer space from the stratosphere in the  $15 \mu$  band of  $CO_2$  and  $O_3$  amount to 310 microcalories/square centimeter/second. Thus, the principal effect of the  $CO_2$  band in the radiation balance of the stratosphere is emission into outer space. These calculations were also based on using the data on transparency of the atmosphere obtained with aircraft flights at an altitude of 11 kilometers.

Owing to the absence of experimental data, the above-named authors could provide only a very rough estimate of the radiation losses in the  $H_2O$  bands.

If it be assumed that all the black-body radiation reaching the earth's surface in this region originates from a  $50 \mu$   $H_2O$  band, it will be found that water vapor radiates 780 microcalories/square centimeter/second. Moreover, if the  $H_2O$  spectrum

STAT

is absolutely black only above 20  $\mu$ , then the water vapor in the stratosphere may absorb relatively little radiation from the earth's surface and the troposphere. This heat is approximately estimated at 100 microcalories/square centimeter/second.

The evaluation of ozone's participation is made even more roughly, since the variability of ozone concentration with altitude presents a more or less satisfactory accuracy of the calculations. From the transparency curve it may be concluded that the 9.6- $\mu$  band of  $O_3$  represents a continuous absorption region with a width of approximately 0.5  $\mu$ , and with an absorption coefficient of 0.5. Consequently, its radiation amounts to one-half of black-body radiation at a temperature of 220°. Hence it follows that ozone loses 30 microcalories/square centimeter/second downward toward the earth's surface. In assuming a temperature of 300° for the earth's surface, it can be found that  $O_3$  absorbs 190 microcalories/square centimeter/second from the radiation emanating from the earth's surface.

If it is assumed that ozone ( $O_3$ ) absorbs 1/12 of the solar radiation incident to the outer boundary of the atmosphere, i. e., 800 microcalories/square centimeter/second, this would mean 800 microcalories/square centimeter/second.

Thus, according to Plass and Strong, the radiation balance of the stratosphere is thus represented:

Heat Losses	
From the 15- $\mu$ bands of $CO_2$ and $O_3$	310 cal/cm <sup>2</sup> -sec
From the 9.6- $\mu$ band of $O_3$	60 "
From the 50- $\mu$ band of $H_2O$	780 "
	<hr/>
	1,150 cal/cm <sup>2</sup> -sec
Heat Gain	
From solar radiation absorbed by $O_3$	800 cal/cm <sup>2</sup> -sec
From the radiation of the earth's surface,	
absorbed in the 9.6- $\mu$ band of $O_3$	190 "
From the radiation of the earth's surface and	
the troposphere, absorbed in the 15- $\mu$ band of $CO_2$	60 "

STAT

Ditto, for the 50- $\mu$  band of H<sub>2</sub>O

100 cal/cm<sup>2</sup>-sec

1,150 cal/cm<sup>2</sup>-sec

The model of the atmosphere adopted by Strong and Plass has subsequently been made more accurate by King [65], Kaplan [65], and Warner [83].

King examined the radiation transport of heat in a non-isothermal atmosphere and came to the following interpretation of the structure of the standard atmosphere: The atmosphere may be divided into three layers differing from each other by the nature of the processes determining its thermal regime:

(1) The stratosphere is heated by the ozone which absorbs solar radiation; this heating or warming effect is compensated at every level by the infrared cooling in the 15- $\mu$  CO<sub>2</sub> band which, like the warming effect from O<sub>3</sub>, has a maximum value at the top of the stratosphere and decreases to zero in the proximity of the tropopause.

(2) The upper troposphere (between the tropopause and the altitude level of approximately 6 kilometers) is the only region of the atmosphere found in infrared radiational equilibrium; the effect of the 15- $\mu$  CO<sub>2</sub> and 5-8- $\mu$  H<sub>2</sub>O bands consists in the heating of this region, which is compensated by the cooling induced by the rotary H<sub>2</sub>O band.

(3) The lower troposphere - is controlled by convective processes; here the radiational transport creates superadiabatic temperature lapse rates, which cause convective-condensational processes; this results in the establishment of lapse rates with values approximating the wet-adiabatic ones; it is only in the lowest, surface-frictional layer, where convection and turbulence are hampered, that the temperature lapse rates approximate their radiative-equilibrium values.

Kaplan investigated the influence of pressure on radiational transfer, on assuming that, according to Lorentz, the half-width of spectral lines varies in proportion to  $p$ . Having considered the outgoing radiation of the atmosphere for three cases of sounding, he came to the conclusion that the effect of the decrease in pressure with altitude leads to an increase of 5 to 8 percent in outgoing radiation (according to Kondrat'yev, the counter-radiation of the atmosphere decreases by

STAT

5 percent [20]). Furthermore, Kaplan assumes that the tropopause area is not in a radiational equilibrium and constitutes rather an outlet for radiational heat.

Warner turned his attention to the asymmetry of the form of spectral lines - the line center is usually displaced in a direction towards the low-frequencies by a value proportional to pressure. The correction for this factor in outgoing radiation is at most only several percent.

The calculations based on the Flass-Strong model provide a different representation of the radiation balance of the stratosphere compared with Goody's calculations: owing to  $\text{CO}_2$  and  $\text{H}_2\text{O}$  the stratosphere is cooled and warmed chiefly by  $\text{O}_3$  (which corresponds with Dobson's hypothesis).

This diversity of results reemphasizes that all the quantitative evaluations of the thermal regime of the atmosphere are as yet tentative and suffer from the lack of accurate experimental data and complete (detailed) theoretical elaborations.

Despite the obvious adequacy of the hypothesis of the radiational equilibrium in the stratosphere from the theoretical point of view, this problem, like all the problems of geophysics, requires direct observations for a reliable determination of the relationship between the radiational and turbulent heat influxes above the tropopause. Here, direct measurements of thermal effects are very difficult, but there are certain possibilities for inferring indirect conclusions about these effects by means of measurements of other values.

The existence of high wind gradients in the proximity of the tropopause has long been known (Dobson, in 1920) [53]. In 1947 [20] it was shown that the tropopause may be a level of very strong localized westerly winds. This appears to be inconceivable if it is assumed that turbulence and advection play a small role in the thermal state of the lower stratosphere.

Prior to the war, in Germany, Koschmieder [64] and Jung [63] conducted observations of the turbulent velocities in the proximity of the tropopause. The results of two series of measurements made by the former investigator during balloon-pilot ascents show extremely strong variations in the rate of ascent in the lower stratosphere. STAT

even if the ascent through the tropopause was fairly stable. As for the latter investigator, on the basis of five measurement series made by balloon-pilots equipped with miniature accelerometers, he also came to the conclusion that turbulence reaches its maximum intensity somewhere in the lower stratosphere. It is difficult to reconcile these results with the generally accepted hypotheses, and, therefore, further research is necessary.

Beside these measurements of a preliminary nature there exists direct and repeatedly verified evidence of the existence of intermixing in the lower stratosphere. Measurements of the concentration of oxygen (E. Regener, 1936) [77] and of helium (Gluckauf and Paneth, 1946) [57] indicate that above the tropopause these two gases are not dissociated by the force of gravity; furthermore their relative concentration does not change, as one must anticipate in the case of a lack of turbulence. Chaket, Paneth and Wilson [49] measured the ratios of helium, neon and argon to nitrogen up to an altitude of 70 kilometers, and found no variations in the relative concentration of these gases.

Ozone is the other component of atmospheric air the altitude distribution of which may provide valuable information about turbulent transport in the stratosphere. This gas forms almost completely above the 20-kilometer altitude, and, consequently, it can be transported downward only through turbulent diffusion. Therefore, it may be assumed that the measurements of the concentration of ozone in the proximity of the tropopause may provide some information about the aforesaid transport. corresponding observations were made by V. Regener [78]; it was found that in the proximity of the tropopause the ozone concentration increases very rapidly with altitude.

Hence it is evident that the physical processes occurring in the stratosphere cannot be explained entirely from the standpoint of the hypothesis of radiational equilibrium. The conditions at which such equilibrium is preserved are not compatible with the turbulent and orderly intermixings of large air masses occurring above the tropopause. In the calculations of Goody and Kaplan it is possible to find indications that the radiational heat influxes in the stratosphere do not compensate each other. STAT

King expresses doubts as to the possibility of the existence of an isothermal temperature distribution in the stratosphere with a radiative equilibrium. The function of atmospheric radiation that he obtained from this condition, proved to be a decreasing function of altitude.

An attempt at clarifying the essential features of the stratosphere's structure - an isothermal state and vertical intermixing insuring a uniform chemical composition of the air with altitude - has been made in [30] and [31]. In these works, the hypothesis of radiative equilibrium is replaced by the assumption that non-adiabatic vertical intermixings of the air take place in the stratosphere. The heat influx is insured by the absorption of solar radiation by the dust contained in the stratosphere. With such an assumption the vertical stability of the stratosphere, induced by the isothermal distribution of temperature which prevents an adiabatic intermixing of the air within it, on the one hand, and the vertical intermixing, on the other hand, are not incompatible phenomena. For this, it is necessary that the ascending air receive from the dust a quantity of heat that would be at least sufficient for the compensation of its cooling as the result of expansion. As for the radiative equilibrium hypothesis, even if it could produce an isothermal stratosphere, it is not capable of resolving the problem of an "intermixed" atmosphere.

With regard to dust, it is logical to assume that it must be predominantly of cosmic origin. Volcanic dust enters the stratosphere comparatively rarely, while cosmic dust is admitted almost continuously; its particles are much smaller and thus may remain in the air for a very long time.

In order to show the possibility of vertical displacements of the air in the stratosphere owing to the thermal effect of dust, it is necessary to estimate the dust concentrations that are, on the one hand, necessary for such displacements, and, on the other, possible under conditions of the stratosphere.

Let us assume that the quantity of the radiation incident onto a dust particle is determined by the geometric shielding law. If  $I_0$  is the quantity of radiation incident per square centimeter of surface area per unit of time, then a quantity

STAT

$\pi r^2 I_0 N$  (of radiation) is incident for every  $N$  of the dust particles with a radius  $r$ , contained in a cubic centimeter of air, out of which a quantity,  $\alpha \pi r^2 I_0 N$  is absorbed, and the remainder is scattered.

Generally speaking, for particles with dimensions smaller than the wave length of the incident radiation, the quantity of the incident energy is proportional to  $r^n$ , where  $n \neq 2$ , because it is determined by diffraction phenomena and not by geometrical shielding. But, inasmuch as the numerical values of  $n$  have not been accurately established for small particles of various dimensions, we shall assume that  $n = 2$ .

The coefficient of radiation absorption by dust is smaller than unity. Since  $\alpha$  is a co-multiplier together with  $r^2$  in the concentration of  $N$  being evaluated in all the expressions incorporating that concentration, as will be evident later on, for simplicity and calculational convenience we shall assume that  $\alpha = 1$ . Then, any obtained quantitative values of  $N$  that are lower than that should be multiplied by a value inverse to the product of  $\alpha \cdot r^{n-2}$  in order to improve their accuracy at a corresponding selection of  $\alpha$  and  $n$ .

Of the various schemes of hypothetical motions reviewed in [31] we shall cite now the first and most elementary one, taking place with the following assumptions which simplify the problem:

- (1) The temperature in the stratosphere  $T_s$  is uniform on all altitudes.
- (2) Horizontal motions are not taken into account, since this is a question of investigating the possibility itself of the vertical ascent of warmed air parcels and not one of an investigation of the vertical velocity value which is distorted by this assumption.
- (3) The process is stationary.
- (4) With regard to heat transfer from dust to the atmosphere, the following most generalized assumption is made: a thermal equilibrium is established in which the influx of heat from the sun to the dust is equal to its efflux from the dust to the atmosphere.
- (5) The pressures in an ascending air mass and in the ambient atmosphere are

STAT

the same.

Let, at altitude  $z$ , one cubic centimeter of ascending air contain  $N(z)$  dust particles, and let  $\rho$  denote its density.

Now let us write the equation of heat influx for a unit of the ascending air mass

$$\frac{QN}{\rho} = c_p \frac{dT}{dt} - \frac{A dp}{\rho dt}$$

where  $Q$  is the quantity of solar heat being absorbed per dust particle,  $T$  and  $p$  are the temperature and pressure of the air, respectively,  $A$  is the thermal equivalent of work, and  $c_p$  is the specific heat of air at constant pressure.

Proceeding from the above assumptions, the equation of continuity has the form of

$$\rho w = \text{const} = K,$$

in which,  $K \neq 0$  (since the process of ascent of air does not extend to the boundaries of the atmosphere). Then, by means of the equations of state and statics, we obtain

$$\frac{QN}{K} = c_p \frac{\partial T}{\partial z} + Ag \frac{T}{T_c}$$

The condition for the possibility of vertical motion in the stratosphere is

$$\frac{\partial T}{\partial z} \gg 0.$$

Consequently, in order that the temperature of the ascending air should not vary and remain approximately the same as that of the ambient stratosphere, the number of dust particles per unit of air volume should satisfy the condition

$$N = \frac{AgK}{Q}.$$

By means of this relation it is possible to carry out quantitative evaluations of the dust content of the stratosphere necessary for bringing about isothermal displacement of air in the stratosphere.

If it is assumed that  $Q = \pi r^2 I_0$  ( $I_0$  — represents the solar constant), then we

STAT



obtain for the 20-kilometer level ( $\rho = 9.2 \cdot 10^{-5}$  grams/cubic centimeter), with a trajectory velocity of  $w = 1$  centimeter/second,  $N = 2$  for  $r = 10^{-4}$  centimeters and  $N = 2 \cdot 10^k$  for  $r = 10^{-5}$  centimeters.

The ratio between  $Q$  and  $w$  is determined with greater accuracy with their higher values.

Let us now examine a second scheme, in which the pressure inside an ascending air mass is lower than in the ambient atmosphere (which is possible with vertical velocities greater than those examined immediately above).

The simplifying assumptions here are the same as those for the first scheme, but an equation of vertical motion of air is included into the set of equations under consideration.

$$\frac{dw}{dt} = -\frac{1}{\rho} \frac{\partial p}{\partial z} - g$$

Having derived this set of equations and discarding the small terms, we obtain

$$\begin{aligned} \rho &= \rho_0 e^{-\int_0^z \frac{R \frac{\partial T}{\partial z} + g}{RT} dz} \\ p &= p_0 e^{\frac{c_p}{AR} \ln \frac{T}{T_0} - \frac{Q}{AKR} \int_0^z N dz} \\ T &= T_0 e^{\frac{c_p}{AR} \ln \frac{T}{T_0} - \frac{Q}{AKR} \int_0^z \frac{N dz}{T} + \int_0^z \frac{R \frac{\partial T}{\partial z} + g}{RT} dz} \\ w &= w_0 e^{\int_0^z \frac{R \frac{\partial T}{\partial z} + g}{RT} dz} \end{aligned}$$

where  $R$  is the gas constant.

Obviously the order of  $w_0$  here should be not below 10 centimeters a second.

Let us determine the initial concentration  $N_0$  of dust necessary for, e. g., increasing the air temperature by 1 degree with an upward displacement of 1 kilometer, and also the pressure differential  $\Delta p = p_0 - p$  resulting with this displacement.

At first we shall make calculations for the 30-kilometer altitude:  $T_0 = 233^\circ \text{C}$ ,  $p_0 = 10$  millibars,  $\rho_0 = 1.5 \cdot 10^{-5}$  grams/cubic centimeters, and the  $231 = 230eV$  relation yields  $y \approx 0$ .

If it is assumed that the  $T$  temperature and the  $\frac{\partial T}{\partial z}$  gradient may be substituted by their mean values for a layer of thickness  $\Delta z$ , then

$$y = \frac{c_p}{AR} \ln \frac{T}{T_0} - \frac{Q}{AKRT} \int N dz + \frac{R \left( \frac{\partial T}{\partial z} \right) + g}{RT} \Delta z.$$

STAT

$$L = \frac{Q \int N dz}{ARR} = 35,$$

Inasmuch as

$$\ln \frac{T}{T_0} \approx 0.$$

If

$$N = N_0 e^{-kx},$$

then

$$N_0 = \frac{LAKRk}{Q(1 - e^{-kx})}$$

At  $k = 10^{-6}$  and  $r = 10^{-6}$  centimeters we obtain  $N_0 = 5 \cdot 10^4$  for  $K = 10^{-4}$  ( $w_0 \approx 10$  centimeters/second).

We find

$$p_1 = p_0 e^x,$$

Inasmuch as

$$x = -\frac{L}{T} = -0.15,$$

$p_1 = 10 \cdot e^{-0.15} = 6.3$  millibars. In the stratosphere at the 31-kilometer altitude,  $p_0 = 9.5$  millibars. Therefore, the pressure drop towards the center of the dust-pollution area is  $\Delta p = 3.2$  millibars. If the radius of that area is  $r = 10^7$  centimeters, then the horizontal pressure gradient is  $32 \cdot 10^{-5}$  dynes/cubic centimeter.

Let us make the same calculations with regard to the 75-kilometer altitude:

$T_0 = 275^\circ$ ,  $p_0 = 6.4 \cdot 10^{-2}$  millibars,  $\rho_0 = 0.8 \cdot 10^{-7}$  grams/cubic centimeter,  $y = 0$ , and  $L = 35$ .

When  $k = 10^{-6}$  and  $r = 10^{-6}$  centimeters,  $N_0 = 5 \cdot 10^2$  for  $K = 10^{-6}$  ( $w_0 \approx 10$  centimeters/second),  $x = -0.127$ ,  $p_1 = 5.3 \cdot 10^{-2}$  millibars,  $p_0 = 6 \cdot 10^{-2}$  millibars,

$\Delta p = 0.007$  millibars, and  $\frac{\partial p}{\partial r} = 7 \cdot 10^{-7}$  dynes/cubic centimeter.

A study of a series of photographic surveys of noctilucent clouds observed on

STAT

29 June 1936 made it possible to discover a cyclonic rotary motion of the air at the 70-80-kilometer altitudes occupying an area of  $5 \cdot 10^4$  square kilometers (rotation velocity: 29 to 34 meters a second). The motion of luminous meteoric tracks also indicates the existence of local air current systems, which systems usually disintegrate towards the night's end. V.V. Fedynskiy has suggested that these air currents are a consequence of the effect of solar radiation.

In order to explain whether similar cyclonic systems may develop even if only approximately as a consequence of atmospheric motion examined according to the second scheme, it is necessary to compare the above-calculated horizontal pressure gradients with the gradients corresponding to the observed rotation velocity.

The radius  $r'$  of the cyclone in the above example is  $10^7$  centimeters, and its velocity  $c$  is of the order of  $3 \cdot 10^3$  centimeters a second. The pressure gradient for this cyclone can be estimated from the following relation

$$\frac{c^2}{r'} + lc - \frac{1}{\rho} \frac{\partial p}{\partial r'} = 0$$

where  $l = 2\omega \sin \varphi$  ( $\omega$  is angular velocity of the earth's rotation,  $\varphi$  is geographical latitude of the locus of observation). When  $\varphi = 30^\circ$ ,  $l = 10^{-4}$  seconds $^{-1}$ .

For the 30-kilometer altitude,  $\frac{\partial p}{\partial r'} = 10^{-5}$  dynes/cubic centimeter, and for the 75-kilometer altitude  $\frac{\partial p}{\partial r'} = 10^{-7}$  dynes/cubic centimeter.

Consequently, in the afore-examined examples the pressure gradients, for the 30- and 75-kilometer altitudes are 30 and 5 times higher, respectively, than those obtained from the corresponding observation data at these altitudes. Such gradients develop with a displacement of air by one kilometer; with further displacement, they should become even greater.

Undoubtedly, the discrepancy between the computed and the actually measured pressure gradients is due to the distorting influence of horizontal motions. But, if it is assumed that the computed gradients will be sufficient anyway to cause the wind velocities computed according to the second scheme to be of the order of the actually observed wind velocities, then the second scheme should provide an explanation for the cyclones which are observed in the stratosphere. For this purpose it is merely STAT

necessary to postulate the possibility of the existence of sufficiently large dust areas in the stratosphere. Then it may be assumed that the noctilucent clouds, which are found at the uppermost portion of the area under cyclonic rotation, disclose that area by their motion. It should be noted that, with such an explanation of the causes of local currents in the stratosphere, one absolutely natural result is their diurnal periodicity noted during observations.

Let us return to the question of the initial vertical velocities of the motion of air containing dust. Let us determine whether it is possible to establish a relationship between the level in the atmosphere at which this motion begins and the magnitude of  $w_0$ , i. e., whether anything may be stated about the altitudinal distribution in the stratosphere of the motions given by the afore-examined schemes.

For altitudes upward of 60 kilometers,  $w_0$  is of the order of  $10^2$  to  $10^3$  centimeters a second, which can be substantiated as follows: It is impossible to assume that there exists a discontinuity between the rate (velocity) of mixing of various portions of a gas as the result of diffusion and the velocity of the initial laminar convective motion of the same portions of the gas. Therefore, at the 75-80-kilometer altitude,  $w_0$  should be of the order of several meters a second. Actually, the expansion rate (velocity) of the gaseous meteoric tracks, where diffusion becomes visible per se owing to the presence of agitated molecules, amounts to 2-10 meters a second. But the diffusion rate (velocity) is proportional to the diffusion coefficient, and the latter is inversely proportional to air density. This is a direct consequence of the expression for the coefficient of diffusion "per se" according to Enskog:

$$D = \frac{3\sqrt{R}}{32\pi} \frac{\sqrt{T}}{N_L} \frac{1}{V\mu^2\psi}$$

where  $\mu$  is molecular weight of gas,  $N_L$  is Avogadro's number, and the  $\psi$ -function depends on the forces of interaction between molecules. Consequently, for any two altitudes in the stratosphere where  $T_1$  and  $T_2$  are of the same order,

$$D_2 = D_1 \frac{\rho_1}{\rho_2}$$

If at the 75-kilometer altitude  $\rho_1 \approx 10^{-7}$  grams/cubic centimeter and  $w_0$  equals STAT

several meters a second, while at the 30-kilometer altitude  $\rho_0 \approx 10^{-5}$  grams/cubic meter, then, for the latter altitude,  $w_0$  is of the order of several centimeters a second.

Consequently, motions in the first scheme may take place in the lower part of the stratosphere (20 to 60 kilometers) and second-scheme motions - in the upper stratosphere (60 to 80 kilometers) where, in addition to the required magnitude of  $w$ , there is also a general decrease of temperature with altitude, which contributes to the development of convection.

The prolonged duration of dust trails (up to 5-6 hours) as compared with luminous night trails, could be also attributed to the low velocity of the vertical displacements of air in the lower stratosphere.

It should be noted that the formulas in both schemes give only the averaged values of  $T$ ,  $p$  and  $\rho$ , which should be related to finite and sufficiently large intervals of time and displacements. These formulas govern macro-motions and they do not give the instantaneous values of the corresponding physical values governing micro-motions. The latter are associated with thermal heterogeneity in moving air, which, of course, should be assumed, since the dust pollution of a certain mass of air may not be uniform.

Let us examine within a dust cloud the motions of air being heated by the dust. In order to isolate these micro-motions from the motions of the cloud itself, let us resolve the stationary problem. The stratification of the stratosphere, as previously, will be assumed as isothermal; the variations in velocities, temperature and pressure will be examined in the  $xz$  plane.

We shall assume the upper and lower boundaries of the cloud to be flat. The dust distribution in the cloud will be such that the dust concentration is  $N = 0$  at the lower ( $z = 0$ ), upper ( $z = h$ ) and lateral ( $x = L$ ) boundaries of the cloud. This may be most simply written in the following form:

$$N = N_0 \frac{z(h-z)(1-bx^2)}{h^2},$$

where  $bx^2 = 1$  with  $x = L$ .

STAT

The maximum dust concentration will be in the center of the cloud

$$N_{\max} = \frac{N_0}{4}$$

In this case, the quantity of heat entering into a unit mass of air per unit of time from a dust with  $N$  concentration equals

$$Q = \frac{\pi r^2 l N_0}{\rho k^2} z (h - z) (1 - bx^2)$$

In order to determine the velocity of motion, temperature and pressure of the air in the dust cloud, it is necessary to derive the following set of equations:

Equations of motion

$$u \frac{\partial u}{\partial x} + w \frac{\partial u}{\partial z} - lv = - \frac{1}{\rho} \frac{\partial p}{\partial x}, \quad (35)$$

$$u \frac{\partial v}{\partial x} + w \frac{\partial v}{\partial z} + lv = 0, \quad (36)$$

$$w \frac{\partial w}{\partial z} = - \frac{1}{\rho} \frac{\partial p}{\partial z} - g; \quad (37)$$

The equation of continuity

$$\frac{\partial u}{\partial x} + \frac{\partial w}{\partial z} = 0; \quad (38)$$

The equation of heat influx

$$u \frac{\partial \theta}{\partial x} + w \frac{\partial \theta}{\partial z} + \Gamma w = \frac{Q(x, z)}{c_p} \quad (39)$$

Here  $u$ ,  $v$  and  $w$  are velocity components of air,  $\theta$  is deviation of temperature from values not affected by dust,  $\Gamma = \gamma_a - \gamma$ , (where  $\gamma_a$  is the adiabatic lapse rate), and  $l$  is the Coriolis parameter.

Let us set the distribution of vertical velocity,  $w$ . It is known that with thermal heterogeneity in the horizontal direction in the atmosphere vertical motions of air develop, while the air within dust clouds is found precisely under thermally heterogeneous conditions. Obviously, there are no vertical motions of air at a certain level under the cloud and at another level above that cloud. The motions outside the cloud we shall assume small in comparison with the motions within it. Therefore, we

STAT

shall relate  $w = 0$  to  $z = 0$ , and we shall not examine  $z = h$  and the motions of the air outside the cloud. Let us further assume that  $w$  is independent of  $x$ , i. e., our estimates of  $w$  will be valid for the parts of the cloud that are remote from its lateral boundaries.

The altitudinal distributions of  $w$  and  $N$  are similar. Then,

$$w = az(h - z)$$

where  $a$  is a constant determining the velocity value that must be determined.

In assuming the above-indicated boundary conditions for  $w$  it obviously should be assumed that thermal heterogeneity is lacking at the lower and upper boundaries of the cloud.

Thus, the problem is resolved with the following boundary conditions:

when  $z = 0$

$$w = Q = \theta = 0,$$

When  $z = h$

$$w = Q = \theta = 0.$$

Let us determine the corresponding values of  $a$ ,  $u$ ,  $v$ ,  $\theta$ , and  $p$ , for various values of  $N_{\max}$ . In addition, let us estimate the  $x = L$  at which the upper boundary of the cloud may still be considered as flat. Obviously, the distribution of velocities, temperature and pressure in the cloud will be stationary so long as variations in the distribution of dust concentration therein do not take place, i. e., so long as there does not occur any considerable deformation of the cloud. Let us estimate the time interval  $\Delta t$ , during which the cloud may be considered undeformed and the distribution of elements therein, stationary. In this way, we shall determine the conditions at which the above-made assumptions remain valid.

Let us proceed to a resolution of the problem.

We shall determine  $u$  from eq. (38):

$$\dot{u} = - \int \frac{\partial w}{\partial z} dx = - ax(h - 2z) + \varphi(z).$$

When  $x = 0$

$$u = \varphi(z) = 0,$$

STAT

therefore,

$$u = -ax(h-2z).$$

The horizontal velocity component  $u$  will have opposite directions at the lower and upper boundaries of the cloud, and it will attain its maximum values when  $z = 0$  and  $z = h$ .

Let us determine  $\theta$  from eq. (39):

$$\frac{\partial \theta}{\partial z} - \frac{x(h-2z)}{z(h-z)} \frac{\partial \theta}{\partial x} + \Gamma = \frac{\alpha(1-bx^2)}{ac_p}$$

where

$$\alpha = \frac{\pi r^2 J_0 N_0}{\rho h^2}$$

The integrals of this equation are:

$$\begin{aligned} C_1 &= xz(h-z), \\ \theta + C_2 &= \left( \frac{\alpha}{ac_p} - \Gamma \right) z + \frac{2xb}{ac_p h^2} x^2 z^2 (h-z)^2 \ln \left( \frac{h}{z} - 1 \right) + \\ &+ \frac{ab}{ac_p h^2} x^2 z (h-z)(h-2z). \end{aligned}$$

It follows from the  $\theta = 0$  condition when  $z = 0$  that  $C_2 = 0$ .

Inasmuch as  $\theta = 0$  when  $z = h$ , therefore,

$$\frac{\alpha}{ac_p} - \Gamma = 0,$$

whence

$$\alpha = \Gamma c_p.$$

Obviously, with any other possible law of the variation of  $w$  with altitude, but with the same boundary conditions and with the condition of the similarity between the variations of  $w$  and  $N$  with altitudes, we obtain the same expression for  $\alpha$ . With these conditions,  $w_{\max}$  and consequently also the order of magnitude of  $w$  have an identical value with a given dust-content of the cloud:

STAT



$$w_{\max} = \frac{1}{c_p \Gamma} \frac{N_{\max}}{\rho}$$

As one should expect, the vertical velocity of air in the cloud is determined by the dust-content of the cloud, the stratification of the atmosphere, and the density of air. The latter is in complete agreement with the previously obtained conclusion about the altitudinal distribution of the vertical motion velocities of dust-filled air masses in the stratosphere.

From the physical standpoint it is perfectly obvious that the form in which  $N(z)$  was given, different from that of  $w$ , cannot, with the same boundary conditions and the same value of  $N_{\max}$ , affect greatly the magnitude of  $w$ .

Let us determine  $v$  from eq. (36):

$$\frac{\partial v}{\partial x} - \frac{x(h-x)}{x(h-2x)} \frac{\partial v}{\partial z} + l = 0.$$

The integrals of the equation are

$$\begin{aligned} C_1 &= xz(h-z), \\ C_2 &= x + \frac{v}{l}. \end{aligned}$$

In which connection,  $C_2 = 0$ , since  $v = 0$  when  $x = 0$ . Whence

$$v = -lx + mxz(h-z).$$

Let us determine the constant  $m$  after having differentiated with respect to  $x$  eqs. (35) and (37) and discarded  $\frac{\partial^2 p}{\partial x \partial z}$  from them:

$$\frac{\partial u}{\partial z} \frac{\partial u}{\partial x} + u \frac{\partial^2 u}{\partial x \partial z} + \frac{\partial w}{\partial z} \frac{\partial u}{\partial z} - l \frac{\partial v}{\partial z} = 0.$$

Whence

$$m = -\frac{2a^2}{l}.$$

Let us find pressure  $b$  from eqs. (35) and (37).

STAT

$$w_{\max} = \frac{1}{c_p \Gamma} \frac{N_{\max}}{\rho}$$

As one should expect, the vertical velocity of air in the cloud is determined by the dust-content of the cloud, the stratification of the atmosphere, and the density of air. The latter is in complete agreement with the previously obtained conclusion about the altitudinal distribution of the vertical motion velocities of dust-filled air masses in the stratosphere.

From the physical standpoint it is perfectly obvious that the form in which  $N(z)$  was given, different from that of  $w$ , cannot, with the same boundary conditions and the same value of  $N_{\max}$ , affect greatly the magnitude of  $w$ .

Let us determine  $v$  from eq. (36):

$$\frac{\partial v}{\partial x} - \frac{x(h-x)}{x(h-2x)} \frac{\partial v}{\partial x} + l = 0.$$

The integrals of the equation are

$$C_1 = xz(h-z),$$

$$C_2 = x + \frac{v}{l}.$$

In which connection,  $C_2 = 0$ , since  $v = 0$  when  $x = 0$ . Whence

$$v = -lx + mxz(h-z).$$

Let us determine the constant  $m$  after having differentiated with respect to  $x$  eqs. (35) and (37) and discarded  $\frac{\partial^2 p}{\partial x \partial z}$  from them:

$$\frac{\partial u}{\partial z} \frac{\partial u}{\partial x} + u \frac{\partial^2 u}{\partial x \partial z} + \frac{\partial w}{\partial z} \frac{\partial u}{\partial z} - l \frac{\partial v}{\partial z} = 0.$$

Whence

$$m = -\frac{2a^2}{l}.$$

Let us find pressure  $b$  from eqs. (35) and (37).

STAT

Evidently,

$$dp = \frac{\partial p}{\partial z} dz + \frac{\partial p}{\partial x} dx$$

or

$$p = \int_h^z \frac{\partial p}{\partial z} dz + \int_0^x \frac{\partial p}{\partial x} dx + C.$$

Here C is atmospheric pressure at the upper boundary of the cloud.

If it is assumed that  $\rho$  is independent of  $z$  within the limits of the cloud,

then

$$\begin{aligned} \int_h^z \frac{\partial p}{\partial z} dz &= -\rho g(z-h) - \rho \frac{a^2 z^2 (h-z)^2}{2}, \\ \int_0^x \frac{\partial p}{\partial x} dx &= \rho \int_0^x (lv - u \frac{\partial u}{\partial x} - w \frac{\partial w}{\partial x}) dx = \\ &= \rho \left[ \frac{lmx(h-z) - l^2}{2} - \frac{a(h-2z)^2}{2} - a^2 z(h-z) \right] x^2. \end{aligned}$$

Now it is possible to estimate the horizontal-direction distance L at which the upper boundary of the cloud may be considered flat. L should satisfy the condition that

$$p|_{h,L} = \int_0^L \frac{\partial p}{\partial x} dx|_{z=h} + C \approx C$$

or

$$\left| \int_0^L \frac{\partial p}{\partial x} dx|_{z=h} \right| \ll C.$$

But we do not ignore values of the order of  $\rho gh$  in the calculation of pressure.

Consequently,

$$\left| \int_0^L \frac{\partial p}{\partial x} dx|_{z=h} \right| < \rho gh$$

or

$$\left( \frac{l^2}{2} + \frac{a^2 h^2}{2} \right) L^2 < gh.$$

STAT

If the cloud is found at the 30-kilometer altitude, then  $\rho = 1.5 \cdot 10^{-5}$  grams/cubic centimeter; when  $N_0 = 10^3$ ,  $r = 10^{-6}$  centimeters and  $h = 5 \cdot 10^4$  centimeters, we obtain  $a = 1.6 \cdot 10^{-11}$  and  $L < 10^8$  centimeters.

The  $N$ -dependent member in comparison with the  $l$ -dependent member may be ignored (with dust concentrations that are even  $10^2 - 10^3$  times higher than the selected one), and the value of  $L$  is determined by the Coriolis parameter and the altitude of the cloud:

$$L < \sqrt{\frac{2gh}{\rho}}$$

Let us calculate the  $w$  and  $u$  for a dust cloud with certain given dimensions and dust content, and let us also evaluate the time interval during which the cloud may be considered undeformed, and the processes therein, as stationary.

Let  $h = 5 \cdot 10^4$  centimeters,  $L = 10^5$  centimeters, and let the cloud be located at an altitude of 30 kilometers, and let  $N_{\max} = 2,500$  ( $N_0 = 10^4$ ).

Then:

$$\begin{aligned} a &= 1.6 \cdot 10^{-10}; \quad w = 0.3 \cdot 10^{-1} \text{ centimeters/second at } z = 0.1h; \\ w &= 0.9 \cdot 10^{-1} \text{ centimeters/second at } z = 0.5h; \quad u = 0.7 \text{ centimeters/second} \\ &\text{at } z = 0; \quad z = h; \quad x = L \end{aligned}$$

If  $N_{\max}$  is displaced from the altitude of  $z = \frac{h}{2}$  to the altitude of  $z = \frac{h}{2} + \Delta z$ , we shall assume that the distribution of dust in the vertical directions remains unchanged if  $|\Delta z| = 0.1h$  ( $|\Delta z|$  for other  $z$ 's will be smaller). This will take place during the time of  $\Delta t_1 = 16$  hours.

If the displacement of the lateral boundaries of the cloud in the horizontal direction amounts to  $0.1L$ , then we assume that the distribution of dust in the horizontal direction has likewise remained unchanged. This occurs during the time  $\Delta t_2 = 4$  hours. Consequently, in the course of several hours during the daylight half of the day, when the above-mentioned motions are possible, these motions may be considered stationary when  $N_{\max} \approx 10^3$ , and all the values calculated in the given problem will apply to them.

It can be shown that viscosity alters the distribution of temperature with altitude but does not affect the magnitude of the vertical velocity of air. Therefore, viscosity can be disregarded in an investigation of the vertical motion of air heated by dust.

It is to be expected that with time the dust cloud will be deformed so that the horizontal dimensions of its lower half will decrease and the dust concentration in that half will increase, while, conversely, the horizontal dimensions of its upper half will increase and dust concentration will decrease. Therefore, in the lower half of the cloud, velocities will increase with time, while in its upper half, they will decrease.

In the course of a 24-hour period the air in a cloud at the 30-kilometer altitude is displaced upward several tens of meters when  $N \approx 10^3$ . With an increase in altitude and a decrease in air density, the velocities, and consequently also diurnal displacement of air increase.

With an increase in the dust content of the cloud there is an increase in the vertical velocities in the cloud; therefore, the time during which the processes of motion may be considered stationary decreases.

As can be concluded from a comparison of the calculations made according to the first two schemes, the consideration of horizontal flows diminishes the magnitude of vertical velocity by approximately 5 times.

Let us consider whether the dust concentrations required for the above-described processes are possible in the stratosphere, and what are the quantity and dimensions in which dust may be present in a suspended state in air continuously forming, as it were, a "dust atmosphere".

It can be shown that the lower limit for a dust concentration continually present in the atmosphere is  $10^3$  if the dimension of dust particles is  $10^{-6}$  centimeters. Let us set up these two fundamental postulates: first, particles with a dimension of  $10^{-6}$  centimeters are suspended in the atmosphere below the 80-kilometer level, since here, with regard to them, Stokes' velocity is smaller than the velocity of Brownian motion (both velocities are calculated by taking into account Cunningham's

STAT

correction for gliding); second, the density of dust in the outer portions of the atmosphere cannot be lower than the density of dust in the interplanetary space. From the physical standpoint, both these postulates are entirely substantiated. In general, the 80-kilometer level is distinctive in many ways: this is the level delineating the lower boundary of polar auroras, the second twilight arc, the lower boundary of the E layer of the ionosphere; and this is the level at which the ionization traces of meteorites cease and dust traces begin, etc. Let us note that dust particles cannot be present in suspended state above that level. This conclusion is confirmed as follows: according to meteorological data, the 80-kilometer level is a boundary above which the air density decreases abruptly; noctilucent clouds are never observed above this level.

Let the mean concentration of the dust particles measuring  $10^{-6}$  centimeters in dimension and suspended in the atmosphere below the 80-kilometer level, amount to  $10^3$ .

Then, the mean density of that dust in the atmosphere amounts to  $2 \cdot 10^{-14}$  grams/cubic centimeter (with a density of dust matter amounting to 3 grams/cubic centimeter). The total quantity of dust in the layer in question, with a volume of  $3.7 \cdot 10^{25}$  cubic centimeters, equals  $4.5 \cdot 10^5$  tons.

Let the total diurnal income  $A$  of cosmic matter conveyed by meteorite bodies into the atmosphere remain constant with time. According to the most recent data, it amounts to 6 tons daily. If the duration of the earth's existence amounts to  $3 \cdot 10^9$  years (according to the radiometric method), then the total amount of the meteorite matter which has entered the atmosphere during that time should amount to  $6.6 \cdot 10^{12}$  tons. Then the  $\beta$ -portion, the amount of cosmic matter which did not settle onto the earth's surface, would be no more than  $10^{-7}$  of the total amount.

Let us examine the question of dust density in the 160-80 kilometers layer. Inasmuch as in that layer the velocity of Brownian motion is smaller than Stokes' velocity, with respect to the  $10^{-6}$  centimeter dust particles, these particles subside downward at a velocity of the order of  $10^2$  centimeters per second (at the 100-kilometer altitude, Stokes' velocity is 8 centimeters per second, while at the 120-kilometer STAT

altitude it is 110 centimeters per second). Accordingly, the dust particles will travel through the path from the 160-kilometer level to the 60-kilometer level during a time  $\tau$  of the order of a 24-hour period.

Obviously, the total quantity of dust particles with a dimension of  $10^{-6}$  centimeters in that layer equals

$$\tau A = \beta \cdot 10^6 \text{ grams}$$

and dust density in that layer amounts to  $\beta \cdot 10^{-19}$  grams/cubic centimeter.

It is known that the density of cosmic dust in outer space is of the order of  $10^{-21}$  to  $10^{-26}$  grams per cubic centimeter. Since the density of dust in the earth's atmosphere cannot be of a value smaller than this value, the obtained value of  $\beta$ , equal to  $10^{-7}$ , is the minimum possible for the atmosphere. Correspondingly, our assumed concentration of  $10^3$  particles suspended in the atmosphere appears to be the minimum one. The actual magnitudes of  $\beta$ , and, consequently, of that concentration also, should be much higher.

In the atmosphere the dust may not be distributed uniformly. The deviations from the mean values of such a distribution are bound to be both spatial and temporal. Actually, observations of noctilucent clouds show that the surface brightness of these clouds sometimes changes abruptly and very sharply, which, obviously, indicates a like abruptness of the change in the dust concentration in these clouds. Sometimes even it seems as if a shadow falls on these clouds, and then vanishes - such is the suddenness with which the intensity of their illumination changes. Usually, luminosity of the clouds changes 10 to 15 times within several minutes. But, there exist also more prolonged perturbations in the dust content of the atmosphere.

In 1944, N.N. Kalitin made a survey of the data based on long-term actinometric observations of a number of stations, in order to explain whether an August transparency minimum does actually exist, and whether it might not be related to the showers of the "Perseids". It was found that the minimum does exist, and it occurs simultaneously at all the selected stations, from Pavlovsk to Yakutsk, in which connection its magnitude is of the same order at all stations which although are

STAT

located under various climatic conditions. Hence, it was concluded that the cause of the August transparency minimum is of non-terrestrial origin, but is instead the result of the "Perseid" meteor shower. The extent of the accumulation of cosmic dust is 70 million kilometers, with the absorbing mass not uniformly distributed in that accumulation. The absorption maximum is situated at a distance of 26 million kilometers from the frontal limit of that accumulation, and the second portion of the accumulation is more dense than the first. The earth enters into the dust cloud on 8 August and leaves it on 5 September.

Preliminary processing of data has shown that together with the August minimum there also exists an April minimum, which might be ascribed to the influence of the "Lyrid" meteor shower. As early as in 1925, studies of the annual course of transparency of the atmosphere over Pavlovsk revealed that the transparency in April is lower than might be obtained from the values of the annual course.

These data corroborate the assumption that the earth on its orbit encounters dust accumulations of various dimensions and various concentrations.

Thus, it may be expected that the conditions required for the above-examined processes of the vertical motion of air are always present in the stratosphere between the 20- and 80-kilometer levels, where there are sufficient quantities of dust and the vertical velocities reach a considerable magnitude.

The intermixing of air and local cyclonic systems reach their maximum intensity during the time when the atmosphere is invaded by large accumulations of cosmic dust.

In concluding let us evaluate the possible order of the diurnal variations of air temperature in the stratosphere caused by the thermal effect of its dust content. For this purpose, let us assume that the air layers are so uniformly dust-filled in the horizontal direction that the formation of vertical currents is not possible.

Let us examine the equation of heat influx related, as previously, to a unit mass of air occupying a specific volume  $v$ :

$$\pi r^2 \rho_0 v N = c_p \frac{dT}{dt} - A v \frac{dp}{dt}$$



Since in the given case the volume of air expands with heating while not being displaced, therefore

$$\frac{dT}{dt} = \frac{\partial T}{\partial t} \text{ and } \frac{\partial p}{\partial t} = 0.$$

And consequently,

$$\ln \frac{T}{T_0} = \frac{\pi^2 IR}{c_p} N(t - t_0).$$

Let us calculate the change in temperature during one day.

Let the time from sunrise to sunset  $t - t_0$  equal 12 hours, and let mean concentration of dust be  $N = 10^3$  ( $10^2$  in the upper half of the stratosphere and  $10^4$  in the lower half thereof).

At the 30-kilometer level:  $T_0 = 230^\circ$ ;  $p_0 = 10$  millibars; and  $\Delta T = 13^\circ$ .

At the 75-kilometer level:  $T_0 = 275^\circ$ ;  $p_0 = 6.4 \cdot 10^{-2}$  millibars; and  $\Delta T = 24.5^\circ$ .

Thus, the daily course of temperature should increase with altitude. In the inversion layers, e.g., in the tropopause, the dust content should deviate from mean conditions, and the daily course should be correspondingly greater than in the upper layers next to the inversion.

In this way, the intermixing of air in the stratosphere, being the result of the afore-surveyed vertical macro- and micro-motions, should impede the establishment of a diffusion equilibrium up to the 80-kilometer altitude.

The intermixing of air with an individual lapse rate of  $\frac{\partial t}{\partial z} \approx 0$  should contribute to the establishment of an isothermal temperature profile in the stratosphere, just the same as the adiabatic displacements of air in the troposphere lead to a decrease of temperature with altitude.

If the hypothesis of the radiation equilibrium of the stratosphere should give relatively satisfactory results, then this may be explained by the circumstance that, in the problems to which it is applied (e.g., the determination of the thermal regime of the stratosphere under conditions averaged for long intervals of time and for extensive spatial regions), the radiative processes are of essential importance.

STAT

Actually the state of radiation equilibrium should be considered the primary state of the atmosphere. But in being hydrostatically unstable (as revealed already by Emden's calculations), this equilibrium is transformed into a convective equilibrium, in the troposphere, owing to the perturbing influence of the earth's surface. Here, the radiation equilibrium itself generates turbulent and convective heat transfer. Such a transformation does not extend to the stratosphere.

In studies of the stratosphere it is necessary to consider, beside the presence of non-radiation heat influxes therein, also the circumstance that the stratosphere is not a region totally isolated from the troposphere. The physical processes above the tropopause are to a major extent affected by the state of the lower layers. The tropopause is not a continuous surface of discontinuity. The break in the tropopause in the middle latitudes, in the area of the jet streams, insures an intensive exchange of tropospheric and stratospheric air masses. There are reasons for assuming that the tropospheric dynamic perturbations (cyclones and anticyclones) cause similar perturbations above the tropopause [32,81].

The concept that the weather-forming processes, originating primarily from the effect of the earth's surface (general circulation and pressure disturbances - cyclones and anticyclones) develop only within the lower few kilometers of the atmosphere (troposphere) should apparently be considered obsolete and not true. This concept developed as a result of the limited possibilities for experimental investigations of the upper layers of the atmosphere.

The low density of the air in the upper layers is another argument in favor of the possibility of their being susceptible to the effect of the processes occurring in the troposphere, since the energy which must be transmitted upward by a certain mechanism, is not significant.

It should be expected that the more intensive the processes in the troposphere, the larger the area of the earth's surface that they occupy, and the longer their duration, the greater is their influence on the upper layers and the higher they must extend.

Let us turn to the experimental data corroborating the foregoing representations. First, there are the statistically processed observational data on temperature and pressure at various levels in cyclones and anticyclones. P.N. Tverskoy cites data on temperature distribution in cyclones and anticyclones up to the tropopause level. A.B. Kalinovskiy provides the distribution of pressure and temperature in cyclones and anticyclones up to an altitude of 20 kilometers. The limitation of observational data to the 20-kilometer level is due to the fact that this level is the mean ceiling of radiosondes. If it were possible to obtain information on temperature and pressure above the tropospheric cyclones and anticyclones, at higher levels, it is entirely probable that this would serve to demonstrate the susceptibility of these higher levels to the effect of dynamic perturbations in the troposphere.

Secondly, we know of various phenomena making it possible to explain the mechanism of the connection between the tropospheric cyclones and anticyclones and the upper layers of the atmosphere. It is becoming possible to show the predominant role of tropospheric processes in the overall development of a perturbation. A separate study [32] is concerned with the explanation of this mechanism. All the necessary experimental data will be cited below insofar as necessary.

With respect to tropospheric cyclones the following is known: Basically, these two stages may be distinguished in the development of a cyclone: (1) the wave stage - the cyclone has a warm sector, and its intensification occurs chiefly owing to advective causes; (2) the vortex stage - the beginning of this stage may be related to the beginning of the occlusion of the cyclone; during this stage the cyclone deepens owing to the dynamic processes associated with the upward displacement of warm air and the release of moist-instability energy.

The vertical thickness of a cyclone depends on the stage of its development, and it increases with the age of the cyclone. During the frontal-wave stage the baric depression is restricted to the lowest kilometers of the troposphere. In proportion with increasing vorticity and deepening of the cyclone, its vertical thickness (towards the time of occlusion) reaches the lower layers of the stratosphere.

STAT

In the occlusion stage, the perturbation is already so well expressed in the upper troposphere that closed cyclonic lines of flow and, consequently, closed cyclonic isobars, are present at the 6-7 kilometer level; the depression center at that level nearly coincides with the lower center of perturbation, i.e., the inclination of the cyclone axis becomes steeper. Occlusion occurs with a sufficiently pronounced pressure drop at the earth's surface. During this stage the cyclone is slightly mobile. In a cyclone, the tropopause and the lower stratosphere, as well, subside downward in order to reestablish the static equilibrium violated by the counter-gradient displacement of air from the deepening cyclone at the 5 to 8 kilometer levels. The altitude of the tropopause decreases in proportion with the development of the cyclone and at the moment of the occlusion, or following that instant, it reaches especially low values. At first, this decrease occurs owing to the meridional advection of the lower tropopause from the north, while during the second stage there occurs a dynamic suction of the tropopause.

By proceeding from the data on the correlation coefficient between pressure at various levels and the altitude of the tropopause  $H$ , it may be assumed that tropospheric processes exert a stronger influence than stratospheric processes at the altitude of the tropopause: the correlation coefficient between  $H$  and  $P_{10}$  amounts to 0.64, and between  $H$  and  $P_5$ , to 0.71; the maximum correlation exists between  $H$  and  $P_5$ .

In the vortex stage, the temperature of the troposphere decreases, while that of the lower stratosphere increases.

The most intense cyclones are already occluded to a major extent and therefore, may be regarded as cold tropospheric vortices.

The dynamic processes developing in an anticyclone, take place in an opposite direction: the vertical velocities are downward-directed, pressure increases, and the tropopause ascends.

Let us set up the problem: let us explain the manner in which the values of meteorological elements at various levels in a vortex cyclone (or anticyclone) vary

with time, if their variation with time at the earth's surface is known. In other words, let us attempt to obtain theoretically the variation in the state of the atmosphere with time at various altitudes on the basis of given changes in that state at the earth's surface, for the case of a vortex cyclone. Obviously, with a proper solution of the task, the results so obtained should approximate the data cited by P.N. Tverskoy, A.B. Kalinovskiy, and others.

Let us examine the set of the equations of hydro- and thermodynamics proceeding from the following representations concerning the principal features of a cyclone in the vortex stage of its development: its isobars are circular, the cyclone is stationary, its axis is vertical, and the process is nonstationary and occurs adiabatically.

Let us write the equations of motion for a cylindrical coordinate system:

$$\begin{aligned} \frac{\partial v_r}{\partial t} + v_r \frac{\partial v_r}{\partial r} - \frac{v_\varphi^2}{r} + \frac{w}{H} \frac{\partial v_r}{\partial \zeta} &= -\frac{1}{\rho} \frac{\partial p}{\partial r} + l v_\varphi, \\ \frac{\partial v_\varphi}{\partial t} + v_r \frac{\partial v_\varphi}{\partial r} + \frac{v_r v_\varphi}{r} + \frac{w}{H} \frac{\partial v_\varphi}{\partial \zeta} &= -l v_r, \\ -\frac{1}{\rho H} \frac{\partial p}{\partial \zeta} - g &= 0; \end{aligned}$$

equation of continuity

$$\frac{\partial v_r}{\partial r} + \frac{v_r}{r} + \frac{1}{H} \frac{\partial w}{\partial \zeta} = 0;$$

equation of heat influx

$$\frac{\partial \theta}{\partial t} + v_r \frac{\partial \theta}{\partial r} + \frac{w}{H} \frac{\partial \theta}{\partial \zeta} + \Gamma w - \frac{A}{c_p} \left( v_r \frac{\partial p}{\partial r} + \frac{\partial p}{\partial t} \right) = 0.$$

In the above formulas  $\zeta = \frac{z}{H}$  is dimensionless vertical coordinate ( $H$  is thickness of the layer in question, i.e., altitude of the tropopause);  $v_r$ ,  $v_\varphi$  and  $w$  are the velocity components for the radius, tangential to the isobar, and vertical, respectively;  $\theta$  is the deviation of temperature from its initial non perturbed value;  $\Gamma = \gamma_a + \frac{\partial T}{\partial z}$  (where  $\gamma_a$  is the adiabatic lapse rate and  $T$  is temperature of the undisturbed atmosphere);  $l$  is Coriolis parameter; and  $t$  is time.

In order to integrate to the end this set of equations, let us give vertical STAT

with time, if their variation with time at the earth's surface is known. In other words, let us attempt to obtain theoretically the variation in the state of the atmosphere with time at various altitudes on the basis of given changes in that state at the earth's surface, for the case of a vortex cyclone. Obviously, with a proper solution of the task, the results so obtained should approximate the data cited by P.N. Tverskiy, A.B. Kalinovskiy, and others.

Let us examine the set of the equations of hydro- and thermodynamics proceeding from the following representations concerning the principal features of a cyclone in the vortex stage of its development: its isobars are circular, the cyclone is stationary, its axis is vertical, and the process is nonstationary and occurs adiabatically.

Let us write the equations of motion for a cylindrical coordinate system:

$$\begin{aligned} \frac{\partial v_r}{\partial t} + v_r \frac{\partial v_r}{\partial r} - \frac{v_\varphi^2}{r} + \frac{w}{H} \frac{\partial v_r}{\partial \zeta} &= -\frac{1}{\rho} \frac{\partial p}{\partial r} + l v_\varphi, \\ \frac{\partial v_\varphi}{\partial t} + v_r \frac{\partial v_\varphi}{\partial r} + \frac{v_r v_\varphi}{r} + \frac{w}{H} \frac{\partial v_\varphi}{\partial \zeta} &= -l v_r, \\ -\frac{1}{\rho H} \frac{\partial p}{\partial \zeta} - g &= 0; \end{aligned}$$

equation of continuity

$$\frac{\partial v_r}{\partial r} + \frac{v_r}{r} + \frac{1}{H} \frac{\partial w}{\partial \zeta} = 0;$$

equation of heat influx

$$\frac{\partial \theta}{\partial t} + v_r \frac{\partial \theta}{\partial r} + \frac{w}{H} \frac{\partial \theta}{\partial \zeta} + \Gamma w - \frac{A}{c_p} \left( v_r \frac{\partial p}{\partial r} + \frac{\partial p}{\partial t} \right) = 0.$$

In the above formulas  $\zeta = \frac{z}{H}$  is dimensionless vertical coordinate (H is thickness of the layer in question, i.e., altitude of the tropopause);  $v_r$ ,  $v_\varphi$  and  $w$  are the velocity components for the radius, tangential to the isobar, and vertical, respectively;  $\theta$  is the deviation of temperature from its initial non perturbed value;  $\Gamma = \gamma_a + \frac{\partial T}{\partial z}$  (where  $\gamma_a$  is the adiabatic lapse rate and T is temperature of the undisturbed atmosphere);  $l$  is Coriolis parameter; and t is time.

In order to integrate to the end this set of equations, let us give vertical STAT

velocity  $w$  in this form:

$$w = \alpha \zeta (1 - \alpha \zeta) f(t),$$

where  $f(t)$  — is arbitrary function of time.

Our assumed  $\zeta$  -dependence of  $w$  may be thus physically substantiated: at the earth's surface  $w$  should equal zero, above that surface, it has positive values, but in the tropopause  $w$  is negative, inasmuch as the tropopause over the cyclone tends to subside. Therefore, it may be assumed that in the layer below, directly contiguous to the tropopause, vortical velocity  $w$  is also negative. Consequently, in the upper troposphere,  $w$  passes through zero. This is the condition for determining the  $\alpha$  coefficient, which varies within fairly narrow limits, inasmuch as the value of  $\zeta$  at which  $w$  reverts to zero is in every case greater than 0.5 and smaller than unity.

Inasmuch as with regard to the  $r$ -dependence of  $w$  it may be merely stated that  $w$  reverts to zero at some distance from the center of the cyclone, the examination of this dependence would require the introduction of new parameters with arbitrarily selected quantitative values. This would not improve the obtained results, and it would merely complicate the calculations; consequently we shall ignore them here.

In its form assumed here,  $w$  reflects satisfactorily the conditions in the central area of the cyclone where  $w$  may be regarded as being independent of  $r$ .

The derivation of the above set of equations is provided in [32]. The formulas obtained in [32] were used to make a calculation of the distribution of temperature and wind at various levels in the atmosphere over a cyclone, under the following conditions:

Given: baric temperature and wind fields at the earth's surface at the moments of  $t = 0$  and  $t = t_k$  in the center of cyclone  $r = 0$  and at a distance  $r_k$  from that center:

$$t = 0:$$

$$r = 0 \quad p_0 = 966 \text{ мб}, \quad \theta = 0.$$

$$r = r_k \quad p_1 = 967,35 \text{ мб}, \quad \theta = 0 \left| \frac{v_r}{v_\varphi} \right| = 8,5 \cdot 10^{-2}.$$

$$t = t_k:$$

$$r = 0 \quad p_2 = 961 \text{ мб}, \quad \theta = 0.$$

$$r = r_k \quad p_3 = 962,35 \text{ мб}, \quad \theta = -0,5^\circ \left| \frac{v_r}{v_\varphi} \right| = 1,5 \cdot 10^{-1}.$$

Furthermore, when  $t = 0$ , the temperature at the earth's surface is  $T_0 = 300^\circ$ , and at the tropopause level,  $T_H = 240^\circ$  ( $H = 6$  kilometers); and  $t_k = 6$  hours (duration of vortex stage), while  $r_k = 200$  kilometers.

The results of the calculations are compiled in Table 3. In this Table,  $\Delta_r p$  denotes the variability of pressure with time at various levels, and  $\Delta_p$  denotes the horizontal pressure difference at point  $r_k$  and in the center of the cyclone at various levels, at the initial and final moments of time.

Table 3

## Distribution of Pressure and Temperature in a Cyclone

(The numerator contains data pertaining to the  $t = 0$  moment of time; the denominator, data pertaining to the  $t = t_k$  moment of time)

z KM	r = 0			r = r <sub>k</sub>		
	$\Delta_r p$	p	$\Delta_p$	$\Delta_r p$	p	$\delta$
0	-5,00	966,00	+1,35	-5,00	967,35	0
		961,00	+1,35		962,35	-0,40
1	-4,64	860,56	+1,16	-3,92	861,72	0
		855,92	+1,88		857,80	-3,38
2	-4,24	763,52	+1,13	-4,23	764,65	0
		759,28	+1,14		760,42	-3,98
3	-3,56	674,44	+1,00	-4,38	675,44	0
		670,88	+0,18		671,06	-3,18
4	-3,56	593,04	+0,85	-4,38	593,89	0
		589,48	+0,03		589,51	-2,40
5	-3,11	518,78	+0,81	-4,39	519,59	0
		515,67	-0,47		515,20	-0,03
6	-2,93	451,35	+0,74	-4,31	452,09	0
		448,42	-0,64		447,78	+4,79

Let us compare the above results with experimental data.

Temperature. P.N. Tverskoy's data: Selected data on soundings on the days of explicitly expressed cyclones and anticyclones; the former, in 46 cases, and the latter, in 39 cases. The selected observations cover the period from December 1903 to December 1915.

The results of the processing of the selected data, illustrated in Fig. 5, show



STAT



the temperature distribution in cyclones and anticyclones and the mean temperature distribution for the four seasons and for the year as a whole. Near the earth's surface the temperature in the cyclones exceeds the temperature in the anticyclones, but, beginning from the altitude of one kilometer, this relation is reversed, while at altitudes above 8.5 kilometers the cyclone temperature again becomes higher than the anticyclone temperature. The difference between the temperatures in the cyclone and in the anticyclone increases at altitudes between 1.0 and 2.5 kilometers, after which it remains nearly constant up to the altitude of 7.0 kilometers, varying within the limits of approximately 3 degrees. Between altitudes from 7.0 to 8.5 kilometers this difference abruptly decreases, and above the 8.5-kilometer altitude it again increases, reaching a value of 6.0 degrees at the 12-kilometer altitude. The course of the curves in the lowest kilometer is explained by the influence of surface conditions.

A.B. Kalinovskiy's Data: The values of the algebraic variability in temperature are of opposite sign in the troposphere as contrasted with the stratosphere (Fig. 6). The change in sign occurs under the tropopause at the altitude of 9.5 kilometers. The maximum of the variability is observed at the altitudes from 6-8 kilometers. The maximum of the variability of opposite sign is observed at the altitude of 12 kilometers, above which its decrease ensues.

Hewson's (E.W.) Data: The mean temperature curves in cyclones and anticyclones over England exhibit the same character as P.N. Tverskoy's curves.

The theoretical curve of temperature variability at various levels, plotted on the basis of the data in Table 3, is very similar to the above-cited experimental curves. The sign of variability in the free atmosphere is negative. In the middle troposphere, variability is very small. The change in sign takes place under the tropopause. The absolute value of the variability, 3-4 degrees, is close to values obtained by aerological observations. The theoretical point of the reversal of sign is lower than the experimentally verified point owing to the lower position of the tropopause assumed in the cited example.

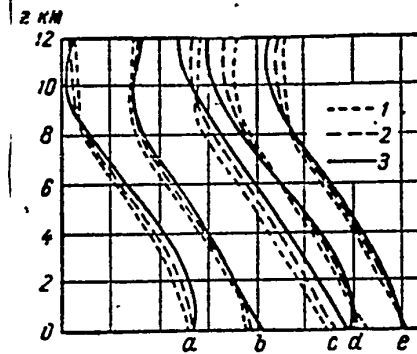


Fig. 5. Vertical Temperature Profile

1. In cyclone; 2. In undisturbed atmosphere; 3. In anticyclone (a - winter; b - spring; c - summer; d - autumn; e - year). One gradation on the scale equals 30 degrees.

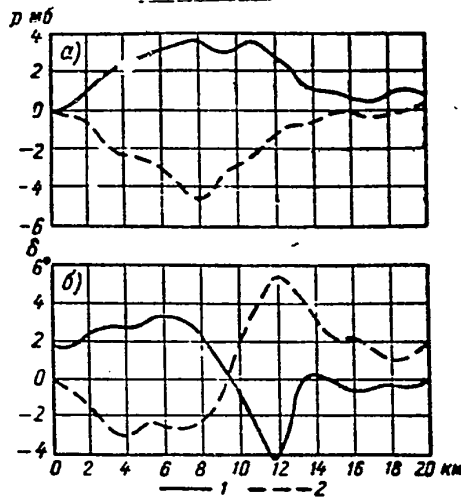


Fig. 6. Algebraic Variability of Pressure (a) and Temperature (b)

1.  $\Delta H_c > 0, \Delta T_c < 0$ ;      2.  $\Delta H_c < 0, \Delta T_c > 0$

$H_c$  and  $T_c$  represent the altitude and temperature of the tropopause,

respectively.

Pressure. According to A.B. Kalinovskiy's data, pressure variability initially increases with altitude, but above 8 kilometers it begins to decrease. This decrease has been traced up to 20 kilometers, in which connection the variabilities in a

STAT

cyclone are of a negative sign, and in an anticyclone, of a positive sign.

According to Hewson, pressure variability with altitude decreases uniformly over England: at the earth's surface, it is 10 millibars, at the 8-kilometer altitude, 8 millibars, at the 12-kilometer altitude, 4 millibars, 16-kilometer, 2 millibars, and 20-kilometer, 2 millibars (Fig. 7).

According to Khromov, the interdiurnal pressure variability in cyclones also decreases with altitude: at the earth's surface, it is 5.1 millibars, at the 8-kilometer altitude, 4.7 millibars, and at the 12-kilometer altitude, 3.5 millibars.

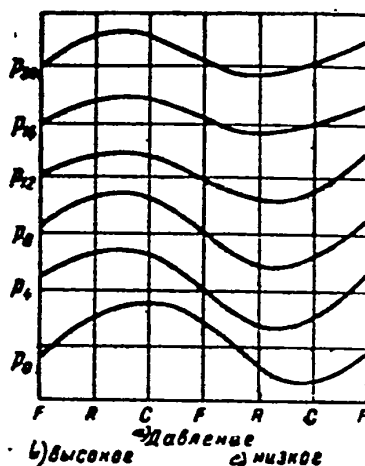


Fig. 7. Change in Pressure at Various Altitudes (From 0 to 20 Kilometers) During the Passage of High- and Low-Pressure Systems

F - forward, C - central, and R - rear portions of pressure systems.

a. Pressure; b. High; c. Low.

According to theoretical data, variability has a negative sign at all altitudes in a cyclone. It uniformly decreases with altitude. Its absolute values likewise approximate the values given by experimental data. In a comparison it is necessary to consider that, e.g., the surface variability calculated by Hewson is twice as large as that assumed for the theoretical calculation. Therefore, this ratio is maintained at all other levels.

It is interesting that the vertical course of the variability of temperature and pressure is independent of the time intervals to which these meteorological

elements are related (theoretical variabilities were computed for 6-hour intervals, whereas the variabilities taken in aerological and other observations are usually related to 24-hour intervals). Here probably, the essential circumstance is that the variations in meteorological elements associated with a change in the synoptic situation, as pointed out by Ye. S. Selezneva, occur mostly during short time intervals and then they gradually increase.

With regard to the other elements, the following should be noted: The order of the computed vertical velocity corresponds with the actually observed value. The computed values of  $w$  for the troposphere are of the order of several centimeters per second.

The radial components of the velocity for the lower layer is directed toward the center. In the upper troposphere, it is directed from the center, with the absolute value of the outflow velocity exceeding that of the inflow velocity. Such a profile of  $v_r$  is conditioned by the given profile of  $w$ . Both profiles reflect very closely the actual directions of the flows in the vortical cyclone. Inasmuch as the outflowing mass of air exceeds the inflowing mass, an intensification of the cyclone occurs.

The tropopause displacement is  $\Delta H = 0.54$  kilometers. If we assume a value of  $a$  or, which amounts to the same thing, of  $w$ , two or three times greater, then the displacement will amount to 1.0-1.5 kilometers, which is close to actual values. (vertical velocities of the order of 5-10 centimeters/second are entirely realistic for a cyclone).

From Figs. 6 and 7 it is evident that both the cyclonic and the anticyclonic perturbations extend from the troposphere into the entire lower stratosphere. The perturbation in the lower stratosphere is of the same nature as that in the troposphere: the uniform decrease in pressure is also observed in the stratosphere, the temperature curves in the troposphere and stratosphere are of an identical character, and the uniform increase in the absolute values of the temperature variability is replaced by a similar uniform decrease in these values.

STAT

Inasmuch as the temperature variabilities below and above the tropopause, respectively, are opposite in sign, it may be concluded that the dynamic perturbations in the troposphere and in the lower stratosphere are likewise opposite in sign. The lower stratosphere over a cyclone is occupied by a vortex disturbance within which there occur vertical motions of air, extending from the tropopause to the maximum altitude of observations (20 kilometers), but, unlike in the troposphere, directed downward rather than upward. Therefore, calculations based on the afore-given scheme of formulas may be also applied to perturbations in the lower stratosphere. The results of such calculations are given in Table 4.

Table 4

Distribution of Pressure and Temperature in an Anticyclone

(see explanatory notes in Table 3).

$t = 0$

$t = t_k$

$w_{max} = -5$  centimeters/sec

$\xi = 0$

$v_r \dots 1.67$  meters/sec     $2.05$  meters/sec

$v_\phi \dots 9.84$  " "     $-1.71$  " "

z km	r=0			r=r <sub>k</sub>		
	$\Delta_r p$	p	$\Delta_r p$	$\Delta_r p$	p	$\theta$
6	-2.93	451.35	+0.74	-4.31	452.09	0
		448.42	-0.64		447.78	4.79
7	-2.86	391.77	-0.31	-4.12	391.46	0
		388.91	-1.57		387.34	8.40
9	-2.05	294.73	-0.13	-2.62	294.60	0
		292.68	-0.56		291.92	13.5
12.5	-1.25	179.18	-0.08	-1.17	179.10	0
		177.93	0.00		177.93	14.3
16	-0.700	108.48	-0.015	-0.425	108.465	0
		107.78	+0.260		108.040	11.4
18	-0.532	81.958	-0.014	-0.197	81.944	0
		81.426	+0.321		81.747	4.79
19	-0.499	71.092	-0.009	-0.078	71.083	0
		70.593	+0.402		71.005	0.7

The thus obtained temperature deviations  $\theta$  initially increase with altitude and reach at the 12.5-kilometer level values exceeding 2-3 times the normal temperature deviations in the troposphere, and then decrease from that level upward. They are



positive in sign.

According to experimental data, the deviations of temperature from mean values over a cyclone in the lower stratosphere are positive at all altitudes. The change in the obtained temperature deviations with altitude agrees satisfactorily with the course of the temperature curve plotted by Kalinovskiy.

In their order of magnitude, the computed deviations likewise approximate the experimental deviations.

Many investigators note that the temperature fluctuations in the lower stratosphere over a cyclone are considerably greater than at the earth's surface. This obviously, is a characteristic feature of vortex cyclones. The calculations also give this peculiarity.

The computed course of pressure variabilities also corresponds to the actually observed course. Pressure variability uniformly decreases with altitude. In their order of magnitude, the computed and the actually observed pressure variabilities agree satisfactorily.

Such an agreement between the computed and actually observed data cannot be considered as fortuitous. The calculations were made for the average cyclone, with typical characteristics, but not for any specific cyclone. Their results were compared also with the mean statistical data of the observations. Accordingly, it is concluded that the theoretical model of a nonstationary cyclone (anticyclone) was satisfactory and reflected with sufficient accuracy the processes actually occurring in the atmosphere. Therefore it should be assumed that the vertical motions and the directly related radial motions are, with regard to the vortex cyclone, of a dominant importance, determining the development of the process as a whole. Above a tropospheric vortex perturbation there develops, in the lower stratosphere, a vortex perturbation that is opposite in sign and, correspondingly also, the vertical motions in the troposphere and in the lower stratosphere, respectively, are opposite in direction. The energy of the perturbation is transmitted upward as a result of the effect of dynamic processes in the troposphere in the pressure and thermal fields

at higher levels, so that as a result, horizontal and vertical flows develop.

With regard to the layers above the 20-kilometer level, experimental data similar to the above are not available. But this, of course, is no reason for concluding that perturbations caused, as in the lower stratosphere, by the effect of tropospheric processes, cannot exist at these altitudes.

Likewise, it cannot be concluded from the decrease of the variability of temperature and pressure with altitude in the lower stratosphere that dynamic perturbations should attenuate with altitude and not be transmitted higher. In the upper troposphere, temperature variability also decreases with altitude and passes through a zero point but, this notwithstanding, such variability occurs again in the lower stratosphere, where in absolute value it even exceeds the tropospheric values.

The relative value of the pressure variability owing to the decrease of pressure with altitude, decreases more gradually than the absolute value. The horizontal pressure gradient is important in the development of perturbations, but it also may pass through a zero point, e.g., in the lower stratosphere directly above the tropopause, and then again attain an appreciable value.

A graphic example of the shift in the sign of dynamic perturbations is shown in Fig. 8, taken from [81], which illustrates the pressure fields at the earth's surface and at the tropopause level on 17 May 1949 for Western Europe: over the cyclone in the troposphere an anticyclone is found in the lower stratosphere.

There are reasons to assume that the effect of tropospheric dynamic perturbations extends above the 20-kilometer level because many data indicate the existence of a relationship between the various phenomena in the upper layers of the atmosphere and between tropospheric cyclones and anticyclones. Let us cite some of these reasons:

1. The amount of ozone exceeds considerably its mean values over a cyclone and is considerably below the mean over an anticyclone.

2. The nacreous clouds observed in the layer from 22 to 27 kilometers are most often accompanied by intense cyclones. Shtermer [1] assumes that such clouds may be

a characteristic feature of the stratosphere over a cyclone; however, they are usually not visible owing to cloudiness accompanying the cyclone in the troposphere.

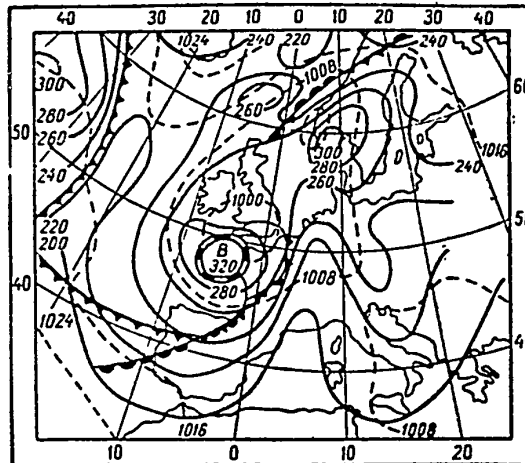


Fig. 8 Isobars at the Tropopause (300 millibars) on 17 May 1949.

(Pressure field at the earth's surface denoted by broken lines)

3. Night observations of the strength of radio reception may be used to conclude that the ion concentration of the E layer is considerably increased over a cyclone and reduced over an anticyclone.

4. The ion concentration in the F layer on "frontal days", i.e., days with cyclonic type of weather, is lower than on ordinary days.

5. The "continental" effect: the ion concentration in the F layer over Siberia (Tomsk) in winter, when a stationary anticyclone is present, is higher than over the European portion of the USSR (Moscow).

The above-enumerated phenomena lead to the assumption that many processes in the upper atmosphere develop simultaneously with cyclonic and anticyclonic activity in the troposphere. It is difficult to conceive that all these phenomena should not be directly interrelated, that there may exist some differing causes exerting a simultaneous effect on all layers and causing in these layers mutually independent variations corresponding to the ones described above. It is more natural to assume that between the various layers of the atmosphere there exists a close thermal and dynamic relationship owing to which a perturbation in a certain atmospheric layer

STAT



exerts an influence on the state of other layers.

All the above-enumerated phenomena prove to be readily explained if it is assumed that in the upper layers - the middle and upper stratosphere and the ionosphere - there are dynamic perturbations of the same nature and that the same alternative sequence of positive and negative signs as in the two first layers - the troposphere and the lower stratosphere exists. Such an assumption appears to be possible not only because it explains the diverse observational data but also because in the upper layers conditions necessary for the origin of such perturbations exist -- i.e., layers of temperature inversion similar to the tropopause. The middle stratosphere is separated from the upper stratosphere by a layer of a pronounced temperature inversion, with the maximum temperature in that layer found at the level of 50-55 kilometers. In the E layer, with which the ionosphere begins, at altitudes of 80 to 100 kilometers, another temperature inversion is found. There are certain reasons for assuming that above 80 - 100 kilometers temperature decreases with altitude and reaches its minimum values at 200 kilometers, but in the F layer - in the upper boundary of the ionosphere, it again begins to increase.

The increase of air temperature in the middle stratosphere is associated with radiative processes - an increase in the absorptivity of the atmosphere in the ozone layer. As for the increase of air temperature in the ionospheric layers, it is related, on the one hand, also to an increase in the absorptivity of the atmosphere with respect to ultraviolet radiation of the sun, and, on the other hand, to the direct increase in the kinetic energy of air molecules in their collisions with the corpuscular particles emitted by the sun.

Inasmuch as the vortex perturbations opposite in sign were formed in the first two layers (i.e., troposphere and lower stratosphere) separated from each other by inversions - the question arises why should not such perturbations likewise be present in the still higher layers, which are likewise separated by inversions from the lower stratosphere and from each other.

Thus, let us assume that a cyclone while developing in the troposphere and

STAT

while rising to the tropopause level exerts an effect not only on the entire lower stratosphere, where it provokes an anticyclonic disturbance, but also on the still higher layers, by provoking cyclonic disturbances in the middle stratosphere and the ionosphere, and anticyclonic disturbances in the upper stratosphere. When an anticyclone develops in the troposphere, the signs of the perturbations in the various layers would then be correspondingly reversed.

In regions with cyclonic perturbations there must be sources of instability energy so as to make possible the development of ascending motions of air in these areas. In the middle stratosphere, the source of instability energy may be in the form of cosmic dust, and in the ionosphere, corpuscular and ultraviolet radiation of the sun. Let us explain the above-indicated phenomena by means of a here proposed scheme of perturbations. Let us examine the case of a cyclone in the troposphere.

The horizontal flows at the 20 to 25 kilometer - levels, directed to the interior of the perturbation region must bring in ozone-rich air. As a consequence there should occur an increase in the ozone content in the area over the cyclone.

The vertical flows directed upward in the 20 to 30 kilometer layer should facilitate the condensation of small quantities of water vapor, which leads to the formation of nacreous clouds in that layer. Such an explanation also sheds light on the circumstance why nacreous clouds accompany only very strong cyclones, i.e., cyclones extending upward to a great distance.

The horizontal fluxes directed towards the interior of the disturbed region at the altitude of the E layer should lead to an increase in air density and, consequently, also to a concentration of ions in that layer in the area over the cyclone. A reversed situation should take place over an anticyclone. It is very important that the increase in the ion concentration in the E layer over the cyclonic area has been recorded at night and, therefore, it may be caused only by dynamic principles. In the absence of solar light, the ordinary physical-chemical processes can result only in a reduction of the number of ions.

The horizontal flows directed outward from the disturbance region at the altitude

of the F layer should carry away ion-rich air from that area. Therefore, on "frontal" days the ion concentration in the F layer decreases.

An opposite process over an anticyclone, gives a "continental" effect.

Let us cite still two more examples of the relationship between weather and ionospheric characteristics, described in [27a]. The weather in Australia is, according to meteorological observations, determined by a fairly regular sequence of anticyclones crossing from the west to the east. In the region between two consecutive anticyclones there is a zone in which the air characteristics change and, ultimately, there forms a cyclonic depression. During 19 months of observations at two stations located along the trajectory of the anticyclone chain, the ionization of the F layer was 6 to 11 percent above its normal values, and a tendency towards a decrease in ionization was observed under "frontal weather conditions". Another case of correlation, observed on the Zikkawei Observatory in Shanghai, has an analogous character. Observations revealed the existence of a relationship between the manifestation of an echo from the E, F<sub>1</sub> and F<sub>2</sub> layers and the subsequent behavior of the three principal air masses - the polar, maritime and equatorial air masses. Observations showed that the occurrence of an echo from the F<sub>1</sub> layer was followed by the appearance of polar (Siberian) air over the station, while the occurrence of echo from the F<sub>2</sub> layer indicated that an arrival of tropical air should be expected or if it had already arrived, its conservation was indicated. If, however, an echo from the E layer occurred it was subsequently followed by the advent of masses of maritime (Pacific-Ocean) air over the region of the station or, if that air had already been present over the region, by its conservation. If the detection of an E-layer echo was made in the presence of a typhoon at a distance of approximately 200 miles on the weather chart, it could be predicted that the air masses advancing from the sea will bring the cyclone to a dangerous proximity to the station. According to the author, these relationships were so definite that they could be used for a sufficiently reliable forecasting of the features of future weather.

From the standpoint of the expounded scheme of relationships among the various

layers, all the above echo relationships are readily explainable. According to the scheme, the  $\text{FO}_2$  concentration in the F layer increases over tropospheric anticyclones and decreases over cyclones; the reverse occurs with regard to the E layer.

Thus, the changes in the state of the upper-air layers observed during cyclonic or anticyclonic weather obtain a simple explanation. Inasmuch as all the above-enumerated phenomena fit into a single scheme, this too can serve as an argument in favor of its possibility.

It should be noted that as long ago as in 1933 E. Palmén, on the basis of processed aerological data, came to the conclusion that over a cyclone in the lower stratosphere there should exist a downward-directed flow of air; it is true, no quantitative theory was provided for these phenomena.

In the problem of the relationship between ozone and the troposphere, the latter must be the primary link. Ozone as the prime cause may be used for a qualitative explanation of the observed close correlation between ozone concentration and potential temperature in the lower stratosphere at the 18-kilometer level. But in quantitative evaluations there develop insurmountable contradictions: the increased concentrations of ozone must be maintained for too long (16 days) a period for bringing about the necessary change in temperature in the given air mass by emission from ozone. Consequently, only the processes in the troposphere may cause both a change in the ozone content over cyclones and anticyclones and also dynamic fluctuations of temperature in the lower stratosphere. From the circumstance that the surface pressure is more closely correlated with stratospheric air density than with ozone, it may be concluded that tropospheric processes exert a direct effect on air density in the stratosphere, while their influence on ozone is secondary and is realized through this intermediate link. In accordance with this empirical fact, in the scheme being expounded the dynamic effect is directly reflected in the air density in the lower stratosphere; and the change in the amount of ozone is the secondary effect.

The changes in ozone concentration are slightly out of phase, i.e., later in time compared with the changes in surface pressure. This is as it should be, considering

that the perturbation extends upward, from the troposphere, and not in the opposite direction.

Inasmuch as the horizontal flows of air usually predominate and, owing to the general circulation, the air masses in various layers flow in different directions and with various velocities, the actual distribution of the motions in the dynamic perturbations will be much more complex than in the afore-surveyed scheme of a nonstationary cyclone.

Let us sum up the foregoing statements. The constructed dynamic model of a nonstationary cyclone (anticyclone) has made it possible to calculate the distribution of pressure, temperature and wind at various altitudes and the changes in these elements with time. Calculations have given a satisfactory agreement between theoretical and experimental data. It was found possible to show that over a tropospheric dynamic perturbation (cyclone or anticyclone) there exists, in the lower stratosphere, a dynamic perturbation that is opposite in sign (anticyclone or cyclone).

Thus, there was also proposed a possible scheme of dynamic disturbances in the upper-air layers (up to the altitude of 200-300 kilometers), verified by various observation data. This scheme explains the mechanism of the action of tropospheric dynamic processes in the upper layers.

Further, it should be assumed that the disturbances, according to this scheme, may be transmitted not only upward from below but also in the opposite direction.

Actually, let, e.g., supplementary warming take place at the altitude of 50-60 kilometers (layer D in the ionosphere). This warming will lead to an increase in the intensity of the anticyclonic perturbation at that altitude. In view of the continuity of horizontal flows at the boundaries between the layers of the scheme, the obtained impulse will reach the troposphere and cause an increase in the intensity of the cyclone, i.e., provoke an additional decrease of pressure and temperature at the earth's surface. Under the same conditions, the tropospheric anticyclone becomes less intense, i.e., pressure and temperature at the earth's surface will likewise decrease. Obviously, in the troposphere, supplementary warming at the altitudes of

200-250 kilometers (F-ionospheric layer) will bring about analogous effects.

If, however, the supplementary warming takes place at altitudes of 100-130 kilometers (E-ionospheric layer), then, in case of a tropospheric cyclone, this will lead to a reduction in the intensity of the entire system of perturbations, i.e., to an increase in the pressure and temperature at the earth's surface. In case of a tropospheric anticyclone, there will be an increase in the intensity of the entire system of perturbations, i.e., again an increase in the surface pressure and temperature.

The sources of supplementary thermal effects may be external - primarily, the ultraviolet and corpuscular radiation by the active regions of the sun. It is known that the wave radiation by these areas is absorbed in the D layer of the ionosphere, while the corpuscular fluxes provoke an anomaly-type ionization of the F layer (ionospheric and magnetic storms) and polar auroras at the altitude of the E layer.

If the absorption of ultraviolet and corpuscular radiation in the D, E and F layers is associated with the warming, then, according to the afore-described scheme, the solar-activity eruptions should lead to an intensification of cyclones and weakening of anticyclones; and only in the high latitudes can the polar auroras be accompanied by an intensification of anticyclonic activity.

A number of experimentally established facts corroborates this conclusion.

With an increase in the index of sunspot frequency (characterizing the intensity of corpuscular fluxes), there is an increase in the number of intense cyclones and a decrease in the number of intense anticyclones (L.A. Vitel's).

Magnetic storms are an index of the penetrations of corpuscular fluxes into the terrestrial atmosphere. Therefore, according to the scheme above, there should be a definite relationship between magnetic storms and the surface pressure: on the days of magnetic disturbances the pressure should decrease (the same applies to temperature). Actually:

1. The intensity of cyclonic circulation at high latitudes increases during very strong magnetic storms, while that of anticyclonic circulation, decreases. During magnetic storms an explicit weakening of anticyclonic circulation can be

detected over Siberia (L.A. Vitel's).

2. On the days of magnetic disturbances the pressure in the regions of the (Northern) Arctic Ocean, Iceland, and West Siberia, decreases two to four millibars (according to observations for the years 1946-1951). The same occurs also in the Braunschweig region (observations for the 1884-1951 period; data by Kärre).

3. The temperature in Washington (D.C.) during the week following a [magnetic] storm is on the average 0.8 degrees lower than during the week preceding the storm, and on the very day of the storm, it is 3 degrees lower (Abbot's data for 73 magnetic storms during the 1923-1946 period).

Polar auroras are accompanied by arctic invasions, i.e., by intensification of anticyclonic activity in the polar latitudes (P.P. Predtechenskiy).

Attention should be turned to the following: on the first day of a magnetic disturbance, the critical frequency of the F layer, and hence also its ionization, decreases. The corpuscle fluxes can only increase the ionization. Therefore, the observed decrease in critical frequency is caused by other processes; this may be an intensification of divergent currents or a weakening of convergent currents postulated in the scheme under the influence of corpuscular fluxes.

The scheme of baric perturbations now being reviewed is not the only scheme based on vertical stratification; but also schemes of the general circulation in the upper layers as proposed by various investigators are analyzed in a vertical direction in which the rotations of the circulation in layers above or below each other are opposite.

Obviously, the breaking-down of dynamic systems, in a vertical direction associated with the presence of planetary layers of temperature inversion in the atmosphere, must be a characteristic peculiarity of atmospheric circulation.

The cause of certain peculiarities in the changes of the earth's climate is considered by many investigators to stem from the effect of solar activity on weather processes, which effect extends also to the heat processes in the atmosphere by causing not only the warming or cooling of individual portions of the terrestrial

sphere but also fluctuations of such a planetary thermal characteristic as the temperature difference between the equator and the pole. Climatic changes caused by the sun may be both comparatively brief (change in the duration of the cold and warm seasons during the 11-year cycle of solar activity) and of geological duration (glacial periods). Inasmuch as the ultraviolet and corpuscular radiations of the active regions of the sun affect directly only atmospheric layers situated at altitudes above 60-70 kilometers, solar activity could not influence the processes in the troposphere without the existence of a certain transmission mechanism. The presently assumed transmission mechanism is one of the possible links between the effect of the active sun and the hydrothermodynamic processes in the atmosphere, and it makes possible to provide the physical basis for certain variations being observed in the horizontal heat exchange and zonal thermal field of the atmosphere.



## Temperature Distribution in the Troposphere

The problem of investigating tropospheric temperature was first correctly set-up by I.A. Kibel' [15], who examined not only the radiation but also the turbulent transfer of heat. Before him, an attempt at improving the results obtained by Emden through taking into account the vertical fluxes was made by A.A. Fridman [39].

For the problem of the mean annual temperature distribution in the atmosphere, examined by I.A. Kibel', eq. (4) assumes the following form:

$$z=0,$$

in which,

$$z = -\operatorname{div} R - \operatorname{div} P, \quad (40)$$

where R and P are the radiation and turbulent fluxes of heat, respectively.

Kibel' wrote the equations of transfer according to the Schwarzschild-Emden scheme (12), (13), and (20), i.e., for "grey-body" radiation with  $\alpha$  and  $\alpha'$  absorption coefficients for the long-wave and short-wave portions of the spectrum, respectively, extending only in the vertical direction (absorbing substance: water vapor, with density  $\rho$ ):

$$\frac{\partial A}{\partial z} = \alpha_2 (A - fE), \quad (41)$$

$$\frac{\partial B}{\partial z} = \alpha_2 (fE - B), \quad (42)$$

$$\frac{\partial S}{\partial z} = \alpha' \rho S, \quad (43)$$

where z is vertical coordinate.

The only difference from Schwarzschild's scheme consists in that Kibel' introduces into the consideration the factor  $f$ , according to Gul'bert [Hulbert 7], which takes into account in a very approximate manner the circumstance that water vapor does not radiate as a "gray" body;  $f$  is a function of temperature.

The following boundary conditions are assumed for integrating eqs. (41) - (43):

When  $z = \infty$

$$A = 0, \quad (44)$$

i.e., only solar radiation approaches the boundary of the atmosphere from above;

$$S = W, \quad (45)$$

where  $W$  is the quantity of solar energy absorbed by the earth-atmosphere system, the calculation of which requires the consideration of the reflection of solar rays from the atmosphere, clouds, and the earth's surface.

When  $z = 0$

$$B = qE, \quad (46)$$

where  $q$  is a parameter taking into account the circumstance that the earth's surface does not radiate as an absolutely black body.

If we examine only the vertical turbulent heat flux, then

$$\text{div } P = -\frac{\partial}{\partial z} \lambda' \frac{\partial T}{\partial z}. \quad (47)$$

It is assumed that the turbulent heat flux is proportional to the absolute temperature gradient in accordance with Ertel's scheme,  $\lambda'$  is the coefficient of vertical turbulent heat conductivity.

Eq. (40) may be written in the following form:

$$\frac{\partial}{\partial z} \lambda' \frac{\partial T}{\partial z} + \alpha p (A + B - 2fE + \beta S) = 0, \quad (48)$$

in which

$$\beta = \frac{\alpha'}{\alpha}.$$

For the integration of this equation, two boundary conditions are required. We select them as follows:

When  $z = \infty$ , radiation equilibrium for mean annual conditions

$$B = W, \quad (49)$$

When  $z = 0$ , equation of heat balance

$$-\lambda' \frac{\partial T}{\partial z} = A + S - B. \quad (50)$$

STAT

Here no account is taken of the heat loss into evaporation and heat fluxes into the soil.

The  $z$ -coordinate is replaced by the variable  $\tau$  (optical "thickness" of the atmosphere for grey-body radiation):

$$\tau = \int_0^{\infty} \alpha p dz.$$

Instead of temperature  $T$ , the function being sought here is  $E = f_0 T^4$ .

For a resolution of the problem we introduce the dimensionless values  $s'$ ,  $a$ ,  $y$ , according to the equalities

$$fE = Ws', \quad B + A = Wa, \quad B - A = Wy.$$

Then, the derivation of eq. (48) is reduced to the integration of the following expression:

$$\frac{dy}{d\tau} - \left(1 + \frac{8\sigma T^3 f}{\lambda' \alpha p}\right) y = -\frac{8\sigma T^3 f}{\lambda' \alpha p} e^{-\tau},$$

at these boundary conditions:

$$\tau = 0 \quad y = 1;$$

$$\tau = \tau_0 \quad y + \frac{q}{f} y' = \left(\frac{q}{f} - 1\right) \left(1 + \int_0^{\tau_0} y d\tau\right).$$

Here

$$y' = \frac{dy}{d\tau}, \quad \tau_0 = \int_0^{\infty} \alpha p dz.$$

The combination of parameters  $\frac{fT^3}{\lambda' \alpha p}$  is considered by I.A. Kibel' to remain constant with altitude. Further, Kibel' introduces the constant  $m$ :

$$\frac{4\sigma T^3 f}{\lambda' \alpha p} = \frac{m^2 - 1}{2} = \text{const.}$$

After determining  $y$ , we find the values of  $a$  and  $s'$  according to the following formulas:

$$a = 1 + \int_0^{\tau_0} y d\tau; \quad s' = \frac{1}{2} \left(1 + \int_0^{\tau_0} y d\tau - \frac{dy}{d\tau}\right).$$

Latitude  $42^{\circ}$  was selected for a specific calculation of the distribution of temperature with altitude, since it may be expected that in the middle latitudes the effect of horizontal turbulent heat transfer is small. The following values of parameters were assumed:

$$m = 1.75; \quad \frac{g}{T} = 1.15; \quad W = 0.138 \quad \text{calories/square centimeter-minute}$$

In order to obtain the last figure, the albedo of the earth-atmosphere system was assumed equal to 0.7 on the average during the year.

The optical thickness of the atmosphere  $\tau$  was determined by means of Hann's empirical law

$$\tau = \int_0^{\infty} \alpha_0 \rho_0 T_0 \frac{10^{-x/l}}{T} dx$$

when  $l = 8 \times 10^5$  centimeters<sup>-1</sup>.  $\rho_0 = 6.2 \times 10^{-6}$  grams/cubic centimeters,  $\alpha_0 = 7.25$  square centimeters/gram, and  $\frac{T_0}{T_{\infty}} = \frac{280}{220}$ . This resulted in obtaining  $\tau_0 = 12.6$  (the "0" subscript indicates that the magnitudes of the corresponding values are assumed at the earth's surface).

The calculated formula for determining T has this form:

$$f_0 T^4 = 0.047 [6.80 - 4.80e^{-0.2x} + 0.57e^{-1.75x} - 0.36e^{1.75(x-12.6)}].$$

Let us cite results of the calculation of T; for comparison, also given are the actual mean values of temperature, based on data from radiosonde ascents for three years (1938-1940) at Omaha (USA):

x kilometers	0.3	0.5	1.0	2.0	3	4	5	6
T° calculated	8	9	9	4.5	-0.5	-6.5	-13.5	-19.5
T° actual	8.1	9.1	8.9	5.2	-0.1	-6.1	-12.2	-19.5
T° corrected	52	52	52	52		49		42

x kilometers	7	8	9	10	11	12	13	∞
T° calculated	-26.5	-33.5	-40.0	-45.0	-49.0	-52.0	-53.0	-55.0
T° actual	-26.4	-33.7	-40.8	-47.15	-52.35	-55.7	-57.7	-
T° corrected		35		30		13		

The agreement between calculated and actual data for mean annual temperatures is entirely satisfactory.

But in this problem far from all the factors determining the air temperature, have been taken into account, e.g., such an important component of the heat balance as the latent heat of condensation (vaporization) in the atmosphere and at the earth's surface. Therefore, the selection of the quantitative values of the parameters considered in this problem was found to be the only possible way of attaining a satisfactory agreement between calculated and experimental temperatures. This refers even to parameters the values of which are considered at present, as determinate. For example, such an important characteristic as the albedo of the earth-atmosphere system, was increased approximately twice, while the mean value of water-vapor density on the earth's surface was reduced in half.

If it is assumed that  $\Gamma = 0.41$  and  $\rho = 13 \text{ g/m}^3$ , which is more valid, then we obtain the distribution given above in the  $T^0$  corrected line (of the Omaha data).

The combination of parameters  $\frac{\sigma T^0 f}{\lambda_{sp}}$  likewise does not remain constant with altitude, owing to the rapid decrease of  $\rho$ . N.R. Malkin showed [24] that, if the distribution of water vapor density is governed by an exponential law, then  $\frac{\sigma T^0 f}{\lambda_{sp}} \approx \frac{1}{\tau}$ . N.R. Malkin provides a derivation of Kibel's differential equation with variable coefficients which he considers proportional to  $\frac{1}{\tau}$  in the  $0 \leq \tau \leq \tau_0$  interval, but he does not cite the quantitative calculation. O.S. Berlyand [6] derives Kibel's equation by assuming that  $\frac{\sigma T^0 f}{\lambda_{sp}} = \text{const.}$  in the troposphere and proportional to  $\frac{1}{\tau}$  in the stratosphere.

It should be noted that the description of selective radiation processes in the atmosphere by means of Hulbert's scheme with only two absorption factors is in itself so rough that it does not permit any hope of obtaining a correspondence between the calculated and the actual temperatures, even if all the principal factors are taken into account and the parameter values are correctly assumed.

Moreover, Hulbert's scheme requires that boundary conditions (49) and (50) should be written in the form of (40):

$$B + (1-f)qE|_{z=0} = W,$$

$$-\lambda \frac{\partial T}{\partial z} = A + S - B - (1-f)qE,$$

i.e., they should be complemented by radiation from the earth's surface in the wave-length interval from 8 to 12 microns, an interval transparent to water vapor, since according to Hulbert's scheme

$$\int_0^8 E_\lambda d\lambda + \int_{12}^{\infty} E_\lambda d\lambda = fE,$$

$$\alpha_1(\lambda) \begin{cases} 0 & 8 < \lambda < 12\mu \\ \alpha & \lambda < 8\mu, \lambda > 12\mu \end{cases}$$

As for condition (46), it appears to be illogical and, as shown by M.I. Yudin [41], it should be written differently. If the earth is a "grey" body, then it should reflect a portion of the back (counter) radiation, and the upward flux from the earth's surface will be

$$B = \delta E + (1 - \delta) A,$$

where  $\delta$  is absorption coefficient for the earth's surface. Consequently, the parameter  $q$  in eq. (46) depends on both the reflecting properties of the underlying surface and the stratification of the atmosphere. Disregard of the latter relationship may lead to a contradiction with the condition of a radiant equilibrium when  $z = \infty$ .

According to I.A. Kibel', a very essential contribution to the solving of the problem of the heat regime in the atmosphere was made by Ye. N. Blinova [7]. She succeeded in taking account of such a fundamentally important factor as the horizontal turbulent heat exchange stipulated by the temperature contrast between the pole and the equator. Accordingly, in her problem, instead of (47) we obtain

$$\operatorname{div} \mathbf{P} = -\frac{\partial}{\partial z} \lambda' \frac{\partial T}{\partial z} - \frac{1}{a_0^2 \sin \theta} \frac{\partial}{\partial \theta} \sin \theta \lambda'' \frac{\partial T}{\partial \theta}, \quad (51)$$

and eq. (40) will give the temperature distribution for the case of a purely zonal circulation in which the meridional components of wind velocity are absent.

In eq. (51)  $\theta = 90^\circ - \varphi$  ( $\varphi$  is geographical latitude),  $a_0$  is radius of the earth, and  $\lambda''$  is the coefficient of the horizontal turbulent heat conductivity.

The equations of radiation transfer are written in the same way as Kibel's eqs.

(41), (42) and (43). As a complement to boundary conditions (44) - (46) and (50), it is assumed that on the upper boundary of the atmosphere the temperatures along the meridians are smoothed out

$$\frac{\partial T}{\partial \theta} = 0. \quad (52)$$

Inasmuch as the mathematical calculations of Ye. I. Blinova are of interest, we shall cite them after complementing her problem by taking into account the quantities of heat lost to evaporation of moisture from the earth's surface and also associated with phase transformations of water vapor in the atmosphere.

In order to take the first factor into account, it is necessary to introduce the following term into the left-hand part of eq. (50):

$$-Lk' \frac{\partial p}{\partial z} = LF,$$

where  $L$  is latent heat of condensation (vaporization),  $F$  is evaporation during a unit of time from a unit of surface, and  $k'$  is the coefficient of turbulence.

In order to take the second factor into account, it is necessary to introduce into eq. (40), in addition to the radiation and turbulent heat fluxes, also the condensational influx of heat. Let us assume that it is proportional to the density of water vapor and is equal to  $Lxp$ , where  $x$  is a proportionality coefficient. The procedure for determining  $x$  will be described later.

Thus, instead of eq. (48), we obtain

$$\sigma p (A + B + \beta S - 2E) + \frac{\partial}{\partial z} \lambda' \frac{\partial T}{\partial z} + \frac{1}{a_0^2 \sin \theta} \frac{\partial}{\partial \theta} \sin \theta \lambda'' \frac{\partial T}{\partial \theta} + Lxp = 0. \quad (53)$$

Instead of the vertical coordinate  $z$ , the dimensionless coordinate  $x$  is introduced:

$$x = \frac{1}{\tau_0} \int_0^{\infty} \sigma p dz,$$

which may be called the reduced optical thickness of the atmosphere

$$\left( \tau_0 = \int_0^{\infty} \sigma p dz \right).$$

(41), (42) and (43). As a complement to boundary conditions (44) - (46) and (50), it is assumed that on the upper boundary of the atmosphere the temperatures along the meridians are smoothed out

$$\frac{\partial T}{\partial \theta} = 0. \quad (52)$$

Inasmuch as the mathematical calculations of Ye. I. Blinova are of interest, we shall cite them after complementing her problem by taking into account the quantities of heat lost to evaporation of moisture from the earth's surface and also associated with phase transformations of water vapor in the atmosphere.

In order to take the first factor into account, it is necessary to introduce the following term into the left-hand part of eq. (50):

$$-Lk' \frac{\partial p}{\partial z} = LF,$$

where  $L$  is latent heat of condensation (vaporization),  $F$  is evaporation during a unit of time from a unit of surface, and  $k'$  is the coefficient of turbulence.

In order to take the second factor into account, it is necessary to introduce into eq. (40), in addition to the radiation and turbulent heat fluxes, also the condensational influx of heat. Let us assume that it is proportional to the density of water vapor and is equal to  $Lx\rho$ , where  $x$  is a proportionality coefficient. The procedure for determining  $x$  will be described later.

Thus, instead of eq. (48), we obtain

$$\alpha p (A + B + \beta S - 2E) + \frac{\partial}{\partial z} \lambda' \frac{\partial T}{\partial z} + \frac{1}{a_0^2 \sin \theta} \frac{\partial}{\partial \theta} \sin \theta \lambda'' \frac{\partial T}{\partial \theta} + Lx\rho = 0. \quad (53)$$

Instead of the vertical coordinate  $z$ , the dimensionless coordinate  $x$  is introduced:

$$x = \frac{1}{\tau_0} \int_0^{\infty} \alpha p dz,$$

which may be called the reduced optical thickness of the atmosphere

$$\left( \tau_0 = \int_0^{\infty} \alpha p dz \right).$$



Obviously,

$$dz = -\frac{\tau_0}{\alpha p} dx.$$

By transforming to variable  $x$  and  $E$ , and by having designated

$$A + B = a, B - A = y, \frac{2}{m^2 - 1} = \frac{\lambda' \alpha p}{4 f_0 T^2}, M = \frac{\lambda'}{4 f_0 T^2 \alpha_0^2 \alpha p},$$

we obtain from (53)

$$(a + \beta S - 2E) + \frac{1}{\tau_0^2} \frac{\partial}{\partial x} \frac{2}{m^2 - 1} \frac{\partial E}{\partial x} + \frac{1}{\sin \theta} M \sin \theta \frac{\partial E}{\partial \theta} + \frac{Lx}{a} = 0. \quad (54)$$

The equations of radiation transfer (41) - (43) and the boundary conditions will be written out in the designations adopted as:

$$\frac{\partial a}{\partial x} = \tau_0 y, \quad (55)$$

$$\frac{\partial y}{\partial x} = \tau_0 (a - 2E), \quad (56)$$

$$\frac{\partial S}{\partial x} = -\beta \tau_0 S; \quad (57)$$

when  $x=0$ :

$$a - y = 0, \quad (58)$$

$$S = W, \quad (59)$$

$$\frac{\partial E}{\partial \theta} = 0, \quad (60)$$

$$\int_{(\Sigma)} (a + y) d\Sigma = 2 \int_{(\Sigma)} W d\Sigma; \quad (61)$$

when  $x=1$ :

$$y + \frac{1}{\tau_0} \frac{\partial y}{\partial x} - 2(q-1)E = 0, \quad (62)$$

$$y + \frac{2}{m^2 - 1} \frac{1}{\tau_0} \frac{\partial E}{\partial x} + \frac{Lk'a}{\tau_0} p \frac{\partial p}{\partial x} = S$$

It is obvious from (57) and (59) that

$$S = W e^{-\beta x}. \quad (63)$$

In excluding from eqs. (54) - (56) the unknowns  $a$  and  $y$ , and in using (63), we obtain the following differential equation for  $E$ :

$$\frac{2}{m^2-1} \frac{\partial^4 E}{\partial x^4} - \frac{2m^2 \tau_0^2}{m^2-1} \frac{\partial^2 E}{\partial x^2} + \frac{M \tau_0^2}{\sin \theta} \left[ \frac{\partial^3}{\partial x^2 \partial \theta} \sin \theta \frac{\partial E}{\partial \theta} - \tau_0^2 \frac{\partial}{\partial \theta} \sin \theta \frac{\partial E}{\partial \theta} \right] - \frac{Lx \tau_0^4}{a} = \beta(1-\beta^2) \tau_0^4 e^{-\beta x} W. \quad (64)$$

For the derivation of eq. (64) the Fourier method is used: the sought function  $E$ , and the known function  $W$  are represented by dissociations into series according to Legendre's polynomials:

$$E(x, \theta) = \sum_{n=0}^{\infty} E_n(x) P_n(\theta), \quad (65)$$

$$W(\theta) = \sum_{n=0}^{\infty} W_n P_n(\theta) \quad (66)$$

Eq. (64) will be thus written for the  $n$ th harmonic of  $E(x, \theta)$ :

$$\frac{2}{m^2-1} \frac{d^4 E_n}{dx^4} - \tau_0^2 \left[ \frac{2m^2}{m^2-1} + Mn(n+1) \right] \frac{d^2 E_n}{dx^2} + M \tau_0^4 n(n+1) E_n - \frac{Lx \tau_0^4}{a} = \beta(1-\beta^2) \tau_0^4 e^{-\beta x} W_n. \quad (67)$$

After having dissociated the functions  $S$ ,  $a' = a + \frac{Lx}{a}$  and  $y$  into series of form (65) we obtain, analogously to (67)

$$S_n = W_n e^{-\beta x}, \quad (68)$$

$$a_n = 2E_n - \frac{2}{\tau_0^2(m^2-1)} \frac{d^2 E_n}{dx^2} + Mn(n+1)E_n - \beta S_n, \quad (69)$$

$$y_n = \frac{2 + Mn(n+1)}{\tau_0} \frac{\partial E_n}{\partial x} - \frac{2}{\tau_0^2(m^2-1)} \frac{d^3 E_n}{dx^3} + \beta^2 S_n. \quad (70)$$

Let us write the boundary conditions for the  $n$ th harmonic:

When  $x=0$ :

$$a'_n - y_n = \begin{cases} \frac{Lx}{a} & n=0 \\ 0 & n>0 \end{cases} \quad (71)$$

$$E_n = 0 \quad n>0 \quad (72)$$

$$a_n + y_n = \begin{cases} 2W_n + \frac{Lx}{a} & n=0 \\ 2W_n & n>0 \end{cases} \quad (73)$$

When  $x=1$ :

$$y_n + \frac{1}{\tau_0} \frac{dy_n}{dx} - 2(q-1)E_n = 0 \quad (74)$$

$$y_n + \frac{2}{(m^2-1)\tau_0} \frac{dE_n}{dx} = \begin{cases} S_n - LF & n=0 \\ S_n & n>0. \end{cases} \quad (75)$$

Let us dwell in some detail on determining the zero harmonic  $E_0(x)$ .

After having integrated (67) twice we reduce the order of the equation

$$\frac{d^2 E_0}{dx^2} - m^2 \tau_0^2 E_0 = \frac{(1-\beta^2)\tau_0^2}{2\beta} (m^2-1) e^{-\beta x} W_0 + \frac{Lx\tau_0^4}{4a} (m^2-1)x^2 + \gamma x + \delta. \quad (76)$$

where  $\gamma$  and  $\delta$  are integration constants.

The derivation of (76) has this form:

$$E_0 = C_1 e^{kx} + C_2 e^{-kx} + C_3 + C_4 x + d_1 x^2 + d_2 e^{-\beta x}, \quad (77)$$

where

$$k = m\tau_0, \quad d_2 = \frac{(1-\beta^2)(m^2-1)}{2\beta(\beta^2-m^2)} W_0, \quad d_1 = -\frac{Lx\tau_0^4(m^2-1)}{4am^2},$$

$$\delta = d_1 - m^2\tau_0^2 C_3, \quad \gamma = -m^2\tau_0^2 C_4.$$

In order to determine the integration constants  $C_1$ ,  $C_2$ ,  $C_3$ , and  $C_4$ , it is necessary to employ the boundary conditions (71) - (75) when  $n = 0$ .

Having substituted (77) into (69) and (70), we obtain

$$a_0' = -\frac{2}{m^2-1} (C_1 e^{kx} + C_2 e^{-kx}) + 2(C_3 + C_4 x) + 2d_1 \left( x^2 - \frac{2}{\tau_0^2(m^2-1)} \right) + \frac{m^2-1}{\beta(\beta^2-m^2)} e^{-\beta x} W_0, \quad (78)$$

$$y_0 = -\frac{2m}{m^2-1} (C_1 e^{m\tau_0 x} - C_2 e^{-m\tau_0 x}) + \frac{2}{\tau_0} C_4 + \frac{4}{\tau_0} d_1 x + \frac{1-m^2}{\beta^2-m^2} e^{-\beta x} W_0. \quad (79)$$

Condition (74) by means of (79), leads to the equality

$$C_4 = \frac{L\tau_0(m^2-1)}{2m^2} \left( \frac{x\tau_0}{a} - F \right). \quad (80)$$

Conditions (71) and (72) will yield (their sum and their difference is taken)

$$-\frac{2}{m^2-1}(C_1 + C_2) + 2C_3 = \left[1 + \frac{m^2-1}{\beta(m^2-\beta^2)}\right] W_0 + \frac{Lx}{a} + \frac{4d_1}{\tau_0^2(m^2-1)} \quad (81)$$

$$\frac{2m}{m^2-1}(C_2 - C_1) + \frac{2}{\tau_0} C_4 = \frac{1-\beta^2}{m^2-\beta^2} W_0. \quad (82)$$

From (75) we obtain

$$\begin{aligned} & \left(\frac{m}{m-1} + q - 1\right) C_1 e^{m\tau_0} + \left(\frac{m}{m+1} + q - 1\right) C_2 e^{-m\tau_0} + \\ & + (q-1)(C_3 + C_4 + d_1) - \frac{C_4}{\tau_0} - \frac{2d_1}{\tau_0} \left(1 + \frac{1}{\tau_0}\right) = \\ & = \frac{m^2-1}{2(m^2-\beta^2)} (1-\beta) \left(q + \frac{q-1}{\beta}\right) e^{-\beta\tau_0} W_0. \end{aligned} \quad (83)$$

Since C enters into (77) as a multiplier with e, C<sub>1</sub> is small compared with C<sub>2</sub> and C<sub>3</sub>. Hence it follows from (81) and (82) that

$$\begin{aligned} C_1 &= \frac{m^2-1}{2m} \left[ \frac{1-\beta^2}{m^2-\beta^2} W_0 - \frac{L(m^2-1)}{m^2} \left(\frac{x\tau_0}{a} - F\right) \right], \\ C_2 &= \frac{1}{2(m^2-\beta^2)} \left[ m^2 - \beta + \frac{m^2-1}{\beta} + \frac{1-\beta^2}{m} \right] W_0 + \\ & + \frac{Lx}{2a} \left(1 - \frac{\tau_0}{m}\right) \frac{m^2-1}{m^2} + LF \frac{m^2-1}{2m^3}. \end{aligned}$$

From (83) we obtain

$$\begin{aligned} C_1 &= \frac{e^{-m\tau_0}}{\left(\frac{m}{m-1} + q - 1\right)} \frac{m^2-1}{2(m^2-\beta^2)} \left[ (1-\beta) \left(q + \frac{q-1}{\beta}\right) e^{-\beta\tau_0} - \right. \\ & \left. - (q-1) \left( \frac{1}{\beta} + \frac{m^2-\beta^2}{m^2-1} + \frac{1-\beta^2}{m(m^2-1)} - \frac{\left(\frac{m}{m+1} + q - 1\right) (1-\beta^2)}{m} e^{-m\tau_0} \right) \right] \times (84) \\ & \times W_0 + \frac{e^{-m\tau_0}}{\left(\frac{m}{m-1} + q - 1\right)} \left\{ \frac{(1-m^2)LF}{2m^2} - \frac{Lx(m^2-1)}{2am^2} - \right. \\ & \left. - (q-1) \left[ \frac{LF(m^2-1)}{2m^2} \left(\frac{1}{m} \tau_0\right) + \frac{Lx(m^2-1)}{2a} \left(1 - \frac{\tau_0}{m} + \frac{\tau_0^2}{2}\right) \right] - \right. \\ & \left. - (mq + q - 1) e^{-m\tau_0} \frac{L}{2m^3} (m-1)(m^2-1) \left(F - \frac{\tau_0^2}{a}\right) \right\}. \end{aligned}$$

Having substituted the constants found into (77), we obtain

$$\begin{aligned}
F_0 = F_0 w_0 + LF \frac{m^2 - 1}{2m^2} & \left\{ \frac{1}{m} - \tau_0 x + \frac{m^2 - 1}{m} e^{-m\tau_0 x} - \right. \\
- \frac{e^{-m\tau_0(1-x)}}{\left(\frac{m}{m-1} + q - 1\right)} & \left[ 1 + (q-1) \left(\frac{1}{m} - \tau_0\right) + (mq + q - 1) \frac{m-1}{m} e^{m\tau_0} \right] \Bigg\} + \\
+ Lx \frac{m^2 - 1}{2m^2} & \left\{ \frac{1}{\alpha} \left(1 - \frac{\tau_0}{m}\right) + \frac{\tau_0^2}{\alpha} x - \frac{\tau_0^2}{2\alpha} x^2 - \frac{m^2 - 1}{m} \frac{\tau_0}{\alpha} e^{-m\tau_0 x} - \right. \\
- \frac{e^{-m\tau_0(1-x)}}{\left(\frac{m}{m-1} + q - 1\right)} & \left[ \frac{1}{\alpha} + \frac{q-1}{\alpha} \left(1 - \frac{\tau_0}{m} + \frac{\tau_0^2}{2}\right) - \right. \\
- \frac{m-1}{m} (mq + q - 1) & \left. \frac{\tau_0}{\alpha} e^{-m\tau_0} \right] \Bigg\}.
\end{aligned} \quad (85)$$

The first term in (85), denoted as  $E_0, W_0$ , and dependent on  $W_0$ , represents the derivation obtained by I.A. Kibel' and Ye. N. Elinova.

The value of the proportionality coefficient  $x$  may be obtained from the equation of water vapor diffusion, in which only vertical transfer is taken into account

$$k' \frac{\partial^2 \rho}{\partial z^2} - x\rho = 0$$

by two different methods.

First, if  $\rho$  is assumed as given according to altitude, e.g., in the form of

$$\rho = \rho_0 e^{-bz},$$

then

$$x = k' b^2.$$

Second, if evaporation  $F$  and water vapor density  $\rho_0$  are given for the earth's surface, then

$$x = \frac{1}{k' \rho_0^2} F^2.$$

Both methods for determining  $x$  give a magnitude of the order of  $10^{-5}$  minutes<sup>-1</sup>.

Let us cite the calculations of the vertical distribution of temperature according to formula (85) for Latitude 35°N when  $F = 3.83 \cdot 10^{-5}$  centimeters/minute,

$k' = 10$  square meters/second; the values of the remaining parameters are taken from [15] and [7]:  $T_w$  is the temperature distribution obtained in [7].

$z$ KM	0	0.5	1.5	2.5	3.5	4.5	6.0	8.0	9.0
$T_w$	287	289	284	279	273	266	257	242	237
$T$	244	252	252	250	247	242	233	225	222

As can be seen from the data cited above, after the introduction of corrections for evaporation and condensation, the scheme of I. A. Kibel' and Ye. N. Blinova, with the parameter values they selected, gives a temperature distribution greatly differing from the actual distribution.

Here it is necessary to stress once more the impermissibility of using the model of a "grey-body" atmosphere in those problems in which radiant heat exchange must be taken into account. This has been pointed out already by other investigators, e.g., in [18] it was noted that Hulbert's factor  $f$  is an essentially integral value characterizing the mean absorptivity of the entire atmosphere; this value is very roughly approximated. This can be ascertained by comparing the transparency of the "grey-body" atmosphere with that of the actual atmosphere. The factor  $f = 0.6$  corresponds to average conditions of the atmosphere. Hence, it follows that the  $1 - f = 0.4$  portion of the terrestrial radiation should go out into outer space. However, the actual mean transparency of the atmosphere is equal to 0.6, inasmuch as  $B_0 = \epsilon q_0 T_0^4 = 0.50$  at  $T_0 = 286^\circ$  and  $q = 0.9$ ,  $B_\infty = \frac{1}{4} (1 - \Gamma) I_0 = 0.317$  when  $\Gamma = 35$  percent and  $I_0 = 1.91$  calories/square centimeter minute. Obviously, Hulbert's scheme reduces the mean transparency of the atmosphere. It is readily explained how the nonselectivity of absorption distorts the fluxes of upward and downward long-wave radiation. For this purpose let us integrate the equations of transfer (41) and (42) at boundary conditions (44) and (46), and let us calculate the outgoing radiation of the atmosphere and the atmospheric back (counter) radiation at Latitude  $40^\circ N$  for mean annual conditions at the usually assumed mean characteristics of "grey-body" atmosphere ( $f = 0.6$ ,  $\alpha = 7.25$  square centimeters/gram) and the actually observed distribution of  $p$  and  $T$  (see Tables 9 and 34). Here we will obtain  $B_\infty = 95$  kilocalories/square centimeter year, whereas according to the most complete existing

radiation diagrams,  $B_{\infty} = 160$  kilocalories/square centimeter year. Consequently, the conventional model of "grey-body" atmosphere diminishes the outgoing radiation considerably. As one should expect, the transparency of the "grey-body" atmosphere amounts to  $\frac{0.182}{0.50} = 0.4$  also according to these calculations. In order to increase the outgoing radiation it is necessary to base the calculations on temperature values artificially higher than the values being observed at all levels of the atmosphere. The mean annual value of back (counter) radiation for the "grey-body" atmosphere at Latitude  $40^{\circ}\text{N}$  is  $A_0 = 155$  kilocalories/square centimeter year. Therefore, the effective radiation of the earth's surface under these condition is  $B_0 - A_0 = 260 - 155 = 105$  kilocalories/square centimeter year, whereas according to Evfimov [18] and T.G. Berlyand [10] it should amount to 50 kilocalories/square centimeter year. If the selectivity of atmospheric absorption is not taken into account, effective radiation is distorted so as to be increased in our example, this radiation is twice what it should be and differs little from  $B_{\infty}$ , whereas it should be approximately three times less than  $B_{\infty}$ .

Hence, it can be seen that the model of the "grey-body" atmosphere actually does not provide an opportunity for determining the correct distribution of temperature and fluxes of long-wave radiation, and therefore, it cannot be used.

A more accurate account of radiation fluxes in Kibel's scheme was obtained by F.N. Shekhter [40]. In describing the selective processes she chose the Ambartsumyan-Lebedinskiy method [1], which at the present time should be considered as the most satisfactory from the view point of accuracy and simplicity.

The idea of the method of V.A. Ambartsumyan consists in that the integration for all the wave lengths  $\lambda$  is realized by these two procedures:

- (1) Integration for the wave lengths  $\lambda$ , the absorption coefficient of which lies within the  $\alpha < \alpha_1 < \alpha + d\alpha_1$  interval, and
- (2) Integration over all  $d\alpha$ 's.

This method was further developed by A.I. Lebedinskiy and applied to the examination of the radiant equilibrium of the earth's atmosphere [23]. Lebedinskiy

introduced the  $\mu(\alpha, T)$ -function, representing that portion of the total black-body radiation in the wave length range for which  $\alpha < \alpha_1 < \alpha + d\alpha$ . This portion depends both on the absorption coefficient and on the emitting-body temperature  $T$ . Lebedinskiy proceeded from approximate equations of the transfer of radiant energy: diffusivity was taken into account by increasing the absorption factor of parallel radiation 1.6 times. Moreover, Lebedinskiy examined only one absorbing substance - water vapor.

F.N. Shekhter extended the applicability of the Ambartsumyan-Lebedinskiy method to the case of an accurate composition of the equation of the transfer of radiant energy (5), by taking into account that two absorbing substances - water vapor and carbon dioxide - participate in radiative processes. In order to obtain total radiation fluxes from (5) it is necessary to complete three integrations:

- (1) For all wave lengths (consideration of selectivity)
- (2) For all directions in space (consideration of diffusivity)
- (3) For all elementary layers composing the finite layer, the radiation of which is being calculated.

The scattering processes were not considered, because the condition of local thermodynamic equilibrium is assumed to be valid.

It should be noted that the influence of diffusivity on temperature was examined by Feygel'son [38], although only for the case of grey-body radiation. Hence, she obtained, at all altitudes, temperatures that were 5-10 degrees higher than in the data cited on page 60 ( $T^0$  calculated).

Let us describe briefly the fundamental stages of the derivation of the equation of the transfer of radiant energy according to F.N. Shekhter.

Eq. (5) assumes the following form with respect to upward- and downward-directed fluxes of monochromatic radiation in the presence of two absorbing substances ( $H_2O$  and  $CO_2$ ):

$$\cos \theta \frac{dI_{\lambda,0}^{(1)}}{dz} = (\alpha_{\lambda}^w \rho + \alpha_{\lambda}^c \rho_c) (\epsilon_{\lambda} - I_{\lambda,0}^{(1)}), \quad (86)$$

$$\cos \theta \frac{dI_{\lambda,0}^{(2)}}{dz} = (\alpha_{\lambda}^w \rho + \alpha_{\lambda}^c \rho_c) (I_{\lambda,0}^{(2)} - \epsilon_{\lambda}). \quad (87)$$



Here  $I_{\lambda,0}^{(1)}, I_{\lambda,0}^{(2)}$  is the intensity of radiation energy of the wave length  $\lambda$  propagating upward (or downward) in a direction forming an angle  $\theta$  with the z-axis;  $\epsilon_{\lambda}$  is intensity of the monochromatic radiation of an absolutely black body;  $\rho$  and  $\rho_c$  are densities of  $H_2O$  and  $CO_2$ , respectively; and  $\alpha_{\lambda}^w$  and  $\alpha_{\lambda}^c$  are the respective coefficients of absorption.

Generally speaking, the absorption coefficients depend on altitude by way of temperature and pressure. The temperature relationship is ignored in view of its insignificance, while the influence of pressure is taken into account by introducing the  $\sqrt{\frac{p}{p_*}}$  factor, where  $p_*$  is the pressure at which the values of the absorption coefficients were (experimentally) determined.

If we introduce the effective coefficient of absorption  $\alpha_{\lambda}$  and the effective humidity  $m$  according to the formulas

$$\alpha_{\lambda} = \alpha_{\lambda}^w + \alpha_{\lambda}^c \frac{p_c}{p}, \quad (88)$$

$$m = \int_0^z \rho \sqrt{\frac{p}{p_*}} dz, \quad (89)$$

then eqs. (86) and (87) will be rewritten as:

$$\cos \theta \frac{dI_{\lambda,0}^{(1)}}{dm} = \alpha_{\lambda} (\epsilon_{\lambda} - I_{\lambda,0}^{(1)}), \quad (90)$$

$$\cos \theta \frac{dI_{\lambda,0}^{(2)}}{dm} = \alpha_{\lambda} (I_{\lambda,0}^{(2)} - \epsilon_{\lambda}). \quad (91)$$

Let us add here the equation of solar energy transfer

$$\cos \theta \frac{dS_{\lambda}}{dm} = \alpha_{\lambda} S_{\lambda}. \quad (92)$$

The set of eqs. (90)-(92) is derived at these boundary conditions:

$$m = 0 \quad (z = 0) \quad I_{\lambda}^{(1)} = \delta \epsilon_{\lambda} + (1 - \delta) I_{\lambda}^{(2)}, \quad (93)$$

$$m = M \quad (z = \infty) \quad I_{\lambda}^{(2)} = 0, \quad S_{\lambda} = S_{\lambda 0} \quad (94)$$

Condition (93) assumes that the temperature of the earth's surface and of the atmosphere immediately above it are equal, and that, with regard to long-wave radiat

the earth may be regarded as a "grey" body with an absorptivity  $\delta$ , reflecting rays as a smooth surface. Condition (94) assumes that only the flux of solar radiation is present at the outer boundary.

Further, according to Lebedinskiy, there is introduced the  $\omega(\alpha, T)$ -function for long-wave radiation and, analogously, the  $\eta(\alpha, T)$ -function for short-wave radiation which satisfies the condition

$$\int_0^{\infty} \omega(\alpha, T) d\alpha = 1,$$

since

$$\varepsilon = \int_0^{\infty} \varepsilon_{\lambda} d\lambda = \int_0^{\infty} d\alpha \left( \int_{\alpha < \alpha_{\lambda} < \alpha + d\alpha} \varepsilon_{\lambda} d\lambda \right) = \int_0^{\infty} \omega(\alpha, T) \varepsilon d\alpha.$$

Eqs. (90)-(92) and the boundary conditions (93)-(94) are integrated for the wave lengths the absorption coefficients  $\alpha_{\lambda}$  of which satisfy the condition

$$\alpha < \alpha_{\lambda} < \alpha + d\alpha, \quad (95)$$

Then, they are thus written:

$$\cos \theta \frac{dI_{\alpha, \theta}^{(1)}}{dm} = \alpha [\omega(\alpha, m) \varepsilon - I_{\alpha, \theta}^{(1)}], \quad (96)$$

$$\cos \theta \frac{dI_{\alpha, \theta}^{(2)}}{dm} = \alpha [I_{\alpha, \theta}^{(2)} - \omega(\alpha, m) \varepsilon], \quad (97)$$

$$\cos \theta \frac{dS_{\alpha}}{dm} = \alpha S_{\alpha} \quad (98)$$

and

$$I_{\alpha}^{(1)} = \delta \omega(\alpha, 0) \varepsilon + (1 - \delta) I_{\alpha}^{(2)} \text{ when } m = 0, \quad (99)$$

$$I_{\alpha}^{(2)} = 0, \quad S_{\alpha} = \eta(\alpha, M) S_0 \text{ when } m = M. \quad (100)$$

After deriving eqs. (96) and (97), determining the integration constants from conditions (99) and (100) and the conversion from radiation intensities to radiation fluxes according to the known formula

$$R_{\alpha} = 2\pi \int_0^{\frac{\pi}{2}} I_{\alpha, \theta} \cos \theta \sin \theta d\theta$$

(which yields  $E' = \pi e$  for radiation by an absolutely black body), we obtain

$$A_*(m) = 2 \int_m^M \omega(\alpha, \tau) E(\tau) d\tau \int_0^{\frac{\pi}{2}} e^{-\alpha \frac{\tau-m}{\cos \theta}} \sin \theta d\theta, \quad (101)$$

$$B_*(m) = 2 \int_0^m \omega(\alpha, \tau) E(\tau) d\tau \int_0^{\frac{\pi}{2}} e^{-\alpha \frac{m-\tau}{\cos \theta}} \sin \theta d\theta + \\ + 2(1-\delta) \int_0^M \omega(\alpha, \tau) E(\tau) d\tau \int_0^{\frac{\pi}{2}} e^{-\alpha \frac{m+\tau}{\cos \theta}} \sin \theta d\theta + \\ + 2\delta \omega(\alpha, 0) E(0) \int_0^{\frac{\pi}{2}} e^{-\alpha m / \cos \theta} \sin 2\theta d\theta. \quad (102)$$

Here are introduced the standard meteorological designations A and B for the respectively downward-and-upward-directed fluxes of long-wave radiation.  $A_*$  and  $B_*$  are fluxes satisfying condition (95).

Into expressions (101) and (102) Gold's function is introduced in accordance with the following relation

$$H_{\frac{1+\beta+\gamma}{\gamma}} = \gamma \int_0^{\frac{\pi}{2}} e^{-\frac{q}{\cos \theta}} \cos^{\beta} \theta \sin \theta d\theta \\ (\gamma > 0, \beta > -(1+\gamma), q > 0)$$

after which, these expressions assume the following form:

$$A_*(m) = 2 \int_m^M \omega(\alpha, \tau) E(\tau) H_2[\alpha(\tau-m)] d\tau, \quad (103)$$

$$B_*(m) = 2 \int_0^m \omega(\alpha, \tau) E(\tau) H_2[\alpha(m-\tau)] d\tau + \\ + 2(1-\delta) \int_0^M \omega(\alpha, \tau) E(\tau) H_2[\alpha(m+\tau)] d\tau + \\ + 2\delta \omega(\alpha, 0) E(0) H_2(\alpha m). \quad (104)$$

Inasmuch as

$$A = \int_0^{\infty} A_* da, \quad B = \int_0^{\infty} B_* da \quad (105)$$

and  $\alpha$  and  $\tau$  are independent variables, we obtain the following expressions for



total fluxes:

$$A(m) = \int_m^M E(\tau) d\tau \int_0^\infty 2\alpha\omega(\alpha, \tau) H_2[\alpha(\tau - m)] d\alpha, \quad (106)$$

$$\begin{aligned} B(m) = & \int_0^m E(\tau) d\tau \int_0^\infty 2\alpha\omega(\alpha, \tau) H_2[\alpha(m - \tau)] d\alpha + \\ & + (1 - \delta) \int_0^M E(\tau) d\tau \int_0^\infty 2\alpha\omega(\alpha, \tau) H_2[\alpha(m + \tau)] d\alpha + \\ & + \delta E(0) \int_0^\infty 2\omega(\alpha, 0) H_2(\alpha m) d\alpha. \end{aligned} \quad (107)$$

Owing to the great distance between the sun and the earth it may be assumed that direct solar radiation passes through the atmosphere in parallel bands of rays. Therefore, the integration of (98) for  $m$  and  $\alpha$  yields under the second condition, (100):

$$S_0(m) = S_0 \int_0^\infty \eta(\alpha, m) e^{-\alpha \frac{M-m}{\cos\theta}} d\alpha. \quad (108)$$

By definition, the transparency function  $D(u)$  is equal to the ratio of the outgoing flux  $R$  from a layer of  $h$  thickness to the incoming flux  $R_0$  into that layer ( $u = \rho h$  is mass of absorbing substance in a column with a unit cross-section perpendicular to the emitting surface).

If  $I_{0,\theta}$  is the total intensity of radiation (summed up for all wave lengths) in the direction of  $\theta$ , of isothermal plane adjacent to the homogeneous layer of the absorbing substance with a thickness,  $h$ , then the total incoming flux  $R_0$  entering that layer will be

$$R_0 = 2\pi \int_0^{\frac{\pi}{2}} I_{0,\theta} \cos\theta \sin\theta d\theta. \quad (109)$$

The magnitude of the total outgoing flux will be obtained if we substitute the initial intensity  $I_{0,\theta}$  in (109) by the intensity weakened as a result of absorption,  $I_\theta$ . The elementary weakening of intensity  $I_{\theta,\lambda}$  as a result of passage through an absorbing but not emitting medium along a direction  $r$ , forming an angle  $\theta$  with the direction of the normal  $h$ , will be

STAT

$$dI_{\theta,\lambda} = -\alpha_\lambda I_{\theta,\lambda} dr,$$

or

$$dI_{\theta,\lambda} = -\alpha_\lambda I_{\theta,\lambda} \frac{pdh}{\cos\theta}.$$

After integrating this expression for  $h$  and  $\lambda$ , we obtain

$$I_\theta = \int_0^\infty I_{0,\theta,\lambda} e^{-\alpha_\lambda \frac{ph}{\cos\theta}} d\lambda. \quad (110)$$

Therefore,

$$R = 2\pi \int_0^\infty d\lambda \int_0^{\frac{\pi}{2}} I_{0,\theta,\lambda} e^{-\alpha_\lambda \frac{ph}{\cos\theta}} \cos\theta \sin\theta d\theta, \quad (111)$$

whence

$$D(u) = \frac{\int_0^\infty d\lambda \int_0^{\frac{\pi}{2}} I_{0,\theta,\lambda} e^{-\alpha_\lambda \frac{ph}{\cos\theta}} \cos\theta \sin\theta d\theta}{\int_0^{\frac{\pi}{2}} I_{0,\theta} \cos\theta \sin\theta d\theta}. \quad (112)$$

For the case of an absolutely black emitting surface, formula (112) is simplified. Inasmuch as emission intensity  $\epsilon_\lambda$  for black bodies is independent of the direction  $\theta$ , therefore, monochromatic flux  $E_\lambda = \pi\epsilon_\lambda$  and total flux  $E = \pi\epsilon$ .

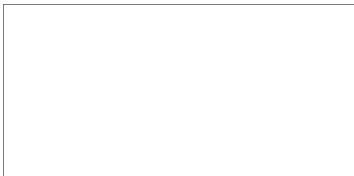
In substituting  $E_{0,\lambda}$  and  $E$  for  $I_{0,\theta,\lambda}$  and  $I_{0,\theta}$ , respectively, in (112), we obtain

$$D(u) = \frac{\int_0^\infty E_{0,\lambda} d\lambda \int_0^{\frac{\pi}{2}} e^{-\alpha_\lambda \frac{ph}{\cos\theta}} \cos\theta \sin\theta d\theta}{E_0 \int_0^{\frac{\pi}{2}} \cos\theta \sin\theta d\theta}, \quad (113)$$

or

$$D(u) = \frac{2}{E_0} \int_0^\infty E_{0,\lambda} H_2(\alpha_\lambda u) d\lambda. \quad (114)$$

For parallel radiation ( $\theta = 0$ )



STAT

$$\bar{D}(u) = \frac{1}{E_0} \int_0^{\infty} E_{0,\lambda} e^{-\alpha \lambda} d\lambda. \quad (115)$$

The transparency functions for diffuse (propagating in all directions) radiation  $D(u)$  and parallel  $\bar{D}(u)$  are associated by the following relationship

$$D(u) = \int_0^{\frac{\pi}{2}} \bar{D}\left(\frac{u}{\cos \theta}\right) \sin 2\theta d\theta. \quad (116)$$

After having used the afore-mentioned Ambartsumyan-Lebedinskiy integration method for (114) and (115), we obtain

$$D(u) = 2 \int_0^{\infty} \omega(\alpha, T) H_3(\alpha u) d\alpha, \quad (117)$$

$$\bar{D}(u) = \int_0^{\infty} \omega(\alpha, T) e^{-\alpha u} d\alpha. \quad (118)$$

Since

$$\frac{dH_n(x)}{dx} = -H_{n-1}(x),$$

therefore

$$D'(u) = -2 \int_0^{\infty} \alpha \omega(\alpha, T) H_2(\alpha, u) d\alpha. \quad (119)$$

In (117) and (118) the author discards the relationship between the transparency function and the temperature of the emitting layer. The reasons for this omission will be explained below.

The transparency functions for the fluxes of radiation from an absolutely black surface can be used to write expressions (106)-(108) in a more simplified form:

$$A(m) = - \int_m^M D'(\tau - m) E(\tau) d\tau, \quad (120)$$

$$B(m) = - \int_0^m D'(m - \tau) E(\tau) d\tau - (1 - \delta) \int_0^M D'(m + \tau) E(\tau) d\tau + \delta D(m) E(0), \quad (121)$$

$$S(m) = S_0 \bar{D}_s \left( \frac{M-m}{\cos \theta} \right) \cos \theta. \quad (122)$$

where  $\bar{D}_s$  is a function of the penetration of solar radiation.

Inasmuch as accurate analytic formulas for the transparency function are not available (instead, they are usually given in the form of graphs or tables), it is expedient to integrate (120) and (121) partially:

$$A(m) = E(m) - E(M) D(M-m) + \int_m^M D(\tau-m) \frac{dE}{d\tau} d\tau, \quad (123)$$

$$B(m) = E(m) - (1-\delta) E(M) D(M+m) + (1-\delta) \int_0^M D(\tau+m) \frac{dE}{d\tau} d\tau - \int_0^m D(m-\tau) \frac{dE}{d\tau} d\tau. \quad (124)$$

Now the problem consists in setting up functions of the penetration for atmospheric and solar radiations on the basis of experimental data pertaining to parallel radiation fluxes. The method of constructing the  $\bar{D}(u)$  for water vapor is described in detail in [40].

Absorption by carbon dioxide is significant only within the range of 13 to 17 microns. In order to take this into account, the penetration function should be written in the following form:

$$\bar{D}(u, u_0) = \frac{1}{E} \left[ \int_0^{13} E_\lambda e^{-\tau_\lambda u} d\lambda + \int_{13}^{17} E_\lambda e^{-\tau_\lambda u - \epsilon_\lambda^c u_c} d\lambda + \int_{17}^{\infty} E_\lambda e^{-\tau_\lambda u} d\lambda \right], \quad (125)$$

or

$$\bar{D}(u, u_c) = \bar{D}_{H_2O}(u) - \bar{D}_{13}^{17} b_{13}^{17} + \bar{D}_{13}^{17} \frac{\int_{13}^{17} E_\lambda e^{-\tau_\lambda u_c} d\lambda}{E}, \quad (126)$$

inasmuch as in the 13-17 micron range the absorption lines in the water-vapor spectrum are weak and the penetration in it will be represented with sufficient accuracy by the exponential law ( $u_c$  is quantity of carbon dioxide on the path of the ray).

The integral in the last term of (126) may be expressed by the function of the absorption by carbon dioxide of the total black-body radiation  $\bar{A}_{CO_2}$  in the corresponding range of wave lengths.

STAT

$$\int_{13}^{17} E_{\lambda} e^{-\epsilon_{\lambda} u_c} d\lambda = E(b_{13}^{17} - \bar{A}_{CO_2}), \quad (127)$$

since

$$\bar{A}_{CO_2} \approx \frac{\int_{13}^{17} E_{\lambda} d\lambda - \int_{13}^{17} E_{\lambda} e^{-\epsilon_{\lambda} u_c} d\lambda}{E} = b_{13}^{17} - \frac{\int_{13}^{17} E_{\lambda} e^{-\epsilon_{\lambda} u_c} d\lambda}{E}. \quad (128)$$

In substituting (126) into (127) we obtain

$$\bar{D}(u_1, u_c) = \bar{D}_{H_2O}(u) - \bar{D}_{13}^{17}(u) \bar{A}_{CO_2}. \quad (129)$$

The  $\bar{A}_{CO_2}(u_c)$  function was constructed by Möller [73] on the basis of experimental data.

In order to express (129) by only one variable - effective humidity  $m$  - there has been established a relationship between the effective humidity and the effective quantity of  $CO_2$  in the atmosphere (associated with each other by baric pressure  $p$ , if it is assumed that the relative concentration of  $CO_2$  is independent of altitude).

The graph of the  $\bar{D}_{H_2O} + CO_2(m)$ -function is satisfactorily approximated by the formula

$$\bar{D}(m) = Q_1 e^{-q\sqrt{m}} + P_1 e^{-p\sqrt{m}},$$

where  $Q_1 = 0.471$ ;  $q = 0.54$ ;  $P_1 = 0.529$ ; and  $p = 6.94$ .

In substituting the thus found  $\bar{D}(m)$  into formula (116) we obtain the transparency function for diffuse radiation

$$D(m) = QH_s(q\sqrt{m}) + PH_s(p\sqrt{m}), \quad (130)$$

where  $Q = 1.884$ ;  $q = 0.54$ ;  $P = 2.116$ ; and  $p = 6.94$

In the determination of the transparency function for solar radiation, its weakening is taken into account only with respect to selective absorption; scattering and nonselective absorption are ignored. Of the numerous empirical formulas providing a relationship between absorbed solar radiation  $W$  and the quantity of water vapor in

STAT



the atmosphere  $u$ , the following formula, derived by V.G. Kastrov [14], was used:

$$W = 0.156u^{0.294} \text{ calories/square centimeter minute.}$$

If solar radiation at the upper boundary of the atmosphere is  $W_0$ , then

$$\bar{D}_s(u) = \frac{W_0 - W}{W_0}, \quad (131)$$

whence

$$\bar{D}_s(u) = 1 - v^2,$$

where  $v = 0.081$ ;  $\eta = 0.294$  when  $I_0 = 1.91$  calories/square centimeter minute.

A certain limitation of the transparency function so-obtained is the ignoring of its relationship to the temperature of the radiation source.

In effect, it follows from the definition

$$\bar{D}(u) = \frac{\int_0^{\infty} E_{\lambda T} e^{-\lambda u} d\lambda}{E_T}$$

that  $\bar{D}(u)$  is independent of the temperature of the emitting substance  $T$  only for "grey-body" absorption. This does not apply to selective absorption in the atmosphere.

A change in the temperature of the emitting body causes a displacement of the energy distribution curve in the radiation spectrum of an absolutely black body, according to Wien's law. However, the known experiments and calculations lead to only a qualitative conclusion about the decrease of absorption with an increase in the emitting body temperature  $T$ , which is inadequate for obtaining the quantitative characteristics [20]. Moreover, absorption increases with an increase in temperature owing to the increase in the intensity of the absorption bands. These two processes compensate each other to a major extent. In any case, the difference in both corrections lies within the limits of the determination of radiation fluxes in the atmosphere.

With an increase of pressure and a decrease in air temperature, the individual absorption bands in the spectrum increase in their half-width<sup>1</sup> in which connection the integral intensity of the line remains unchanged but its form (contour) does vary.

1 Half-width is the name used for the distance from the center of the line at which its intensity decreases by half.

As a result, with a decrease in pressure, absorption increases more in the center of the line, whereas on the line flanks the  $\alpha_\lambda$  may even decrease.

For different wave lengths the transition from absorption in line center to absorption on line flanks occurs with varying thicknesses of the layer of the absorbing substance, owing to the extremely great differences in their absorption coefficients. This leads to a complex combination of the processes of increase and decrease in absorption with variation of air pressure. In a layer of sufficient thickness the decrease in pressure leads to a decrease in absorption. But theory and experiment provide differing quantitative characteristics of this relationship. It follows from the majority of experiments that the absorption coefficients for  $H_2O$  vary proportionately to  $\sqrt{p}$ . Lorentz's theory of the expansion of spectral lines during collisions establishes a relationship between the absorption coefficient and the first power of pressure  $p$ . Goody assumes a proportionality to  $p$  with respect to  $CO_2$ , [58]. With respect to  $H_2O$ , Möller assumes a more complex relationship with  $p$  [69]. Therefore, the relationship between  $k_\lambda$  and  $\sqrt{p}$  as assumed by Shekhter for both absorbing substances -  $H_2O$  and  $CO_2$  - is not convincing.

The works of S. Ye. Kuznetsov [21, 22] occupy a special place among the studies determining the temperature of the earth's atmosphere. In his works, attention is focused chiefly on a thorough theoretical investigation of the processes of the radiative transfer of heat. Kuznetsov has developed methods of integrating the equations of transfer, by taking into account the influence of horizontal surfaces of discontinuity, the albedo of clouds and the dissipation of radiant energy. However, so far quantitative calculations were made solely for a "grey-body" atmosphere characterized by one or two absorption coefficients. This is due to the unwieldiness of the developed method of calculation.

STAT

Climatological Studies of the Heat Balance of the  
Atmosphere. The Earth's Albedo.

The solution of the problem of the thermal regime of the atmosphere is closely related to the investigation of the various components of heat balance at the earth's surface. The income - outgo thermal processes which are determined by these characteristics of the balance, by being decisive in many diverse manifestations of physical-chemical and biological life on the earth, also are responsible for certain fundamental spatial and temporal features of the temperature field of the atmosphere. Therefore, the equation of heat balance is employed as a boundary condition in all theoretical problems regarding the determination of the temperature of the atmosphere.

Some of the components of the heat balance include the sought-for function - temperature of the atmosphere  $T$  (effective radiation, turbulent heat flux), and therefore, generally speaking, they can be determined directly, theoretically together with  $T$ . The remaining components - heat losses to evaporation and heat flux into the soil - should be given (a priori) if the theoretical problem of the heat exchange in the atmosphere is not resolved in conjunction with the problem of moisture exchange and of temperature distribution in the soil. The heat-balance characteristics are thus necessary for verifying the reliability of the theoretical calculations of temperatures, and in addition they may be assumed as parameters for the appropriate research problems. Hence, the distinct importance of developing and perfecting the methods of both the direct, experimental measurements of the heat balance and the indirect determination of the components of that balance by means of large scale observational data for the principal meteorological elements.

The problem of investigating the heat balance of the earth's surface was set-up, first by A.I. Voyeykov (1884). Subsequently, S.I. Savinov and V.V. Shuleykin made a major contribution to the advancement of climatological research in the heat balance. Particular attention has been turned to this problem in the last 10-20 years.

In particular, the (I.A. Voyeykov) Central Geophysical Observatory had completed in 1953 a climatological study of the heat balance of the earth's surface, the

STAT

purpose of which was the perfection of methods of computing the components of that balance and of compiling appropriate charts and the corresponding map for both the sea and land surfaces [10]. In these studies, special attention was given to the development of methods of independent determination of all components of the heat balance, for evaluating the accuracy of the completed calculations according to the completion of the equation of balance [9].

As a result, it was found possible to plot, for the first time in the world literature, the following maps of the components of the radiation and heat balances:

- (a) Total radiation on the earth's surface - monthly and annual charts or maps.
- (b) Radiation balance of earth's surface - monthly and annual charts or maps.
- (c) Heat losses to evaporation - annual map for land surface and monthly charts for ocean surfaces.
- (d) Turbulent exchange of heat between the surface interfaces (underlying surfaces) and the atmosphere - annual map for land surface and monthly charts for ocean surfaces.
- (e) Annual chart of the quantity of the heat received or lost by the surface of the oceans, in connection with the effect of sea currents.

Altogether, a total of 53 charts and maps of the components of the radiation and heat balances were plotted.

Let us dwell very briefly on the methods employed in determining the components of the heat balance in plotting these charts (maps) by referring the reader to articles [10], [11] for further details.

The equation of the heat balance of the surface interface (underlying surface) was written in the following form:

$$R + LF + P + U = 0 \quad (132)$$

Here R is the radiation balance of the surface interface (underlying surface); LF is loss of heat to evaporation, P is turbulent exchange of heat between the underlying surface and the atmosphere, and U is exchange of heat between the underlying surface and the underlying layers.

In connection with the form of equation adopted above, all terms in the balance STAT

(which yields  $E = \pi e$  for radiation by an absolutely black body), we obtain

$$A_*(m) = 2 \int_m^M \omega(\alpha, \tau) E(\tau) d\tau \int_0^{\frac{\pi}{2}} e^{-\alpha \frac{\tau-m}{\cos \theta}} \sin \theta d\theta, \quad (101)$$

$$B_*(m) = 2 \int_0^m \alpha \omega(\alpha, \tau) E(\tau) d\tau \int_0^{\frac{\pi}{2}} e^{-\alpha \frac{m-\tau}{\cos \theta}} \sin \theta d\theta + \\ + 2(1-\delta) \int_0^M \alpha \omega(\alpha, \tau) E(\tau) d\tau \int_0^{\frac{\pi}{2}} e^{-\alpha \frac{m+\tau}{\cos \theta}} \sin \theta d\theta + \\ + 2\delta \omega(\alpha, 0) E(0) \int_0^{\frac{\pi}{2}} e^{-\frac{\alpha m}{\cos \theta}} \sin 2\theta d\theta. \quad (102)$$

Here are introduced the standard meteorological designations A and B for the respectively downward-and-upward-directed fluxes of long-wave radiation.  $A_*$  and  $B_*$  are fluxes satisfying condition (95).

Into expressions (101) and (102) Gold's function is introduced in accordance with the following relation

$$H_{\frac{1+\beta+\gamma}{\gamma}} = \gamma \int_0^{\frac{\pi}{2}} e^{-\frac{q}{\cos \theta}} \cos^{\beta} \theta \sin \theta d\theta \\ (\gamma > 0, \beta > -(1+\gamma), q > 0)$$

after which, these expressions assume the following form:

$$A_*(m) = 2 \int_m^M \alpha \omega(\alpha, \tau) E(\tau) H_2[\alpha(\tau-m)] d\tau, \quad (103)$$

$$B_*(m) = 2 \int_0^m \alpha \omega(\alpha, \tau) E(\tau) H_2[\alpha(m-\tau)] d\tau + \\ + 2(1-\delta) \int_0^M \alpha \omega(\alpha, \tau) E(\tau) H_2[\alpha(m+\tau)] d\tau + \\ + 2\delta \omega(\alpha, 0) E(0) H_2(\alpha m). \quad (104)$$

Inasmuch as

$$A = \int_0^{\infty} A_* d\alpha, \quad B = \int_0^{\infty} B_* d\alpha \quad (105)$$

and  $\alpha$ , and  $\tau$  are independent variables, we obtain the following expressions for

STAT

total fluxes:

$$A(m) = \int_m^M E(\tau) d\tau \int_0^\infty 2\alpha\omega(\alpha, \tau) H_2[\alpha(\tau - m)] d\alpha, \quad (106)$$

$$B(m) = \int_0^m E(\tau) d\tau \int_0^\infty 2\alpha\omega(\alpha, \tau) H_2[\alpha(m - \tau)] d\alpha + \\ + (1 - \delta) \int_0^M E(\tau) d\tau \int_0^\infty 2\alpha\omega(\alpha, \tau) H_2[\alpha(m + \tau)] d\alpha + \\ + \delta E(0) \int_0^\infty 2\omega(\alpha, 0) H_2(\alpha m) d\alpha. \quad (107)$$

Owing to the great distance between the sun and the earth it may be assumed that direct solar radiation passes through the atmosphere in parallel bands of rays. Therefore, the integration of (98) for  $m$  and  $\alpha$  yields under the second condition, (100):

$$S_0(m) = S_0 \int_0^\infty \eta(\alpha, m) e^{-\alpha \frac{M-m}{\cos \theta}} d\alpha. \quad (108)$$

By definition, the transparency function  $D(u)$  is equal to the ratio of the outgoing flux  $R$  from a layer of  $h$  thickness to the incoming flux  $R_0$  into that layer ( $u = \rho h$  is mass of absorbing substance in a column with a unit cross-section perpendicular to the emitting surface).

If  $I_{0,\theta}$  is the total intensity of radiation (summed up for all wave lengths) in the direction of  $\theta$ , of isothermal plane adjacent to the homogeneous layer of the absorbing substance with a thickness,  $h$ , then the total incoming flux  $R_0$  entering that layer will be

$$R_0 = 2\pi \int_0^{\frac{\pi}{2}} I_{0,\theta} \cos \theta \sin \theta d\theta. \quad (109)$$

The magnitude of the total outgoing flux will be obtained if we substitute the initial intensity  $I_{0,\theta}$  in (109) by the intensity weakened as a result of absorption,  $I_\theta$ . The elementary weakening of intensity  $I_{\theta,\lambda}$  as a result of passage through an absorbing but not emitting medium along a direction  $r$ , forming an angle  $\theta$  with the direction of the normal  $h$ , will be

$$dI_{\theta,\lambda} = -\alpha_\lambda I_{\theta,\lambda} dr,$$

or

$$dI_{\theta,\lambda} = -\alpha_\lambda I_{\theta,\lambda} \frac{r dh}{\cos \theta}.$$

After integrating this expression for  $h$  and  $\lambda$ , we obtain

$$I_\theta = \int_0^\infty I_{0,\theta,\lambda} e^{-\alpha_\lambda \frac{r h}{\cos \theta}} d\lambda. \quad (110)$$

Therefore,

$$R = 2\pi \int_0^\infty d\lambda \int_0^{\frac{\pi}{2}} I_{0,\theta,\lambda} e^{-\alpha_\lambda \frac{r h}{\cos \theta}} \cos \theta \sin \theta d\theta, \quad (111)$$

whence

$$D(u) = \frac{\int_0^\infty d\lambda \int_0^{\frac{\pi}{2}} I_{0,\theta,\lambda} e^{-\alpha_\lambda \frac{r h}{\cos \theta}} \cos \theta \sin \theta d\theta}{\int_0^{\frac{\pi}{2}} I_{0,\theta} \cos \theta \sin \theta d\theta}. \quad (112)$$

For the case of an absolutely black emitting surface, formula (112) is simplified. Inasmuch as emission intensity  $\epsilon_\lambda$  for black bodies is independent of the direction  $\theta$ , therefore, monochromatic flux  $E_\lambda = \pi \epsilon_\lambda$  and total flux  $E = \pi \epsilon$ .

In substituting  $E_{0,\lambda}$  and  $E$  for  $I_{0,\theta,\lambda}$  and  $I_{0,\theta}$ , respectively, in (112), we obtain

$$D(u) = \frac{\int_0^\infty E_{0,\lambda} d\lambda \int_0^{\frac{\pi}{2}} e^{-\alpha_\lambda \frac{r h}{\cos \theta}} \cos \theta \sin \theta d\theta}{E_0 \int_0^{\frac{\pi}{2}} \cos \theta \sin \theta d\theta}, \quad (113)$$

or

$$D(u) = \frac{2}{E_0} \int_0^\infty E_{0,\lambda} H_2(\alpha_\lambda u) d\lambda. \quad (114)$$

For parallel radiation ( $\theta = 0$ )

STAT

$$\bar{D}(u) = \frac{1}{E_0} \int_0^{\infty} E_{0,\lambda} e^{-u\lambda} d\lambda. \quad (115)$$

The transparency functions for diffuse (propagating in all directions) radiation  $D(u)$  and parallel  $\bar{D}(u)$  are associated by the following relationship

$$D(u) = \int_0^{\frac{\pi}{2}} \bar{D}\left(\frac{u}{\cos \theta}\right) \sin 2\theta d\theta. \quad (116)$$

After having used the afore-mentioned Ambartsumyan-Lebedinskiy integration method for (114) and (115), we obtain

$$D(u) = 2 \int_0^{\infty} \omega(\alpha, T) H_3(\alpha u) d\alpha, \quad (117)$$

$$\bar{D}(u) = \int_0^{\infty} \omega(\alpha, T) e^{-\alpha u} d\alpha. \quad (118)$$

Since

$$\frac{dH_n(x)}{dx} = -H_{n-1}(x),$$

therefore

$$D'(u) = -2 \int_0^{\infty} \alpha \omega(\alpha, T) H_2(\alpha, u) d\alpha. \quad (119)$$

In (117) and (118) the author discards the relationship between the transparency function and the temperature of the emitting layer. The reasons for this omission will be explained below.

The transparency functions for the fluxes of radiation from an absolutely black surface can be used to write expressions (106)-(108) in a more simplified form:

$$A(m) = - \int_m^M D'(\tau - m) E(\tau) d\tau, \quad (120)$$

$$B(m) = - \int_0^m D'(m - \tau) E(\tau) d\tau - (1 - \delta) \int_0^M D'(m + \tau) E(\tau) d\tau + \delta D(m) E(0), \quad (121)$$



$$S(m) = S_0 \bar{D}_s \left( \frac{M-m}{\cos \theta} \right) \cos \theta. \quad (122)$$

where  $\bar{D}_s$  is a function of the penetration of solar radiation.

Inasmuch as accurate analytic formulas for the transparency function are not available (instead, they are usually given in the form of graphs or tables), it is expedient to integrate (120) and (121) partially:

$$A(m) = E(m) - E(M) D(M-m) + \int_m^M D(\tau-m) \frac{dE}{d\tau} d\tau, \quad (123)$$

$$B(m) = E(m) - (1-\delta) E(M) D(M+m) + (1-\delta) \int_0^m D(\tau+m) \frac{dE}{d\tau} d\tau - \int_0^m D(m-\tau) \frac{dE}{d\tau} d\tau. \quad (124)$$

Now the problem consists in setting up functions of the penetration for atmospheric and solar radiations on the basis of experimental data pertaining to parallel radiation fluxes. The method of constructing the  $\bar{D}(u)$  for water vapor is described in detail in [40].

Absorption by carbon dioxide is significant only within the range of 13 to 17 microns. In order to take this into account, the penetration function should be written in the following form:

$$\bar{D}(u, u_0) = \frac{1}{E} \left[ \int_0^{13} E_\lambda e^{-\tau_\lambda u} d\lambda + \int_{13}^{17} E_\lambda e^{-\tau_\lambda u - \epsilon_\lambda u_c} d\lambda + \int_{17}^{\infty} E_\lambda e^{-\tau_\lambda u} d\lambda \right], \quad (125)$$

or

$$\bar{D}(u, u_c) = \bar{D}_{H_2O}(u) - \bar{D}_{13}^{17} b_{13}^{17} + \bar{D}_{13}^{17} \frac{\int_{13}^{17} E_\lambda e^{-\tau_\lambda u_c} d\lambda}{E}, \quad (126)$$

inasmuch as in the 13-17 micron range the absorption lines in the water-vapor spectrum are weak and the penetration in it will be represented with sufficient accuracy by the exponential law ( $u_c$  is quantity of carbon dioxide on the path of the ray).

The integral in the last term of (126) may be expressed by the function of the absorption by carbon dioxide of the total black-body radiation  $\bar{A}_{CO_2}$  in the corresponding range of wave lengths.

STAT

$$\int_{13}^{17} E_{\lambda} e^{-\tau_{\lambda}^{u_c}} d\lambda = E(b_{13}^{17} - \bar{A}_{CO_2}), \quad (127)$$

since

$$\bar{A}_{CO_2} \approx \frac{\int_{13}^{17} E_{\lambda} d\lambda - \int_{13}^{17} E_{\lambda} e^{-\tau_{\lambda}^{u_c}} d\lambda}{E} = b_{13}^{17} - \frac{\int_{13}^{17} E_{\lambda} e^{-\tau_{\lambda}^{u_c}} d\lambda}{E}. \quad (128)$$

In substituting (126) into (127) we obtain

$$\bar{D}(u_1, u_c) = \bar{D}_{H_2O}(u) - \bar{D}_{13}^{17}(u) \bar{A}_{CO_2}. \quad (129)$$

The  $\bar{A}_{CO_2}(u_c)$  function was constructed by Möller [73] on the basis of experimental data.

In order to express (129) by only one variable - effective humidity  $m$  - there has been established a relationship between the effective humidity and the effective quantity of  $CO_2$  in the atmosphere (associated with each other by baric pressure  $p$ , if it is assumed that the relative concentration of  $CO_2$  is independent of altitude).

The graph of the  $\bar{D}_{H_2O} + CO_2(m)$ -function is satisfactorily approximated by the formula

$$\bar{D}(m) = Q_1 e^{-q\sqrt{m}} + P_1 e^{-p\sqrt{m}},$$

Where  $Q_1 = 0.471$ ;  $q = 0.54$ ;  $P_1 = 0.529$ ; and  $p = 6.94$ .

In substituting the thus found  $\bar{D}(m)$  into formula (116) we obtain the transparency function for diffuse radiation

$$D(m) = QH_s(q\sqrt{m}) + PH_s(p\sqrt{m}), \quad (130)$$

where  $Q = 1.884$ ;  $q = 0.54$ ;  $P = 2.116$ ; and  $p = 6.94$

In the determination of the transparency function for solar radiation, its weakening is taken into account only with respect to selective absorption; scattering and nonselective absorption are ignored. Of the numerous empirical formulas providing a relationship between absorbed solar radiation  $W$  and the quantity of water vapor in

STAT

the atmosphere  $u$ , the following formula, derived by V.G. Kastrov [14], was used:

$$W = 0.156u^{0.294} \text{ calories/square centimeter minute.}$$

If solar radiation at the upper boundary of the atmosphere is  $W_0$ , then

$$\bar{D}_s(u) = \frac{W_0 - W}{W_0}, \quad (131)$$

whence

$$\bar{D}_s(u) = 1 - v^2,$$

where  $v = 0.081$ ;  $\eta = 0.294$  when  $I_0 = 1.91$  calories/square centimeter minute.

A certain limitation of the transparency function so-obtained is the ignoring of its relationship to the temperature of the radiation source.

In effect, it follows from the definition

$$\bar{D}(u) = \frac{\int_0^\infty E_{\lambda T} e^{-\eta \lambda u} d\lambda}{E_T}$$

that  $\bar{D}(u)$  is independent of the temperature of the emitting substance  $T$  only for "grey-body" absorption. This does not apply to selective absorption in the atmosphere.

A change in the temperature of the emitting body causes a displacement of the energy distribution curve in the radiation spectrum of an absolutely black body, according to Wien's law. However, the known experiments and calculations lead to only a qualitative conclusion about the decrease of absorption with an increase in the emitting body temperature  $T$ , which is inadequate for obtaining the quantitative characteristics [20]. Moreover, absorption increases with an increase in temperature owing to the increase in the intensity of the absorption bands. These two processes compensate each other to a major extent. In any case, the difference in both corrections lies within the limits of the determination of radiation fluxes in the atmosphere.

With an increase of pressure and a decrease in air temperature, the individual absorption bands in the spectrum increase in their half-width<sup>1</sup> in which connection the integral intensity of the line remains unchanged but its form (contour) does vary.

<sup>1</sup> Half-width is the name used for the distance from the center of the line at which its intensity decreases by half.

As a result, with a decrease in pressure, absorption increases more in the center of the line, whereas on the line flanks the  $\alpha_\lambda$  may even decrease.

For different wave lengths the transition from absorption in line center to absorption on line flanks occurs with varying thicknesses of the layer of the absorbing substance, owing to the extremely great differences in their absorption coefficients. This leads to a complex combination of the processes of increase and decrease in absorption with variation of air pressure. In a layer of sufficient thickness the decrease in pressure leads to a decrease in absorption. But theory and experiment provide differing quantitative characteristics of this relationship. It follows from the majority of experiments that the absorption coefficients for  $H_2O$  vary proportionately to  $\sqrt{p}$ . Lorentz's theory of the expansion of spectral lines during collisions establishes a relationship between the absorption coefficient and the first power of pressure  $p$ . Goody assumes a proportionality to  $p$  with respect to  $CO_2$ , [58]. With respect to  $H_2O$ , Möller assumes a more complex relationship with  $p$  [69]. Therefore, the relationship between  $k_\lambda$  and  $\sqrt{p}$  as assumed by Shekhter for both absorbing substances -  $H_2O$  and  $CO_2$  - is not convincing.

The works of S. Ye. Kuznetsov [21, 22] occupy a special place among the studies determining the temperature of the earth's atmosphere. In his works, attention is focused chiefly on a thorough theoretical investigation of the processes of the radiative transfer of heat. Kuznetsov has developed methods of integrating the equations of transfer, by taking into account the influence of horizontal surfaces of discontinuity, the albedo of clouds and the dissipation of radiant energy. However, so far quantitative calculations were made solely for a "grey-body" atmosphere characterized by one or two absorption coefficients. This is due to the unwieldiness of the developed method of calculation.

STAT

Climatological Studies of the Heat Balance of the  
Atmosphere. The Earth's Albedo.

The solution of the problem of the thermal regime of the atmosphere is closely related to the investigation of the various components of heat balance at the earth's surface. The income - outgo thermal processes which are determined by these characteristics of the balance, by being decisive in many diverse manifestations of physical-chemical and biological life on the earth, also are responsible for certain fundamental spatial and temporal features of the temperature field of the atmosphere. Therefore, the equation of heat balance is employed as a boundary condition in all theoretical problems regarding the determination of the temperature of the atmosphere.

Some of the components of the heat balance include the sought-for function - temperature of the atmosphere  $T$  (effective radiation, turbulent heat flux), and therefore, generally speaking, they can be determined directly, theoretically together with  $T$ . The remaining components - heat losses to evaporation and heat flux into the soil - should be given (a priori) if the theoretical problem of the heat exchange in the atmosphere is not resolved in conjunction with the problem of moisture exchange and of temperature distribution in the soil. The heat-balance characteristics are thus necessary for verifying the reliability of the theoretical calculations of temperatures, and in addition they may be assumed as parameters for the appropriate research problems. Hence, the distinct importance of developing and perfecting the methods of both the direct, experimental measurements of the heat balance and the indirect determination of the components of that balance by means of large scale observational data for the principal meteorological elements.

The problem of investigating the heat balance of the earth's surface was set-up, first by A.I. Voyeykov (1884). Subsequently, S.I. Savinov and V.V. Shmileykin made a major contribution to the advancement of climatological research in the heat balance. Particular attention has been turned to this problem in the last 10-20 years.

In particular, the (I.A. Voyeykov) Central Geophysical Observatory had completed in 1953 a climatological study of the heat balance of the earth's surface, the

STAT

purpose of which was the perfection of methods of computing the components of that balance and of compiling appropriate charts and the corresponding map for both the sea and land surfaces 10. In these studies, special attention was given to the development of methods of independent determination of all components of the heat balance, for evaluating the accuracy of the completed calculations according to the completion of the equation of balance 9.

As a result, it was found possible to plot, for the first time in the world literature, the following maps of the components of the radiation and heat balances:

- (a) Total radiation on the earth's surface - monthly and annual charts or maps.
- (b) Radiation balance of earth's surface - monthly and annual charts or maps.
- (c) Heat losses to evaporation - annual map for land surface and monthly charts for ocean surfaces.
- (d) Turbulent exchange of heat between the surface interfaces (underlying surfaces) and the atmosphere - annual map for land surface and monthly charts for ocean surfaces.
- (e) Annual chart of the quantity of the heat received or lost by the surface of the oceans, in connection with the effect of sea currents.

Altogether, a total of 53 charts and maps of the components of the radiation and heat balances were plotted.

Let us dwell very briefly on the methods employed in determining the components of the heat balance in plotting these charts (maps) by referring the reader to articles 10, 11 for further details.

The equation of the heat balance of the surface interface (underlying surface) was written in the following form:

$$R + LF + P + U = 0. \quad (132)$$

Here R is the radiation balance of the surface interface (underlying surface); LF is loss of heat to evaporation, P is turbulent exchange of heat between the underlying surface and the atmosphere, and U is exchange of heat between the underlying surface and the underlying layers.

In connection with the form of equation adopted above, all terms in the balance STAT

characterizing the influx of heat to an active surface are positive, while all terms characterizing the expenditure of heat are negative.

The total radiation included in R, owing to the insufficient amount of data on actinometric observations, was calculated according to the Savinov-Ångström formula, which takes into account the influence of cloudiness on solar radiation. This method of calculating total radiation was verified according to all the available data on actinometric observations. It was found that the mean monthly values of total radiation are determined with a mean error of 10 percent, while its mean yearly values involve a mean error of less than 5 percent.

For determining the expenditure portion of the radiation balance - effective radiation, the formula obtained by E.M. Berlyand was used (it takes into account cloudiness, and the temperature difference between the underlying surface and the air). This formula is corroborated very well by the present large-scale measurements of effective radiation [4].

The methods of the climatological calculation of the loss of heat to evaporation and of the turbulent heat exchange differ for the conditions of the ocean and the land, owing to the difference in the available initial data.

The availability of data on the temperature of the surface of oceans makes it possible to employ the following experimental formula of V.V. Shuleykin in the calculations of heat loss to evaporation:

$$LF = -L_{av}(q^* - q).$$

Here  $\underline{v}$  is wind velocity,  $q^*$  is specific humidity of air saturated with water vapor at the water-surface temperature,  $q$  is specific humidity of air, and  $a$  is proportionality coefficient.

An analogous formula may be written, by means of Bowen's relations, for the turbulent exchange of heat between the ocean surface and the atmosphere:

$$P = -c_p a v (T_s - T).$$

STAT

where  $T_w$  and  $T$  are the temperatures of the water surface and of the air, respectively, (the latter is measured on a ship).

The coefficient  $\alpha$  was determined by means of the equation of heat balance written for the mean annual conditions of the entire universal ocean ( $U = 0$ ).

It follows from

$$R + LF + P = 0$$

that

$$\alpha = \frac{R}{Lv(q^* - q) + c_p v (T_w - T)}$$

For the calculation of the right-hand part of the above relation the authors had at their disposal detailed data for the entire territory of the universal ocean, except for the Arctic and Antarctic regions, which could not affect appreciably the accuracy of determining the  $\alpha$ , inasmuch as the area of these regions represents only 9 percent of the total area of the universal ocean. The assumption is that, in the plotting of schematic world charts, the possible variations in  $\alpha$  under various climatic conditions, may be ignored.

After determining the first three components of the heat balance, the last component - the magnitude of the heat exchange between the ocean surface and its lower layers - may be found as a remaining term of the equation of heat balance. For mean annual conditions, the magnitude of  $U$  proves to be equal to the influx or expenditure of heat as the result of the horizontal heat exchange related basically to the effect of sea currents. Despite the fact that  $U$  is determined with a maximum error (equal to the sum of the errors in determining all other components of the heat balance), on the chart of the mean annual magnitudes of this value there is a satisfactory correspondence noted between the areas of higher positive values (which corresponds to the influx of heat to the ocean surface) and warm currents, as well as between the areas of the lower negative values and cold currents.

The lack of large scale data on the temperature of soil surface and the influence of the humidification of the upper layers of the soil on evaporation make it impossible

STAT



to calculate LF and P for the land (continental) conditions by means of formulas as simple as those applied for oceanic conditions. For land, the mean annual totals of evaporation may be determined from the equation of the hydrological balance by means of data on the measurements of river run-off  $f$ , or if such data are not available, by means of various methods based on the relationships involving evaporation, precipitation and heat fluxes. The authors applied one of such methods - the "equation of relationship" - derived by M.I. Budyko from a combined analysis of the equations of the hydrological and heat balances [12]. This equation gives a relationship between the ratio of the mean annual evaporation to the precipitation  $\frac{F}{r}$  and the ratio of the radiation balance to the quantity of heat required for the complete evaporation of the annual total of precipitation  $\frac{R}{Lr}$ .

It is clear from the general representations that the mean totals of the evaporation from a land surface depend on both the quantity of precipitation  $r$  and the flux of radiation  $R$ .

With an increase in  $R$  and a decrease in  $r$  there is an increase in the dryness of the soil:  $f \rightarrow 0$  or  $\frac{F}{r} \rightarrow 1$  (since  $r = F + f$ ) when  $\frac{R}{Lr} \rightarrow \infty$ .

With sufficiently high totals of  $r$  and a sufficiently small  $R$ , a state of constant overhumidification of the top layer of the soil will be attained. But, even with these optimum conditions for evaporation  $F$  will always be  $< R$  (since the turbulent heat flux is always directed away from the earth's surface), and  $LF \rightarrow R$  or  $\frac{F}{r} \rightarrow 0$  when  $\frac{R}{Lr} \rightarrow 0$ .

Consequently, the following relation should exist between  $R$ ,  $r$  and  $F$ :

$$\frac{F}{r} = \Phi\left(\frac{R}{Lr}\right),$$

which is called the "equation of relationship".

These approximate calculations of evaporation are based on the mean latitudinal values of the radiation balance for the conditions of potentially possible evaporation (evaporability - for the humidified surface). As for areas for which run-off data was available, parallel calculations were made for the evaporation on the basis of STAT

the equation of the hydrological balance - which gave an entirely satisfactory agreement between the two methods.

The mean annual value of the turbulent heat exchange between the land surface and the atmosphere was determined as a residual term of the equation of heat balance.

The constructed annual maps (charts) can be used as the basis for determining the course of all the components of the heat balance. The corresponding values are cited in Table 5 which is copied from [10].

Map data were used with respect to areas between Latitude 60°N and Latitude 60°S. Data for arctic and antarctic areas were determined by supplementary approximate calculations.

The data in Table 5 and in the analogous table in [13] are the only data ever obtained on the basis of a complete and detailed climatological analysis of the equation of heat balance and of available observational data.

Table 5

Mean Latitudinal Values of the Components of Heat Balance  
(kilocalories/square centimeter year)

Latitude	Oceans					Inland				The Earth				
	S	R	LF	P	U	S	R	LF	P	S	P	LF	P	U
60-50°C	88	34	-34	-18	18	93	23	-19	-4	91	28	-25	-10	7
50-40	109	54	-51	-15	12	119	38	-22	-14	114	46	-36	-15	5
40-30	136	78	-73	-12	7	159	56	-26	-30	146	69	-53	-20	4
30-20	151	100	-85	-7	-8	184	64	-23	-41	163	86	-60	-20	-6
20-10	156	110	-89	-5	-16	182	74	-36	-38	163	101	-75	-14	-12
10-0	149	107	-76	-5	-26	149	79	-58	-21	149	101	-72	-9	-20
0-10 K	152	107	-81	-7	-19	143	75	-59	-16	150	99	-76	-9	-14
10-20	155	107	-97	-9	-1	161	69	-44	-25	156	99	-85	-13	-1
20-30	147	94	-87	-10	3	169	62	-29	-33	152	87	-74	-15	2
30-40	128	73	-77	-12	16	149	55	-29	-26	130	71	-72	-14	15
40-50	104	53	-57	-5	9	112	39	-24	-15	104	53	-55	-5	8
50-60	84	31	-37	-12	18	80	26	-18	-8	83	31	-37	-12	18
The Earth as a whole	128	77	-68	-9	0	132	46	-27	-19	129	68	-56	-12	0

STAT

The theoretical determination of the temperature field of the atmosphere requires not only the knowledge of heat-balance characteristics but also the knowledge of the reflectivity of the earth. In effect, the magnitude of the albedo of the earth-atmosphere system enters into the boundary condition for the flux of solar energy in the problem under review [see, e.g., eq. (45)].

The study of that value encounters many difficulties, and therefore up to the present the albedo has been determined only for individual underlying surfaces or for the planet as a whole.

The experimental determination of the value of the planetary albedo may be realized only by means of a body found outside the earth's atmosphere, because clouds make a major contribution of the earth's albedo, and their reflectivity varies greatly. Such measurements have been made by Danjon [51], who observed the moon by means of an appropriate photometer. The moon is illuminated by two light sources. The bright side of the moon is illuminated directly by the sun, while its dark side is illuminated by the earth. The light from the earth is solar light reflected by the earth. Consequently, the ratio of the brightness of the dark side of the moon to that of its bright side is a measure for the solar light reflected by the earth, i.e., a value of the earth's planetary albedo. However, photometric measurements can give the value of the albedo only in the visible portion of the spectrum - the so-called visual albedo. Such a procedure was also used by N.P. Barabashev [2] and M.S. Orlova [28] for obtaining the earth's albedo. Their measurements yielded 43 and 40 percent, respectively. According to the data accumulated by Danjon in the course of 9 years of photometric observations of the moon, the mean visual albedo of the earth was 39 percent. In order to make the transition from a visual albedo to a total energetic albedo it is necessary also to take into account the reflection of solar energy in the ultraviolet and infrared portions of the spectrum. Fritz's calculations gave for that value, 35 percent [56]. Somewhat different estimates of the total albedo were obtained earlier, during the selection of other values for the albedo of clouds and for the quantity of energy absorbed by the atmosphere and the clouds. Aldrich

STAT

obtained 43 percent [43], while Baur and Phillips obtained 41.5 percent [48].

In view of the insufficient accuracy of the methods of albedo determination used by various investigators, the divergence in their results by several percent is entirely permissible. For example, the determination of the visual albedo through photometric observations of the moon involves an error consisting in that the spectral composition of terrestrial light differs from the spectral composition of solar light owing to the selectivity of reflection from two surfaces - terrestrial and lunar. Likewise, the assumptions about the scattering capacity of the particles of dust and water vapor suspended in the atmosphere are also indeterminate. The value obtained by Fritz probably should be considered as too low, since he cited a mean value (low mean value of 2-3 percent) two to three percent too low for the albedo of the earth's surface, because he did not take into account the distribution of land (continents) and oceans.

We cannot remain satisfied with knowing only the mean value of the planetary albedo. For theoretical calculations it is necessary to have a concept of the geographical distribution of the albedo of the earth-atmosphere system and of its temporal course. The most complete study of this problem was made by A.I. Fedoseyeva [37]. Using the published information about the albedo of various underlying surfaces, duration of the vegetative period, dates of the establishment and the disappearance of the snow cover, limit of ice (sea), distribution of cloudiness, etc., she succeeded in constructing 12 monthly tables of the latitudinal and longitudinal distribution of the albedo and, on their basis, four charts for the most indicative months.

Fig. 9 illustrates the latitudinal course of the albedo for January, July, and the year as a whole. Only the calculations for the zones of Latitude 30-90°N and 70-90°S are omitted, owing to the lack of adequate data on cloudiness. The mean annual value of the planetary albedo was obtained at 41 percent, which, within the limits of accuracy of the calculations made agrees quite satisfactorily with the results obtained by other investigators.

STAT

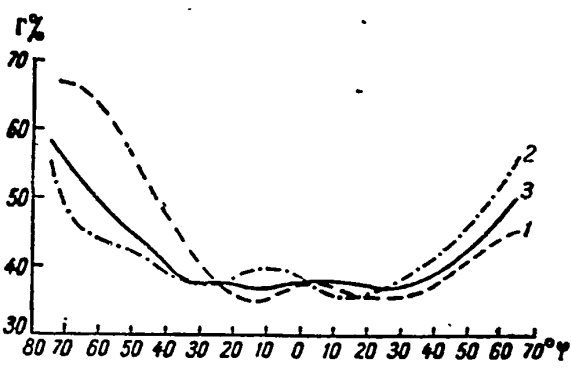


Fig. 9. Latitudinal Course of Zonal Magnitudes of the Albedo of the Earth-Atmosphere System for January (1), July (2) and the Year (3), according to A.I. Fedoseyeva.

STAT

## Chapter II

## THE ZONAL THERMAL FIELD OF THE ATMOSPHERE.

The Setting-up and the Solution of the Problem of the Zonal and Nonzonal  
Distribution of Temperature in the Atmosphere.

The survey of the studies of the heat regime in the atmosphere leads quite definitely to the conclusion that a physically well-founded theory of temperature distribution in the atmosphere cannot be framed without taking into account the entire complex whole of the fundamental factors determining the thermal state of the atmosphere. This entails the necessity of posing and solving the problem of thermal structure of the atmosphere on the planetary scale as comprehensively as is possible at the present time.

This Chapter describes a solution of the problem concerning the stationary zonal distribution of temperature, averaged over large intervals of time.

The following should obviously be included among the primary factors for determining such a distribution of temperature:

1. Radiation heat fluxes. Essential are: latitudinal distribution of solar radiation; latitudinal distribution of the albedo conditioned by the reflectivity of the clouds, the underlying surface and the atmosphere; selectivity of the absorption of solar radiation in the atmosphere; and selectivity of the absorption and diffusivity of the propagation of long-wave radiation.
2. Turbulent heat fluxes - the vertical and the horizontal. Here there is no foundation for taking into account the latitudinal changes in turbulence characteristics [e.g., the coefficient of horizontal turbulence varies within the limits of  $(3.8-3.1) \cdot 10^6$  square meters/second<sup>2</sup>].
3. Quantities of heat associated with condensation and evaporation. It is necessary to take into account the change in the quantity of the condensing and evaporating moisture with change in latitude, since this change is considerable.
4. Distribution of water vapor and carbon dioxide in the atmosphere. Since

radiation is absorbed and emitted principally by water vapor and CO<sub>2</sub>, it is necessary to take into account the relationship between the optical mass of the atmosphere and latitude. The density of water vapor at the earth's surface varies from the equator to the pole at the rate of 20 to 1.5 grams per cubic meter.

These factors are considered in the problem described below, insofar as possible.

It is assumed, in accordance with K. Ya. Kondrat'yev's research [19a], that ozone does not affect the thermal state of the atmosphere below the 16-kilometer altitude.

During the calculations special attention was given to the experimental and physical substantiation of the values of the required parameters.

Thus, the thermal regime of the atmosphere will be investigated here in a climatological cross-section - for long intervals of time and extensive spatial areas.

Let us consider what climatological data may be used for comparing the calculated values of zonal temperatures with the actually observed values. Although the network of meteorological stations has collected extensive temperature data, only a comparatively minor part of that information has been subjected to generalizing climatological processing for the entire northern hemisphere. Basically, this information represents tables and maps of mean monthly temperatures of air at the earth's surface, since the availability of data is well ensured here - the longest sequences of observations and the greatest number of stations.

In the "World Agroclimatological Handbook" [27] are cited the mean monthly air temperatures at the earth's surface for the meteorological stations of the northern hemisphere. The works of Ye. S. Rubinshteyn [34] deserve special attention for air temperature determinations over the USSR. She processed data from 1,000 stations of which only about 12 percent had observational series of less than 10 years. The "Great Soviet World Atlas" [8] contains world charts of mean air temperatures at sea level for January and July, compiled by Ye. S. Rubinshteyn. For the "Marine Atlas" [25] such charts were compiled by V. Ya. Sharova and I.A. Berlin; on which are recorded the deviations of mean air temperatures in January and July from their mean latitudinal

STAT

values. Maps of the surface (air) temperatures for each month are found in [68].

As for the studies concerned with the climatological processing of observations of temperature in the free atmosphere, their number is even smaller. Here only the "Climatological Atlas of the Northern Hemisphere" [85] can be cited.

It is necessary to keep in mind that temperature data provided by various investigators may differ by several degrees owing to the heterogeneity of the material used by them. This can be revealed, e.g., by comparing the corresponding maps in [25, 68].

The initial equation in our problem is the equation of the heat influx to a unit volume of air

$$c_p \rho_0 \frac{dT}{dt} - A \frac{dp}{dt} = \epsilon. \quad (1)$$

In application to the problem in question, eq. (1) can be simplified. In effect, in the individual derivative  $\frac{dp}{dt}$ ; the local change in pressure  $\frac{\partial p}{\partial t} = 0$ , is for stationary conditions; the sum of the advective terms also turns to zero with geostrophic conditions.

We obtain instead of (1)

$$c_p \rho_0 \frac{dT}{dt} - A w \frac{\partial p}{\partial z} = \epsilon. \quad (2)$$

In the problem concerning the stationary distribution of temperature  $T$ , the latter can always be represented in the form of the sum of two terms which are the functions of spatial coordinates; we shall select the spherical coordinates as such coordinates: latitude  $\varphi$ , longitude  $\lambda$  and altitude  $z$ .

$$T(\varphi, \lambda, z) = \bar{T}(\varphi, z) + T'(\varphi, \lambda, z). \quad (3)$$

The first term  $\bar{T}(\varphi, z)$  represents the so-called zonal temperature, averaged by latitude.  $T'(\varphi, \lambda, z)$  gives the deviation of temperature at a given point in space from its corresponding zonal value. This deviation may be called spatial anomaly of temperature.

STAT



In substituting (3) into (2) we obtain two equations. One for determining zonal temperatures  $\bar{T}$ , and the other for determining deviations  $T'$ :

$$c_p \rho_a \left[ \frac{v_\theta}{a_0} \frac{\partial}{\partial \theta} T + \frac{v_\lambda}{a_0 \sin \theta} \frac{\partial}{\partial \lambda} (\bar{T} + T') + w \frac{\partial}{\partial z} T \right] - A w \frac{\partial p}{\partial z} = \bar{\epsilon} + \epsilon' \quad (4)$$

where  $\bar{\epsilon}(\varphi, z)$  — is the portion of the heat influx creating the zonal distribution of temperature,  $\epsilon'(\varphi, \lambda, z)$  — is the part of heat influx responsible for  $T'$ , and  $\frac{\partial \bar{T}}{\partial \lambda} = 0$  according to (3).

The term containing  $\frac{\partial T}{\partial \lambda}$  should be related to the equation for determining  $T'$ , inasmuch as it is a function of longitude; the same pertains also to the terms containing  $w$  ( $w = 0$  for a strictly zonal circulation).

Therefore, eq. (4) gives for zonal temperatures

$$w = 0 \quad (5)$$

and for spatial anomalies

$$c_p \rho_a \left[ \frac{v_\lambda}{a_0 \sin \theta} \frac{\partial}{\partial \lambda} T' + \frac{v_\theta}{a_0} \frac{\partial}{\partial \theta} T' + w \frac{\partial}{\partial z} T' \right] - A w \frac{\partial p}{\partial z} = \epsilon' \quad (6)$$

where  $v_\lambda$  and  $v_\theta$  are the latitudinal and longitudinal components of wind velocity, respectively;  $\theta = 90^\circ - \varphi$ ,  $a_0$  — is the earth's radius;  $\rho_a$  is air density; and  $A$  is the thermal equivalent of work.

Let us now determine zonal temperatures  $\bar{T}$ .

The heat influx  $\bar{\epsilon}$  towards a certain mass of air in the earth's atmosphere is realized by: (1) transfer of long-wave and short-wave radiation; (2) turbulent transfer of heat; and (3) influx of heat associated with phase transformations of water.

The above-indicated portions of the total heat influx  $\bar{\epsilon}$  will be designated correspondingly as  $\epsilon_1$ ,  $\epsilon_2$ ,  $\epsilon_3$ . By definition

$$\epsilon_1 = -\text{div} R \quad (7)$$

$$\dot{\epsilon}_2 = -\operatorname{div} P, \quad (8)$$

$$\dot{\epsilon}_2 = LQ. \quad (9)$$

Here  $R$  and  $P$  are radiative and turbulent heat fluxes, respectively;  $L$  is latent heat of condensation (vaporization); and  $Q$  is the quantity of condensed water vapor (evaporated water). The signs (—) in (7) and (8) denote that the divergence in heat fluxes leads to the cooling of the air particle.

Inasmuch as the change in the radiation properties of the atmosphere occurs chiefly in the vertical direction (the scale of horizontal inhomogeneities is greater by two or three orders of magnitude than the scale of vertical ones), therefore

$$\operatorname{div} R = -\frac{\partial}{\partial x}(A - B + S), \quad (10)$$

where  $A$  and  $B$  are the fluxes of long-wave radiation passing through the area from an upper and lower hemisphere, respectively; and  $S$  is the flux of solar radiation.

The turbulent flux of heat  $P$  we shall consider proportional to the difference between the actual and the equilibrium temperature gradients, according to M. I. Yudin [42], i.e.,

$$P = -\lambda^* (-\nabla T + \beta), \quad (11)$$

where  $\lambda^*$  is coefficient of turbulent heat conduction, and  $\beta$  is equilibrium gradient of temperature.

Therefore,

$$\operatorname{div} P = -\frac{\partial}{\partial x} \lambda^* \left( \frac{\partial T}{\partial x} + \beta \right) - \frac{1}{\lambda_0^2 \sin \theta} \left( \frac{\partial}{\partial \theta} \sin \theta \lambda^* \frac{\partial T}{\partial \theta} + \frac{\partial \lambda^*}{\partial \lambda \sin \theta} \frac{\partial T}{\partial \lambda} \right). \quad (12)$$

inasmuch as the components of the equilibrium gradient  $\beta_x = \beta_y = 0$ .

Let us assume that the quantity of condensed water vapor  $Q$  is proportional to the density of water vapor

$$Q = \epsilon p. \quad (13)$$

Such an assumption is natural because from the equation of water vapor diffusion, an exponential distribution of  $\rho$  corresponding to the experimental data is obtained.

The drawback of this assumption consists in that the condensation of water vapor extends from a layer of clouds throughout the entire height of the atmosphere. However, inasmuch as  $\rho$  decreases rather rapidly with altitude, condition (13) cannot introduce any substantial error. At three to four kilometers above a condensation level  $z_1$ , the heat influx  $Q$  represents one fifth of its value on the  $z_1$  level, or the total quantity of moisture being condensed in the three to four kilometer layer exceeds four times the amount which is condensed above it.

Eq. (5) is thus written for zonal temperatures  $\bar{T}$ :

$$\frac{\partial}{\partial z}(A - B + S) + \frac{\partial}{\partial z} \lambda \left( \frac{\partial \bar{T}}{\partial z} + \beta \right) + \frac{1}{a_0^2 \sin^2 \theta} \frac{\partial}{\partial \theta} \sin \theta \lambda^2 \frac{\partial \bar{T}}{\partial \theta} + L \rho = 0. \quad (14)$$

The above equation is derived under the following boundary conditions. At the earth's surface, where  $z = 0$ , the equation of heat balance is satisfied

$$-\lambda \left( \frac{\partial \bar{T}}{\partial z} + \beta \right) = (A - B + S) - LF. \quad (15)$$

Here  $F$  is the quantity of moisture evaporating from a unit surface during a unit time; the fluxes of heat into the soil may be ignored, because they are small compared with  $LF$ .

At the upper boundary of the atmosphere, where  $z = \infty$  the turbulent heat flux  $P = 0$ .

On an average for a year, for the earth as a whole, this condition will correspond to the radiant equilibrium of the earth-atmosphere system.

Let us give the distribution of water vapor density with altitude in the conventional form:

$$\rho = \rho_0(\theta) e^{-\alpha z}. \quad (16)$$

In the zonal problem it is necessary to take into account only the latitudinal changes in  $\rho$ . Here it is assumed that the surface values of water vapor density

change with latitude, and that  $\alpha$  is independent of  $\theta$ , i.e., water vapor density decreases uniformly with altitude at all latitudes. Such an assumption can be made, because the relationship between the surface values of  $\rho$  and latitude is expressed much more explicitly than the relationship between  $\alpha$  and  $\theta$ .

Let us pass over from the vertical dimensional coordinate  $z$  to the dimensionless coordinate  $x$ :

$$x = \frac{1}{M} \int_0^{\infty} \rho dz. \quad (17)$$

where

$$M = \int_0^{\infty} \rho dz = \frac{p_0(\theta)}{\alpha}.$$

Then,

$$\rho = \rho_0(\theta) x.$$

From temperature  $T$  we now pass over to the function of emission  $E$ . Instead of eq. (14) we obtain

$$\begin{aligned} -\alpha x \frac{\partial}{\partial x} (A - B + S) + \alpha^2 x \frac{\partial}{\partial x} \frac{\lambda^r}{4\sigma T^2} \frac{\partial E}{\partial x} - \alpha x \frac{\partial}{\partial x} \lambda^r \beta + \\ + \frac{1}{\alpha_0^2 \sin \theta} \frac{\partial \lambda^r \sin \theta}{\partial \theta} \frac{\partial E}{4\sigma T^2} + L \rho_0(\theta) x = 0. \end{aligned} \quad (18)$$

Let us introduce the designations

$$N(x) = \frac{\alpha x \lambda^r}{4\sigma T^2}, \quad (19)$$

$$G(x) = \frac{\lambda^r}{4\sigma T^2 \alpha_0^2 x}. \quad (20)$$

Then, eq. (18), after being divided by  $\alpha x$  assumes the form:

$$\begin{aligned} -\frac{\partial}{\partial x} (A - B + S) + \frac{\partial}{\partial x} N(x) \frac{\partial E}{\partial x} - \frac{\partial}{\partial x} \lambda^r \beta + G(x) \frac{1}{\sin \theta} \frac{\partial}{\partial \theta} \sin \theta \frac{\partial E}{\partial \theta} + \\ + \frac{Lx}{\alpha} \rho_0(\theta) = 0. \end{aligned} \quad (21)$$

We shall seek for the function of emission  $E$  in the form of the series

STAT

$$E(x, \theta) = \sum_{n=0}^{\infty} E_n(x) P_n(\theta). \quad (22)$$

Here  $P_n(\theta)$  — is Legendre's polynomial of the  $n$ th power,  $E_n(x)$  is the  $n$ th harmonic of the dissociation (22). The following functions may be presented in the same manner:

$$\left. \begin{aligned} A(x, \theta) &= \sum_{n=0}^{\infty} A_n(x) P_n(\theta) \\ B(x, \theta) &= \sum_{n=0}^{\infty} B_n(x) P_n(\theta) \\ S(x, \theta) &= \sum_{n=0}^{\infty} S_n(x) P_n(\theta) \\ \rho_0(\theta) &= \sum_{n=0}^{\infty} \rho_n P_n(\theta) \\ LF &= \sum_{n=0}^{\infty} F_n P_n(\theta) \end{aligned} \right\} \quad (22')$$

Let us note that, in view of the properties of Legendre's polynomials

$$\frac{1}{\sin \theta} \frac{\partial}{\partial \theta} \sin \theta \frac{\partial E}{\partial \theta} = - \sum_{n=0}^{\infty} n(n+1) E_n(x) P_n(\theta).$$

Then, for the  $n$ th harmonic of the E-function, eq. (21) will assume the following form:

$$\begin{aligned} - \frac{d}{dx} (A_n - B_n + S_n) + \frac{d}{dx} N(x) \frac{dE_n}{dx} - \frac{d}{dx} \lambda' \beta - \\ - n(n+1) G(x) E_n + \frac{L_n}{\alpha} \rho_{0n} = 0 \end{aligned} \quad (23)$$

(the  $\beta$ -containing term is absent in the equations for  $n > 0$ .)

Let us resolve a two-layer problem.

In the first, quasistationary surface layer, the coefficient of the vertical turbulent heat conduction  $\lambda'$  increases linearly with altitude, while in the second layer, the free atmosphere,  $\lambda'$  is an arbitrary function of altitude.

The First Layer. By assumption

$$\lambda' = \lambda_0 + \beta z,$$

STAT

where  $\lambda_0$  is coefficient of molecular heat conduction, or

$$\lambda' = \lambda_0 - \frac{b}{a} \ln x.$$

For the quasistationary surface layer it may be assumed that its radiation balance does not change with altitude and that the horizontal turbulent exchange is considerably smaller than the vertical. This important circumstance has been demonstrated both theoretically and empirically [42, 5].

The influx of heat owing to condensation is equal to zero on an average for long intervals of time.

With the foregoing assumptions, eq. (23) is reduced to a simpler one:

$$\frac{d}{dx} \left[ N(x) \frac{dE_n}{dx} - \lambda' \beta \right] = 0, \quad (24)$$

in which

$$N(x) = \eta x \left[ \lambda_0 + \frac{b}{a} (1-x) \right], \quad (25)$$

inasmuch as  $\ln x \approx x-1$ , at  $x \approx 1$

$$\eta = \frac{a}{4\sigma T^3}.$$

Let us integrate eq. (24)

$$N(x) \frac{dE_n}{dx} - \lambda' \beta = \tilde{C}_{0n},$$

whence

$$\frac{dE_n}{dx} = \frac{1}{N(x)} \left[ \tilde{C}_{0n} + \lambda' \beta \right] = \frac{\tilde{C}_{0n}}{\eta \left[ \lambda_0 + \frac{b}{a} (1-x) \right] x} + \frac{\beta}{\eta x},$$

inasmuch as  $\lambda_n \ll 1$ ,  $x \approx 1$ , therefore

$$E_n = -\frac{\tilde{C}_{0n}}{\eta} \frac{a}{b} \ln \left[ \lambda_0 + \frac{b}{a} (1-x) \right] + \frac{\beta}{\eta} \ln x + \tilde{C}_{1n}. \quad (26)$$

The integration constant  $\tilde{C}_{0n}$  is determined from the equation of heat balance (15) at the earth's surface

STAT

$$\bar{C}_{1n} - (A_n - B_n + S_n)|_{x=1} + F_n = 0.$$

The constant  $\bar{C}_{1n}$  will be determined later from the condition of the continuity of the derivations of eq. (23) for the first and second layers.

The Second Layer  $\lambda'(x)$ .

Let us integrate eq. (23) from the altitude of the surface layer  $x_0$  up to a certain variable altitude  $x$

$$\begin{aligned} (A_n - B_n + S_n) - N(x) \frac{dE_n}{dx} + \lambda' \beta(x) + n(n+1) \int_{x_0}^x G(y) E_n dy - \\ - \frac{Lx}{n} \rho_{0n}(x - x_0) = (A_n - B_n + S_n)_{x=x_0} - N(x_0) \frac{dE_n}{dx} \Big|_{x=x_0} + \lambda' \beta(x_0). \end{aligned} \quad (27)$$

We obtained an equation of heat balance for the layer according to which the heat fluxes through the upper and lower boundaries of the layer are mutually equal.

Since for the surface layer of the atmosphere we assume that its radiation balance does not change with altitude, we find by means of the equation of heat balance for the earth's surface, that

$$\begin{aligned} (A_n - B_n + S_n)|_{x=x_0} = (A_n - B_n + S_n)_{x=1} = N(1) \frac{dE_n}{dx} \Big|_{x=1} - \\ - \lambda_0 \beta(1) + F_n \end{aligned}$$

and we thus rewrite eq. (27):

$$\begin{aligned} N(x) \frac{dE_n}{dx} = (A_n - B_n + S_n) + n(n+1) \int_{x_0}^x G(y) E_n dy - \\ - \frac{Lx}{n} \rho_{0n}(x - x_0) - F_n + \lambda' \beta(x). \end{aligned} \quad (28)$$

Let us undertake the derivation of eq. (28)

The variable

$$m = \int_0^x \rho dz$$

is associated with the  $x$ -coordinate by the relationship

$$m = M(1 - x).$$

STAT

Since

$$M = \frac{m(\theta)}{a};$$

therefore  $m$  is a function of  $x$  and  $\theta$ . Hence, the transparency functions for long-wave and short-wave radiations  $D$  and  $\bar{D}_s$ , which are functions of  $m$ , can be dissociated into series according to Legendre's polynomials

$$D(m) = D(x, \theta) = \sum_{n=0}^{\infty} D_n(x) P_n(\theta) = D_0(x) + \sum_{n=1}^{\infty} D_n(x) P_n(\theta), \quad (29)$$

$$\bar{D}_s(m) = \bar{D}_s(x, \theta) = \sum_{n=0}^{\infty} \bar{D}_{sn}(x) P_n(\theta) = \bar{D}_{s0}(x) + \sum_{n=1}^{\infty} \bar{D}_{sn}(x) P_n(\theta). \quad (30)$$

The values of  $D_0(x)$  and  $\bar{D}_{s0}(x)$  are determined as an averaged distribution of  $m(z)$ , according to latitude, i.e., the same as an averaged distribution of  $\rho(z)$  according to latitude.

The additions  $\sum_{n=1}^{\infty} D_n(x) P_n$  and  $\sum_{n=1}^{\infty} \bar{D}_{sn}(x) P_n$  are determined by the deviations of water vapor density at various latitudes from its mean values for a given level.

The emission function  $E(x, \theta)$  is conveniently represented in the following form:

$$E(x, \theta) = F(x, \theta) + E(x, \theta). \quad (31)$$

where  $E(x, \theta)$  — is the portion of the emission function determined by the deviation of water vapor density from its mean distribution, and  $F(x, \theta)$  is the portion of the emission function determined by the mean distribution of water vapor density with altitude and by all the other factors being considered in the problem.

The  $F(x, \theta)$ -function may be called the "basic background" of the emission function. Obviously,  $E$  may be considered as minor additions to  $F$ .

The radiation flux of heat across the variable  $m$  is, in accordance with formulas (122), (123) and (124) in Chapter I, determined in the following manner:

$$A - B + S = S_0 D_s(M - m) - E(M) |D(M - m) - \Delta D(M + m)| - \int_0^M |\Delta D(m + \tau) - D|m - \tau| \left| \frac{\partial E}{\partial \tau} \right| d\tau, \quad (32)$$



since

$$\int_{-M}^M D(\tau - m) \frac{\partial E}{\partial \tau} d\tau + \int_0^M D(m - \tau) \frac{\partial E}{\partial \tau} d\tau = \int_0^M D|m - \tau| \frac{\partial E}{\partial \tau} d\tau.$$

For eq. (28) we have to obtain the expression for the  $n$ th harmonic of the radiation balance.

We shall rewrite eq. (32) taking into account (31), in the dimensionless coordinate  $x$ , as follows:

$$\begin{aligned} A - B + S = & \sum_{n=0}^{\infty} S_{0n} P_n \left[ D_{0n}(1-x) + \sum_{n=1}^{\infty} D_{nn}(1-x) P_n \right] - \\ & - \left[ \sum_{n=0}^{\infty} F_n(0) P_n + \sum_{n=0}^{\infty} E_n(0) P_n \right] \left\{ \left[ D_0(1-x) + \sum_{n=1}^{\infty} D_{nn}(1-x) P_n \right] - \right. \\ & - \Delta \left[ D_0(x-1) + \sum_{n=1}^{\infty} D_{nn}(x-1) P_n \right] \left. - \int_0^1 \Delta \left[ D_0(x+y-1) + \right. \right. \quad (33) \\ & \left. \left. + \sum_{n=1}^{\infty} D_{nn}(x+y-1) P_n \right] - \left[ D_0|1+x-y| + \sum_{n=1}^{\infty} D_{nn}|1+x-y| P_n \right] \right\} \left[ \sum_{n=0}^{\infty} \frac{dF_n}{dy} P_n + \sum_{n=0}^{\infty} \frac{dE_n}{dy} P_n \right] dy. \end{aligned}$$

where  $\Delta = 1 - \delta$ .

The transition, in the transparency functions, from arguments in the variable  $m$  to arguments in the variable  $x$  is made in the following manner. A certain argument  $\bar{m}$  in the variable  $m$  is associated with a certain argument  $\bar{x}$  in the  $x$ -variable by the following relationship:

$$\bar{m} = M(1 - \bar{x}).$$

Therefore, for the case of  $\bar{m} = M - m$ , we obtain  $\bar{x} = 1 - x$ , inasmuch as

$$\bar{m} = M - M(1 - x) = M(1 - \bar{x}).$$

The same applies when  $\bar{m} = M + m$   $\bar{x} = x - 1$ .

For  $\bar{m} = m + \tau$   $\bar{x} = (x + y - 1)$ , and for  $\bar{m} = m - \tau$   $\bar{x} = (1 + x - y)$ . The  $m$ -variable varies from 0 to  $2M$ , which corresponds to the change in  $x$  within the limits between 1 and -1.

In expression (33) let us discard the products of the form

$$\sum_{n=1}^{\infty} D_n(x) P_n \sum_{n=0}^{\infty} \left( E_n \frac{dE_n}{dy} \right) P_n$$

as small in comparison with the remaining terms (the corresponding evaluations are cited later on).

Then

$$\begin{aligned} A - B + S = & D_{0n}(1-x) \sum_{n=0}^{\infty} S_{0n} P_n + \sum_{n=0}^{\infty} S_{0n} P_n \sum_{n=1}^{\infty} D_{0n}(1-x) P_n - \\ & - \sum_{n=0}^{\infty} F_n P_n [D_0(1-x) - \Delta D_0(x-1)] - \\ & - \sum_{n=0}^{\infty} F_n P_n \left[ \sum_{n=1}^{\infty} D_n(1-x) P_n - \Delta \sum_{n=1}^{\infty} D_n(x-1) P_n \right] - \\ & - \sum_{n=0}^{\infty} E_n P_n [D_0(1-x) - \Delta D_0(x-1)] - \\ & - \int_1^0 \left\{ [\Delta D_0(x+y-1) - D_0|1+x+y|] \sum_{n=0}^{\infty} \frac{dF_n}{dy} P_n + \right. \\ & + [\Delta D_0(x+y-1) - D_0|1+x-y|] \sum_{n=0}^{\infty} \frac{dE_n}{dy} P_n \left. \right\} dy - \\ & - \int_1^0 \left[ \Delta \sum_{n=1}^{\infty} D_n(x+y-1) P_n - \right. \\ & \left. - \sum_{n=1}^{\infty} D_n|1+x-y| P_n \right] \sum_{n=0}^{\infty} \frac{dF_n}{dy} P_n dy. \end{aligned} \quad (34)$$

The double products of the series, entering into (34), can also be presented in the form of a dissociation of certain functions into series according to Legendre's polynomials

$$\begin{aligned} \sum_{n=0}^{\infty} S_{0n} P_n \sum_{n=1}^{\infty} D_{0n}(1-x) P_n &= \sum_{n=0}^{\infty} \xi_n(x) P_n, \\ \sum_{n=0}^{\infty} F_n(0) P_n \left[ \sum_{n=1}^{\infty} D_n(1-x) P_n - \Delta \sum_{n=1}^{\infty} D_n(x-1) P_n \right] &= \\ &= \sum_{n=0}^{\infty} \zeta_n(x) P_n. \end{aligned} \quad (34^1)$$

$$\int_1^0 \sum_{n=1}^{\infty} [\Delta D_n(x+y-1) - D_n|1+x-y|] P_n \sum_{n=0}^{\infty} \frac{dF_n}{dy} P_n dy = \quad (34^2)$$

$$= \sum_{n=0}^{\infty} Q_n(x) P_n. \quad (34''')$$

Therefore, the nth harmonic of the radiation balance for the  $E$ -function will have the form of

$$\begin{aligned} A_n - B_n + S_n = & D_{0n}(1-x)S_{0n} - F_n(0)[D_0(1-x) - \Delta D_0(x-1)] - \\ & - F_n(0)[D_0(1-x) - \Delta D_0(x-1)] - \int_1^0 [\Delta D_0(x+y-1) - \\ & - D_0|1+x-y|] \frac{dF_n}{dy} + [\Delta D_0(x+y-1) - \\ & - D_0|1+x-y|] \frac{dE_n}{dy} dy + \epsilon_n - \zeta_n - Q_n \end{aligned} \quad (35)$$

Whence the radiation balance for the  $F_n$  function is

$$\begin{aligned} A_n - B_n + S_n = & D_{0n}(1-x)S_{0n} - F_n(0)[D_0(1-x) - \Delta D_0(x-1)] - \\ & - \int_1^0 [\Delta D_0(x+y-1) - D_0|1+x-y|] \frac{dF_n}{dy} dy; \end{aligned} \quad (36)$$

and for the  $E_n$  function

$$\begin{aligned} A_n - B_n + S_n = & - F_n(0)[D_0(1-x) - \Delta D_0(x-1)] - \\ & - \int_1^0 [\Delta D_0(x+y-1) - D_0|1+x-y|] \frac{dE_n}{dy} dy + \epsilon_n - \zeta_n - Q_n. \end{aligned} \quad (37)$$

Now eq. (28) can be subdivided into two equations, one for  $F_n(\tau)$ , and the other for  $E_n(x)$ .

The first equation

$$\begin{aligned} N \frac{dF_n}{dx} = & S_{0n} D_{0n}(1-x) - F_n(0)[D_0(1-x) - \Delta D_0(x-1)] - \\ & - \int_1^0 [\Delta D_0(x+y-1) - D_0|1+x-y|] \frac{dF_n}{dy} dy + \\ & + n(n+1) \int_{x_n}^x G(y) F_n dy - \frac{L(x_{0n})}{2} (x-x_0) - F_n + \lambda' \beta \end{aligned} \quad (38)$$

The second equation

STAT

$$\begin{aligned}
& N \frac{dE_n}{dx} = S_0 D_0 (1-x) E_n(0) \{D_0(1-x) - \Delta D_0(x, 1)\} \\
& - \int_1^0 [\Delta D_0(x+y-1) - D_0|1+x-y|] \frac{dE_n}{dy} dy + \\
& + n(n+1) \int_{x_0}^x G(y) E_n dy + \zeta_n - \zeta_n - Q_n - \\
& - \frac{L(x_0)_n}{a} (x-x_0) - F_n + \lambda' \beta.
\end{aligned} \tag{39}$$

The condensation term is discarded from (38) when ' $n > 0$ '.

These equations differ from each other only by their expressions for the free term. Therefore, it will be sufficient to examine the derivation of only one of these equations.

Let us examine the derivation of eq. (38), which contains the unknown  $F_n$ -function necessary for determining  $\zeta_n$  and  $Q_n$ .

For the  $F_n$ -function, the two-layer problem is resolved in the same way as for the  $E_n$ -function (and hence this refers to the  $E_n$ -function). The same equation of heat influx in the surface layer of the atmosphere as that applied to the  $E$ -function, corresponds to the averaged distribution of water vapor by latitude. In the first layer we obtain accordingly, by analogy with expressions (24) and (26):

$$\begin{aligned}
& \frac{d}{dx} \left[ N(x) \frac{dF_n}{dx} - \lambda' \zeta \right] = 0, \\
& F_n = -\frac{C_{0n}}{\eta} \frac{a}{b} \ln \left[ \lambda_0 + \frac{b}{a} (1-x) \right] + \frac{\beta}{\eta} \ln x + C_{1n}.
\end{aligned}$$

The integration constant  $C_{0n}$ , as well as  $\tilde{C}_{0n}$ , is determined from the equation of heat balance for the earth's surface

$$C_{0n} - (A_n - B_n + S_n)_{x=1} + F_n = 0. \tag{40}$$

only in determining  $C_{0n}$  must formula (36) be used for the radiation balance while formula (35) must be used in determining  $\tilde{C}_{0n}$ .

The Second Layer. In eq. (38) we transform the term corresponding to the horizontal turbulent heat flux. After integrating it by parts, we obtain

$$\begin{aligned} \int_{x_0}^x G(y) F_n(y) dy &= [H(x) F_n(x) - H(x_0) F_n(x_0)] - \int_{x_0}^x H(y) \frac{dF_n}{dy} dy = \\ &= H(x) \left[ F_n(x_0) + \int_{x_0}^x \frac{dF_n}{dy} dy \right] - H(x_0) F_n(x_0) - \int_{x_0}^x H(y) \frac{dF_n}{dy} dy = (41) \\ &= F_n(x_0) [H(x) - H(x_0)] + \int_{x_0}^x [H(x) - H(y)] \frac{dF_n}{dy} dy, \end{aligned}$$

where

$$H(y) = \int G(y) dy.$$

After the substitution of (41), eq. (38) assumes the form

$$\begin{aligned} N(x) \frac{dF_n}{dx} &= S_{0n} D_{0n} (1-x) - F_n(0) [D_0(1-x) - \Delta D_0(x-1)] - \\ &\quad - \int_1^0 [\Delta D_0(x+y-1) - D_0|1+x-y|] \frac{dF_n}{dy} dy + (42) \\ &\quad + n(n+1) \int_{x_0}^x [H(x) - H(x_0)] \frac{dF_n}{dy} dy - \frac{L^2 \rho_{0n}}{a} (x-x_0) - \\ &\quad - F_n + n(n+1) F_n(x_0) [H(x) - H(x_0)] + \lambda \beta. \end{aligned}$$

The sought-for function  $\frac{dF_n}{dy}$  of eq. (42) will be denoted by  $\varphi_n(y)$ .

Furthermore, we introduce the following other designations:

$$\begin{aligned} f_n(x) &= S_{0n} \bar{D}_{0n} (1-x) - F_n(0) [D_0(1-x) - \Delta D_0(x-1)] - \\ &\quad - \frac{L^2 (\rho_{0n})}{a} (x-x_0) - F_n + n(n+1) F_n(x_0) [H(x) - H(x_0)] + \lambda \beta - \\ &\quad - \int_1^{x_0} [\Delta D_0(x+y-1) - D_0|1+x-y|] \left[ \frac{C_{0n}}{\gamma \left[ \lambda_0 + \frac{b}{a}(1-y) \right]} + \frac{\beta}{\gamma} \right] dy, (43) \end{aligned}$$

$$K_1(x, y) = D_0|1+x-y| - \Delta D_0(x+y-1),$$

$$K_2(x, y) = n(n+1) [H(x) - H(y)].$$

Then, eq. (42) will be written in the following form:

STAT

$$N(x)\varphi_n(x) - \int_{x_0}^0 K(x, y)\varphi_n(y) dy = f_n(x). \quad (44)$$

In this manner, the derivation of eq. (38), as well as of eq. (39), is reduced to deriving the integral equation (44) of the Fredholm type of the second kind;  $f_n(x)$  is the free term of this equation, while  $K(x, y)$  is its core.

$$K(x, y) = \begin{cases} K_1 + K_2 = [D_0|1+x-y| - \Delta D_0(x+y-1)] + \\ + n(n+1)[H(x) - H(y)] & \text{when } y > x \\ K_1 = [D_0|1+x-y| - \Delta D_0(x+y-1)] & \text{when } y < x \end{cases}$$

Inasmuch as the first derivative of the  $K(x, y)$  - core has a discontinuity along  $y$  when  $y=x$ , eq. (43) should be written thus:

$$\varphi_n(x) \left[ N(x) - \int_{x_0}^0 K(x, y) dy \right] - \int_{x_0}^0 K(x, y) [\varphi_n(y) - \varphi_n(x)] dy = f_n(x). \quad (45)$$

Eq. (45) is obtained from (43) by adding and subtracting  $\varphi_n(x)$  from the subintegral  $\varphi_n(y)$ -function.

Integral equations of type (44) are usually derived by approximate methods. Let us use any one of the formulas of approximate squaring, according to which

$$\int_a^b F(y) dy = \sum_{j=1}^r A_j F(y_j). \quad (46)$$

Here  $y_j$  are points being given in the (b-a)-interval in a definite manner;  $A_j$  are coefficients determining the weights of the components in sum (46). Then, from eq. (45) we obtain a set  $r$  of algebraic equations for determining  $r$  values  $\varphi_n(x_j)$  of the unknown  $\varphi_n(x)$ -function:

$$\begin{aligned} & \varphi_n(x_j) \left[ N(x_j) - \int_{x_0}^0 K(x_j, y) dy \right] - \\ & - \sum_{j=1}^r A_j K(x_j, x_j) [\varphi_n(x_j) - \varphi_n(x_j)] = f_n(x_j). \end{aligned} \quad (47)$$

The character of the convergence of the approximate derivations of eq. (44) to the exact one, and of the magnitude of possible errors in determining temperature  $T$ , are explained in [41]. After determining  $\varphi_n(x_j)$ , the derivation for the

$F_n$ -function in the second layer may be constructed according to (48)

$$F_n(x) = \int_{x_0}^x \varphi_n(y) dy + C_{2n}. \quad (48)$$

Let us now pass over to determining the integration constants. In resolving the two-layer problem involving a second-order differential equation, we should obtain four integration constants for the determination of which it is necessary to write out four more equations in addition to the  $r$  equations of set (47).

Eq. (40), for determining  $C_{0n}$ , has already been written. Inasmuch as (40) is obtained from (47) when  $x = x_0$ , another equation must be found for determining  $\varphi_n(x_0)$ . Let us write out the condition of continuity when  $x = x_0$  for the  $\varphi_n(x)$  function:

$$\varphi_n(x_0) = \frac{C_{0n}}{N(x_0)} + \frac{\beta}{\eta x_0}. \quad (49)$$

The constants  $C_{1n}$  and  $C_{2n}$  are associated with each other by the condition of continuity of the emission function when  $x = x_0$

$$-\frac{C_{0n}}{\eta} \frac{a}{b} \ln \left[ \lambda_0 + \frac{b}{a} (1 - x_0) \right] + C_{1n} + \frac{\beta}{\eta} \ln x_0 = C_{2n}. \quad (50)$$

The constant  $C_{2n}$  is related to the fourth integration constant by equation (48) when  $x = 0$ .

$$F_n(0) = \int_{x_0}^0 \varphi_n(y) dy + C_{2n}. \quad (51)$$

Let us determine  $F_n(0)$  from (47) with  $x = 0$ , assuming that

$$\varphi_n(0) = 0, \quad (52)$$

i.e., we find that, as in the preceding investigations [7] made with respect to a latitudinally independent quantity of water vapor in the atmosphere ( $M(\theta) = \text{const}$ ), the latitudinal course of temperature in the stratosphere is the same as in the troposphere.

In the construction of the  $E_n(x, \theta)$ -function, the equations for determining

STAT

the integration constants will differ somewhat. The first three equations will be analogous to (49)-(51), except that they include  $\tilde{C}_n$  instead of  $\tilde{C}_n$ ;  $E_n(0)$  is determined from a set analogous to (47) but with a free term for the  $E_n(x)$ -function with  $x=0$ . In this connection, we use the upper boundary condition applied to eq. (14):

$$P|_{x=0} = 0.$$

In calculating  $E_n(x)$  we shall assume that

$$\psi_n(0) = \left. \frac{dE_n}{dx} \right|_{x=0} \neq 0.$$

Let us turn our attention to the circumstance that the sought-for function  $\psi_n(x)$  varies little in the lower part of the (1-0) integration interval, in the 0-1 kilometer layer, i.e., it may be assumed that here  $\frac{\partial \psi}{\partial x} = 0$ , or, which is the same thing,

$$\psi_n(x_j) = \psi_n(x_{j+1}), \quad (53)$$

where  $x_j$  and  $x_{j+1}$  are neighboring points of (46) located in the lower part of the integration interval.

To take into account, with a variable optical mass, the change in  $E_n(x)$  in the stratosphere [with  $M(\theta) \neq \text{const}$ ;  $\psi_n(0) \neq 0$ ], is very important since this ensures the observed reversal in the sign of the equator-pole temperature contrast: in the stratosphere, the temperature over the equator is lower than over the pole, whereas at all levels in the troposphere, up to an altitude of 10 kilometers, temperature decreases from the equator toward the pole. The fact that, with a changing optical mass of the layer in question, the changes in temperature at its upper and lower boundaries, respectively, are opposite in sign, has been demonstrated in [22].

Therefore, let us relate  $\psi_n(0) \neq 0$  to the  $E_n(x)$ -function being determined with  $M(\theta) \neq \text{const}$ ., after having closed by means of (53) the set of equations necessary for its determination.

With this we terminate our review of the theoretical portion of the problem

STAT



concerning the zonal temperatures of the atmosphere. The calculation portion of this problem is set forth in detail in the following sections.

Let us pass over to deriving eq. (6) for nonzonal deviations of temperature  $T'$ .

The right-hand part of eq. (6) has the form

$$e' = \frac{\partial}{\partial z} \lambda' \frac{\partial T'}{\partial z} + Lx\rho',$$

since

$$e'_1 < e'_2 \text{ и } e'_2,$$

i.e., the spatial anomalies of radiation heat fluxes may be ignored [3].

For long intervals of time, it may be assumed that on an average  $w = 0$ .

Let us resolve the two-layer problem.

In the surface layer of the atmosphere ( $0 \leq z' \leq z_0$ ) the  $T'$  anomalies develop solely on account of the diversity of the thermal properties of the underlying surface, and (6) is reduced to

$$\frac{\partial}{\partial z'} \lambda' \frac{\partial T'}{\partial z'} = 0,$$

whence

$$T' = -\frac{P'(0)}{b} \ln(\lambda_0 + bz') + C, \quad (54)$$

where  $P'(0)$  and  $\rho'$  are the deviations of the vertical turbulent heat flux at the underlying surface and the deviations of the water vapor density from its zonal values they are assumed as known.

For the free atmosphere ( $0 \leq z \leq h$ ), as a first approximation, we discard

$\frac{\partial T'}{\partial \theta}$  from eq. (6) and rewrite it thus:

$$\frac{\partial^2 T'}{\partial z^2} - \frac{c_p \rho_b}{\lambda'} \frac{v_\lambda}{a_0 \sin \theta} \frac{\partial T'}{\partial \lambda} = \frac{c_p \rho_b}{\lambda'} \frac{v_\theta}{a_0} \frac{\partial T'}{\partial \theta} - \frac{Lx}{\lambda'} \rho'.$$

Let us derive the designations

$$V = \frac{c_p \rho_b}{\lambda'} \frac{v_\lambda}{a_0 \sin \theta}, \quad \Phi = \frac{c_p \rho_b}{\lambda'} \frac{v_\theta}{a_0} \frac{\partial T}{\partial \theta} - \frac{Lx}{\lambda'} \rho'.$$

STAT

We shall obtain

$$\frac{\partial T'}{\partial z^2} - V \frac{\partial T'}{\partial \lambda} = \Phi.$$

We shall seek the derivation of this equation in the form

$$T' = M + \left(1 - \frac{z}{h}\right) h \frac{P'(0)}{\lambda'}.$$

The  $M(z, \lambda)$ -function should satisfy the following conditions:

$$\begin{aligned} \text{when } z=0 & \quad \frac{\partial M}{\partial z} = 0 \quad \left( \frac{\partial T'}{\partial z} = -\frac{P'(0)}{\lambda_0 + \partial z_0} \right), \\ \text{when } z=h & \quad M=0 \quad (T'=0), \end{aligned}$$

inasmuch as at the upper boundary of the surface layer of its atmosphere the heat fluxes are continuous, while at an  $h$ -altitude the temperature assumes zonal values.

We obtain the following equation for determining  $M$ :

$$\frac{\partial^2 M}{\partial z^2} - V \frac{\partial M}{\partial \lambda} = \Phi + V \left(1 - \frac{z}{h}\right) h \frac{\partial}{\partial \lambda} \frac{P'(0)}{\lambda'}.$$

Let us designate

$$N = \Phi + V \left(1 - \frac{z}{h}\right) h \frac{\partial}{\partial \lambda} \frac{P'(0)}{\lambda'}.$$

then

$$\frac{\partial^2 M}{\partial z^2} - V \frac{\partial M}{\partial \lambda} = N. \quad (55)$$

We shall seek the  $M$ -function in the form of a trigonometric series

$$M = \sum_{n=1}^{\infty} u_n(\lambda) \cos\left(\frac{2n-1}{2} \frac{\pi}{h} z\right).$$

Let us substitute  $M$  into (55):

$$-\sum_{n=1}^{\infty} u_n \left[\frac{2n-1}{2} \frac{\pi}{h}\right]^2 \cos\left(\frac{2n-1}{2} \frac{\pi}{h} z\right) - V \sum_{n=1}^{\infty} \frac{\partial u_n}{\partial \lambda} \cos\left(\frac{2n-1}{2} \frac{\pi}{h} z\right) = N.$$

Let us multiply this equation by  $\frac{2}{h} \cos\left(\frac{2j-1}{2} \frac{\pi}{h} z\right)$

and integrate with respect to  $z$  the thus obtained expression from 0 to  $h$ .

STAT

Since

$$\int_0^h \cos \frac{2n-1}{2} \frac{\pi}{h} z \cos \frac{2j-1}{2} \frac{\pi}{h} z dz = \begin{cases} 0 & n \neq j \\ \frac{h}{2} & n = j \end{cases}$$

we obtain

$$u_j \left[ \frac{2j-1}{2} \frac{\pi}{h} \right]^2 + \sum_{n=1}^{\infty} \frac{\partial u_n}{\partial \lambda} A_{nj} = -N_j. \quad (56)$$

Here

$$A_{nj} = \frac{2}{h} \int_0^h V \cos \frac{2n-1}{2} \frac{\pi}{h} z \cos \frac{2j-1}{2} \frac{\pi}{h} z dz,$$

$$N_j = \frac{2}{h} \int_0^h \Phi \cos \frac{2j-1}{2} \frac{\pi}{h} z dz + 2 \frac{\partial P'(0)}{\partial \lambda} \int_0^h V \left(1 - \frac{z}{h}\right) \cos \frac{2j-1}{2} \frac{\pi}{h} z dz.$$

Let us isolate the term containing  $A_{jj}$ , in eq. (56), and then this equation will be rewritten as:

$$A_{jj} \frac{\partial u_j}{\partial \lambda} + \left[ \frac{2j-1}{2} \frac{\pi}{h} \right]^2 u_j + \sum_{n=1}^{\infty} A_{nj} \frac{\partial u_n}{\partial \lambda} = -N_j. \quad (57)$$

The asterisk denotes that the sum does not contain terms with  $j = n$ .

Let us dissociate all the known functions into a Fourier series:

$$A_{jj} = \sum_{l=-\infty}^{\infty} A_{jjl} e^{i l \lambda},$$

$$A_{nj} = \sum_{l=-\infty}^{\infty} A_{njl} e^{i l \lambda},$$

$$N_j = \sum_{l=-\infty}^{\infty} N_{jl} e^{i l \lambda}.$$

Let us likewise seek for a derivation of eq. (57) in the form of a Fourier series:

$$u_n = \sum_{k=-\infty}^{\infty} u_{nk} e^{i k \lambda}.$$

The double asterisk denotes that the sum does not contain a term with  $k = 0$ ,

since  $u_{n0} = 0$ .

Obviously,

$$\frac{\partial u_n}{\partial \lambda} = i \sum_{k=-\infty}^{\infty} k u_{nk} e^{i k \lambda}.$$

STAT

In eq. (57) let us collect the terms with identical  $e^{ikz}$ -powers

$$\left[\frac{2j-1}{2} \frac{\pi}{h}\right]^2 u_{jk} + i \sum_{r=-m}^m A_{jr} (k-r) u_{j(k-r)} +$$

$$+ i \sum_{n=-m}^m \sum_{r=-m}^m A_{nr} (k-r) u_{n(k-r)} = -N_{jk}. \quad (58)$$

Let us isolate from (58) the term with  $r = 0$

$$\left[\left(\frac{2j-1}{2} \frac{\pi}{h}\right) + ikA_{j0}\right] u_{jk} + i \sum_{r=-m}^m A_{jr} (k-r) u_{j(k-r)} +$$

$$+ i \sum_{n=-m}^m \sum_{r=-m}^m A_{nr} (k-r) u_{n(k-r)} = -N_{jk}.$$

As a first approximation

$$u_{nk} = - \frac{N_{nk}}{\left[\frac{2n-1}{2} \frac{\pi}{h}\right]^2 + ikA_{nn}}.$$

As a second approximation

$$u_{nk} = - \frac{N_{nk}}{\left[\frac{2n-1}{2} \frac{\pi}{h}\right]^2 + ikA_{nn}} + i \sum_{r=-m}^m \frac{(k-r) A_{nr} N_{n(k-r)}}{\left[\frac{2n-1}{2} \frac{\pi}{h}\right]^2 + ikA_{nn}} +$$

$$+ i \frac{1}{\left[\frac{2n-1}{2} \frac{\pi}{h}\right]^2 + ikA_{nn}} \sum_{j=-m}^m \sum_{r=-m}^m A_{nr} (k-r) \frac{N_{j(k-r)}}{\left[\frac{2j-1}{2} \frac{\pi}{h}\right]^2 + ikA_{nn}}.$$

Knowing  $u_{nk}$  we shall find  $H$  and the  $T'$  values being sought. The integration constant  $C$  in (54) is determined from the condition of continuity of  $T'$  at the upper boundary of the surface layer of the atmosphere.

Let us analyze the obtained results. In the surface layer of the atmosphere temperature anomalies develop chiefly owing to the diversity of the thermal properties of the underlying surface, which (properties) are determined by the deviation of the turbulent heat flux at the earth's surface from the zonal values. As a consequence of the continuity of the distribution of temperature with altitude, heat advection and water-vapor condensation in the free atmosphere also exert an influence on the surface anomalies of the temperature. However, the influence of advection becomes fundamental only in the regions where the values of the turbulent heat flux approximate its zonal values, i. e., on the boundaries between continents

STAT

and oceans. In all the remaining area the signs of the anomalies of temperature and turbulent heat flux agree.

Owing to the continuity of the lapse rates, the thermal properties of the underlying surface exert an influence on the temperature anomalies in the free atmosphere; here this influence also becomes fundamental. Experimental data indicate that up to an altitude of 6 kilometers the correspondence of signs between  $T'$  and  $P'(0)$  takes place in at least 70 percent or more of the cases. Therefore, the contribution of the function  $M$  to  $T'$  in the majority of cases should be smaller than the contribution of the second term containing  $P'(0)$ .

Unfortunately, owing to the lack of sufficiently reliable preliminary data, the quantitative calculations based on the above-derived formulas cannot give the necessary accuracy, and therefore, we confine ourselves only to a theoretical examination of the problem concerning  $T'$ .

### Selecting the Quantitative Values of the Parameters.

Calculations of the zonal thermal field were made for the summer (April-September) and winter (October-March) 6-month periods.

Let us begin with a selection of the values of the parameters entering into the expression for an effective flux of solar energy

$$S_0 = (1 - \Gamma) W,$$

which we refer to the upper boundary of the atmosphere.

For  $W$ , with a solar constant value of  $I_0 = 1.91$  calories/square centimeter minute, we have the latitudinal distribution shown in Table 6, according to Milankovich [24].

Table 6

Latitudinal Distribution of Solar Radiation Reaching the  
Upper Boundary of the Atmosphere  
( $W$  calories/square centimeter minute)

6-Month Period	Latitude									
	0	10	20	30	40	50	60	70	80	90
Summer	0,585	0,620	0,636	0,635	0,620	0,587	0,540	0,508	0,490	0,484
Winter	0,585	0,536	0,470	0,393	0,307	0,217	0,123	0,049	0,012	0

During the warm 6-month period  $W$  changes relatively little, as it reaches a maximum value at the  $20^\circ$ -latitude, while during the cold 6-month period  $W$  abruptly decreases with latitude, reaching zero at the Pole.

The albedo of the earth-atmosphere system, as calculated with a consideration of the reflection of solar radiation from the earth's surface, clouds, and air molecules, has, according to Fedoseyeva [37], the latitudinal course shown in Table 7.

In the low latitudes the albedo is nearly the same during both 6-month periods. In the middle and high latitudes, the albedo in winter is greater than in summer,

owing to the presence of snow cover.

Table 7

Albedo of the Earth-Atmosphere System ( $\bar{\rho}$  in percent)

6-Month Period	$\varphi^\circ$							
	0-10	10-20	20-30	30-40	40-50	50-60	60-70	70-80
Summer	37	38	38	37	41	45	51	67
Winter	38	35	38	40	48	47	64	58

On the basis of Tables 6 and 7 we obtain for  $S_0$  the values cited in Table 8.

Table 8

Effective Flux of Solar Radiation ( $S_0$  calories/cm<sup>2</sup>-minute)

6-Month Period	$\varphi^\circ$							
	0	10	20	30	40	50	60	70
Summer	0,364	0,385	0,395	0,398	0,379	0,335	0,282	0,234
Winter	0,370	0,343	0,296	0,240	0,173	0,113	0,050	0,017

If the  $S_0$ -function given in this manner is dissociated into a series according to Legendre's polynomials

$$S_0 = \sum_{n=0}^{\infty} S_{0n} P_n(\theta), \quad (59)$$

then the harmonics of dissociation (59) will have the following values:

$S_{00} = 0.335$ ,  $S_{02} = -0.124$ ,  $S_{04} = 0.092$ ,  $S_{06} = 0.006$ , - for the summer 6-month period.

$S_{00} = 0.221$ ,  $S_{02} = -0.253$ ,  $S_{04} = 0.032$ ,  $S_{06} = 0.001$ , - for the winter 6 month period.

The subscript  $n$  assumes only even values, since only one hemisphere, the northern hemisphere, is being examined.

In order to calculate the transparency functions  $\bar{D}_s(x, \theta)$  and  $D(x, \theta)$  it is

STAT

necessary to know the distribution of water vapor density  $\rho$  in the atmosphere.

In order to determine the surface values of  $\rho$  the averaged 6 months' period values of water-vapor pressure ( $e$ ) from the Climatological Handbook for the USSR, and Phillips' data for the oceans were used; for the remaining land areas of the earth, the only available data could be found in the monthly charts of Szawa-Kovats [82] for January and July. After their averaging by latitude,  $e_0$  and  $\rho_0$  were assigned the values given in Table 9.

Table 9

Surface Values of Water-Vapor Pressure ( $e_0$  millimeters Hg) and Density ( $\rho_0$  grams/cubic meter)

$\varphi^\circ$	0	10	20	30	40	50	60	70
Summer 6-Month Period								
$e_0$ . . . . .	22,0	22,6	20,0	17,3	12,6	8,8	6,9	4,8
$\rho_0$ . . . . .	21,4	21,9	19,3	16,7	12,3	8,8	7,0	5,0
Winter 6-month Period								
$e_0$ . . . . .	22,0	20,8	16,0	10,7	7,1	4,2	2,5	1,2
$\rho_0$ . . . . .	21,4	20,1	15,7	10,8	7,4	4,6	2,8	1,4

The given values were used to compute the pressure  $e$  of water vapor according to the known formula

$$\rho = 1,06 \frac{e}{1 + \alpha t} \text{ g/m}^3.$$

The zonal temperatures on the earth's surface necessary for calculating  $\rho$  were taken from [35] for July and January (Table 10).

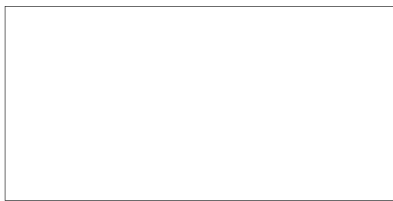




Table 10

## Zonal Temperatures at the earth's Surface [35]

6-Month Period	$\varphi^\circ$			
	10	30	50	70
Summer	299,1	299,9	291,1	280,2
Winter	298,4	285,8	265,3	246,1

The temperature corrections for  $e$  were found to be insignificant, and therefore it is unimportant that mean monthly temperature values were taken instead of the mean semianual values.

The dissociation of  $\rho_0$  into series

$$\rho_0 = \sum_{n=0}^{\infty} \rho_{0n} P_n(\theta) \quad (60)$$

yielded the harmonics of  $\rho_{0n}$  in grams/cubic meter for the summer 6 month period

$$\rho_{00} = 15,2; \rho_{02} = -13,8; \rho_{04} = 2,4; \rho_{06} = 1,3;$$

and for the winter 6 month period

$$\rho_{00} = 11,4; \rho_{02} = -15,1; \rho_{04} = 5,8; \rho_{06} = -2,4.$$

The vertical profile of  $\rho$  was approximated by the exponential function

$$\rho = \rho_0 e^{-\alpha z} \quad (61)$$

For the determination of the dependence of the coefficient  $\alpha$  on latitude and season, Nakorenko's calculations of the distribution of relative humidity  $q$  in the atmosphere up to the altitude of 5 kilometers over the following stations were used: Koko-Solo ( $\varphi = 9^\circ 22' N$ ;  $\lambda = 79^\circ 53' W$ ), Rensokola ( $\varphi = 50^\circ 25' N$ ;  $\lambda = 87^\circ 13' W$ ), Trömsö ( $\varphi = 69^\circ 42' N$ ;  $\lambda = 19^\circ 02'$ ), E. Long, based on the data in [61].

The averaging of monthly values by 6 month periods led to the obtainment of the  $q$  values in grams per kilogram cited in Table 11.

STAT

Table 11

## Vertical Profile of Specific Humidity

(  $q$  in grams/kilogram - upper line;  $\lg \frac{q_0}{q}$  - lower line )

Station	z in kilometers						
	0.01	0.5	1.0	2.0	3.0	4.0	5.0
Summer 6-Month Period							
Koko-Solo	18.4 0	16.5 0.041	14.7 0.079	11.0 0.204	7.4 0.398	5.7 0.505	4.0 0.633
Rensokola	14.3 0	12.9 0.041	10.9 0.114	7.7 0.255	5.2 0.431	3.6 0.591	2.4 0.771
Tromso	4.7 0	4.8 -0.046	4.2 0.41	3.1 0.176	2.4 0.279	1.6 0.462	1.1 0.623
Winter 6-Month Period							
Koko-Solo	17.3 0	16.1 0.041	14.0 0.079	9.9 0.230	6.0 0.447	4.1 0.623	2.9 0.771
Rensokola	7.2 0	6.8 0.021	5.9 0.079	4.3 0.204	3.0 0.390	2.0 0.556	1.4 0.70*
Tromso	2.8 0	2.8 0	2.5 0.041	1.8 0.176	1.3 0.322	0.8 0.544	0.5 0.748

If the values of  $\lg \frac{q_0}{q}$  are plotted on a graph as a function of altitude for various latitudes and seasons, it will be found that the seasonal and latitudinal fluctuations in  $\lg \frac{q_0}{q}$  are not large (Fig 10). This confirms the assumption about the  $\theta$ -independence of  $\alpha$ . Therefore, let us select a single mean value of the slope of the  $\lg \frac{q_0}{q}$ -curve toward the z-axis, equal to  $1.4 \cdot 10^{-6}$  centimeters<sup>-1</sup>.

Consequently,

$$q = q_0 \cdot 10^{-1.4 \cdot 10^{-6} z} = q_0 e^{-0.32 \cdot 10^{-5} z}$$

Since

$$\rho \approx \rho_0 e^{-\frac{p_0 z}{0.622}} = \frac{1}{0.622} p_0 q_0 e^{-\left(\frac{p_0}{RT} + 0.32 \cdot 10^{-5}\right) z} = \frac{1}{0.622} p_0 q_0 e^{-\alpha z}$$

therefore

$$\alpha = \frac{p_0}{RT} + 0.32 \cdot 10^{-5} = 0.46 \cdot 10^{-5} \text{ cm}^{-1}$$

with a mean atmospheric temperature of  $T = 245^\circ$ .



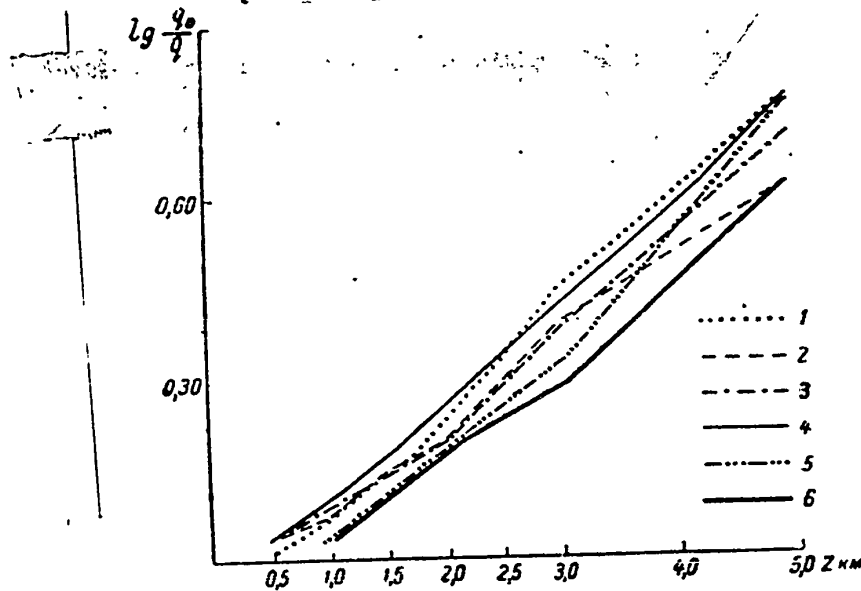


Fig. 10. Vertical Profiles of  $\lg \frac{q_0}{q}$ .

1.  $\varphi = 9^{\circ}22'N$ , winter 6 months; 2. The same summer 6 months;
3.  $\varphi = 30^{\circ}25'N$ , winter 6 months; 4. The same, summer 6 months;
5.  $\varphi = 69^{\circ}42'N$ , winter 6 months; 6. The same, summer 6 months.

The approximate squarings in (47) are based on the Gaussian formula. The points  $x_j$  in the (0.976-0.000)-interval were selected in the following manner: 3 points are taken from  $x_0 = 0.976$  to the condensation level ( $x = 0.665$ ,  $z = 1$  kilometer) and 4 points are taken beyond up to  $x = 0$ . This gives

$x_1$	$x_2$	$x_3$	$x_4$	$x_5$	$x_6$	$x_7$
0,941	0,820	0,702	0,621	0,446	0,218	0,047

( $x_0$  corresponds to the height of the surface layer of the atmosphere  $z_0 = 50$  meters).

In the calculations of  $x$  it was duly considered that Hann's empirical law governs water vapor pressure rather than density.

The calculations of the transparency function for short-wave radiation  $\bar{D}_s(x, \theta)$  are based on Moller's formula for the depletion of solar radiation by water vapor

$$\Delta S = 0,172m^{0,308}.$$

STAT

By means of this formula, Table 9, and formula (61) it was possible to find the distribution of  $\bar{D}_s$  at various altitudes and latitudes (Table 12).

Table 12

## Vertical Profile of the Transparency Function for Solar Radiation

$x$	$z$	$\theta^\circ$								
		0	10	20	30	40	50	60	70	
Summer 6-Month Period										
0,000	16	1	1	1	1	1	1	1	1	1
0,001	14	0,905	0,904	0,910	0,910	0,914	0,922	0,925	0,932	
0,004	12	0,890	0,890	0,892	0,900	0,906	0,915	0,916	0,924	
0,010	10	0,876	0,875	0,880	0,890	0,898	0,908	0,910	0,917	
0,035	8	0,866	0,865	0,875	0,880	0,892	0,904	0,910	0,914	
0,063	6	0,864	0,860	0,870	0,880	0,890	0,900	0,910	0,913	
0,159	4	0,862	0,860	0,870	0,880	0,890	0,900	0,908	0,912	
0,398	2	0,860	0,860	0,870	0,880	0,890	0,900	0,908	0,912	
0,631	1	0,860	0,860	0,870	0,880	0,890	0,900	0,908	0,911	
1,000	0	0,860	0,860	0,870	0,880	0,890	0,900	0,908	0,910	

## Winter 6-Month Period

0,000	16	1	1	1	1	1	1	1	1
0,001	14	0,905	0,908	0,910	0,917	0,926	0,935	0,940	0,964
0,004	12	0,890	0,890	0,900	0,910	0,916	0,926	0,933	0,950
0,010	10	0,877	0,880	0,890	0,910	0,912	0,918	0,928	0,940
0,035	8	0,865	0,870	0,885	0,910	0,908	0,917	0,925	0,938
0,063	6	0,860	0,866	0,883	0,908	0,907	0,916	0,925	0,938
0,159	4	0,860	0,865	0,880	0,898	0,907	0,915	0,924	0,938
0,398	2	0,860	0,865	0,880	0,898	0,907	0,914	0,924	0,938
0,631	1	0,860	0,865	0,880	0,898	0,907	0,913	0,924	0,938
1,000	0	0,860	0,865	0,880	0,898	0,907	0,913	0,924	0,938

The greater is the quantity of water vapor in the air column traversed by the solar ray, the lower is the value of the transparency of  $\bar{D}_s$ . Therefore, the transparency function increases with an increase in latitude during the cold 6 months somewhat more than during the warm 6 months, this difference being more considerable at high latitudes.

The dissociation of  $\bar{D}_s(x, \theta)$  into a series according to Legendre's polynomials gives the values of  $D_{sm}(x)$  harmonics cited in Table 13.

Table 13

Values of the  $D_n(x)$ -Function

$\bar{x}$	$D_{20}$	$D_{12}$	$D_{11}$	$D_{10}$	$D_{20}$	$D_{12}$	$D_{11}$	$D_{10}$
Summer 6-Month Period					Winter 6-Month Period			
	1	0	0	0	1	0	0	0
0,000	0,913	0,022	-0,004	0,003	0,925	0,041	-0,002	0,009
0,001	0,903	0,026	-0,006	0,006	0,913	0,045	-0,014	0,015
0,004	0,888	0,034	-0,008	0,006	0,906	0,044	-0,008	0,028
0,010	0,881	0,039	-0,010	0,006	0,901	0,051	-0,008	0,031
0,035	0,877	0,042	-0,011	0,006	0,895	0,055	-0,008	0,025
0,063	0,876	0,042	-0,011	0,006	0,895	0,055	-0,008	0,023
0,159	0,876	0,040	-0,012	0,006	0,895	0,054	-0,007	0,022
0,398	0,876	0,040	-0,014	0,006	0,895	0,054	-0,007	0,022
0,631	0,875	0,039	-0,015	0,007	0,895	0,054	-0,007	0,022
1,000	0,875	0,039	-0,015	0,007	0,895	0,054	-0,007	0,022

By means of Table 13 the terms in eqs. (38) and (39) dependent on the flux of solar energy (Table 14) were calculated

Table 14

Values of the  $S_n$ -and  $\xi_n$ -Functions

in calories/square centimeter minute

$x$	$S_0$	$S_2$	$S_4$	$S_6$	$\xi_0$	$\xi_2$	$\xi_4$	$\xi_6$
Summer 6-Month Period								
0,976	0,296	-0,110	-0,081	0,005	-0,001	0,012	-0,008	-0,001
0,941	0,297	-0,110	-0,082	0,005	-0,001	0,011	-0,007	-0,001
0,820	0,298	-0,110	-0,083	0,005	-0,001	0,010	-0,005	-0,001
0,702	0,300	-0,111	-0,083	0,005	-0,001	0,009	-0,004	-0,001
0,621	0,302	-0,112	-0,083	0,005	-0,001	0,008	-0,003	-0,001
0,446	0,305	-0,113	-0,084	0,005	-0,001	0,007	-0,004	-0,001
0,218	0,308	-0,114	-0,084	0,005	-0,001	0,006	-0,003	-0,001
0,047	0,320	-0,118	-0,088	0,006	0,000	0,003	-0,002	0,000
0,000	0,335	-0,124	-0,092	0,006	0,000	0,000	-0,000	0,000
Winter 6-Month Period								
0,976	0,197	-0,226	0,029	0,001	-0,003	0,008	-0,009	0,002
0,941	0,198	-0,227	0,029	0,001	-0,003	0,009	-0,008	0,003
0,820	0,199	-0,228	0,029	0,001	-0,002	0,007	-0,008	0,002
0,702	0,199	-0,228	0,029	0,001	-0,002	0,006	-0,005	0,000
0,621	0,201	-0,230	0,029	0,001	-0,002	0,006	-0,005	0,000
0,446	0,201	-0,231	0,029	0,001	-0,002	0,007	-0,007	0,002
0,218	0,204	-0,235	0,030	0,001	0,002	0,007	-0,006	0,002
0,047	0,212	-0,244	0,031	0,001	-0,002	0,006	-0,005	0,001
0,000	0,221	-0,253	0,032	0,001	0,000	0,000	0,000	0,000

From Table 14 it is evident that the consideration of the latitudinal course of

STAT

water vapor density (large quantities of water vapor at low latitudes and small quantities at high latitudes) leads to a lessening of the contrast in the flux of solar energy between the pole and the equator. In Table 14,  $S_n = S_{0n} \bar{D}_{s0}(1-x)$  and  $t_n$  were obtained from (34<sup>'''</sup>).

The  $t_n$ -harmonics, just like the harmonics of the series (34<sup>'''</sup>) and (34<sup>''''</sup>), were calculated by means of the following relation

$$\sum a_n P_n \sum b_n P_n = \sum c_n P_n$$

which gives (with n equal to 0, 2, 4)

$$\begin{aligned} c_0 &= a_0 b_0 + 0,200 a_2 b_2 + 0,111 a_4 b_4, \\ c_2 &= a_0 b_2 + b_0 a_2 + 0,286 (a_2 b_4 + a_4 b_2) + 0,286 a_2 b_2 + 0,145 a_4 b_4, \\ c_4 &= a_0 b_4 + a_4 b_0 + 0,514 a_2 b_2 + 0,259 (a_2 b_4 + b_4 a_2) + 0,162 a_4 b_4, \\ c_6 &= 0,454 (a_2 b_4 + b_4 a_2) + 0,202 a_4 b_4 \dots \end{aligned}$$

The calculations of the transparency function for atmospheric radiation  $D(x, \theta)$  are based on formula (130) in Chapter I. These calculations are made exactly in the same way as for  $\bar{D}_s(x, \theta)$ , and they are presented in Table 15.

Table 15

Vertical Profile of the Transparency Function for  
Atmospheric Radiation at Various Latitudes

x	$\varphi^\circ$							
	0	10	20	30	40	50	60	70

Summer 6-Month Period

1	1	1	1	1	1	1	1	1
0,631	0,185	0,183	0,192	0,206	0,233	0,267	0,287	0,313
0,398	0,145	0,143	0,153	0,163	0,188	0,215	0,238	0,273
0,159	0,120	0,120	0,125	0,138	0,161	0,188	0,210	0,241
0,063	0,115	0,111	0,120	0,130	0,155	0,180	0,200	0,230
0,035	0,112	0,109	0,118	0,127	0,151	0,179	0,196	0,227
0,010	0,110	0,107	0,116	0,126	0,150	0,177	0,195	0,226
0,004	0,108	0,105	0,115	0,125	0,149	0,176	0,194	0,225
0,001	0,107	0,104	0,115	0,124	0,148	0,175	0,193	0,224
0,000	0,107	0,104	0,115	0,124	0,148	0,175	0,193	0,224

STAT

Winter 6-Month Period									
1	1	1	1	1	1	1	1	1	1
0.631	0.184	0.188	0.210	0.245	0.280	0.320	0.350	0.403	
0.398	0.145	0.150	0.170	0.200	0.234	0.280	0.327	0.355	
0.159	0.120	0.125	0.143	0.174	0.204	0.249	0.292	0.345	
0.063	0.114	0.120	0.135	0.163	0.194	0.236	0.282	0.335	
0.035	0.112	0.117	0.130	0.162	0.192	0.235	0.278	0.335	
0.010	0.110	0.115	0.129	0.161	0.190	0.234	0.277	0.334	
0.004	0.108	0.114	0.128	0.160	0.189	0.233	0.276	0.333	
0.001	0.107	0.114	0.127	0.159	0.188	0.232	0.275	0.332	
0.000	0.107	0.114	0.127	0.159	0.188	0.232	0.275	0.332	

The dissociation of  $D(x, \theta)$  into series (29) gives the values of  $D_n(x)$  harmonics cited in Table 16.

The latitudinal course of the optical mass of the atmosphere leads to an increase in the transparency function for long-wave radiation with latitude. In winter this effect is more distinctly expressed than in summer.

Table 16

Values of the $D_n(x)$ -Function									
$x$	$D_0$	$D_2$	$D_4$	$D_6$	$D_0$	$D_2$	$D_4$	$D_6$	
Summer 6-Month Period					Winter 6-Month Period				
1	1	0	0	0	1	0	0	0	
0.631	0.228	0.104	0.007	-0.015	0.262	0.166	0.007	0.010	
0.398	0.183	0.100	0.015	-0.004	0.218	0.166	0.012	0.010	
0.159	0.158	0.093	0.015	-0.004	0.196	0.166	0.024	0.010	
0.063	0.143	0.092	0.015	-0.037	0.187	0.164	0.028	0.010	
0.035	0.145	0.092	0.014	-0.007	0.186	0.164	0.028	0.011	
0.010	0.145	0.092	0.012	-0.007	0.184	0.164	0.028	0.012	
0.004	0.142	0.092	0.012	-0.007	0.183	0.164	0.028	0.012	
0.001	0.142	0.092	0.012	-0.007	0.183	0.164	0.028	0.013	
0.000	0.142	0.092	0.012	-0.006	0.170	0.163	0.028	0.015	
-0.200	0.129	0.086	0.012	-0.010	0.156	0.162	0.038	0.015	
-0.400	0.121	0.085	0.012	-0.014	0.150	0.160	0.038	0.015	
-0.600	0.111	0.082	0.011	-0.026	0.139	0.158	0.037	0.016	
-0.800	0.078	0.040	0.028	-0.019	0.131	0.156	0.035	0.016	
-1.000	0.077	0.054	0.019						

For convenience in the integration of expressions including the zero (th) harmonic  $D_0(x)$ , the latter is approximated by the sum of five exponential functions of  $x$ . Since  $D_0(x)$  corresponds to the latitudinally averaged optical mass ( $\bar{m}$ ) of the atmosphere, therefore

$$D_0(x) = 0,2 \sum_{i=1}^5 e^{-\sigma_i \bar{m} (1-x)} \quad (62)$$

Here

$$\bar{m} = \frac{m}{\sigma}$$

STAT

For the summer 6 months,  $\bar{M} = 3.3$ ; for the winter 6 months,  $\bar{M} = 2.5$

The  $\alpha_i$  coefficients have the following values:  $\alpha_1 = 0.133$ ,  $\alpha_2 = 1.250$ ,

$\alpha_3 = 17.000$ ,  $\alpha_4 = 76.700$ , and  $\alpha_5 = 1,080.0$ .

The calculations based on formula (62) yield a satisfactory agreement with the tabulated values of  $D_0(x)$  (Table 17).

Table 17

Values of $D_0(x)$ Based on Approximation Formula (62)									
6-Month Period	$x$								
	0.976	0.941	0.820	0.702	0.621	0.446	0.218	0.047	0.000
Summer	0.431	0.358	0.280	0.240	0.211	0.177	0.150	0.137	0.132
Winter	0.455	0.376	0.302	0.258	0.235	0.199	0.170	0.154	0.151

Into the values of  $m$ , and consequently also of  $x$ , there is not introduced any correction for the dependence of the transparency function on the pressure and temperature of the medium traversed by the ray, for the reason that this dependence is extremely indeterminate in the quantitative sense, especially for the case of two absorbing media. Therefore, it does not seem expedient to consider this dependence, since the introduction of new parameters with non-substantiated quantitative values would not improve the accuracy of the calculations.

The approximation expression (62) is used for calculating the integral

$$\int_{x_0}^0 K(x, y) dy \text{ and } f_n(x) \text{ in set (47)}$$

The calculations of the quantity of the heat of condensation being liberated in the various latitudinal zones were based on the assumption that, in every latitudinal zone, precipitation is equal to the amount of the condensed moisture, i.e., there is no interlatitudinal transfer of cloud masses.

In eq. (21) the term associated with the heat influx caused by condensation has the form

$$\frac{\partial \Phi}{\partial x} = \frac{L}{a} x \rho_0$$

Whence:

$$\Phi(x) = -\frac{L}{a} x \rho_0 (x - x')$$

STAT



where  $x^0$  is condensation level.

By equating precipitation  $r$  to the amount of the moisture being condensed throughout the entire height of the atmosphere, we obtain

$$r = x \int_{x'}^{\infty} \rho_0 e^{-\alpha z} dz = \frac{x \rho_0}{\alpha} e^{-\alpha x'}$$

From the expression for the  $n$ th harmonic of  $r$  we obtain

$$(x \rho_0)_n = r_n \alpha e^{\alpha x'}$$

Now the harmonics  $\phi_n(x)$  and  $r_n$  are readily associated:

$$\phi_n(x) = -L r_n e^{\alpha x'} (x - x') \quad (65)$$

The zonal distribution of precipitation at the earth's surface was taken from Möller [74]. In summing up his seasonal data we obtain the precipitation distribution by 6-month periods cited in Table 18.

Table 18

Precipitation Distribution by Latitudes.  
(in millimeters)

6-Month Period

$\varphi^\circ$	Summer	Winter	Year
0	688	622	1310
10	708	661	1369
20	333	307	640
30	356	316	672
40	351	389	741
50	369	382	751
60	241	293	534
70	102	114	216
80	58	66	124
90	50	53	103

The values of the annual totals in Table 18 agree satisfactorily with the annual totals of precipitation cited in the data of Meynardus and L'vovich, generalized by M.I. Budyko [12]. The greatest divergence occurs at the equator, where it amounts to 12 percent.

After dissociating the data in Table 18 into a Legendre polynomial series we obtain the following values of the harmonics of  $r_n$  in centimeters<sup>-1</sup> minutes<sup>-1</sup>. STAT

For the summer 6 months

$$r_0 = 16,90 \cdot 10^{-5}, r_2 = -12,23 \cdot 10^{-5}, r_4 = 1,32 \cdot 10^{-5},$$

$$r_6 = -8,37 \cdot 10^{-5}, r_8 = 5,73 \cdot 10^{-5};$$

For the winter 6 months

$$r_0 = 15,88 \cdot 10^{-5}, r_2 = -9,55 \cdot 10^{-5}, r_4 = 0,22 \cdot 10^{-5}$$

$$r_6 = -9,16 \cdot 10^{-5}, r_8 = 6,14 \cdot 10^{-5}.$$

The altitude of the condensation level  $z'$  was selected at 1 kilometer.

By means of (63) we obtain the altitudinal distribution of the harmonics of  $\Phi_n(x)$  cited in Table 19.

The 6-month zonal sums of heat losses to evaporation are determined by means of monthly charts of evaporation from the oceans, plotted by L.I. Zubenok, and annual totals of evaporation from continents [10]. In this connection, it was assumed that north of Latitude  $30^\circ\text{N}$  there is no evaporation from inland areas in the winter 6 months while south of that latitude, (including Latitude  $30^\circ\text{N}$ ) the annual totals of evaporation from land areas are about equally divided between the two 6-month periods. The results of the calculations are cited in Table 20.

Table 19

Values of  $\Phi_n(x)$ -Function in calories/square centimeter-minute

$x$	$\Phi_0$	$\Phi_2$	$\Phi_4$	$\Phi_6$	$\Phi_8$
-----	----------	----------	----------	----------	----------

Summer 6-Month Period

0,621	$0,73 \cdot 10^{-2}$	$-0,533 \cdot 10^{-2}$	$0,575 \cdot 10^{-3}$	$-0,365 \cdot 10^{-2}$	$0,249 \cdot 10^{-2}$
0,446	3,53	-2,560	2,770	-1,760	1,200
0,218	7,17	-5,180	5,600	-3,560	2,425
0,047	9,90	-7,200	7,780	-4,940	3,350
0,000	10,70	-7,740	8,370	-5,300	3,620

Winter 6-Month Period

0,621	$0,69 \cdot 10^{-2}$	$-0,415 \cdot 10^{-2}$	$0,096 \cdot 10^{-3}$	$-0,400 \cdot 10^{-2}$	$0,267 \cdot 10^{-2}$
0,446	3,30	-1,985	0,459	-1,910	1,275
0,218	6,67	-4,020	0,932	-3,870	2,580
0,047	9,26	-5,570	1,288	-5,360	3,590
0,000	9,90	-6,000	1,388	-5,780	3,860

STAT

Table 20

## Heat Losses to Evaporation LF in kilocalories

6-Month Periods	$\varphi^\circ$					
	0	10	20	30	40	50
Summer	34	37	47	47	50	43
Winter	38	35	33	14	3	2

The harmonics of series (27) have the following values:

for the summer 6 months

$$F_0 = 0,153, F_2 = -0,035, F_4 = -0,107;$$

for the winter 6 months

$$F_0 = 0,053, F_2 = -0,148, F_4 = 0,053.$$

The altitude of the first layer, inside which layer the heat fluxes may be considered constant (quasistatic surface layer of the atmosphere was assumed to be

equal to 50 meters. Above that level, in the troposphere, it was assumed that

$\lambda' = \left(\frac{T}{T_0}\right)^6 \cdot 10^3$  cal/cm<sup>2</sup> min. degrees.<sup>1</sup> In eq. (25) this yields  $b = 0.20$  calories/square centimeter-minute-degree. In the stratosphere,  $\lambda'$  decreases with altitude until it reaches 0 at the upper boundary.

In eq. (25), for the summer 6 months

$$\eta = 0.535 \cdot 10^{-3} \text{ minute-degrees/calorie when } T_0 = 296^\circ$$

For the winter 6 months

$$\eta = 0.597 \cdot 10^{-3} \text{ minute-degrees/calories when } T_0 = 285^\circ$$

Let us construct the vertical profile of the  $N(x) = \eta \lambda' \left(\frac{T_0}{T}\right)^6 x$  function (Table 21). The mean temperature profile for summer and winter was taken from

[84].

1 Such a form of  $\lambda'$  corresponds with the accepted representations about the vertical profile of turbulence characteristics: the constancy of  $\lambda'$  in the lowest kilometer, and the observed values of the exchange coefficient at the 3-4 kilometer altitude (50-70 degrees/centimeter second).

STAT

Table 21

Values of the N Function (in centimeters<sup>-1</sup>)

x	6-Month Period			
	Summer		Winter	
	T	N	T	N
0.976	296	0.535	285	0.597
0.941	295	0.500	284	0.562
0.820	293	0.430	283	0.479
0.702	292	0.356	282	0.410
0.621	291	0.315	281	0.355
0.445	286	0.213	277	0.243
0.218	276	0.095	270	0.110
0.047	255	0.016	249	0.019
0.000	214	0	210	0

For calculations in the surface layer of the atmosphere the value of the equilibrium gradient was assumed  $\beta = 6 \cdot 10^{-5}$  degrees/centimeter. Its quantitative value for the free atmosphere is not essential for this problem. Actually, above the surface layer of the atmosphere  $\beta$  is a function of an altitude  $z$ , the form of which is unknown at present. Therefore, in the calculations,  $\beta$  may be assumed equal to a certain constant value for all altitudes. Thus, e.g., if above the surface layer of the atmosphere  $\beta = 0$ , then  $\lambda' = 10^3 \left(\frac{T}{T_0}\right)^6$  calories/centimeter-minute degrees in the troposphere; with the same temperature distribution in the atmosphere for other values of  $\beta$ , we obtain the values of  $\lambda'$  cited in Table 22.

Table 22

Values of the Function  $\lambda' = 10^3$ 

$\beta$	Summer 6-Months			Winter 6-Months		
	$x_1$	$x_5$	$x_7$	$x_1$	$x_5$	$x_7$
0	1.00	0.72	0.41	1.00	0.84	0.46
$10^{-5}$	1.32	1.00	0.44	1.30	1.10	0.51
$3 \cdot 10^{-5}$	3.70	2.00	0.59	3.10	2.80	0.72
$6 \cdot 10^{-5}$	—	—	1.27	—	—	2.00

Hence, it is evident that in the formula (11) for the turbulent flux  $P$  a change in the value of  $\beta$  is compensated by a change in the value of  $\lambda'$ . Inasmuch as for

the free atmosphere the exact value of  $\lambda'$  and its vertical profile are likewise unknown, the calculations may be made after having selected any one of the above-cited distributions of  $\beta$  and  $\lambda'$ . For simplicity, the first-listed of these distributions, i.e.,  $\beta = 0$ , was selected. Here, it is essential that the magnitude of the turbulent heat flux is independent of the thus selected  $\beta$  and  $\lambda'$ , since it is determined by the remaining components of the heat balance of the atmosphere.

The data on the coefficient of horizontal exchange  $A_\phi$  was taken from [62], which contains a table of its annual variations for northern latitudes from 35 to 70°N, for the period from 1928 to 1937, and also from [76].

At latitude 35°N the mean value of that coefficient for the summer 6 months is

$$A_\phi = 4,47 \cdot 10^7 \text{ centimeters}^{-1} \text{ gram seconds}^{-1}$$

and for the winter 6 months

$$A_\phi = 5,16 \cdot 10^7 \text{ centimeters}^{-1} \text{ gram seconds}^{-1}$$

Since  $\lambda'' = c_p A_\phi$ , therefore, the latitudinally averaged  $\lambda''$  for the summer 6 months is

$$\lambda'' = 6,46 \cdot 10^8 \text{ calories/minute centimeter degree}$$

and for the winter 6 months

$$\lambda'' = 7,43 \cdot 10^8 \text{ calories/minute centimeter degree}$$

According to [72], in the troposphere

$$\lambda'' = 1,6 \cdot 10^8 \text{ calories/minute centimeter degree in May and}$$

$$\lambda'' = 7,9 \cdot 10^8 \text{ calories/minute centimeter degree in February.}$$

In the stratosphere the values of  $\lambda''$  are smaller.

The vertical profile

$$\rho(x) = H(x) - H(x_0).$$

is approximated [41] in the form:

$$\rho(x) = \sum_i \rho_i e^{-\tau_i x}$$

The following values were selected for the calculations:



STAT

For the summer 6 months

$$\rho_1 = -0,29, \quad \rho_2 = -2,00, \quad \rho_3 = 12,05, \quad \rho_4 = -10,16, \quad r_1 = 3,8,$$

$$r_2 = 10,0, \quad r_3 = 18,0, \quad r_4 = 21,0;$$

For the winter 6 months

$$\rho_1 = -0,0253, \quad \rho_2 = -0,0658, \quad \rho_3 = -0,1392, \quad r_1 = 0,44, \quad r_2 = 6,9,$$

$$r_3 = 170$$

With such values of  $\rho_i$  and  $r_i$ ,  $\lambda''(x)$  is of the order indicated above:  $\lambda'' = 0$  when  $x = 0$ .

The Calculation of the Zonal Distribution of Temperatures and of the Components of the Heat Balance of the Atmosphere. Analysis of the Obtained Results.

Let us proceed to construct the set (47) which determines the  $\varphi_n(x)$ -function.

The weights of  $A_j$  corresponding to the selected points  $x_j$  have the following values:

$$A_1 \quad A_2 \quad A_3 \quad A_4 \quad A_5=A_6 \quad A_7 \quad A_8$$

$$-0,086 \quad -0,137 \quad -0,086 \quad -0,115 \quad -0,217 \quad -0,115 \quad -0,022$$

Then, the values of the function  $-A_j K_1(x_i, x_j)$  are reduced to the values in Table 23.

Table 23

Values of the  $A_j K_1(x_i, x_j)$  Function

$x_i$	$x_j$								$-\Sigma A_j K_1$
	0,941	0,820	0,702	0,621	0,446	0,218	0,047	0,000	
Summer 6-Month Period									
0,976	0,030	0,036	0,019	0,023	0,035	0,030	0,015	0,003	0,192
0,941	0,083	0,039	0,020	0,023	0,033	0,032	0,015	0,003	0,253
0,820	0,024	0,135	0,025	0,029	0,042	0,031	0,016	0,003	0,308
0,702	0,020	0,040	0,085	0,039	0,052	0,039	0,017	0,003	0,295
0,621	0,017	0,035	0,029	0,115	0,059	0,041	0,020	0,004	0,319
0,446	0,015	0,027	0,020	0,031	0,217	0,053	0,022	0,004	0,387
0,218	0,013	0,021	0,015	0,022	0,052	0,217	0,032	0,005	0,377
0,047	0,011	0,019	0,013	0,020	0,042	0,059	0,116	0,008	0,288
0,000	0,011	0,019	0,013	0,018	0,042	0,055	0,042	0,022	0,223

Winter 6-Month Period

0,976	0,032	0,039	0,020	0,024	0,039	0,033	0,017	0,003	0,237
0,941	0,084	0,042	0,021	0,027	0,041	0,036	0,017	0,003	0,270
0,820	0,026	0,136	0,026	0,031	0,046	0,038	0,018	0,003	0,323
0,702	0,021	0,041	0,085	0,039	0,055	0,042	0,020	0,004	0,308
0,621	0,020	0,038	0,029	0,114	0,062	0,045	0,022	0,004	0,332
0,446	0,016	0,029	0,022	0,033	0,214	0,058	0,025	0,005	0,400
0,218	0,014	0,024	0,017	0,024	0,058	0,214	0,034	0,006	0,390
0,047	0,013	0,022	0,014	0,022	0,047	0,063	0,115	0,008	0,303
0,000	0,012	0,021	0,014	0,021	0,045	0,058	0,044	0,022	0,237

The  $\int_{x_0}^0 K(x_1, y) dy$ -integrals calculated from [62] are cited in Table 24.

Table 24

Values of  $\int_0^{x_1} K(x_1, y) dy$

6-Month Period	$x_1$								
	0,976	0,941	0,820	0,702	0,621	0,446	0,218	0,047	0,000
Summer	-0,191	-0,205	-0,230	-0,245	-0,251	-0,255	-0,243	-0,217	-0,200
Winter	-0,208	-0,224	-0,249	-0,265	-0,271	-0,276	-0,263	-0,236	-0,213

The functions entering into the free term  $f_a(x)$

$$a_1 = [D_0(1-x) - \Delta D_0(x-1)]$$

and

$$a_2 = \int_1^{x_1} [\Delta D_0(x+y-1) - D_0|1+x-y|] \frac{dy}{\eta \left[ \lambda_0 + \frac{b}{a}(1-y) \right]}$$

have for various  $x_1$ , the values cited in Table 25.

Table 25

Values of Functions  $a_1$  and  $a_2$

$x_1$	Summer 6-Month Period		Winter 6-Month Period	
	$a_1$	$a_2$	$a_1$	$a_2$
0,976	0,117	0,225	0,134	0,198
0,941	0,127	0,185	0,135	0,164
0,820	0,138	0,143	0,156	0,132
0,702	0,149	0,120	0,167	0,112
0,621	0,159	0,108	0,178	0,102
0,446	0,190	0,090	0,208	0,098
0,218	0,251	0,076	0,269	0,074
0,047	0,362	0,069	0,380	0,067
0,000	0,993	0,067	0,990	0,065

STAT

Let us write set (47) for  $n = 0$  for the two 6 month periods

$$\begin{array}{l}
 x_i \qquad \text{(a) Summer 6 months} \\
 0,976 \quad 1,225C_{00} - \sum A_j K_1(x_0, x_j) \varphi(x_j) + 0,117F_0(0) = \\
 \qquad \qquad \qquad \qquad \qquad \qquad \qquad \qquad \qquad \qquad \qquad \qquad \qquad \qquad = 0,143 \\
 0,941 \quad 0,452\varphi_1 - \sum A_j K_1(x_1, x_j) \varphi(x_j) + 0,127F_0(0) + \\
 \qquad \qquad \qquad \qquad \qquad \qquad \qquad \qquad \qquad \qquad \qquad \qquad \qquad \qquad + 0,185C_{00} = 0,144 \\
 0,820 \quad 0,352\varphi_2 - \sum A_j K_1(x_2, x_j) \varphi(x_j) + 0,138F_0(0) + \\
 \qquad \qquad \qquad \qquad \qquad \qquad \qquad \qquad \qquad \qquad \qquad \qquad \qquad \qquad + 0,143C_{00} = 0,146 \\
 0,702 \quad 0,306\varphi_3 - \sum A_j K_1(x_3, x_j) \varphi(x_j) + 0,149F_0(0) + \\
 \qquad \qquad \qquad \qquad \qquad \qquad \qquad \qquad \qquad \qquad \qquad \qquad \qquad \qquad + 0,120C_{00} = 0,147 \\
 0,621 \quad 0,247\varphi_4 - \sum A_j K_1(x_4, x_j) \varphi(x_j) + 0,159F_0(0) + \\
 \qquad \qquad \qquad \qquad \qquad \qquad \qquad \qquad \qquad \qquad \qquad \qquad \qquad \qquad + 0,108C_{00} = 0,156 \\
 0,446 \quad 0,081\varphi_5 - \sum A_j K_1(x_5, x_j) \varphi(x_j) + 0,190F_0(0) + \\
 \qquad \qquad \qquad \qquad \qquad \qquad \qquad \qquad \qquad \qquad \qquad \qquad \qquad \qquad + 0,090C_{00} = 0,187 \\
 0,218 - 0,039\varphi_6 - \sum A_j K_1(x_6, x_j) \varphi(x_j) + 0,251F_0(0) + \\
 \qquad \qquad \qquad \qquad \qquad \qquad \qquad \qquad \qquad \qquad \qquad \qquad \qquad \qquad + 0,076C_{00} = 0,227 \\
 0,047 - 0,055\varphi_7 - \sum A_j K_1(x_7, x_j) \varphi(x_j) + 0,362F_0(0) + \\
 \qquad \qquad \qquad \qquad \qquad \qquad \qquad \qquad \qquad \qquad \qquad \qquad \qquad \qquad + 0,069C_{00} = 0,266 \\
 0,000 - 0,023\varphi_8 - \sum A_j K_1(0, x_j) \varphi(x_j) + 0,993F_0(0) + \\
 \qquad \qquad \qquad \qquad \qquad \qquad \qquad \qquad \qquad \qquad \qquad \qquad \qquad \qquad + 0,067C_{00} = 0,289
 \end{array} \tag{64}$$

$$\begin{array}{l}
 x_i \qquad \text{(b) Winter 6 months} \\
 0,976 \quad 1,198C_{00} - \sum A_j K_1(x_0, x_j) \varphi(x_j) + 0,134F_0(0) = \\
 \qquad \qquad \qquad \qquad \qquad \qquad \qquad \qquad \qquad \qquad \qquad \qquad \qquad \qquad = 0,144 \\
 0,941 \quad 0,516\varphi_1 - \sum A_j K_1(x_1, x_j) \varphi(x_j) + 0,135F_0(0) + \\
 \qquad \qquad \qquad \qquad \qquad \qquad \qquad \qquad \qquad \qquad \qquad \qquad \qquad \qquad + 0,164C_{00} = 0,145 \\
 0,820 \quad 0,405\varphi_2 - \sum A_j K_1(x_2, x_j) \varphi(x_j) + 0,156F_0(0) + \\
 \qquad \qquad \qquad \qquad \qquad \qquad \qquad \qquad \qquad \qquad \qquad \qquad \qquad \qquad + 0,132C_{00} = 0,146 \\
 0,702 \quad 0,367\varphi_3 - \sum A_j K_1(x_3, x_j) \varphi(x_j) + 0,167F_0(0) + \\
 \qquad \qquad \qquad \qquad \qquad \qquad \qquad \qquad \qquad \qquad \qquad \qquad \qquad \qquad + 0,112C_{00} = 0,146 \\
 0,621 \quad 0,294\varphi_4 - \sum A_j K_1(x_4, x_j) \varphi(x_j) + 0,178F_0(0) + \\
 \qquad \qquad \qquad \qquad \qquad \qquad \qquad \qquad \qquad \qquad \qquad \qquad \qquad \qquad + 0,102C_{00} = 0,154 \\
 0,446 \quad 0,119\varphi_5 - \sum A_j K_1(x_5, x_j) \varphi(x_j) + 0,208F_0(0) + \\
 \qquad \qquad \qquad \qquad \qquad \qquad \qquad \qquad \qquad \qquad \qquad \qquad \qquad \qquad + 0,088C_{00} = 0,181 \\
 0,218 - 0,017\varphi_6 - \sum A_j K_1(x_6, x_j) \varphi(x_j) + 0,269F_0(0) + \\
 \qquad \qquad \qquad \qquad \qquad \qquad \qquad \qquad \qquad \qquad \qquad \qquad \qquad \qquad + 0,074C_{00} = 0,218 \\
 0,047 - 0,048\varphi_7 - \sum A_j K_1(x_7, x_j) \varphi(x_j) + 0,380F_0(0) + \\
 \qquad \qquad \qquad \qquad \qquad \qquad \qquad \qquad \qquad \qquad \qquad \qquad \qquad \qquad + 0,067C_{00} = 0,252 \\
 0,000 - 0,024\varphi_8 - \sum A_j K_1(0, x_j) \varphi(x_j) + 0,990F_0(0) + \\
 \qquad \qquad \qquad \qquad \qquad \qquad \qquad \qquad \qquad \qquad \qquad \qquad \qquad \qquad + 0,065C_{00} = 0,267
 \end{array} \tag{65}$$

Condition (49) yields for the summer 6 months

$$\varphi_0(x_0) = 1,870C_{00} + 0,115,$$

and for the winter 6 months

$$\varphi_0(x_0) = 1,700C_{00} + 0,100,$$

if it is assumed that in the quasistationary surface layer of the atmosphere the vertical turbulent heat flux  $P$  is proportional to  $\left(\frac{\partial T}{\partial z} + \dot{\varphi}\right)$ .

STAT



Eqs. (64) and (65) together with (49), (51) and (52) represent two sets of 12 equations each of which gives  $F_0(0)$ ,  $C_{00}$ ,  $C_{10}$ , and 9 values of  $\varphi(x_j)$  (Table 26).

Table 26

Characteristics of the $F_0(x)$ -Function												
6-Month Period	$\varphi(x_0)$	$\varphi_1$	$\varphi_2$	$\varphi_3$	$\varphi_4$	$\varphi_5$	$\varphi_6$	$\varphi_7$	$\varphi_8$	$C_{00}$	$F_0(0)$	$C_{10}$
Summer	0,192	0,084	0,090	0,087	0,096	0,208	0,454	2,942	0	0,044	0,124	0,572
Winter	0,182	0,086	0,086	0,081	0,094	0,172	0,446	2,363	0	0,048	0,120	0,519

Now, by means of (48), the altitudinal distribution of  $F_0(x)$  (Table 27) is readily obtained.

Table 27

Altitudinal Distribution of $F_0(x)$											
z in kilometers											
6-Month Period	0	0,05	1	2	3	4	6	8	10	16	
Summer	0,585	0,561	0,530	0,497	0,455	0,411	0,266	0,212	0,132	0,124	
Winter	0,539	0,515	0,493	0,463	0,438	0,388	0,228	0,182	0,125	0,120	

In order to obtain sets for  $n \neq 0$ , the following terms should be added to the right-hand portions of eqs. (64) and (65):

$$-n(n+1) \sum_j A_j [H(x_i) - H(x_j)] \varphi_n(x_j)$$

and

$$-n(n+1) F_n(x_0) [H(x_i) - H(x_0)].$$

The free terms of the sets are composed according to formula (43) by means of Tables 13, 14, and 19. With  $n \neq 0$ , the functions being sought assume the values cited in Table 28.

STAT

Table 28

Characteristics of  $F_2(x)$  - and  $F_4(x)$  - Functions

$n$	$\psi(x_0)$	$\psi_1$	$\psi_2$	$\psi_3$	$\psi_4$	$\psi_5$	$\psi_6$	$\psi_7$	$\psi_8$	$C_{0n}$	$F_n(0)$	$C_{1n}$
-----	-------------	----------	----------	----------	----------	----------	----------	----------	----------	----------	----------	----------

Summer 6 Months

2	-0.092	-0.072	-0.071	-0.063	-0.079	0.071	-0.051	-0.641	0	-0.042	-0.013	-0.153
4	0.033	0.033	0.029	0.024	0.030	0.015	0.012	0.019	0	0.018	0	0.025

Winter 6 Months

2	-0.065	-0.039	-0.039	-0.037	-0.018	0.031	-0.172	-0.930	0	-0.039	-0.030	-0.200
4	-0.032	0.020	-0.021	-0.025	-0.027	-0.033	-0.018	-0.047	0	-0.019	-0.007	-0.031

Now it is possible to construct series  $(\zeta_n)$  and  $(\Omega_n)$ , and also the  $F(x, \theta)$  function. The values of the harmonics of  $\zeta_n$  and  $\Omega_n$  are cited in Table 29.

Table 29

Values of the  $\zeta_n$  - and  $\Omega_n$  - Functions

$x$	$\zeta_0$	$\zeta_2$	$\zeta_4$	$\Omega_0$	$\Omega_2$	$\Omega_4$
-----	-----------	-----------	-----------	------------	------------	------------

Summer 6 Months

0.976	0,000	0,010	0,001	-0,001	0,006	0,000
0.941	0,000	0,010	0,001	-0,001	0,007	0,000
0.820	0,000	0,011	0,001	-0,001	0,003	-0,002
0.702	0,000	0,011	0,001	-0,001	0,003	-0,002
0.621	0,000	0,011	0,001	-0,001	0,004	-0,002
0.446	0,000	0,013	0,000	-0,001	0,003	0,000
0.218	0,000	0,013	0,001	-0,001	0,002	0,000
0.047	0,000	0,008	0,000	-0,001	0,002	0,000
0,0,0	0,000	-0,001	0,000	0,000	0,017	0,000

Winter 6 Months

0.976	-0,001	0,017	0,001	0,000	0,008	-0,003
0.941	-0,001	0,017	0,001	0,000	0,007	0,000
0.820	-0,001	0,017	0,000	0,000	0,003	-0,002
0.702	-0,001	0,016	0,000	0,000	0,007	-0,002
0.621	-0,001	0,016	-0,001	0,000	0,007	-0,002
0.446	-0,001	0,017	-0,001	0,000	0,005	-0,004
0.218	-0,001	0,018	-0,002	0,000	0,002	-0,006
0.047	-0,001	0,014	-0,002	0,000	0,002	-0,005
0,000	0,000	-0,002	0,000	0,000	0,010	-0,002

After the terms associated with  $F(x, \theta)$  in (39) are determined, it is possible to calculate directly the emission function  $E(x, \theta)$  with which we are concerned.

The values of the  $\psi_n(x)$ -gradients and the integration constants for the  $E_n(x)$ -function are presented in Table 30.



STAT

Table 30

Characteristics of the  $E_n(x)$ -Function

$n$	$\psi(x_0)$	$\psi_1$	$\psi_2$	$\psi_3$	$\psi_4$	$\psi_5$	$\psi_6$	$\psi_7$	$\psi_8$	$C_{0n}$	$E_n(0)$	$C_{1n}$
Summer 6 Months												
0	0,194	0,082	0,082	0,082	0,083	0,190	0,435	2,200	4,000	0,042	0,162	0,595
2	-0,077	-0,076	-0,074	-0,074	-0,078	-0,078	-0,066	0,000	-7,90	-0,041	0,069	-0,167
4	0,021	0,022	0,018	0,018	0,015	0,015	0,012	0,021	0	0,011	0,006	0,018
Winter 6 Months												
0	0,175	0,078	0,076	0,076	0,082	0,148	0,389	1,882	3,200	0,044	0,153	0,535
2	-0,085	-0,041	-0,038	-0,038	-0,053	-0,063	-0,178	0,204	-9,60	-0,045	0,055	-0,249
4	-0,042	-0,033	-0,030	-0,030	-0,030	-0,038	-0,005	0,037	-0,046	-0,025	0	-0,033

Formulas (26) and (48) [the latter being written in terms of the  $E_n(x)$ -function] provide an opportunity for finding the altitudinal distribution of  $E_n(x)$ . The calculations are presented in Table 31.

Table 31

Altitudinal Distribution of  $E_n(x)$ 

$n$	z in kilometers									
	0	0,05	1	2	3	4	6	8	10	16
Summer 6 Months										
0	0,607	0,584	0,549	0,517	0,495	0,456	0,375	0,320	0,236	0,162
2	-0,175	-0,155	-0,137	-0,122	-0,112	-0,105	-0,099	-0,094	-0,039	0,069
4	0,021	0,015	0,009	0,007	0,006	0,006	0,006	0,006	0,006	0,006
Winter 6 Months										
0	0,547	0,525	0,511	0,486	0,456	0,428	0,352	0,302	0,203	0,153
2	-0,257	-0,235	-0,213	-0,196	-0,176	-0,164	-0,147	-0,136	-0,030	0,055
4	-0,038	-0,026	-0,014	-0,011	-0,008	-0,007	-0,002	-0,001	0,000	0,000

At the height of the surface layer of the atmosphere and at the earth's surface, the emission function was calculated according to these formulas:

For the summer 6 months

$$E_n(x_0) = -0,300\tilde{C}_{0n} + \tilde{C}_{1n}$$

$$E_n(1) = 0,248\tilde{C}_{0n} + \tilde{C}_{1n}$$

STAT

For the winter 6 months

$$E_n(x_0) = -0,268\bar{C}_{0n} + \bar{C}_{1n}$$

$$E_n(1) = 0,222\bar{C}_{0n} + \bar{C}_{1n}$$

[when  $n=0$ ], the  $\frac{P}{\eta}$  in  $x$  term adds 0.002 more to  $E_0(x)$ ].

The gradients of the emission function in the stratosphere  $\psi(0)$  prove to be larger owing to the smaller quantity of water vapor. As it is evident even from Table 30, in the stratosphere, temperature decreases with altitude at the equator and increases at the pole - as is observed in reality. This determines the characteristics of the latitudinal course of temperature in the stratosphere.

Let us compare the values of the sums of  $\Sigma E_n P_n$  with the corresponding values of the sums of  $\Sigma E_n P_n$  [sic] (Table 32).

Table 32

Components of the Emission Function  $E(z, \varphi)$ :

$F(z, \varphi)$  (upper line);  $E(z, \varphi)$  (lower line)

z in kilometers	$\varphi^\circ$				$\varphi^\circ$			
	0	30	60	90	0	30	60	90
	Summer 6-Months				Winter 6-Months			
0	0,685 0,026	0,599 0,024	0,463 0,016	0,436 0,004	0,649 0,032	0,580 0,015	0,385 -0,020	0,258 -0,042
3	0,506 0,047	0,465 0,042	0,395 0,029	0,368 0,021	0,516 0,030	0,461 0,020	0,336 0,005	0,263 0,001
6	0,286 0,141	0,269 0,116	0,243 0,070	0,234 0,042	0,259 0,165	0,238 0,133	0,185 0,075	0,152 0,051
10	0,140 0,118	0,132 0,107	0,124 0,083	0,124 0,079	0,142 0,076	0,129 0,078	0,104 0,080	0,091 0,080
16	0,132 -0,003	0,132 0,019	0,116 0,089	0,116 0,121	0,135 -0,009	0,124 0,022	0,101 0,086	0,089 0,119

The condition  $E(x, \theta) < F(x, \theta)$  postulated on the basis of taking into account the latitudinal dependence of the optical mass of the atmosphere, is observed throughout all space except for the stratosphere above the pole.

The altitudinal distribution of the harmonics of  $F_n(x)$  cited in Table 33 was used for the construction of  $\bar{F}(x, \theta)$ .

In calculating  $\bar{F}(x, \theta)$ , after having assumed that  $\varphi(0) = 0$ , we obtain at the

16-kilometer altitude a temperature distribution approximately the same as on the 10-kilometer altitude, i.e., we obtain an isothermal temperature distribution over all stratospheric latitudes (see Table 32).

Table 33

Altitudinal Distribution of the  $F_2(x)$ - and  $F_4(x)$ -Functions

		z in kilometers									
n		0	0.05	1	2	3	4	6	8	10	16
Summer 6 Months											
2		-0.178	-0.154	-0.125	-0.105	-0.094	-0.080	-0.037	-0.022	-0.013	-0.013
4		0.029	0.020	0.014	0.010	0.007	0.006	0.005	0.005	0.005	0.005
Winter 6 Months											
2		-0.246	-0.222	-0.204	-0.184	-0.163	-0.133	-0.068	-0.050	-0.033	-0.030
4		-0.035	-0.026	-0.021	-0.016	-0.012	-0.010	-0.008	-0.007	-0.007	-0.007

By means of the harmonics of  $E_n(x)$  from Table 31, the temperature distribution with altitude in the atmosphere at various latitudes (Table 34) is readily constructed.

Table 34

Zonal Temperature for the Northern Hemisphere (Theoretical - Upper Line, and Experimental - Lower Line)

z in kilometers	$\varphi^\circ$									
	0	10	20	30	40	50	60	70	80	90
Summer 6 Months										
0	304	303	299	295	289	283	279	275	273	272
		301	300	297	292	285	280	272		
1	294	293	291	287	283	278	274	270	268	267
2	290	289	287	283	279	275	271	267	265	264
3	286	285	283	280	276	272	268	265	263	262
		284	284	282	278	271	266	262		
4	280	280	278	274	270	266	262	259	257	256
6	268	267	265	261	257	252	248	245	243	242
		267	266	264	258	253	248	243		
8	259	258	255	251	247	244	237	233	231	230
10	236	236	234	232	229	227	225	224	223	223
		239	237	235	230	226	224	223		
16	199	200	202	206	211	218	223	228	230	231
		197	200	204	210	218	224	228		

STAT

## Winter 6 Months

0	299	298	296	291	283	273	262	249	242	235
		299	296	290	281	270	261	252		
1	294	293	291	286	278	269	260	251	245	235
2	289	288	286	281	274	266	257	249	243	242
3	284	283	281	276	270	263	254	247	241	239
		283	281	276	268	261	255	250		
4	279	278	276	271	265	258	250	243	238	236
6	268	267	264	259	253	245	237	230	225	223
		267	264	258	250	242	235	232		
8	256	256	252	247	241	232	226	219	214	211
10	227	227	225	224	222	220	217	216	214	214
		230	235	229	223	220	219	219		
16	197	198	202	206	211	214	218	221	223	224
		198	199	204	209	215	220	222		

Monthly charts of isotherms on various altitudes taken from  $\overline{85}$  were used for comparing the theoretical with the experimental temperatures.

A comparison of the calculated and the experimental temperature values indicates that they agree satisfactorily. Their differences are less than 3 to 4 degrees (except for the 10-kilometer level over the lower latitudes in winter). Obviously, also the accuracy of the values obtained in this manner does not exceed this limit either. Actually, the values of the parameters entering into the problem are determined with insufficient accuracy. For example, such an essential parameter as the albedo is determined with an absolute error of as much as 10 percent, while evaporation is determined with an error of 5 to 10 percent, and so forth.

The calculated altitudinal distribution of the temperature lapse rates agrees with that actually observed. These lapse rates increase with altitude and reach their greatest values, 0.7-0.8 degrees/100 meters, in the middle and upper troposphere, but above the troposphere they begin to decrease. They decrease with an increase in latitude. In summer, in the lowest kilometer layer of air, the lapse rates are greater.

It should be noted that an inversional temperature distribution in the lowest kilometer is found during the winter 6 months in the high latitudes. This also corresponds with the experimental data.

The distribution calculated in this manner is characterized by a normal course

of temperature in the stratosphere and by decrease in the altitude of the tropopause poleward from the equator. This corresponds with reality: above 8 kilometers, the lapse rates over the equator are still large, but over the pole they already assume negative values.

In Table 35 are presented the altitude and temperature of the tropopause at various latitudes, as obtained from Table 34.

In our problem we have taken into account all the first-order factors conditioning the zonal distribution of temperature. Let us emphasize again that the values of the required parameters were selected in a physically substantiated manner. Therefore, it should be assumed that in Table 34 are presented theoretically obtained values of zonal temperature of the earth's atmosphere in the layer below 16 kilometers.

Table 35

Latitudinal Course of the Altitude  $H_T$  in kilometers and

Temperature  $T_T$  (in °K) of the Tropopause

(Upper line - calculated values; lower line - actually observed values according to Flen)

6-Month Period		$\varphi^\circ$								
		10	20	30	40	50	60	70	80	90
Summer	$H_T$	16 16,6	15 16,0	14 15	13 13	12 11,5	10 10,2	9 9,5	9 9	9 9
	$T_T$		202 198	206 208	211 214	218 218	223 221	223 225	223 226	223 227
Winter	$H_T$	16 16,4	15 15,8	14 13,6	12 11,0	11 9,6	10 8,8	9 8,6	8 8,5	8 8,5
	$T_T$		202 203	206 212	211 216	214 216	217 215	215 213	214 210	211 208

The completeness of the factors taken into account can be judged also by the satisfactory correspondence between the calculated and the actually measured temperatures. Such a correspondence could not have been possible if certain basic factors had been overlooked in the selected values of the parameters.

In order to explain how the atmosphere's temperature is formed let us investigate

STAT

the individual components of the heat balance of the atmosphere at various altitudes by means of the fundamental equation in our problem, and let us evaluate their contribution to the thermal regime of the atmosphere.

Certain calculations in this direction already were made in [33].

Let us write the expression for the nth harmonic of the effective radiation of the atmosphere. From (35) it follows that

$$(A_n - B_n) = \int_{x_0}^0 K_1 \frac{\partial E_n}{\partial y} dy - E_n(0) [D_0(1-x) - \Delta D_0(x-1)] - (\xi_n + \Omega_n) + \int_0^{x_0} K_1 \frac{c_{0n}}{\gamma \left[ \lambda_0 + \frac{b}{a}(1-x) \right]} dy. \tag{66}$$

Let us write the values of the harmonics of the individual components of the heat balance at  $n = 0$  (Table 36, in calories/square centimeter minute) characterizing the thermal regime of the entire earth as a whole.

The four terms in the second columns of Table 36 correspond to the terms in the relationship (66). Other, tables presented previously are used for the remaining components.

Table 36

Harmonics of the Heat-Balance Components for Various Altitudes ( $n = 0$ )

$x$	$A_0 - B_0$	$S_0$	$R_0$	$P_0$	$F_0$	$\phi_0$
Summer 6 Months						
0.976	-0.073-0.019 + 0.001-0.009 -0.100	0.296-0.001 0.295	0.195	0.042	0.153	
0.941	-0.074-0.021 + 0.001-0.008 -0.102	0.297-0.001 0.296	0.194	0.041	0.153	
0.820	-0.083-0.022 + 0.001-0.006 -0.110	0.299-0.001 0.298	0.188	0.035	0.153	
0.702	-0.090-0.024 + 0.001-0.005 -0.118	0.300-0.001 0.299	0.181	0.028	0.153	
0.621	-0.099-0.026 + 0.001-0.005 -0.129	0.302-0.001 0.301	0.172	0.026	0.153	0.007
0.446	-0.111-0.031 + 0.001-0.004 -0.145	0.305-0.001 0.304	0.159	0.041	0.153	0.035
0.218	-0.142-0.041 + 0.001-0.003 -0.185	0.308-0.001 0.307	0.122	0.041	0.153	0.072
0.047	-0.170-0.09 + 0.001-0.003 -0.231	0.320 0.320	0.089	0.035	0.153	0.099
0.000	-0.124-0.162 + 0.000-0.003 -0.289	0.335 0.335	0.046	0.000	0.153	0.107
Winter 6 Months						
0.976	-0.058-0.021 + 0.001-0.009 -0.097	0.197-0.003 0.194	0.097	0.044	0.053	
0.941	-0.071-0.021 + 0.001-0.007 -0.098	0.198-0.003 0.195	0.097	0.044	0.053	
0.820	-0.076-0.024 + 0.001-0.006 -0.105	0.199-0.003 0.196	0.091	0.038	0.053	
0.702	-0.084-0.026 + 0.001-0.005 -0.114	0.199-0.003 0.196	0.082	0.029	0.053	
0.621	-0.092-0.027 + 0.001-0.004 -0.122	0.200-0.003 0.197	0.075	0.029	0.053	0.007
0.446	-0.107-0.032 + 0.001-0.004 -0.142	0.201-0.003 0.198	0.056	0.036	0.053	0.033
0.218	-0.130-0.041 + 0.001-0.003 -0.173	0.204-0.003 0.201	0.028	0.042	0.053	0.067
0.047	-0.154-0.058 + 0.001-0.003 -0.214	0.212-0.002 0.210	-0.004	0.036	0.053	STAT
0.000	-0.111-0.152 -0.001-0.003 -0.267	0.221 0.221	-0.046	0.000	0.053	STAT



From Table 36 it is evident that the mean effective radiation of the atmosphere for the earth as a whole increases with altitude - evidently owing to the decrease in atmospheric back radiation with altitude. The mean radiation balance decreases with altitude. The contribution of the surface layer of the atmosphere to the radiation balance is small, in summer amounting to 5 percent, and in winter, to 10 percent of the values of the balance at the earth's surface. At the upper boundary of the atmosphere the annual total of radiation balance is equal to zero. The annual contribution of evaporation and condensation to the heat balance of the earth-atmosphere system also is equal to zero.

The annual course of effective radiation, like that of the turbulent heat flux, fluctuates little at all altitudes.

At the altitudes of 0.1, 1, 2, and 11 kilometers, effective radiation amounts to, according to K. Ya. Kondrat'yev, 56, 66, 90, and 192 kilocalories/square centimeter year, respectively  $\overline{18}$ ; or according to A. N. Lebedinskiy, 66, 72, 91, and 102, respectively  $\overline{18}$ ; while according to Table 36, the corresponding values are 53, 66, 82, and 147. The correspondence between the values of fluxes in the troposphere is satisfactory. The values of outgoing radiation, amounting to 192 and 102 kilocalories/square centimeter year, do not correspond to a condition of radiant equilibrium with a terrestrial albedo of 35 to 40 percent.

According to Baur and Phillips  $\overline{67}$ , the mean effective radiation at the earth's surface in winter amounts to 5 and in summer, to 6 kilocalories/square centimeter month, and at the upper boundary of the atmosphere it correspondingly amounts to 14 and 13 kilocalories/square centimeter month, while according to Table 36 and corresponding values for the earth's surface and the upper boundary of the atmosphere are 4 and 4 and 14 and 12 kilocalories/square centimeter month, respectively.

In order to evaluate the latitudinal course of the components of the heat balance let us compile tables analogous to Table 36 for the remaining harmonics. The values presented in these tables will satisfy the equation

$$R_n + \Phi_n - F_n - P_n + \Pi_n = 0,$$

(67)

STAT

or, which is the same thing, eq. (39) for function  $E_n (F_{th}[\pi])$  is horizontal turbulent heat flux).

From Tables 37-38 it is evident that effective radiation of the atmosphere decreases poleward from the equator.

The decrease in water-vapor density poleward from the equator leads to a decrease in effective radiation and in the flux of solar radiation in the low latitudes, and to an increase of these fluxes in the high latitudes with respect to their values with an average  $\rho$ . The equator-pole drop in the values of effective radiation and fluxes of solar radiation increases with altitude; in winter it is greater than in summer. In this connection, the effective radiation of the atmosphere experiences relatively greater variations than solar radiation. This, in summer, at the earth's surface, with an average  $\rho$ , the effective radiation decreases poleward from the equator at the rate of 0.052 calories/square centimeter minute, but with  $\rho$  decreasing poleward, its rate is only 0.025 calories/square centimeter minute. In winter the drop in effective radiation poleward from the equator in the former case, amounts to 0.083, and in the latter case, 0.045 calories/square centimeter minute. The corresponding rates for the drop in solar radiation between the equator and pole are, in summer, 0.216 and 0.201, and in winter, 0.321 and 0.314 calories/square centimeter minute, respectively, with an average  $\rho$  and with  $\rho$  varying with latitude. Therefore, the consideration of the latitudinal course of water-vapor density results in increasing the radiation balance poleward from the equator. From the data cited above it is obvious that in summer at the earth's surface, the drop in radiation poleward from the equator increases by 0.012, and in winter, 0.031 calories/square centimeter minute, or by 7 to 13 percent in relation to its values with a mean  $\rho$ .

Table 37

Harmonics of Radiation-Balance Components for Various Altitudes (n = 2)

x	A <sub>2</sub> -B <sub>2</sub>	S <sub>2</sub>	R <sub>2</sub>	P <sub>2</sub>	F <sub>2</sub>	Φ <sub>2</sub>	Π <sub>2</sub>
Summer 6 Months							
0.976	0,036 - 0,008 - 0,016 + 0,009 0,021	-0,110 + 0,012 - 0,098	-0,077	-0,041	-0,036		0,000
0,941	0,037 - 0,009 - 0,017 + 0,008 0,019	-0,110 + 0,011 - 0,099	-0,080	-0,040	-0,036		0,004
0,820	0,042 - 0,010 - 0,014 + 0,007 0,025	-0,110 + 0,010 - 0,100	-0,075	-0,034	-0,036		0,005
0,702	0,043 - 0,010 - 0,014 + 0,005 0,024	-0,111 + 0,009 - 0,102	-0,078	-0,029	-0,036		0,013
0,621	0,051 - 0,011 - 0,015 + 0,005 0,030	-0,112 + 0,003 - 0,104	-0,074	-0,025	-0,036	-0,005	0,018
0,446	0,052 - 0,013 - 0,016 + 0,004 0,027	-0,113 + 0,007 - 0,106	-0,079	-0,017	-0,036	-0,026	0,052
0,218	0,057 - 0,017 - 0,015 + 0,003 0,028	-0,114 + 0,006 - 0,108	-0,080	-0,008	-0,036	-0,052	0,088
0,047	0,089 - 0,025 - 0,010 + 0,003 0,057	-0,118 + 0,003 - 0,115	-0,058	-0,001	-0,036	-0,072	0,092
0,000	0,159 - 0,069 - 0,016 + 0,003 0,077	-0,124 - 0,124	-0,047	0,000	-0,036	-0,077	0,086
Winter 6 Months							
0.976	0,049 - 0,006 - 0,025 + 0,007 0,025	-0,226 + 0,008 - 0,218	-0,193	-0,045	-0,148		0,000
0,941	0,050 - 0,008 - 0,024 + 0,006 0,024	-0,227 + 0,009 - 0,218	-0,194	-0,022	-0,148		0,024
0,820	0,054 - 0,010 - 0,020 + 0,006 0,030	-0,228 + 0,007 - 0,221	-0,191	-0,019	-0,148		0,024
0,702	0,062 - 0,010 - 0,023 + 0,004 0,033	-0,228 + 0,006 - 0,222	-0,189	-0,016	-0,148		0,025
0,621	0,064 - 0,011 - 0,023 + 0,009 0,039	-0,230 + 0,006 - 0,224	-0,185	-0,014	-0,148	-0,004	0,027
0,446	0,080 - 0,011 - 0,022 + 0,003 0,050	-0,231 + 0,007 - 0,224	-0,174	-0,010	-0,148	-0,020	0,036
0,218	0,090 - 0,017 - 0,020 + 0,003 0,056	-0,235 + 0,007 - 0,228	-0,172	-0,004	-0,148	-0,040	0,060
0,047	0,112 - 0,023 - 0,016 + 0,002 0,075	-0,244 + 0,006 - 0,238	-0,163	-0,001	-0,148	-0,056	0,070
0,000	0,157 - 0,061 - 0,008 + 0,002 0,090	-0,253 - 0,253	-0,163	0,000	-0,148	-0,060	0,075

Table 38

Harmonics of Radiation-Balance Components for Various

Altitudes (n = 4)

x	A <sub>4</sub> -B <sub>4</sub>	S <sub>4</sub>	R <sub>4</sub>	P <sub>4</sub>	F <sub>4</sub>	Φ <sub>4</sub>	Π <sub>4</sub>
Summer 6 Months							
0.976	-0,003 - 0,001 - 0,003 - 0,002 - 0,009	-0,081 - 0,008 - 0,089	-0,096	0,011	-0,107		0,000
0,941	-0,003 - 0,001 - 0,003 - 0,002 - 0,009	-0,082 - 0,007 - 0,089	-0,098	0,010	-0,107		0,000
0,820	-0,003 - 0,001 - 0,004 - 0,002 - 0,010	-0,082 - 0,005 - 0,087	-0,097	0,008	-0,107		-0,002
0,702	-0,003 - 0,001 - 0,005 - 0,001 - 0,011	-0,083 - 0,004 - 0,087	-0,098	0,006	-0,107		-0,003
0,621	-0,005 - 0,001 - 0,005 - 0,001 - 0,012	-0,083 - 0,003 - 0,086	-0,093	0,005	-0,107	0,001	-0,005
0,446	-0,004 - 0,001 - 0,002 - 0,001 - 0,008	-0,084 - 0,004 - 0,083	-0,096	0,003	-0,107	0,003	-0,011
0,218	-0,004 - 0,002 - 0,001 - 0,001 - 0,008	-0,084 - 0,003 - 0,087	-0,095	0,001	-0,107	0,006	-0,017
0,047	-0,003 - 0,002 - 0,002 - 0,001 - 0,008	-0,088 - 0,002 - 0,090	-0,098	0,000	-0,107	0,008	-0,017
0,000	-0,003 - 0,006 - 0,000 - 0,001 - 0,010	-0,092 - 0,000 - 0,092	-0,102	0,000	-0,107	0,008	-0,013
Winter 6 Months							
0.976	0,004 + 0,002 + 0,005 0,011	0,029 - 0,009 0,020	0,031	-0,025	0,058		0,002
0,941	0,007 + 0,001 + 0,004 0,010	0,029 - 0,008 0,021	0,031	-0,019	0,058		0,008
0,820	0,006 + 0,003 + 0,003 0,012	0,029 - 0,008 0,021	0,033	-0,014	0,058		0,012
0,702	0,008 + 0,002 + 0,003 0,013	0,029 - 0,005 0,024	0,037	-0,012	0,058		0,009
0,621	0,007 + 0,003 + 0,003 0,013	0,029 - 0,005 0,024	0,037	-0,011	0,058		0,010
0,446	0,007 + 0,005 + 0,002 0,014	0,029 - 0,007 0,022	0,036	-0,009	0,058		0,013
0,218	0,006 + 0,008 + 0,002 0,016	0,030 - 0,006 0,024	0,040	-0,001	0,058	-0,001	0,008
0,047	0,008 + 0,007 + 0,002 0,017	0,031 - 0,005 0,026	0,043	-0,001	0,058	-0,001	0,015
0,000	0,005 + 0,002 + 0,002 0,009	0,032 0,032	0,041	0,000	0,058	-0,001	0,018

The contribution of horizontal turbulent exchange  $F_t, h(\pi)$  in the heat balance increases with altitude and leads to a decrease in air temperature over the low

STAT

latitudes and to an increase in air temperature over the high latitudes.

By means of Tables 36-38 the spatial distribution of the various components of the heat balance may be readily obtained. First of all, let us construct the mean heat balance for the earth as a whole (in kilocalories) for the year on the basis of the data obtained, and let us compare it with the calculations of M.I. Budyko [13] and Houghton [59] (Table 39).

The presently computed values of the heat-balance components agree satisfactorily with the data of other investigators. The low value of the short-wave radiation absorbed by the atmosphere is explained by the circumstance that Moller's formula does not take into account the absorption of solar radiation by clouds.

Table 39

## Mean Heat Balance for the earth

Components of the Heat Balance	Symbol	Annual Sum	6-month Period		According to	
			Summer	Winter	Budyko	Houghton
1. Radiation Balance of the Earth-Atmosphere System <sup>1</sup>						
Solar radiation absorbed by the earth-atmosphere system	$S_0$	146	88	58	145	145
	$(B-A)_s$	146	76	70	145	145
Outgoing radiation						
2. Heat Balance of the Earth's Surface						
Solar radiation absorbed by the earth's surface	$S$	130	78	52	110	104
Effective radiation of the earth's surface	$(B-A)$	52	26	26	50	31
Radiation balance of the earth's surface	$R$	78	52	26	60	73
Heat losses to evaporation	$LF$	54	40	14	46 (56)	50

<sup>1</sup> The radiation balance of the system is equal to zero for the year as a whole. For shorter intervals of time, the condition of radiat equilibrium for the earth-atmosphere system is not realized: in summer, +12, while in winter, -12.

Turbulent heat emission to the atmosphere	$P$	24	12	12	14	22
--	-----	----	----	----	----	----

3. Heat Balance of the Atmosphere

Solar radiation absorbed by the atmosphere	$S_a$	16	10	6	35	42
Latent heat of condensation	$\bullet$	54	28	26	46	50
Turbulent heat emission by the earth's surface	$P$	24	12	12	14	22
Effective radiation into outer space	$(B-A)_s$	94	50	44	95	114

Let us calculate the latitudinal course of effective radiation by the earth's surface (Table 40).

In Table 40 are presented the mean annual data for effective radiation under a condition of average cloudiness, obtained by Evfimov [18], and climatological calculations for the two 6 months' periods based on data by T.G. Berlyand [10]. The agreement with the data presented in Table 40 is satisfactory.

Table 40

Effective Radiation of the Earth's Surface B--A (in kilocalories)

Effective Radiation	$\varphi^\circ$									
	0	10	20	30	40	50	60	70	80	90
Summer 6 months	29	29	28	26	24	22	22	22	22	22
Winter 6 Months	27	27	27	27	25	24	21	18	16	15
Year	56	56	55	53	49	46	43	40	38	37
According to N.P. Evfimov (average cloudiness)	46	53	58	58	51	43	39	34	28	28
According to T.G. Berlyand										
Summer 6 Months	19	17	24	27	26	24	23			
Winter 6 Months	17	23	25	28	24	20	18			

STAT

Let us construct the latitudinal course of the radiation balance at the earth's surface (Table 41).

Table 41

Radiation Balance at the Earth's Surface  $R = (S - E + A)$   
in kilocalories

Components of Radiation Balance	$\varphi^\circ$									
	0	10	20	30	40	50	60	70	80	90

Summer 6 Months

S	80	82	85	87	84	74	60	45	33	28
R	51	53	57	61	60	52	38	23	11	6

Winter 6 Months

S	77	75	69	59	46	30	19	11	7	0
R	50	48	42	32	21	6	-2	-7	-9	-15

The mean annual values of the radiation balance at the earth's surface may be compared with the data provided in [10] (Table 42).

Table 42

Mean Annual Values of the Components of the Radiation Balance at  
the Earth's Surface

$\varphi^\circ$	S		R	
	Calculated	Observed <u>[10]</u>	Calculated	Observed <u>[10]</u>
0	157	136	101	100
10	157	145	102	100
20	154	148	99	93
30	146	134	93	78
40	130	110	81	58
50	104	80	58	37

The ignoring of the absorption of radiation by clouds has resulted in higher values of S, and consequently also of R, at the earth's surface. If it is assumed that short-wave radiation is depleted by 5 to 10 percent owing to absorption by clouds, then by reducing the calculated values of R by 5 to 15 calories, we obtain

values that correspond better with the results of climatological calculations.

Let us calculate the latitudinal course of the radiation outgoing from the upper boundary of the atmosphere (Table 43).

Table 43

Outgoing Atmospheric Radiation  $(B-A)_g$  in kilocalories

6-Month Period	Latitude: $\varphi^\circ$									
	0	10	20	30	40	50	60	70	80	90
Summer	84	83	80	77	73	70	67	66	65	64
Winter	81	80	78	74	68	62	55	50	45	44
Annual	165	163	158	151	141	132	122	116	110	108
According to Muegge-Möller for the year	171	170	169	166	159	152	144	133	128	127

For comparison in Table 43 are presented the mean annual values of outgoing radiation calculated by means of the Muegge-Möller radiation diagram [19] for average cloudiness conditions. Their correspondence with the data in Table 44 is satisfactory.

Let us construct the latitudinal distribution of the radiation balance of the earth-atmosphere system (Table 44).

Table 44

Radiation Balance of the Earth-Atmosphere System

$$R_g = S_0 - (B-A)_g \text{ in kilocalories}$$

(upper line -  $S_0$ ; lower line -  $R_g$ )

6-Month Period	$\varphi^\circ$									
	0	10	20	30	40	50	60	70	80	90
Summer	94	95	98	98	93	83	67	49	36	31
	9	10	16	21	22	16	4	-11	-23	-27
Winter	95	90	79	64	46	30	16	7	2	0
	13	10	2	-10	-22	-31	-38	-42	-43	-44
Annual	184	165	177	162	133	113	79	56	38	31
	22	20	18	11	0	-15	-34	-53	-66	-71

The mean annual  $R_g$  changes in sign at the middle latitudes; during the warm 6 months  $R_g$  passes through its zero values at the lower latitudes, and during the cold 6 months, at the higher latitudes.

The heat influx to an air column with a cross-section area of 1 square centimeter

STAT

passing through the entire atmosphere,

$$\Pi = \sum n(n+1) P_n \int_0^\pi G(y) E_n dy$$

and the heat flux across a latitudinal circle

$$Z = 2\pi a_0^2 \sum n(n+1) \int_0^\pi G(y) E_n dy \int_0^\pi \sin \theta P_n d\theta,$$

are conditioned by horizontal turbulent exchange and are distributed latitudinally in the following manner (Table 45).

From Table 45 it is evident that the heat influx  $F_{t,h}(\Pi)$  is negative south of Latitude 40°N and positive north of that latitude. In the high latitudes, heat influx is greater during the colder 6 months of the year than during the warmer 6 months. The greatest quantity of heat is transported by horizontal turbulent fluxes in the middle latitudes. The transport of heat at all latitudes is directed poleward from the equator. Comparison of data in Tables 44 and 45 indicates that horizontal turbulent exchange is of essential importance to the heat balance of the earth-atmosphere system.

Table 45

Influxes and Fluxes of Macroturbulent Heat

(Upper line  $F_{t,h}$  (i.e.,  $\Pi$ ) in kilocalories; lower line -  $Z \cdot 10^{12}$  kilocalories/minute)

6-Month Period	0	10	20	30	40	50	60	70	80	90
Summer	-11	-9	-6	-3	3	8	13	17	19	20
Winter	0	25	12,5	17,5	25,0	27,5	22,5	15,0	5,0	0
	-9	-8	-6	-4	0	9	13	18	23	24
		2,5	12,5	20,0	25,0	22,5	15,0	7,5	0	0
Annual	-20	-17	-12	-7	3	17	26	35	42	44
	0	2,5	12,5	18,8	25,0	25,0	18,8	11,2	2,5	0

We obtain the latitudinal distribution of the components of the radiation balance of the atmosphere as the difference of  $R_s - R_0$  by means of Tables 41 to 44.

Obviously, the radiation field of the earth-atmosphere system is such that the earth's surface - except for the polar areas in winter - represents a source of radiation heat, while the atmosphere at all latitudes is an outlet of radiative heat. This outlet is uniform throughout the year at middle and low latitudes. The latitudinal distribution of the components of heat balance for any layer of the atmosphere bounded

STAT



by the earth's surface below and by a certain level aloft, can be constructed by means of Tables 36-38.

However, if for the two limiting levels, the earth's surface and the upper boundary of the atmosphere, it is possible to find data in meteorological literature although only partially for the comparisons, then no climatological and theoretical calculations of the heat balance components can be found for the inner levels.

It should be noted that previously no success had been achieved in obtaining any heat balance characteristics of the atmosphere in view of the major limitations in setting up the problem, as the result of which an equation of heat balance essentially was not realized. However, quantitative investigations of heat fluxes represent a very essential part of the problem of formulating the thermal regime of the atmosphere, since they are inseparably associated with the theoretical determination of temperature. In this connection, the investigation of heat fluxes will be continued in Chapter 3, in which there is given detailed analysis of heat transmission processes characteristic for a circulation differing from a strictly zonal circulation.

The theory developed by us makes it possible to construct a mean distribution of temperatures and of heat balance components for intervals of time of the order of a month. However, owing to the lack of necessary data on evaporation, precipitation and heat fluxes into the soil, it is not yet possible to make such calculations.

Once the absorption of short-wave radiation by clouds will have been investigated, the application of corresponding corrections to heat balance calculations will involve no difficulties; this will consist in altering the value of the free term in eq. (15) which determines the magnitude of vertical turbulent heat flux. However, at present, no theoretical investigation of this nature has been undertaken.

Let us recapitulate the results of this Chapter. The problem of the stationary zonal distribution of temperature in the atmosphere has been posed and resolved by taking into account all the fundamental factors, these factors having been examined as thoroughly as possible at the present time. The zonal temperature field calculated up to the 16-kilometer level was found to agree satisfactorily with the field actually

STAT

observed.

In view of the sufficient completeness of the approach to the present problem, and also considering that the quantitative values of the required parameters taken for the calculations are experimentally substantiated, the data in Tables 34-35 should be considered as the first theoretical distribution of a stationary zonal temperature in the atmosphere.

It was found possible to evaluate the contribution of various factors to the thermal regime of the atmosphere. It is essential that such evaluations may be realized only theoretically. Any other methods cannot isolate the influence of individual factors in its pure form (e.g., the influence of factors varying with latitude, (density of water vapor  $\rho$  or the albedo  $\sqrt{\tau}$ ). By means of the equation of the heat balance of a given atmospheric layer, which is the basis of the problem, the values of heat-balance components at various levels and at various latitudes in the atmosphere are calculated after the determination of the temperature. In this connection, it is also possible to construct distributions of the components that cannot be established by any other method - the heat balance of limited layers of the atmosphere. Whereas the climatological statistical methods require processing of an immense mass of observational data for calculating the zonal values of the heat-balance components, the theoretical method developed above makes it possible to determine these characteristics without difficulty.

All this makes it possible to consider the presently set forth theory of the zonal distribution of atmospheric temperature as the most complete and most conclusive of the theories existing at the present time.

## Chapter III

## HEAT ADVECTION IN THE ATMOSPHERE.

## Integral Characteristics of Heat Advection.

The question of evaluating the advective transfer of heat is essential in solving problems of general circulation of the atmosphere.

In the present Chapter a method of computing nonturbulent heat advection is proposed, examples of its application are given and a physical analysis of its results is made.

Let us write the equation of heat transfer in a spherical coordinate system

$$\frac{\partial T}{\partial t} + \frac{v_\lambda}{a_0 \sin \theta} \frac{\partial T}{\partial \lambda} + \frac{v_\theta}{a_0} \frac{\partial T}{\partial \theta} + (\gamma_s - \gamma) w = \frac{\epsilon}{c_p \rho} \quad (1)$$

Here  $T$  is air temperature;  $v_\lambda$ ,  $v_\theta$ , and  $w$  are the latitudinal, longitudinal and vertical wind components, respectively;  $\gamma_s$  and  $\gamma$  are the dry-adiabatic and stratification gradients, respectively;  $\epsilon$  is heat influx to a volume unit of air;  $t$  is time;  $a_0$  is radius of the earth;  $\lambda$  is longitude;  $\theta$  is complement to geographical latitude; and  $\rho$  is air density.

Let us assume for the basic state a stationary, purely zonal, circulation.

Let us carry out a linearization of eq. (1) in relation to the basic state, after having represented  $T$ ,  $v_\lambda$ ,  $v_\theta$ ,  $w$ , and  $\epsilon$  in the form of the sum of zonal values and of the deviations from them.

$$v_\lambda = \bar{v}_\lambda(\theta, z) + v'_\lambda(\theta, \lambda, z, t),$$

$$v_\theta = v'_\theta(\theta, \lambda, z, t),$$

$$w = w'(\theta, \lambda, z, t),$$

$$T = \bar{T}(\theta, z) + T'(\theta, \lambda, z, t),$$

$$\rho = \bar{\rho}(\theta, z) + \rho'(\theta, \lambda, z, t),$$

$$\epsilon = \bar{\epsilon}(\theta, z) + \epsilon'(\theta, \lambda, z, t),$$

inasmuch as it follows from the definition of the purely zonal stationary circulation that

$$\bar{v}_\theta = \bar{w} = 0.$$

STAT

For the basic state, eq. (1) assumes the form

$$\bar{v}(\theta, z) = 0,$$

and the deviations from that state are determined by the following equation

$$\frac{\partial T'}{\partial t} + \frac{\bar{v}_\lambda}{a_0 \sin \theta} \frac{\partial T'}{\partial \lambda} + \frac{v'_\theta}{a_0} \frac{\partial T'}{\partial \theta} + (\gamma_s - \gamma) w' = \frac{e'}{c_p p}. \quad (2)$$

By means of the equation of statics

$$\frac{\partial \ln p}{\partial z} = -\frac{g}{RT} \quad (3)$$

and the equations of the geostrophic wind

$$2\omega p \cos \theta v_\lambda = \frac{1}{a_0} \frac{\partial p}{\partial \theta}, \quad (4)$$

$$2\omega p \cos \theta v_\theta = -\frac{1}{a_0 \sin \theta} \frac{\partial p}{\partial \lambda} \quad (4')$$

we obtain the relations determining the thermal wind

$$\frac{\partial T}{\partial \theta} = \frac{f a_0 T}{g} \frac{\partial v_\lambda}{\partial z} - \frac{f a_0 v_\lambda}{g} \frac{\partial T}{\partial z}, \quad (5)$$

$$\frac{\partial T}{\partial \lambda} = -\frac{f a_0 T \sin \theta}{g} \frac{\partial v'_\theta}{\partial z} + \frac{f a_0 \sin \theta}{g} v'_\theta \frac{\partial T}{\partial z}. \quad (6)$$

Here

$$f = 2\omega \cos \theta.$$

On the basis of (5) and (6), eq. (2) is rewritten as:

$$\frac{\partial T'}{\partial t} - \frac{fT}{g} \left( \frac{\partial v'_\theta}{\partial z} - v'_\theta \frac{\partial v_\lambda}{\partial z} \right) + \frac{fT}{g} v'_\lambda v'_\theta + (\gamma_s - \gamma) w' = \frac{e'}{c_p p}. \quad (7)$$

Zonal velocity for the basic state is determined conventionally by means of the circulation index  $\alpha$

$$\bar{v}_\lambda = a_0 \alpha(z) \sin \theta.$$

For deviations  $v'_\lambda(\theta, \lambda, z, t)$  we obtain from formula (4)

$$v'_\lambda = \frac{1}{f a_0} \frac{\partial p'}{\partial \theta}. \quad (8)$$

STAT

Here

$$a' = \frac{d}{dx} a$$

The discarding of  $v'\lambda$  would be equivalent to ignoring the values of  $\frac{\partial p'}{\partial \theta}$  and  $\frac{\partial T'}{\partial \lambda}$  [see (4') and (5)].

Let us also represent  $T'$  and  $v'_0$  as a p-function.

It follows from (5) that

$$T' = \frac{RT'^2}{g} \frac{\partial}{\partial x} \frac{p'}{p}. \quad (9)$$

Eq. (4'') yields

$$v'_0 \sin \theta = -\frac{1}{a_0 f p} \frac{\partial p'}{\partial \lambda}. \quad (10)$$

It follows from (5) that

$$\frac{\partial \sin \theta v'_0}{\partial x} = -\frac{\gamma}{T'} v'_0 \sin \theta - \frac{g}{f a_0 T'} \frac{\partial T'}{\partial \lambda},$$

or, on the basis of (10)

$$\frac{\partial \sin \theta v'_0}{\partial x} = \frac{R}{f a_0} \left( \frac{\gamma}{p} \frac{\partial p'}{\partial \lambda} - \frac{g}{RT} \frac{\partial T'}{\partial \lambda} \right).$$

Ultimately, by means of (9), we obtain

$$\frac{\partial \sin \theta v'_0}{\partial x} = \frac{R}{f a_0} \left[ \frac{\gamma}{p} \frac{\partial p'}{\partial \lambda} - T' \frac{\partial^2}{\partial \lambda \partial x} \frac{p'}{p} \right] = -\frac{R}{f a_0} \frac{\partial}{\partial x} \left( T' \frac{\partial}{\partial \lambda} \frac{p'}{p} \right) \quad (11)$$

Eqs. (8) and (10) yield

$$\begin{aligned} \frac{\gamma}{g} v'_0 v'_0 + \frac{\gamma T'}{g} v'_0 \frac{\partial v'_0}{\partial x} &= -\frac{1}{g f a_0^2 \sin \theta} \left[ \frac{\gamma}{p} \frac{\partial p'}{\partial \theta} + T' \frac{\partial}{\partial x} \left( \frac{1}{p} \frac{\partial p'}{\partial \theta} \right) \right] \frac{\partial p'}{\partial \lambda} \\ &= -\frac{1}{g f a_0^2 \sin \theta} \frac{\partial p'}{\partial \lambda} \left[ \frac{\partial}{\partial x} \left( T' \frac{1}{p} \frac{\partial p'}{\partial \theta} \right) + 2\gamma \frac{1}{p} \frac{\partial p'}{\partial \theta} \right]. \end{aligned}$$

Now (7) can be rewritten in the following manner:

$$\begin{aligned} \frac{RT'^2}{g} \frac{\partial^2}{\partial x \partial t} \frac{p'}{p} + \frac{RT'}{g} \frac{\partial}{\partial x} \left( T' \frac{\partial}{\partial \lambda} \frac{p'}{p} \right) - \frac{a' T \partial p'}{g p \partial \lambda} \\ - \frac{1}{g f a_0^2 \sin \theta} \frac{\partial p'}{\partial \lambda} \left[ \frac{\partial}{\partial x} \left( T' \frac{\partial p'}{\partial \theta} \right) + 2\gamma \frac{\partial p'}{\partial \theta} \right] + (\gamma_a - \gamma) w' = \frac{a'}{c_p p} \end{aligned} \quad (12)$$

STAT

or

$$\begin{aligned} \frac{pT}{g} \frac{\partial^2}{\partial x \partial t} \frac{p'}{p} + \frac{ap}{g} \frac{\partial}{\partial x} \left( T' \frac{\partial}{\partial \lambda} \frac{p'}{p} \right) - \frac{T a' \partial p'}{g \partial \lambda} \\ - \frac{1}{g f a_0^2 \sin \theta} \frac{\partial p'}{\partial \lambda} \left[ \frac{\partial}{\partial x} \left( T' \frac{\partial p'}{\partial \theta} \right) + 2\gamma \frac{\partial p'}{\partial \theta} \right] + (\gamma_a - \gamma) w' p = \frac{a'}{c_p}. \end{aligned}$$

Here

$$\epsilon' = \frac{d}{dz} \epsilon$$

Let us integrate (12) with respect to  $z$  from 0 to  $z$ . Inasmuch as

$$\begin{aligned} \frac{1}{g} \int_0^z p \bar{T} \frac{\partial^2 p'}{\partial x \partial t} dz &= \frac{\bar{T}}{g} \frac{\partial p'}{\partial t} \Big|_0^z + \left[ \frac{1}{g} + \frac{1}{R} \right] \int_0^z \frac{\partial p'}{\partial t} dz, \\ \int_0^z \frac{\alpha p}{g} \frac{\partial}{\partial x} \left( T \frac{\partial p'}{\partial \lambda} \right) dz &= \frac{\alpha T \partial p'}{g} \Big|_0^z + \frac{1}{R} \int_0^z \alpha \frac{\partial p'}{\partial \lambda} dz - \frac{1}{g} \int_0^z \alpha' T \frac{\partial p'}{\partial \lambda} dz, \\ \int_0^z \frac{\partial p'}{\partial \lambda} \frac{\partial}{\partial x} \left[ \frac{T \partial p'}{p \partial \theta} \right] dz &= \frac{T \partial p'}{p} \frac{\partial p'}{\partial \theta} \Big|_0^z + g \int_0^z T \frac{\partial p'}{\partial \theta} \frac{\partial \ln p}{\partial \lambda} dz, \end{aligned}$$

therefore (12) gives

$$\begin{aligned} \frac{T}{g} \frac{\partial p'}{\partial t} \Big|_0^z + \left[ \frac{1}{g} + \frac{1}{R} \right] \int_0^z \frac{\partial p'}{\partial t} dz + \frac{\alpha T \partial p'}{g} \Big|_0^z + \frac{1}{R} \int_0^z \alpha \frac{\partial p'}{\partial \lambda} dz - \\ - \frac{2}{g} \int_0^z \alpha' T \frac{\partial p'}{\partial \lambda} dz - \frac{1}{g f a_0^2 \sin \theta} \left[ \frac{T \partial p'}{p} \frac{\partial p'}{\partial \theta} \Big|_0^z + g \int_0^z T \frac{\partial p'}{\partial \theta} \frac{\partial \ln p}{\partial \lambda} dz + \right. \\ \left. + 2\gamma \int_0^z \frac{1}{p} \frac{\partial p'}{\partial \theta} \frac{\partial p'}{\partial \lambda} dz \right] + \int_0^z (\gamma_a - \gamma) p w' dz = \frac{1}{c_p} \int_0^z \epsilon' dz. \end{aligned} \quad (13)$$

Let us integrate (13) with respect to time from  $t_0$  to  $t$ . Inasmuch as

$$\begin{aligned} \frac{1}{g} \int_{t_0}^t \left( T \frac{\partial p'}{\partial t} \Big|_z - \bar{T} \frac{\partial p'}{\partial t} \Big|_0 \right) dt &= \frac{1}{g} [T p'(z) - T p'(0)] \Big|_{t_0}^t, \\ \int_{t_0}^t dt \int_0^z \frac{\partial p'}{\partial t} dz &= \int_0^z dz \int_{t_0}^t \frac{\partial p'}{\partial t} dt = \int_0^z [p'(t) - p'(t_0)] dz. \end{aligned}$$

therefore

$$\begin{aligned} \frac{1}{g} (T p' \Big|_z - T p' \Big|_0) \Big|_{t_0}^t + \left[ \frac{1}{g} + \frac{1}{R} \right] \int_0^z p' \Big|_{t_0}^t dz + \int_{t_0}^t \left[ \frac{\alpha T \partial p'}{g} \Big|_0^z + \right. \\ \left. + \frac{1}{R} \int_0^z \alpha \frac{\partial p'}{\partial \lambda} dz - \frac{2}{g} \int_0^z \alpha' T \frac{\partial p'}{\partial \lambda} dz - \frac{1}{g f a_0^2 \sin \theta} \left[ \frac{T \partial p'}{p} \frac{\partial p'}{\partial \theta} \Big|_0^z + \right. \right. \\ \left. \left. + g \int_0^z T \frac{\partial p'}{\partial \theta} \frac{\partial \ln p}{\partial \lambda} dz + 2\gamma \int_0^z \frac{1}{p} \frac{\partial p'}{\partial \theta} \frac{\partial p'}{\partial \lambda} dz \right] + \right. \\ \left. + \int_0^z (\gamma_a - \gamma) p w' dz \right) dt = \frac{1}{c_p} \int_{t_0}^t dt \int_0^z \epsilon' dz. \end{aligned} \quad (14)$$

STAT

Let us examine in (13) the terms pertaining to heat advection:

$$\begin{aligned}
 A = c_p \left\{ -\frac{\alpha T}{g} \frac{\partial p'}{\partial \lambda} \Big|_z - \frac{1}{R} \int_0^z x \frac{\partial p'}{\partial \lambda} dz + \frac{2}{g} \int_0^z x' T \frac{\partial p'}{\partial \lambda} dz + \right. \\
 \left. + \frac{1}{g/a_0^2 \sin \theta} \left[ \frac{T}{p} \frac{\partial p'}{\partial \lambda} \frac{\partial p'}{\partial \theta} \Big|_0^z - \int_0^z \frac{RT^2}{p} \frac{\partial p'}{\partial \theta} \frac{\partial p'}{\partial x \partial \lambda} dz + \right. \right. \\
 \left. \left. + 2\gamma \int_0^z \frac{1}{p} \frac{\partial p'}{\partial \theta} \frac{\partial p'}{\partial \lambda} dz \right] \right\}. \quad (15)
 \end{aligned}$$

Here  $A$  is the advective transfer of heat during a unit of time ( $A < 0$  corresponds to an advection of cold). The mean change in the heat content of an air column with an altitude of  $z$  during the  $t-t_0$  time interval is determined by the following formula:

$$\Delta = \frac{c_p}{t-t_0} \left\{ \frac{1}{g} (\overline{T p'} \Big|_z - \overline{T p'} \Big|_0) + \left( \frac{1}{g} + \frac{1}{R} \right) \int_0^z p' \Big|_{t_0}^t dz \right\}. \quad (16)$$

According to formulas (15) and (16) it is possible to calculate  $A$  and  $L$  for time intervals of the order of a week and longer.

The problem consists in calculating advection  $A$  and the variation of the heat content on the basis of the known distribution of pressure and temperature in the atmosphere. For greater accuracy, the integral terms in (15) and (16) must be calculated according to the greatest possible number of points in the  $(0, z)$  interval.

Usually, the  $p$  and  $T$  distributions are constructed for some standard equations 3 to 4 kilometers apart.

By means of the interpolation formula cited below, it is possible to determine the pressure at intermediate levels (i.e., between standard levels) with sufficient accuracy for our calculations.

The interpolation formula in its form, is an analogue of the barometric formula for the polytropic layer in the atmosphere of an altitude  $H$ , found between two standard levels.

The use of this formula involves the stipulation of pressure  $p_0$  and temperature

STAT

$P_0$  at the lower standard level, and the coefficient  $\beta$  is selected so as to obtain, at  $z = H$ , the following pressure of the upper standard level:

$$P = P_0 \left[ 1 - \frac{\beta}{T_0} z \right]^{\frac{g}{R\beta}} \tag{17}$$

In order to determine the degree of reliability of formula (17), the pressure curves for several radiosonde and airplane soundings were computed according to it and then were compared with the actually recorded pressures, (Table 46).

In Table 46 are presented the values of the observed pressure  $P_{\text{observed}}$  computed pressure  $P_{\text{computed}}$  and temperature  $T$  at the standard  $z$ -levels. The interpolation formula (17) reduces the pressure at intermediate levels with an error not exceeding 0.5 percent. However, (15) and (16) include pressure derivatives which can be substituted by finite differences in the calculations. Therefore, it is necessary that the areas plotted according to the actual pressure differences are sufficiently well represented by areas plotted on the basis of the computed differences. By means of Table 46, 10 examples of such comparisons may be obtained.

Table 46

Aerological Data						
$z$	$T$	$P_{\text{observed}}$	$P$	$T$	$P_{\text{observed}}$	$P$
Pakhta-Aral						
Radiosonde						
13 July, 1200 hours				14 July 0800 hours		
3	292,5	712	632,8	286	710	
4		633	561,2		630	629,3
5		561			557	556,0
6	270,8	496	436,7	265,8	490	
7		436	383,3		430	430,1
8		383	335,6		376	376,3
9		335			327	328,0
10	247,1	293		245,8	285	
Kiev						
Airplane				Radiosonde		
18 June, 1600 hours				2 July, 0400 hours		
-0	302	1010	900,5	293,5	1020	
1		899	800,4		904	906,5
2		799			802	803,6
3	279,5	708	625,8	277,2	710	
4		626	551,6		628	627,3
5		551			554	553,2
6	261,4	485		261,3	487	

STAT



Table 46 (continued)

Airplane			
16 August, 1600 hours			
0	297,0	1015	
1		902	902,8
2		800	801,1
3	273,0	707	
4		623	622,9
5		547	547,2
6	254,4	479	

The areas plotted according to the computed and the actually observed data approximate each other closely in value. The mean error in the determination of the areas on the basis of data in Table 46 amounts to 7 percent.

Consequently, interpolation formula (17) provides the possibility for a sufficiently reliable determination of the integral terms in (15) and (16)

Calculating the Components of Nonturbulent Advection. Evaluating the Horizontal Turbulent Heat Transfer.

To illustrate the applicability of formula (15) for computing advection  $A$ , this formula has been used to determine the annual course in the 0-10 kilometer layer for Odessa ( $\varphi = 46^{\circ}30'$ ,  $\lambda = 30^{\circ}40'$ ), Riga ( $\varphi = 56^{\circ}57'$ ;  $\lambda = 24^{\circ}05'$ ) and Sverdlovsk ( $\varphi = 56^{\circ}50'$ ;  $\lambda = 60^{\circ}38'$ ). The initial data on pressure and temperature were taken from [85] where the standard levels are: 0, 3, 6, 10, 13, and 16 kilometers.

In calculating the  $p$  differences for Odessa and Sverdlovsk the following intervals were adopted: for latitude -  $20''$ , and for longitude -  $10''$ , while for Riga,  $10''$  for both latitude and longitude.

Special nomograms were constructed for interpolating pressure between standard levels by means of (17). On these nomograms, the  $E = \lg p - \lg p_0$  differences were marked off along the axis of the abscissas, while the coefficient  $\beta$  was marked off along the axis of ordinates. Isolines of  $T_0$  were plotted in this coordinate system. The nomograms were designed for altitude intervals  $\Delta z$  equal to 1, 2, 3 and 4 kilometers, respectively.

Work with nomograms. has the following procedure: from a nomogram on which

STAT

$\Delta z$  is equal to the distance between adjacent standard levels,  $\beta$  is computed according to the given  $N$  and  $T_0$ , and from nomograms on which  $\Delta z$  is equal to the distance between the lower standard level and the given intermediate level,  $N$  is computed according to the obtained  $\beta$  and the given  $T_0$ . Then according to  $N$  the  $p$  at that level is calculated.

The rating formulas

$$A = \sum_{i=1}^n A_i \quad \text{calories/square centimeter minute}$$

$$i = 1, 2, \dots, 6$$

for the various seasons are presented in Table 47 and below

$$A_1 = \frac{1.50}{\sin \theta} 10^{-5} \frac{T^2}{p} \Delta_\lambda p \Delta_\lambda p' \Big|_0^z$$

$$A_2 = \frac{0.30}{\sin \theta} \int_0^z \gamma \frac{T}{p} \Delta_\lambda p \Delta_\lambda p' dz$$

$$A_3 = -\frac{1.50}{\sin \theta} 10^{-5} \int_0^z \frac{T^2}{p} \Delta_\lambda p' \Delta_\lambda^2 z p dz$$

Table 47

Calculated Formulas for Advection A in calories/square centimeter minute

Advection Component	Layer in kilometers	
	0-10	10-16
Spring		
$A_1$	$-0.046 \Delta_\lambda p_{10}$	$0.046 \Delta_\lambda p_{10} - 0.026 \Delta_\lambda p_{16}$
$A_2$	$-0.700 \cdot 10^{-4} \int z \Delta_\lambda p dz$	$-0.700 \cdot 10^{-4} \int_{10}^{16} \Delta_\lambda p dz +$ $+ 10^{-4} \int_{13}^{16} (z-13) \Delta_\lambda p dz$
$A_3$	$0.403 \cdot 10^{-5} \int T \Delta_\lambda p dz$	$-0.585 \cdot 10^{-5} \int_{13}^{16} T \Delta_\lambda p dz$
Summer		
$A_1$	$-0.045 \Delta_\lambda p_{10}$	$0.045 \Delta_\lambda p_{10} - 0.022 \Delta_\lambda p_{16}$
$A_2$	$-0.680 \cdot 10^{-4} \int z \Delta_\lambda p dz$	$-0.680 \cdot 10^{-4} \int_{10}^{16} \Delta_\lambda p dz +$ $+ 1.150 \cdot 10^{-4} \int_{12}^{15} (z-13) \Delta_\lambda p dz$
$A_3$	$0.393 \cdot 10^{-5} \int T \Delta_\lambda p dz$	$-0.673 \cdot 10^{-5} \int_{13}^{16} T \Delta_\lambda p dz$

		Autumn	
$A_1$	$-0,059 \cdot \Delta_\lambda p_{10}$	$0,059 \Delta_\lambda p_{10}$	$-0,037 \Delta_\lambda p_{16}$
$A_2$	$-0,895 \cdot 10^{-4} \int z \Delta_\lambda p dz$	$-0,900 \cdot 10^{-3} \int_{10}^{16} \Delta_\lambda p dz +$	$+ 1,110 \cdot 10^{-4} \int_{13}^{16} (z-13) \Delta_\lambda p dz$
$A_3$	$0,515 \cdot 10^{-5} \int T \Delta_\lambda p dz$	$-0,650 \cdot 10^{-5} \int_{13}^{16} T \Delta_\lambda p dz$	
		Winter	
$A_1$	$-0,059 \Delta_\lambda p_{10}$	$0,059 \Delta_\lambda p_{16}$	$-0,047 \Delta_\lambda p_{16}$
$A_2$	$-0,895 \cdot 10^{-4} \int z \Delta_\lambda p dz$	$-0,900 \cdot 10^{-3} \int_{10}^{16} \Delta_\lambda p dz +$	$+ 0,600 \cdot 10^{-4} \int_{13}^{16} (z-13) \Delta_\lambda p dz$
$A_3$	$0,515 \cdot 10^{-5} \int T \Delta_\lambda p dz$	$-0,345 \cdot 10^{-5} \int_{13}^{16} T \Delta_\lambda p dz$	

In Table 47 it is assumed that 100 meters = 1 unit of length. The p-difference is formed for 20° intervals by latitude ( $\Delta_\lambda p$ ) and 10° intervals by longitude ( $\Delta_\lambda p$ ). The circulation indexes for the troposphere and stratosphere are taken from the data of S.A. Mashkovich and V.V. Bykov. In the troposphere  $\alpha$  is approximated by the linear function of altitude

$$z = \alpha'_{0-10} z.$$

In the stratosphere at altitudes from 10 to 13 kilometers  $\alpha$  has a constant value  $\alpha_{10-13} = \text{const.}$ , while at altitudes from 13 to 16 kilometers it decreases with altitude

$$\alpha = \bar{\alpha}_{10-13} + n(z - 13).$$

Let us cite the values of the parameters determining the  $\alpha$  in various layers

	Spring	Autumn
$\alpha'_{0-10} \text{ cm}^{-1} \text{ min}^{-1}$	$2,93 \cdot 10^{-10}$	$3,75 \cdot 10^{-10}$
$\alpha_{10-13} \text{ min}^{-1}$	$2,93 \cdot 10^{-4}$	$3,75 \cdot 10^{-4}$
$n \text{ cm}^{-1} \text{ min}^{-1}$	$4,20 \cdot 10^{-10}$	$4,68 \cdot 10^{-10}$
	Summer	Winter
$\alpha'_{0-10} \text{ cm}^{-1} \text{ min}^{-1}$	$2,85 \cdot 10^{-10}$	$3,75 \cdot 10^{-10}$
$\alpha_{10-13} \text{ min}^{-1}$	$2,85 \cdot 10^{-4}$	$3,75 \cdot 10^{-4}$
$n \text{ cm}^{-1} \text{ min}^{-1}$	$4,83 \cdot 10^{-10}$	$2,50 \cdot 10^{-10}$

The results of the calculations of advection A according to formula (15) are given in Table 48.

Table 48

Heat Advection in the Troposphere (kilocalories/s.cm. month)

Station	I	II	III	IV	V	VI	VII	VIII	IX	X	XI	XII
Odessa	5.3	3.5	3.6	1.3	-1.1	-2.0	-3.0	-1.0	1.0	6.4	5.8	5.2
Riga	6.1	4.1	4.8	2.0	-2.6	-5.6	-3.4	-2.8	1.8	7.2	6.2	5.2
Sverdlovsk	3.3	5.0	2.0	-1.1	-1.9	-1.7	-2.1	-1.1	0.9	2.0	2.6	3.6

Let us compare these direct calculations with the indirect calculations made by T.G. Berlyand [3] who derived advection as the residual term of the equation of heat balance for the earth-atmosphere system, a term including all the errors in determining the remaining components in the equation of heat balance, and also including such factors not considered in [3] as variations in heat content, heat fluxes caused by horizontal turbulent exchange, and heat fluxes into the soil (Table 7)

The agreement between the values of A computed by the author and those obtained by various methods in [3] is satisfactory. The existing differences should be attributed primarily to the above mentioned inaccuracy of determining A in [3].

On having ascertained the quantitative reliability of the obtained values of A (Table 48) let us now subject them to a physical analysis and also calculate the advection for areas not covered in [3].

Let us isolate the latitudinal and meridional components from A.

The latitudinal component is

$$A_{\lambda} = c_p \left\{ -\frac{\alpha T}{g} \frac{\partial p'}{\partial \lambda} \right\}_z - \frac{1}{R} \int_0^z \alpha \frac{\partial p}{\partial \lambda} dz + \frac{\alpha'}{g} \int_0^z T \frac{\partial p}{\partial \lambda} dz \right\}. \quad (18)$$

The meridional component is

$$A_{\theta} = c_p \left\{ \frac{\alpha'}{g} \int_0^z T \frac{\partial p}{\partial \lambda} dz + \frac{1}{g f a_0^2 \sin \theta} \left[ \frac{T}{p} \frac{\partial p'}{\partial \lambda} \frac{\partial p'}{\partial \theta} \right]_0^z - \int_0^z \frac{RT^2}{p} \frac{\partial p'}{\partial \theta} \frac{\partial p'}{\partial z \partial \lambda} dz + 2\gamma \int_0^z \frac{1}{p} \frac{\partial p}{\partial \theta} \frac{\partial p}{\partial \lambda} dz \right\}. \quad (19)$$

Meridional heat transfer  $A_{\theta}$  may, in turn, be subdivided into two components  $A_{\theta 1}$  and  $A_{\theta 2}$ . The first component,  $A_{\theta 1}$ , is conditioned by the mean annual zonal

STAT

value of the meridional temperature gradient  $\frac{\partial T}{\partial \theta}$  [first term of (19)], while the second component,  $A_{20}$ , is determined by the deviations of  $\frac{\partial T}{\partial \theta}$  from the mean zonal values [sum of all remaining terms in (19)].

In figs. 11-13 are presented the values of the  $A_1$ ,  $A_2$  and  $A_3$  components.

It is evident from these graphs that the latitudinal component  $A_1$  has the same annual course as total advection  $A$ ; it is positive in winter, negative in summer, and passes through zero values during the transitional seasons (i.e., spring and autumn).

Heat Advection (Computed by the Heat-Balance Method)

Table 49

in kilocalories/square centimeter month

Station	I	II	III	IV	V	VI	VII	VIII	IX	X	XI	XII
Odessa	6.8	5.2	2.9	0.2	-3.0	-3.3	-1.9	-0.4	2.2	4.1	5.4	7.4
Riga	7.4	5.2	4.8	1.1	-2.2	-4.1	-3.0	-1.3	1.9	4.8	5.6	6.7
Sverdlovsk	8.0	6.2	5.9	4.0	-0.8	-2.9	-2.2	0.1	2.3	5.5	7.5	8.1

In the graph the meridional component  $A_1$  is a double wave with maximum (positive) values in the transitional seasons (autumn and spring) and minimum values (positive and negative) in summer and winter.

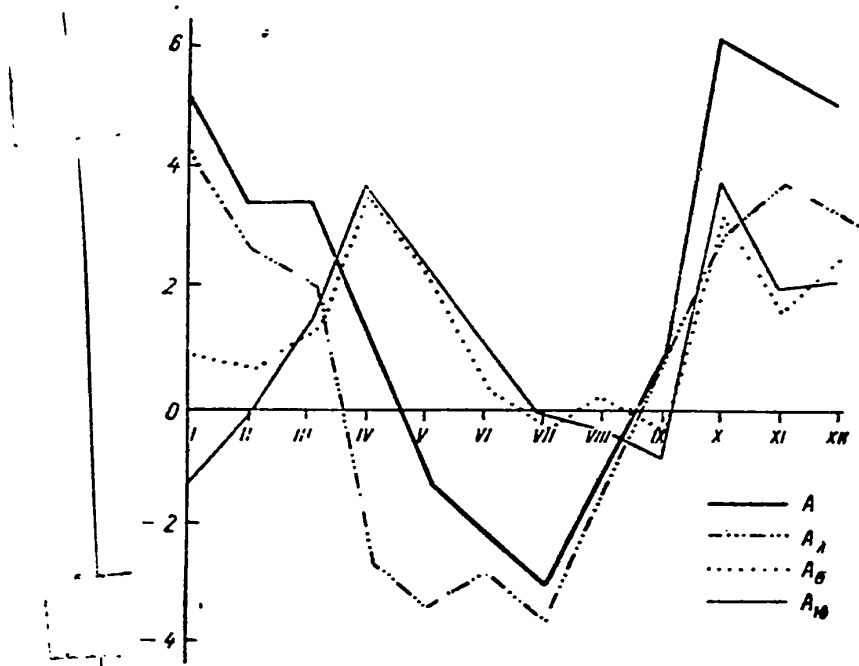


Fig. 11. Yearly Course of Heat Advection. Odessa (10-kilometer layer).  
a. kilocalories/square centimeter month

STAT

The causes for this are as follows: The annual course of  $A_\lambda$  in the middle latitudes (where a west-east transfer of air masses predominates and where the mean monthly values of  $\alpha$  remain steady in sign) is determined by the annual course of the longitudinal differences in temperature between the continent and the ocean; in winter in the European territory of the USSR ("ETS"), westerly winds transport from the Atlantic Ocean warm air masses, while in summer, they transport cold air masses. During the transitional seasons, when these differences are close to zero, the latitudinal advection of heat is small.

The annual course of  $A_\theta$  must be conditioned by the annual course of the meridional component of wind for the entire height of the atmosphere ( $\frac{\partial T}{\partial \theta}$  does not change in sign throughout the year and, likewise, it varies little in value). Consequently, the positive values of  $A_\theta$  may be associated with the transfer of air masses from the south, while its negative values may be associated with the transfer of air masses from the north.

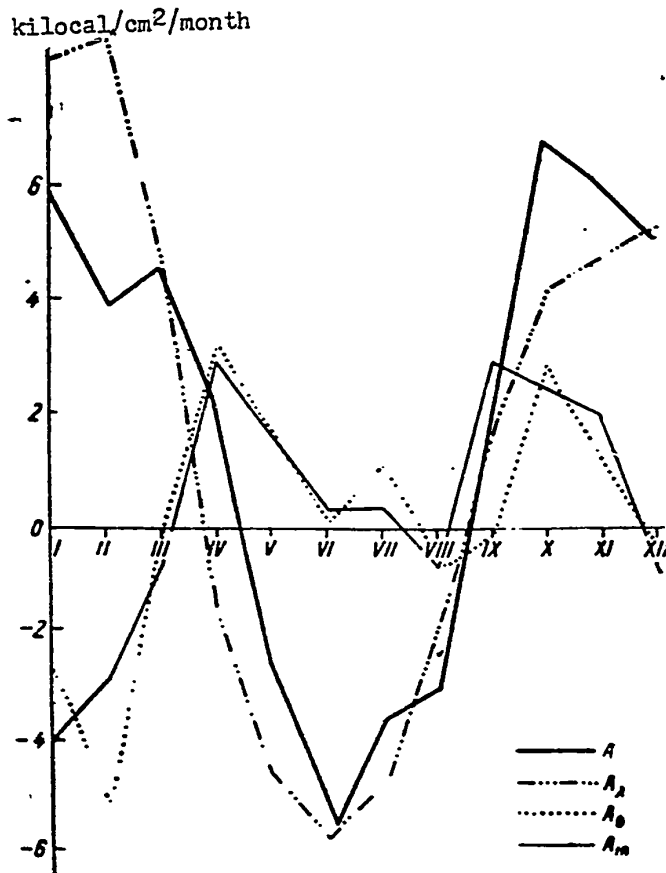


Fig. 12. Annual Course of Heat Advection. Riga (10-kilometer layer)

STAT

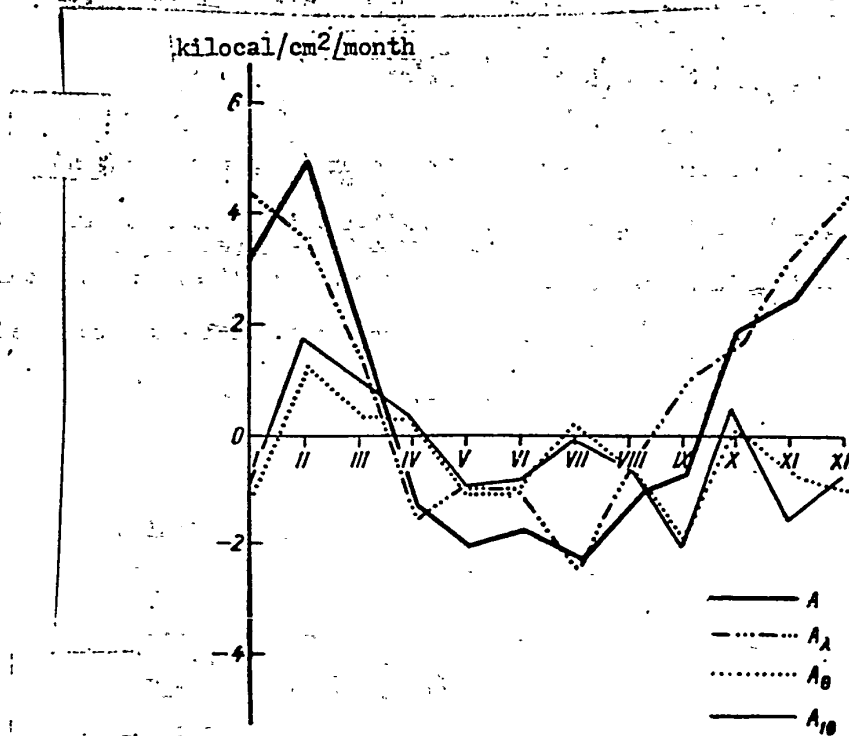


Fig. 13. Annual Course of Heat Advection. Sverdlovsk (10-kilometer layer)

The basic conclusion which may be made from a review of the Figs. 11-13 is: total heat advection over the European Portion of USSR is determined chiefly by the latitudinal component, i.e., by west-east transfer, a conclusion agreeing with the existing concepts of the nature of the general circulation over the European USSR.

It follows hence from all three graphs that during the transitional seasons (spring and autumn) over European USSR heat advection takes place from the south, in summer the meridional transfer of heat is very small; and in winter the advection may proceed both from the south and the north. However, the total meridional transfer is approximately the same for either the 6 months' cold period, from October to March, and the warm 6 months, from April to September.

As for the relationship between  $A_{10}$  and  $A_2$ , the total meridional transfer  $A$ , generally follows the course of  $A_{10}$ , i.e., its principal value is, on the average,

STAT

determined by the zonal value of  $\frac{\partial f}{\partial \theta}$ , while the influence of  $A_p$  is found to be significant only in certain individual months.

The calculated formula for  $\Lambda$  has the form of

$$\Lambda = 0,028 [\overline{Tp'}_t - \overline{Tp'}_{t_0}]'_t + 0,114 \int_0^t p' dz.$$

In this formula 100 meters of altitude are equal to one (1) unit of length. In the determination of time differences for the moment of time  $t$ ,  $p'$  is taken for the succeeding month (in relation to the month for which  $\Lambda$  is being calculated), and for the  $t_0$  moment - for the preceding month.

The calculations based on (20) led to results presented in Table 50.

Table 50

Variation in Heat Content of Air  $\Lambda$  (kilocalories/sq. cm. month)

Station	I	II	III	IV	V	VI	VII	VIII	IX	X	XI	XII
Odessa	-0,2	0,2	0,6	0,8	0,8	0,6	0,2	-0,4	-0,8	-0,8	-0,8	-0,6
Riga	-0,4	0,2	0,7	0,7	0,9	0,6	0,2	-0,4	-0,8	-0,6	-0,6	-0,3
Sverdlovsk	-0,1	0,1	0,9	1,0	1,1	0,9	0,2	-0,2	-1,1	-1,0	-0,8	-0,5

The values of  $\Lambda$  are not large. The annual course of  $\Lambda$ , has the form of a simple-wave curve. During the first half of the year,  $\Lambda > 0$ , while during the second half,  $\Lambda < 0$ .  $\Lambda$  passes through its zero values during the January-February and July-August periods. Its maximum positive values occur in May, and maximum negative, in September. Obviously, during the first half of the year a warming up of the air occurs (reaching its maximum in the spring), while during the second half of the year the cooling which takes place has its maximum value in the autumn months. The obtained values of  $\Lambda$  approximate vary closely the data of G.G. Trolle [36].

Let us examine the advection in January and July on the  $50^\circ N$  segment of the latitudinal circle, between Longitudes  $140^\circ W$  and  $20^\circ E$ , i.e., over North America, the Atlantic Ocean and a part of Europe. The data for the  $p$  and  $T$  at standard levels were taken also from [85]. The calculation of  $p$  differences was based on 20-degree

STAT



intervals by latitude and longitude. The obtained values of advection  $A$  and its components are presented in Figs. 14 and 15. In January, the latitudinal component of advection has positive values over continents and negative values over the ocean. A reverse picture was obtained for the meridional component.

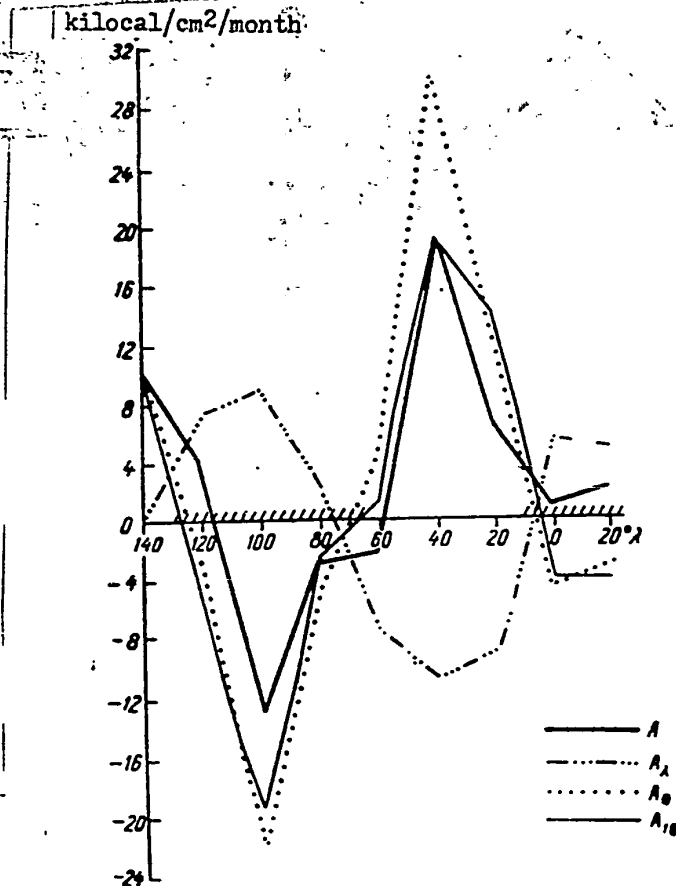


Fig. 14. Longitude-Dependence of Heat Advection for 50th Parallel No. Latitude. January (10-kilometer layer)

Total advection has the same longitudinal distribution as its meridional component.

The distribution of  $A_{\lambda}$  is conditioned by the temperature contrasts between continents and oceans during the winter months. In winter, warm air blows from the oceans to the continents, while cold air travels from the continents to the oceans.

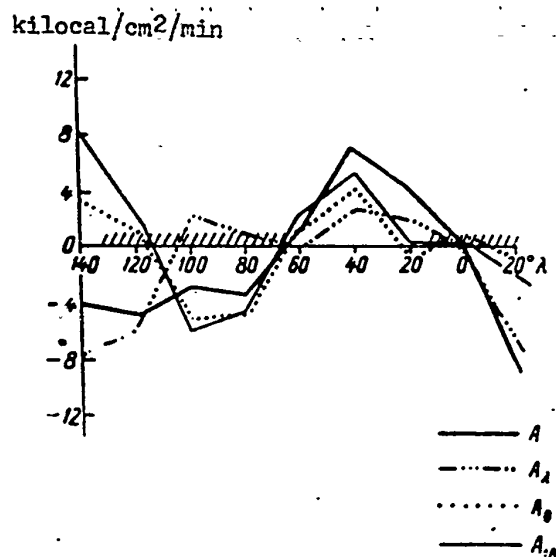


Fig. 15. Relationship between Heat Advection and Longitude for the 50th Parallel No. Latitude. July (10-Km. layer)

The distribution of  $A_0$  is explained by the effect of the steady pressure minimum, situated during the winter months in the northwestern part of the Atlantic Ocean (the Icelandic "center of action" of the atmosphere). In the rear portion of the depression Arctic air comes into the North American continent ( $\bar{A}_0 < 0$ ), while in its fore portion part, situated over the ocean, a transfer of air masses from the lower latitudes ( $A_0 > 0$ ) takes place. Since the baric depression is very deep and the meridional transfers of air masses predominate over the latitudinal transfers over the investigated segment of the 50th No. Latitude parallel, the meridional transfer of heat determines also the longitudinal course of total advection: total advection is negative in the area of the transfer of arctic air masses and positive in the area where the air masses come from lower latitudes.

Since the pressure gradients in the investigated area are much higher than over the European territory of the USSR (except for the "low" over the Atlantic Ocean, a polar frontal zone is found over North America in winter), therefore the values of

advection  $A$ , too, are found to be considerably higher than over the European territory of the USSR.

The higher values of  $A_1$  should also be attributed to a higher inhomogeneity of the pressure field.

In July the values of  $A$  are considerably lower than in January.

The latitudinal component  $A_1$  is negative on the eastern shores of the continents and positive on their western shores and over the ocean, i.e., its sign is determined by the longitudinal distribution of temperatures. The meridional component  $A_2$  along the parallel is distributed the same as in winter, but is lower in value. The Icelandic "low" is present in summer also, but with a greatly "dissipated" pressure field; in its rear portion there occurs a comparatively limited cold advection, while over the ocean heat advection takes place. Total advection in summer is determined by both the meridional and the latitudinal components - on the eastern shores of continents, where the effect of the Icelandic minimum no longer manifests itself.

Consequently, in this example also, we have obtained a satisfactory agreement between computed advection and the character of general circulation in the investigated region. In Figs. 16-20 are given the values of total advection  $A$  and its components in the lower 5-kilometer layer (of the atmosphere) for the examples examined above.

From Figs. 16-20 it is evident that the relationships between total advection and its components and their yearly courses in the 5-kilometer layer of the atmosphere are the same as in the 10-kilometer layer. The quantitative differences between the values of advection in both layers, however, are significant. This is explained primarily by the circumstance that in the middle latitudes (where the regions in question are situated) owing to the increase in west-east transfer with altitude, the contribution of the upper layers of the atmosphere to the advective transfer of heat is comparable with the contribution of the lower layers.

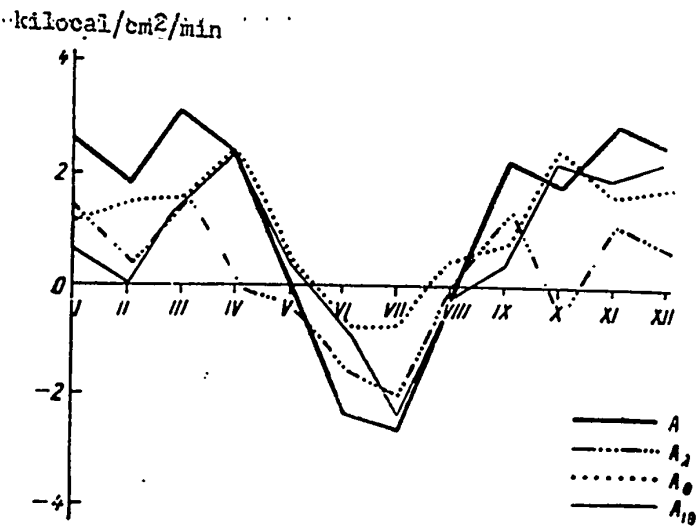


Fig. 16. Annual Course of Heat Advection. Odessa (5-kilometer layer).

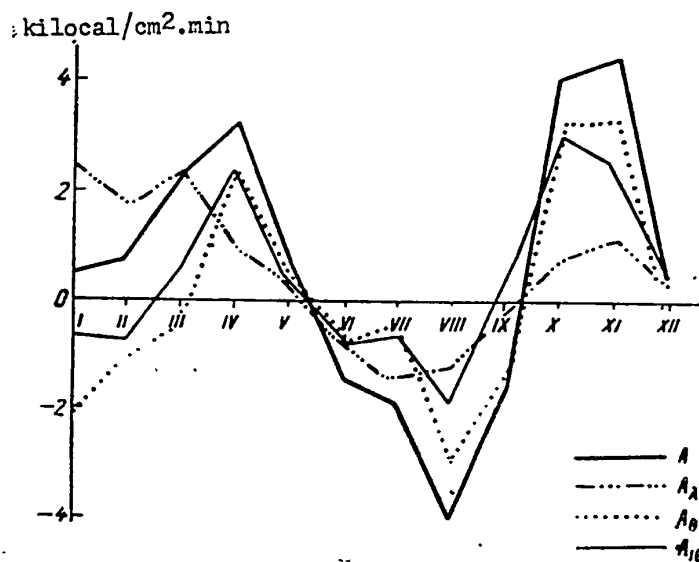


Fig. 17. Annual Course of Heat Advection. Riga (5-kilometer layer)

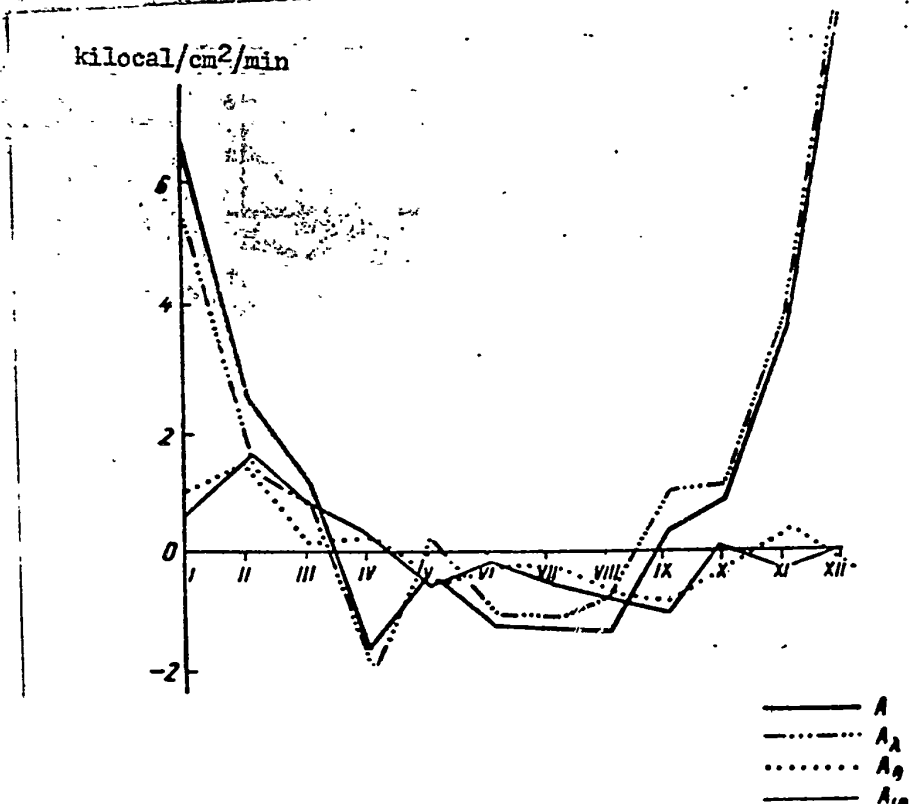


Fig. 18. Annual Course of Heat Advection. Sverdlovsk (5-kilometer layer)

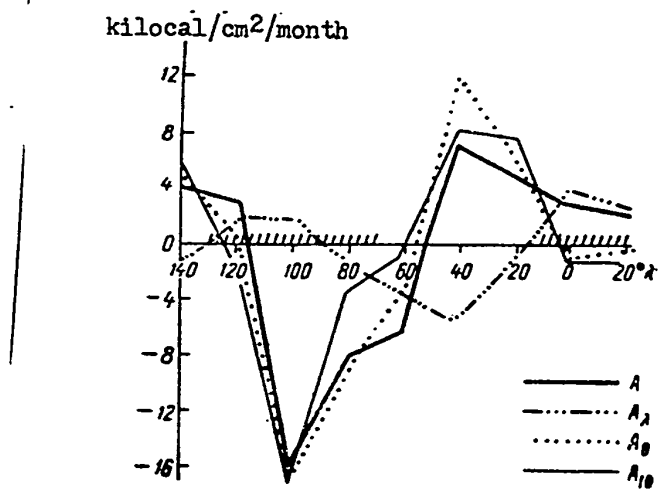


Fig. 19. The Relationship between Heat Advection and Longitude for 50°N in the 50° No. Latitude parallel. January (5-km. layer)

STAT

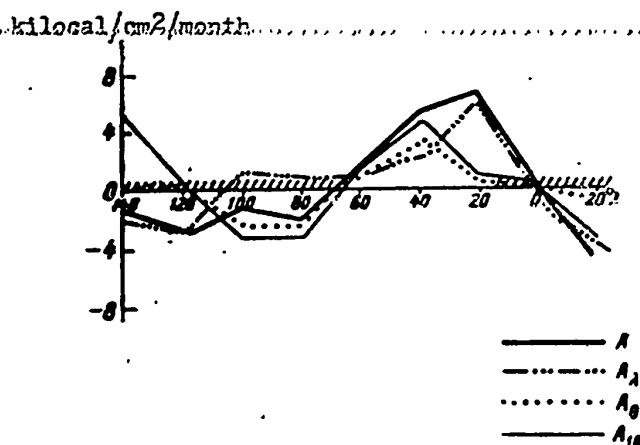


Fig. 20. Relationship between Heat Advection and Longitude for the 50° No. Latitude Parallel. July (5-Km. layer)

The results of the calculation of advection and its components in the layer of 16 kilometers' thickness are illustrated in Figs. 21-25.

The variations in  $A$  and its components with time and space in the 16-kilometer layer have in general the same character as such variations in the 5- and 10-kilometer layers. From the quantitative standpoint,  $A$  in the 16-kilometer layer does not differ greatly from the transfer of advective heat occurs chiefly in the troposphere, where the spatial temperature contrasts are expressed more sharply than in the stratosphere.

Of interest are the variations in  $A$  and its components from layer to layer. In tables 51-54 the respective contributions of the 5 to 10 kilometers and the 10- to 16-kilometer layers to the total advective heat transfer are given.

The contribution of the stratosphere to meridional advection is much smaller than its contribution to latitudinal transfer. In the upper troposphere the nature of variations in  $A_1$  and  $A_2$  is the same as in the lower troposphere.

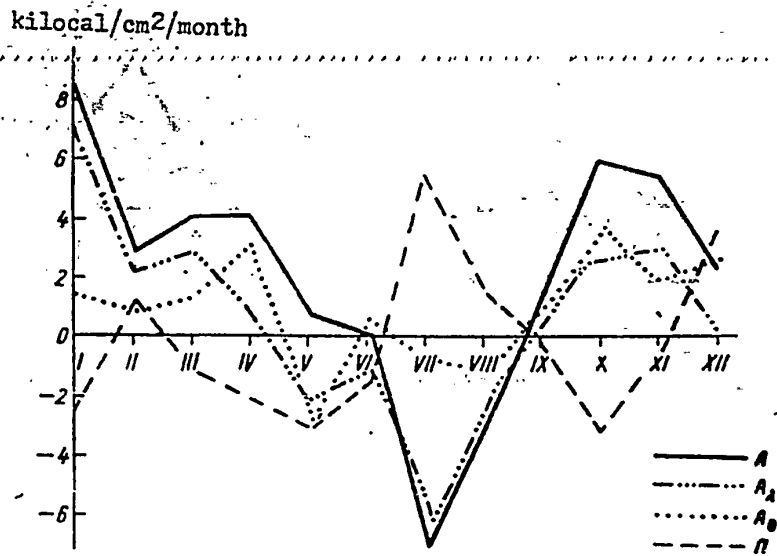


Fig. 21. Annual Course of Advection and of Horizontal Turbulent Transfer of Heat.  
Odessa

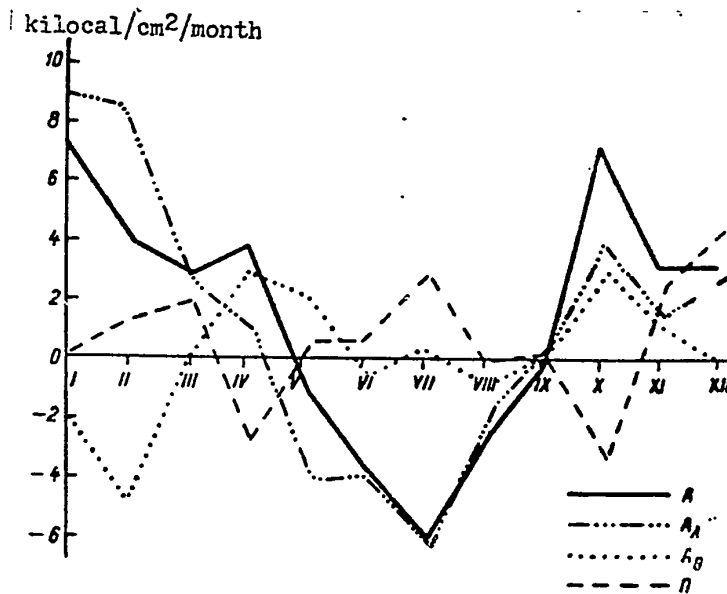


Fig. 22 Annual Course of Advection and horizontal Turbulent Transfer of Heat.  
Riga

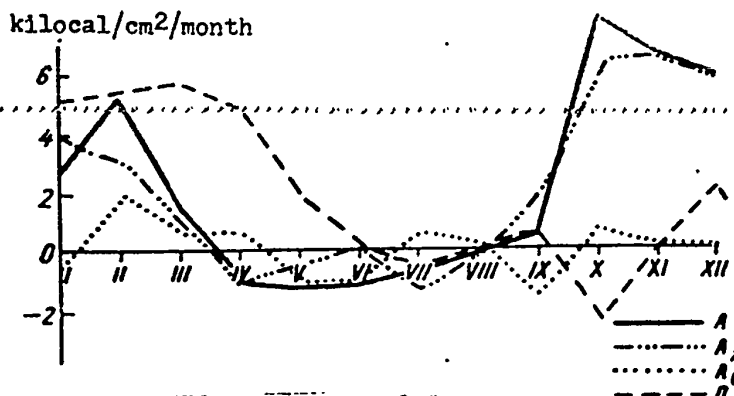


Fig. 23. Annual Course of Advection and of Horizontal Turbulent Transfer of Heat.

Sverdlovsk

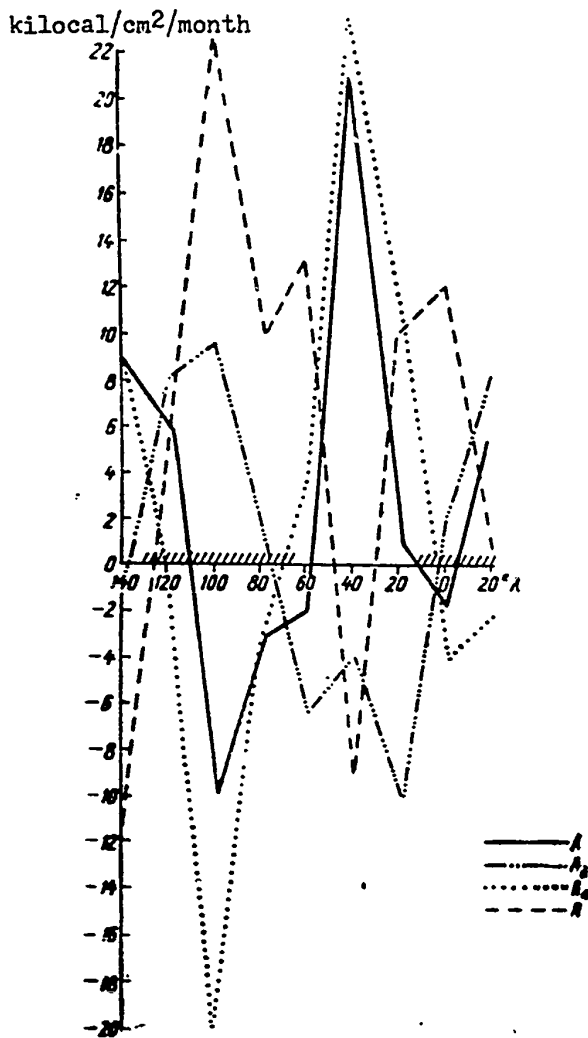


Fig. 24. Advection and Horizontal Turbulent Transfer of Heat on a Segment of the 50° No. Latitude Parallel -- January.

STAT



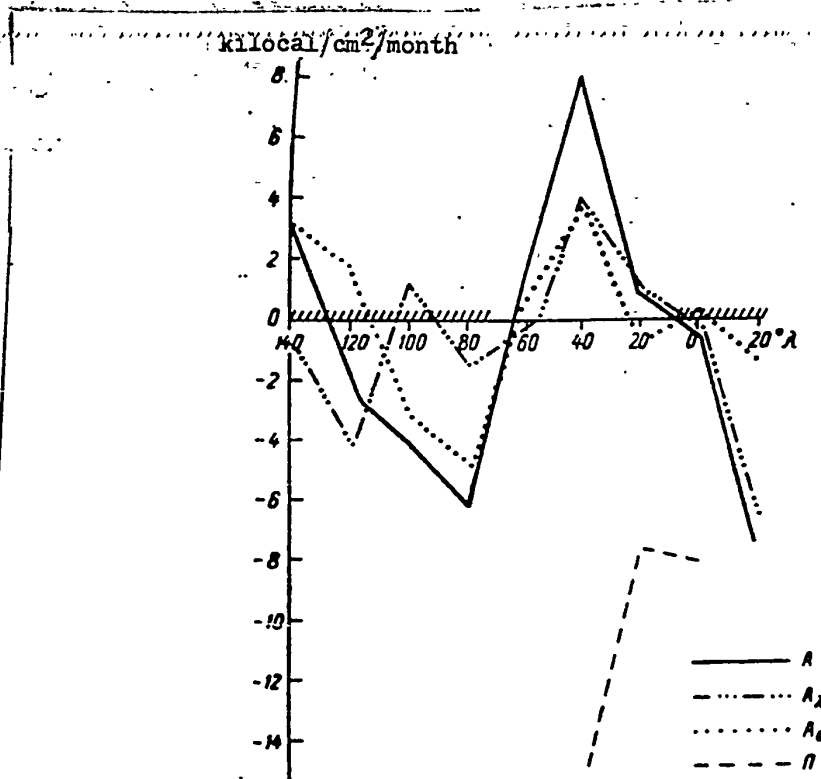


Fig. 25. Advection and Horizontal Turbulent Transfer of Heat on a Segment of the 50° No. Latitude parallel — July.

Table 51

Contribution of the 5-10 Kilometer Layer to Heat Advection  
(in kilocalories/sq. cm. month)

Characteristic of Heat Advection	I	II	III	IV	V	VI	VII	VIII	IX	X	XI	XII
Odessa												
AA	2.7	1.6	0.4	-1.1	-1.1	0.3	-0.4	-1.2	-1.3	4.5	2.8	2.6
AA <sub>1</sub>	2.9	2.4	0.7	-2.4	-3.0	-1.2	-1.0	-1.1	-0.4	3.6	2.8	1.8
AA <sub>2</sub>	-0.2	-0.8	-0.3	1.3	1.9	1.5	0.6	-0.1	-0.7	0.9	0	0.8
Riga												
AA	5.6	3.3	2.7	-1.3	-3.6	-4.2	-1.6	1.1	0.4	3.1	1.7	5.2
AA <sub>1</sub>	6.1	7.3	2.3	-2.3	-4.7	-4.9	-3.2	-1.0	1.8	3.5	3.8	5.1
AA <sub>2</sub>	-0.5	-4.0	0.4	1.0	1.1	0.7	1.6	2.1	-1.4	-0.4	-2.1	0.1

STAT

Sverdlovsk

AA	-3.5	2.3	0.8	0.5	-1.7	-0.6	-1.0	0.2	0.6	1.0	-1.2	-5.2
AA <sub>1</sub>	-1.1	4.4	0.6	0.4	-1.1	0.3	-1.4	0.1	-0.1	0.6	-0.1	-4.6
AA <sub>2</sub>	-2.4	-2.1	0.2	0.1	-0.6	-0.9	0.4	0.1	0.7	0.4	-1.1	-0.8

Table 52

Contribution of the 5-10 Kilometer Layer to Heat Advection along  
Latitude 50°N

(kilocalories/square centimeter month)

Characteristic of Heat Advection	λ°									
	140	120	100	80	60	40	20	0	20	
January										
AA	6.3	0.6	2.2	5.8	3.8	12.7	1.2	-2.0	-0.2	
AA <sub>1</sub>	1.6	4.8	7.1	3.9	-4.1	-4.3	-5.6	1.7	2.4	
AA <sub>2</sub>	4.7	-4.2	-4.9	1.9	7.9	17.0	6.8	-0.3	-2.6	
July										
AA	-2.7	-1.5	-1.9	-1.4	-0.1	1.9	-2.6	0.2	-4.0	
AA <sub>1</sub>	-5.8	-3.1	1.0	0.7	-0.8	0.6	-1.9	0.2	-3.9	
AA <sub>2</sub>	3.1	1.6	-2.9	-2.1	0.7	1.3	-0.7	0	-0.1	

Table 53

Contribution of the 10-16 Kilometer Layer to Heat Advection

(Kilocalories/square centimeter month)

Characteristics of Heat Advection	Month											
	I	II	III	IV	V	VI	VII	VIII	IX	X	XI	XII
Odessa												
AA	2.9	-0.3	0.7	2.5	1.8	2.0	-4.3	-2.2	0.4	-0.1	-0.5	-2.7
AA <sub>1</sub>	2.3	-0.3	0.6	3.2	1.1	1.9	-3.5	-0.9	-0.1	-0.3	-0.7	-2.7
AA <sub>2</sub>	0.6	0	0.1	-0.7	0.7	0.1	-0.8	-1.3	0.5	0.2	0.2	0
Riga												
AA	0.9	-0.2	-1.6	2.0	1.3	1.7	-2.9	0.2	-1.8	0	-3.2	-2.2
AA <sub>1</sub>	0.4	-0.3	-1.8	2.2	0.6	2.0	-2.2	0.4	-2.0	-0.4	-3.2	-2.6
AA <sub>2</sub>	0.5	0.1	0.2	-0.2	0.7	-0.3	-0.7	-0.2	0.2	0.4	0	0.4

Sverdlovsk

ΔA	0	-0.2	-0.4	0.4	0.8	0.5	1.4	0.7	1.7	5.9	4.0	2.2
ΔA <sub>1</sub>	-0.4	-0.4	-0.5	-0.3	0.4	-0.6	1.3	0.4	-1.3	5.1	3.5	-1.7
ΔA <sub>2</sub>	0.4	0.2	0.1	0.1	0.4	-0.1	0.1	0.3	0.4	0.8	0.5	0.5

Table 54

Contribution of the 10-16 Kilometer Layer to Heat Advection along  
the 50th Parallel No. Latitude.  
(kilocalories/square centimeter month)

Characteristic of Heat Advection	λ°									
	140	120	100	80	60	40	20	0	20	
January										
ΔA	-1.9	2.6	2.8	-0.5	0.4	4.3	-5.5	-3.2	3.7	
ΔA <sub>1</sub>	-1.1	1.4	1.0	-1.3	1.2	5.8	-3.7	-3.8	2.7	
ΔA <sub>2</sub>	-0.8	1.2	1.8	0.8	-0.8	-1.5	-1.8	0.6	1.0	
July										
ΔA	7.1	2.5	-1.3	-2.6	-0.2	1.5	-2.9	-0.3	0.8	
ΔA <sub>1</sub>	7.2	2.6	-1.3	-2.6	-0.2	1.5	-2.9	-0.3	0.9	
ΔA <sub>2</sub>	-0.1	-0.1	0	0	0	0	0	0	-0.1	

The equation of heat balance of the atmosphere makes it possible to make an evaluation of the magnitudes of the heat transported by horizontal turbulent inter-mixing.

Let us write the equation of the heat balance of an atmospheric column with an altitude of z kilometers, and limited below by the earth's surface.

$$A + K + \int_0^z \epsilon dz = \Delta.$$

Here ε is the heat influx to a unit of volume of air during a unit of time and K is convective transfer of heat.

The influx ε is realized by radiation and turbulent processes and also by phase transformations of water in the atmosphere

$$\int_0^z dz = R(z) - R(0) - P(z) + P(0) + \Phi(z) + \Pi(z).$$

Here:  $R(0)$  and  $R(z)$  are radiation balances at the earth's surface and at the altitude  $z$ , respectively;  $P(0)$  and  $P(z)$  are vertical turbulent fluxes of heat at the same respective altitudes,  $F_{t,h}(z)$  is the influx of heat to an atmospheric column with an altitude of  $z$ , realized by horizontal turbulent exchange; and  $\Phi(z)$  is the quantity of heat being liberated as a result of phase transformations of water within the column.

If  $z = \infty$ , then

$$\left. \begin{aligned} R(\infty) &= R_s = (S - B)_{z=\infty}, \\ P(\infty) &= 0, \quad \Phi(\infty) = Lr, \quad K(\infty) = 0, \end{aligned} \right\} \quad (20)$$

where  $R_s$  is radiation balance of the earth-atmosphere system, equal to the difference between the fluxes of solar radiation and long-wave atmospheric radiation at the upper boundary of the atmosphere,  $r$  is precipitation, and  $L$  is latent heat of condensation.

As is known, the equation of heat balance of the underlying surface has the form of

$$R(0) = P(0) + LF + V. \quad (21)$$

Here  $F$  is the evaporation from the underlying surface and  $V$  represents heat fluxes from the underlying surface into the soil.

The equation of heat balance of a 10-kilometer high column in the atmosphere will be written on taking account of (21) as:

at  $z > 10$  kilometers,  $R = R_s$ , and  $\Phi = Lr$

$$A + K + R_s + L(r - F) + \Pi - P - V = \Lambda. \quad (22)$$

The equation of heat balance of the earth-atmosphere system, including the entire atmosphere up to  $z = \infty$ , has the form of

STAT

$$A + R_s + L(r - F) + \Pi - V = \Lambda \quad (23)$$

In practice, the 16-kilometer level may be considered as the upper boundary of the atmosphere at which the above-formulated conditions (20) are satisfied.

Obviously, it may be assumed that

$$\bar{\Pi} = \bar{\Pi} + \bar{\Pi}$$

$F_{t,h}(\theta)$  denotes the mean annual meridional longitudinally averaged turbulent heat exchange, calculated in Chapter II, while  $F_{t,h}(\theta, \lambda, t)$  denotes the variation in  $F_{t,h}$  dependent on time  $t$  and on  $\lambda$ .

The value of  $\bar{F}_{t,h}$  is determined from (23) after its averaging for the year, along the latitude parallel.

$$\bar{\Pi} = -\bar{R}_s - L(\bar{r} - \bar{F})$$

since  $\bar{A} = \bar{V} = \bar{\Lambda} = 0$ .

The values of all the components entering in eqs. (22) and (23), except for  $K$ ,  $\Pi$  and  $P$ , may be determined by independent methods.

In order to calculate the residual terms in eqs. (22) and (23) let us use the data concerning  $R_s$ ,  $LF$ ,  $V$ , and  $Lr$ , from [10] and [44], (Table 55), and also the values of  $A$  and  $\Lambda$  that we obtained (owing to the smallness of  $\Lambda$ , its variations at altitudes above 10 kilometers are not taken into consideration.

Table 55

Components of Heat Balance (kilocalories/sq. cm. month)

Components of the Heat Balance	I	II	III	IV	V	VI	VII	VIII	IX	X	XI	XII
Odessa												
$R_s$	-8.0	-5.5	-1.9	1.3	4.7	4.6	3.5	1.5	-2.2	-5.2	-7.3	-8.9
$LF$	0	0.2	1.5	3.4	3.8	3.4	3.1	2.0	1.3	0.8	0.5	0
$V$	-0.5	-0.3	0.2	0.3	0.5	0.5	0.4	0.2	-0.2	-0.2	-0.4	-0.5
$Lr$	1.4	1.0	1.2	1.5	1.8	2.8	1.9	1.8	1.5	2.1	1.6	1.5

Riga

$R_s$	-10.3	-7.5	-5.4	-0.3	3.7	5.3	3.3	0.9	-3.2	-7.5	-9.7	-10.9
$LF$	0	0	0	2.0	4.3	5.0	4.8	3.5	2.0	0.5	0	0
$V$	-0.5	-0.3	-0.2	0.3	0.5	0.5	0.4	-0.2	-0.2	-0.4	-0.5	
$L_r$	2.2	1.9	1.9	2.1	2.7	3.9	5.2	5.0	3.7	3.5	3.3	2.7

Sverdlovsk

$R_s$	-10.3	-8.1	-7.1	-3.1	1.9	4.1	2.2	-1.1	-4.3	-8.0	-10.1	-11.0
$LF$	0	0	0	0.9	3.7	4.6	4.8	2.7	1.1	1.0	0	0
$V$	-0.8	-0.5	0.3	0.5	0.8	0.8	0.6	0.4	-0.3	-0.4	-0.6	-0.8
$L_r$	1.0	0.8	1.0	1.2	2.9	3.9	4.6	4.0	2.5	1.9	1.6	1.3

The horizontal turbulent influxes of heat in the 16-kilometer layer of the atmosphere have the values presented in Table 56 and in Figs. 21-25.

Table 56

Station	I	II	III	IV	V	VI	VII	VIII	IX	X	XI	XII	Year
Odessa	-2.3	1.4	-1.3	-2.1	-2.1	-2.0	5.6	1.7	-0.4	-3.4	-0.3	3.8	-2.0
Riga	0.2	1.6	2.2	-2.8	0.6	0.8	3.2	0	0.5	-3.5	2.4	4.4	9.6
Sverdlovsk	5.1	1.9	5.8	5.0	1.8	-0.5	-0.3	0.3	0.8	-2.2	0.5	2.5	20.5

It is quite obvious from Figs. 21-25 that the values of the horizontal turbulent transfer of heat for the entire depth of the atmosphere have a definite annual course; over the European USSR they are positive primarily during the summer and winter months and negative during the transitional seasons.

The obtained values of  $F_{t,h}$  reflect correctly the characteristics of macroturbulent mixing in various regions (Tables 56 and 57). The values of  $F_{t,h}$  are small for the individual months and years in the regions with a stable west-east transfer. In regions with a mountainous relief or a complex and unstable system of air currents, where the contribution of horizontal turbulent fluxes to the heat transfer must be considerably greater, the values of  $F_{t,h}$  and  $A$  are comparable.

Table 57

Horizontal Turbulent Heat Influx  $F_{t,h}$  (kilocalories/sq. cm. month)

Month	$\lambda^\circ$									
	140	120	100	80	60	40	20	0	20	
January	-12.0	0.6	19.2	9.9	13.7	-9.1	9.9	12.3		0.5
July	-12.0			-2.3		-14.9	-7.7	-7.9		

Table 59

This indicates that the heat-balance method of evaluating the horizontal turbulent transfer of heat which is indirect and hence insufficiently accurate, may nevertheless provide a correct idea about the magnitude of this transfer and its variations in space and time.

Attention should be turned to one peculiarity of the time and spatial variations in the values of  $F_{t,h}$  and  $A$ : their variations are opposite in phase (Figs. 21-25). This indicates a sufficiently good correlation between advective and turbulent transfers of heat in the atmosphere. After having plotted the corresponding correlation graph it is possible to ascertain that the algebraic values of  $F_{t,h}$  display a tendency to decrease with an increase in the algebraic values of  $A$ .

Of interest is an analysis of the residual term of eq. (22). Its annual course is of the same character as that of  $F_{t,h}$  (Table 58).

Table 58

The Residual Term of Eq. (22)  $F_{t,h} 10 + K_{10} - P_{10}$ 

Station	I	II	III	IV	V	VI	VII	VIII	IX	X	XI	XII	Year
Odesa	0,6	1,1	-0,6	0,4	-0,3	-0,9	1,3	-0,5	0	-3,5	-0,8	1,1	-2,1
Riga	1,1	1,4	0,6	-0,8	1,9	2,5	0,3	0,2	-1,3	-3,5	-0,8	2,2	3,8
Sverdloysk	5,1	1,7	5,4	5,4	2,6	0	0,9	1,0	2,5	3,7	4,5	4,7	37,5

The presence of  $K$  in the residual term of eq. (22) need not violate the annual course of  $F_{t,h}$ , because variations in the values of  $K$  and  $A$ , the same as  $F_{t,h}$  and  $A$ , are opposite in phase. Heat advection ( $A > 0$ ) is accompanied by ascending vertical currents ( $K > 0$ ), while cold advection ( $A < 0$ ) is accompanied by descending vertical currents ( $K < 0$ ). This is reflected in the obtained results.

Having carried out a preliminary verification of the method of computing non-turbulent advection, and having explained its possibilities, let us pass over to a calculation of advection for the stations characterizing the principal climates of the earth (Table 59).

Table 59

Stations Characterizing the Principal Climates of the  
Terrestrial Sphere

Station	Coordinates		Climate
	$\phi$	$\lambda$	
Azsuan	24°N	32°53'E	Tropical continental
Krasnovodsk	40	53	Subtropical continental
Barnaul	53°20'	84	Temperate continental
Turukhansk	66	88	Subarctic continental
Shanghai	31	121°30'	Subtropical, monsoon, eastern seacoast
Vladivostok	43	132	Temperate, monsoon, of eastern coasts (of continents)
Bombay	20	73	Equatorial monsoon
Lisbon	38°42'	9	Subtropical, of western seacoast
Philadelphia	40	75	Subtropical of eastern seacoast
Batumi	41°36'	43°30'	Subtropical, humid, black-Sea
New Orleans	30	90	Subtropical of the western periphery of oceanic anti- cyclones

The values of  $A$ ,  $A_{\lambda}$ , and  $A_{\phi}$ , at these stations for the four months (December, March, June, September) for the 10- and 15-kilometer layers are given in Table 60 and illustrated in Figs. 26-36.

Table 60

Heat Advection and Horizontal Turbulent Heat Transfer  
in the Principal Climates of the Earth  
(kilocalories/sq.cm. month)



Table 60 (cont'd)

Characteristic of the Advection and Turbulent Exchange of heat	Assuan				Krasnovodsk			
	XII	III	VI	IX	XII	III	VI	IX
$A_{10}$	4.5	-1.3	10.6	-9.3	12.3	4.4	-6.2	2.9
$A_{110}$	1.6	2.4	0.7	-1.8	6.1	-1.6	-4.4	-3.4
$A_{110}$	2.9	-3.7	9.9	-7.5	6.2	6.0	-1.8	-6.3
$A_{16}$	2.9	1.4	8.2	-12.6	14.2	5.8	-4.8	4.2
$A_{16}$	-0.1	3.8	-2.6	-5.1	7.6	0.4	-2.2	-1.7
$A_{16}$	3.0	-2.4	10.8	-7.5	6.6	5.4	-2.6	5.9
$\Pi$	1.4	-0.4	-4.2	13.1	-8.2	-3.8	2.8	-2.2
Barnaul					Turukhansk			
$A_{10}$	3.9	1.4	-4.2	0	3.5	1.4	2.3	2.9
$A_{110}$	1.6	2.2	2.0	0.8	7.2	3.6	1.7	3.4
$A_{110}$	2.3	-0.8	-6.2	-0.8	-3.6	-2.2	0.6	-0.5
$A_{16}$	5.1	2.2	-6.0	1.0	2.9	0.5	2.0	4.0
$A_{16}$	2.8	2.4	-0.6	1.6	6.0	2.3	1.2	4.1
$A_{16}$	2.3	-0.2	-5.4	-0.6	-3.1	-1.8	0.8	-0.1
$\Pi$	2.9	2.8	4.0	1.0	5.1	5.5	-4.0	-1.0
Shanghai					Vladivostok			
$A_{5}$	-1.1	4.9	1.4	0.4	-9.8	0.3	6.8	-0.6
$A_{5}$	4.5	1.3	2.3	0.3	2.4	5.6	5.5	-0.6
$A_{10}$	-5.6	3.6	-0.9	0.1	-12.2	-5.3	1.3	0
$A_{10}$	-3.8	1.4	5.5	0.7	-7.1	-5.9	4.3	-4.7
$A_{110}$	2.9	5.7	5.5	1.9	7.5	-1.8	5.5	-4.0
$A_{110}$	-6.7	-4.3	0	-1.2	-14.6	-4.1	-1.2	-0.7
$A_{16}$	-5.9	3.5	5.6	1.1	-2.0	-2.1	8.6	-6.8
$A_{16}$	0.6	6.5	5.8	1.5	11.5	0.4	7.1	-5.5
$A_{16}$	-6.5	-3.0	0.2	-0.4	-13.5	-2.5	1.5	-1.3
$\Pi$	10.7	-0.5	-16.9	0.5	9.2	5.4	-13.8	5.4
Bombay					Lisbon			
$A_{5}$	4.2	2.9	-1.2	0	6.1	2.9	-8.4	-1.7
$A_{5}$	3.5	0.4	-0.6	0	8.5	4.0	-4.2	2.0
$A_{10}$	0.7	2.5	-0.6	0	-2.4	-1.1	-4.2	-3.7
$A_{10}$	2.6	3.6	-1.2	0	-3.2	-3.8	-6.5	-4.7
$A_{110}$	3.6	1.0	-0.6	0	4.5	-1.7	-6.4	-0.8
$A_{110}$	-1.0	2.6	-0.6	0	-7.7	-2.1	-0.1	-3.9
$A_{16}$	6.8	7.0	-1.2	0	-4.2	-9.8	-9.4	-4.3
$A_{16}$	7.4	3.8	-0.6	0	2.5	-6.8	-7.8	-1.0
$A_{16}$	-0.6	3.2	-0.6	0	-6.7	-3.0	-1.6	-3.3
$\Pi$	-2.8	3.0	-4.8	1.0	5.9	8.9	6.6	1.9
Philadelphia					Batumi			
$A_{10}$	8.6	-4.8	-1.1	-2.7	7.1	3.1	-2.0	1.1
$A_{110}$	2.4	-1.2	2.2	-5.0	2.1	1.0	-2.7	-1.8
$A_{110}$	6.2	-3.6	-3.3	2.3	5.0	2.1	0.7	2.9
$A_{16}$	3.0	-8.4	3.7	3.3	5.6	4.6	-1.4	-1.6
$A_{16}$	-2.8	-1.6	4.6	-0.2	1.6	2.2	-2.4	-4.0
$A_{16}$	5.8	-6.8	-0.9	3.5	5.0	2.4	1.0	2.4
$\Pi$	7.8	11.5	-12.0	1.5	-4.6	-6.6	3.8	6.8

New Orleans

$A_{10}$	-3,7	5,8	-0,1	7,4
$A_{110}$	-2,9	1,1	-1,6	4,7
$A_{810}$	-0,8	4,7	1,5	2,7
$A_{16}$	0,7	6,0	-0,9	7,0
$A_{116}$	1,3	1,2	-0,9	3,6
$A_{816}$	-0,6	4,8	1,8	3,4
$\Pi$	7,7	-8,6	-10,7	-7,9

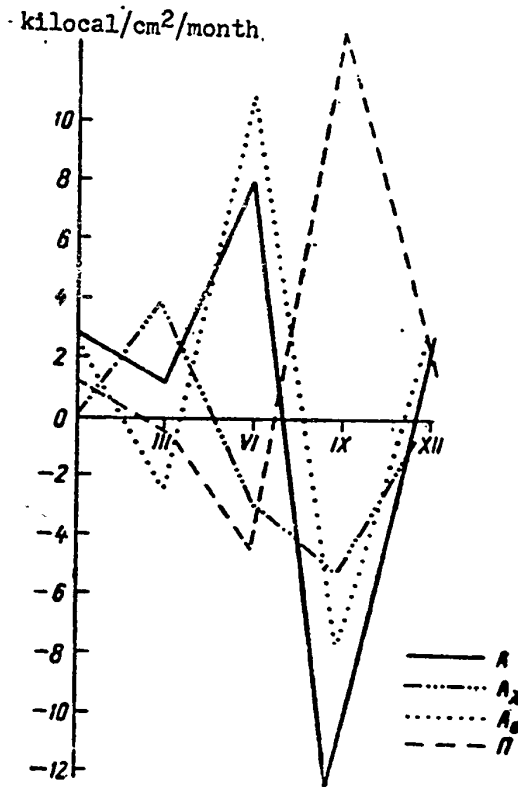


Fig. 26. Annual Course of the Advection and Horizontal Turbulent Transfer of Heat.

Assuan.

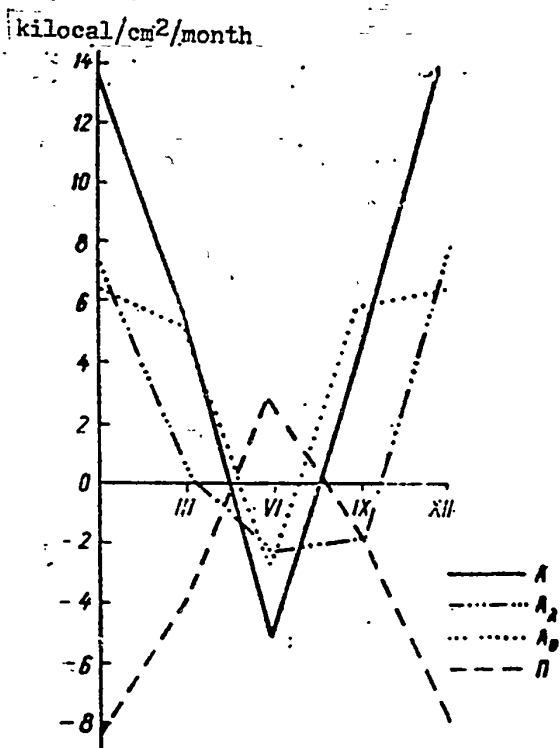


Fig. 27. Annual Course of the Advection and Horizontal Turbulent Transfer of Heat.  
Krasnovodsk.

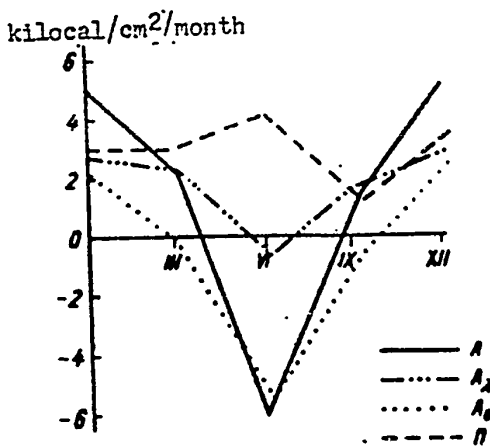


Fig. 28 Annual Course of the Advection and Horizontal Turbulent Transfer of Heat. Barnaul.

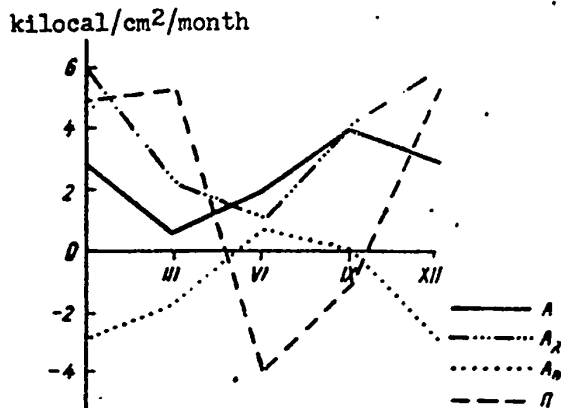


Fig. 29. Annual Course of the Advection and Horizontal Turbulent Transfer of Heat. Turukhansk.

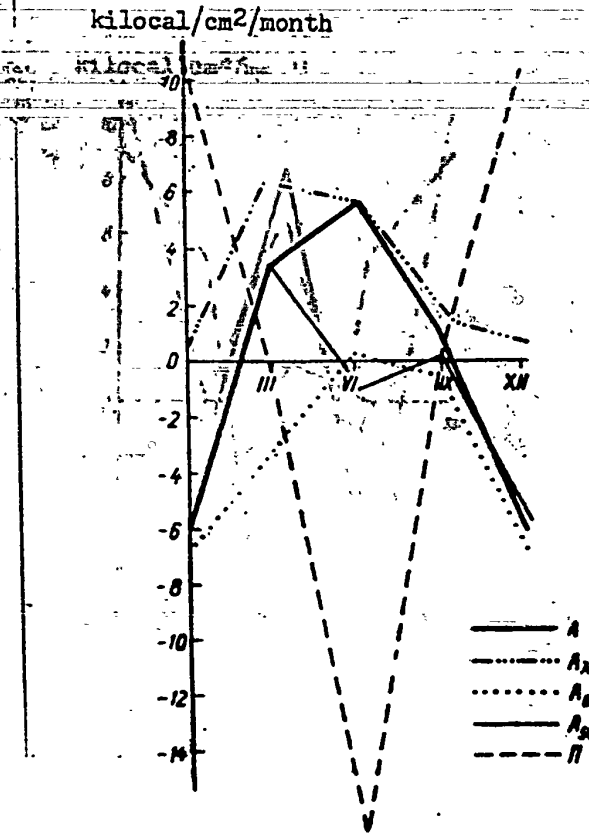


Fig. 30. Annual Course of the Advection and Horizontal Turbulent Transfer of Heat. Shanghai.

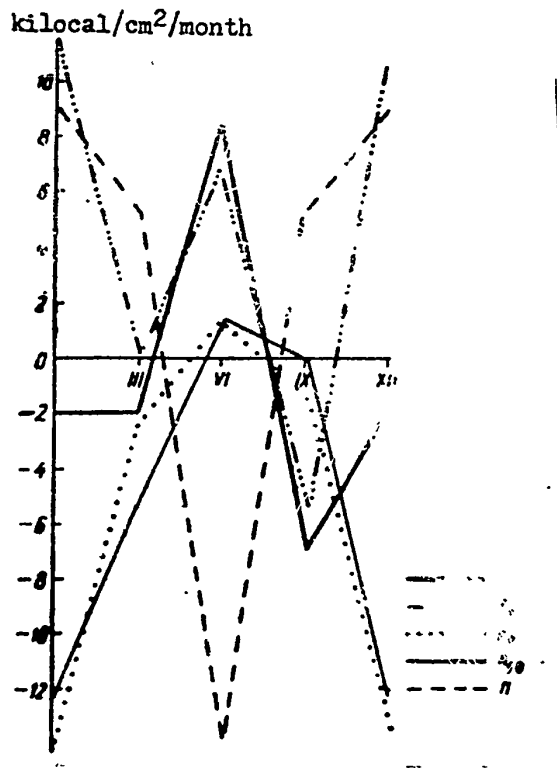


Fig. 31. Annual Course of the Advection and Horizontal Turbulent Transfer of Heat. Vladivostok.

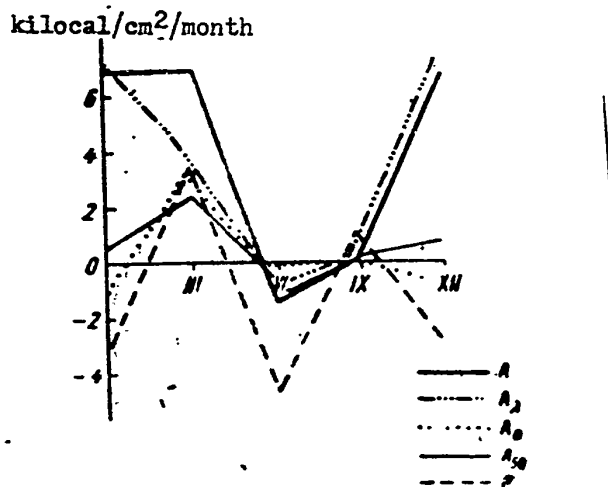


Fig. 32. Annual Course of the Advection and Horizontal Turbulent Transfer of Heat. Bombay.

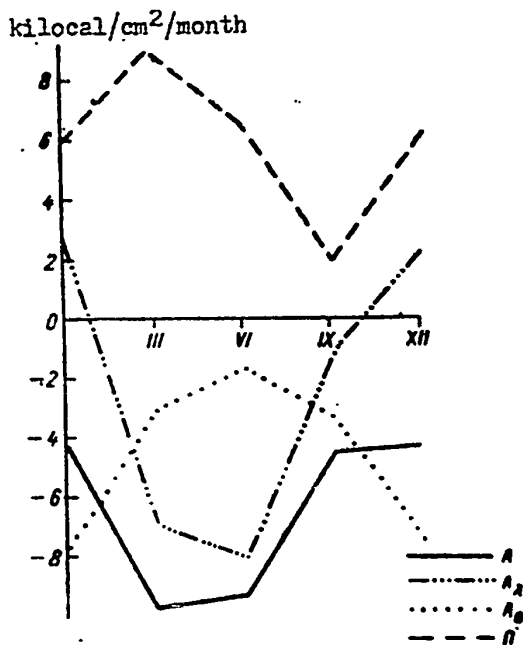


Fig. 33. Annual Course of the Advection and Horizontal Turbulent Transfer of Heat. Lisbon.

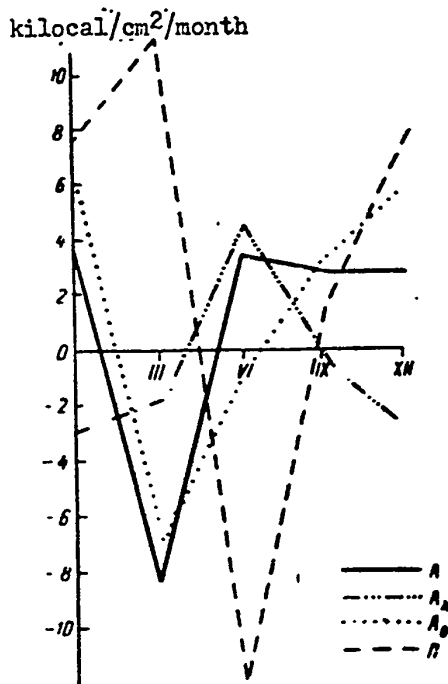


Fig. 34. Annual Course of the Advection and Horizontal Turbulent Transfer of Heat. Philadelphia.

STAT

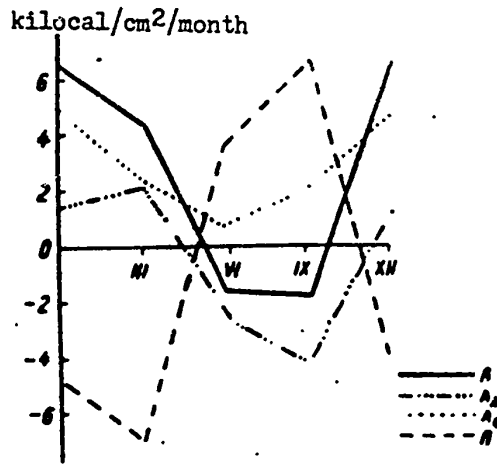


Fig. 35. Annual Course of the Advection and Horizontal Turbulent Transfer of Heat.  
Batumi

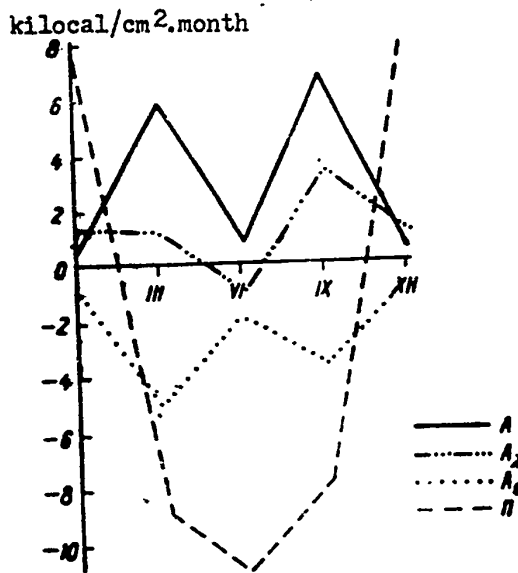


Fig. 36. Annual Course of Advection and Horizontal Turbulent Transfer of Heat.  
New Orleans.



Examination of Table 60 and the graphs in Figs. 26-36 will reveal some quite definite principles in the spatial and temporal distribution on nonturbulent heat transfer in the atmosphere.

First of all, the latitudinal component of advection  $A_\lambda$  is, as a rule, positive in winter months and negative in summer months for all regions having a continental climate and for the western seacoasts of the oceans. We have already obtained the same results with regard to the European portion of the Soviet Union. Along the eastern seacoasts of Asia and North America the values of  $A_\lambda$  are positive in summer months (Vladivostok, Shanghai, Philadelphia). Such an annual course of  $A_\lambda$  is explained, as noted above by the annual course of temperature contrast between the continents and oceans.

In winter the westerly flow brings warm air masses from the oceans to the continents and cold air masses from the continents to the oceans. In summer the converse takes place. The meridional component  $A_\theta$  reflects the characteristic features of the regime of general circulation in various regions in greater detail than  $A_\lambda$ .

Let us examine regions with a monsoon climate. For Shanghai and Vladivostok the meridional component  $A_\theta$  is negative in winter months and close to zero during summer. Such an annual course of  $A_\theta$  is closely related to the seasonal change in monsoon currents in that region. In winter, under the influence of the Siberian anticyclone, cold winds blow from the northwest, while in summer, there arrives from the southeastern part of the Pacific Ocean subtropical air having thermal properties differing little from the air of the more northern seacoast regions. For Bombay the meridional component  $A_\theta$  is small both in winter and in summer, since the thermal properties of the air masses transferred in the subtropics in the meridional direction differ but little owing to the smallness of the meridional temperature gradients.

In order to ascertain that the annual course of  $A_\theta$  at the stations named above is caused viz., by a monsoonal circulation, we have calculated the  $A_\theta$  for the lowest 5-kilometer layer in which the monsoon currents are distributed. The values of  $A_\theta$  for that layer are given in Table 60 (Shanghai, Vladivostok, Bombay) and are illustrated

in Figs. 30, 31, and 32, from which it is evident that the annual course of  $A_0$  characteristic of the monsoon climate is formed in the lower troposphere.

Let us note that in the subtropical climate of the eastern<sup>1</sup> coast of the Atlantic Ocean (Lisbon) the values of  $A_0$  in the course of the year are negative, and the annual curve of  $A_0$  agrees with the corresponding curves for the monsoon regions in the same latitudes. As for the eastern<sup>1</sup> seacoast, however, the negative values of  $A_0$  reflect the influence of the Azores' "High" under which during the course of the year northwest winds blow from the ocean; the northwest winds bring cold air masses from the middle latitudes, in both winter and summer.

The effect of the subtropical high-pressure belt manifests itself also in North Africa (Assuan). Here, in summer, blow northwesterly winds transporting from the area of the Azores' "High" considerably more heat in summer than in winter.

On the Atlantic seacoast of North America (Philadelphia) the effect of the subtropical "High" manifests itself also, but its tendency in the annual course is opposite to that which takes place in North Africa.

In winter a relatively greater amount of heat than in summer arrives from the southeastern periphery of the subtropical anticyclone into the higher latitudes.

In Siberian regions with a temperate continental climate (Barnaul) the influence of the Siberian anticyclone in winter manifests itself; the anticyclone transports relatively warm air masses along its southeastern periphery, while in summer northwesterly flows of cold air from the Arctic Ocean penetrate into this region.

In the northern portion of Siberia (Turukhansk) cold winds blow in winter from the northern periphery of the Siberian anticyclone, and therefore, cold advection is distinctly expressed here during the winter months.

---

1 It is assumed that the "western coast" in the original Russian text is an error especially with respect to Lisbon. The translated version is therefore changed to read "eastern coast".

In addition to the latitudinal cross-section of advection A (along 50° No. Latitude) it is also of interest to construct its meridional cross-section. Let us select longitude 180°, crossing the Pacific Ocean. The values of A for the 10- and 16-kilometer layers in December and June are presented in Table 61 and in Figs. 37 and 38. The latitudinal course of  $A_\lambda$  in December reflects the wintertime temperature contrasts between the Asiatic Continent and the Pacific Ocean at various latitudes. In the temperate belt, cold air masses come to the ocean from the continent, while in the subtropics and tropics the incoming air masses are warm. In summer the longitudinal temperature contrasts between the continent and the ocean in the middle latitudes decrease in absolute value and become positive. Therefore, in June the values of  $A_\lambda$  here are small and positive. In the low latitudes they are positive both in winter and in summer. The meridional component  $A_\theta$  is positive in both winter and summer at all latitudes except for the tropics, since in the region of longitude 180° warm winds from the southeastern periphery of the Pacific "Low" and the northeastern periphery of the subtropical "High" blow during the entire year. The tendency of  $A_\theta$  to decrease in the tropics manifests the effect of trade winds, which transport cold air ( $A_\theta < 0$ ) into the low latitudes from the northeast in winter. As for the anti-trade wind, its effects do not manifest themselves in  $A_\theta$ , since it is essentially a westerly current.

The above analysis indicates that in the computed values of nonturbulent advection A, and its components there are also expressed, rather clearly the peculiarities of the various climates of the earth, which are associated with the character of the general circulation and the distribution of continents and oceans. Therefore, a detailed study of the values of nonturbulent advection both on the basis of mean long-period data and on the basis of data for individual years may be of definite interest to climatology and long-range synoptics.

Table 61

Heat Advection and Horizontal Turbulent Heat Transfer for  
180°E Longitude

Characteristic of the Advection and Turbulent Exchange of Heat	$\varphi^\circ$					
	70	60	50	40	30	20
December						
$A_{10}$	0	-4.4	-0.5	2.4	3.1	-2.9
$A_{110}$	-5.9	-9.3	-1.8	-1.1	1.7	0.2
$A_{110}^*$	5.9	4.9	1.3	3.5	1.4	-3.1
$A_{16}$	2.5	-3.9	-6.6	2.9	4.5	-1.9
$A_{116}$	-3.2	-10.6	-7.6	-0.5	3.1	1.1
$A_{116}^*$	5.7	6.7	1.0	3.4	1.4	-3.0
$\Pi$	5.5	4.9	2.1	-5.9	-4.5	3.9

June						
$A_{10}$	0.8	3.1	4.2	2.6	3.6	-2.3
$A_{110}$	-2.9	0.7	0.6	0.3	1.6	-2.4
$A_{110}^*$	3.7	2.4	3.6	2.3	2.0	0.1
$A_{16}$	3.3	5.1	4.3	0.8	3.8	-1.6
$A_{116}$	-0.4	2.0	0.7	-0.5	1.7	-1.5
$A_{116}^*$	3.7	3.1	3.6	1.3	2.1	-0.1
$\Pi$	-3.3	-7.1	-6.3	-1.4	-3.8	1.6

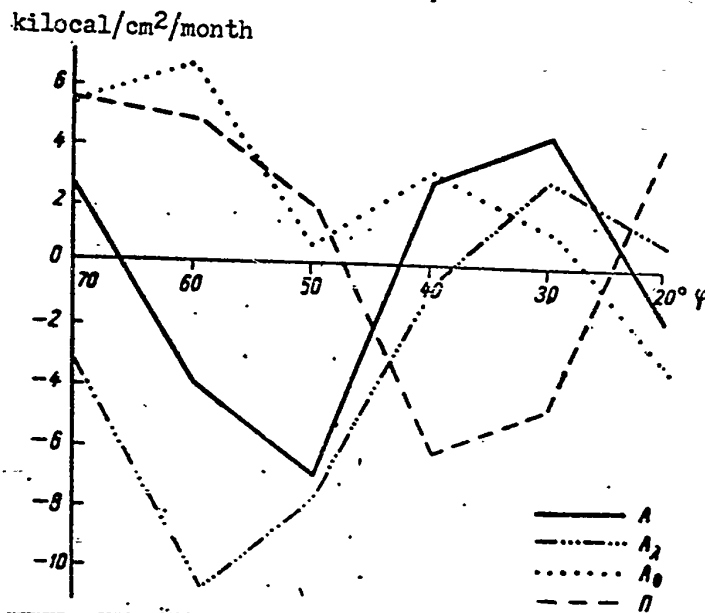


Fig. 37. Heat Advection and Horizontal Turbulent Heat Transfer for Longitude 180°E.

December

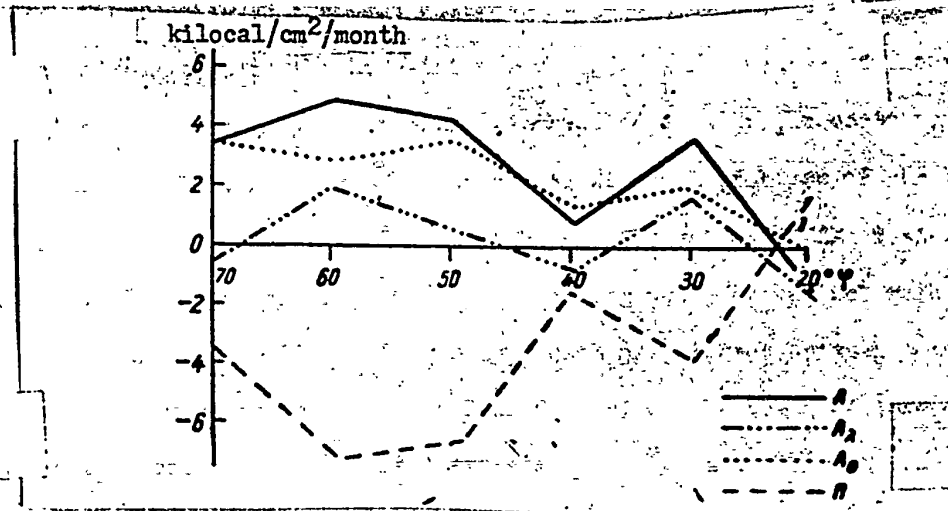


Fig. 38. Heat Advection and Horizontal Turbulent Heat Transfer for Longitude 180°E.—

June

In using the data on total advection from [3] it is possible to estimate horizontal turbulent transfer  $F_{t,h}(\Pi)$ . The values of these fluxes are presented in Tables 60 and 61 and in Figs. 26-38. In all cases concerning the values of  $F_{t,h}$  the tendency already mentioned previously is manifested; their variations in time and space are opposite in phase with respect to variations of  $A$ .

Knowing  $F_{t,h}$  and having estimated the Laplacian of the temperature

$$\frac{\partial^2 T}{\partial x^2} + \frac{1}{\sin \theta} \frac{\partial^2 T}{\partial \lambda^2},$$

it is possible to calculate the mean values of the coefficient of horizontal turbulence for the entire atmosphere. In their order of magnitude ( $10^6$  square meters/second) they correspond with the results of calculations by other investigators.

The horizontal turbulent fluxes of heat in the atmosphere are conditioned on the one hand by temperature contrasts between the equator and pole and, on the other hand, by temperature contrasts between the continents and oceans.

Obviously, meridional transfer does not change the sign of the turbulent fluxes of heat  $F_{t,h}$  in the annual course inasmuch as it is always directed poleward from the equator. Its contribution to the heat content of the atmosphere is negative in the low latitudes and positive in the high latitudes. The annual course of the obtained values of  $F_{t,h}$  is conditioned by the thermal interaction between the continents and oceans. As is known, V.V. Shuleykin was concerned with the problems of the horizontal macro-turbulent transport of heat in the atmosphere. The values of the deviations of temperature at various stations from its corresponding mean latitudinal values were selected by Shuleykin as the index of turbulent exchange of heat between continents and oceans. The isanomaly charts plotted (by S.T. Pagava) on the basis of this data indicate the directions of the turbulent transfer of heat in the atmosphere - it is directed perpendicularly to the isanomalies. Owing to eddy diffusion, heat spreads in all directions from the areas of positive values of the isanomalies and flows into the areas of negative values of the isanomalies. Therefore, the annual course of influxes  $F_{t,h}$  must be associated with the seasonal shift in the signs of the isanomalies. Let us analyze from this standpoint the obtained values of  $F_{t,h}$ .

In summer the continents are, as a rule, occupied by areas of positive isanomalies, and turbulent heat must flow out from the continents. And, in effect, negative values of  $F_{t,h}$  have been obtained in the regions located near oceans in the summer months (Assuan, Bombay, Shanghai, Vladivostok, Turukhansk, New Orleans, Philadelphia). In winter, the source regions of heat are displaced to oceans, while turbulent heat flows toward the continents, and therefore positive values of  $F_{t,h}$  are obtained at the same stations in the winter months. For the Bombay station there is a marked tendency toward attenuation in the annual course of  $F_{t,h}$  which is obviously associated with the general attenuation of seasonal difference in the climate of tropical latitudes. The positive values of  $F_{t,h}$  in summer for Lisbon and Batumi should be associated with the influxes of heat from the source region of heat situated in North Africa, and also from the subtropical belt of anticyclones.

In the interior areas of the continents and oceans the signs of turbulent heat

STAT

fluxes must be conditioned by the interaction between adjacent source regions of heat and cold. Thus, the positive values of  $F_{t,h}$  during summer months for Krasnovodsk and Barnaul may be associated with the influx of heat from the source region of positive isanomalies, located north of the Aral Sea, while the negative values of  $F_{t,h}$  during winter months for Krasnovodsk are associated with the efflux of turbulent heat toward the source regions of cold situated north of the Aral Sea and in the basin of the Lena river. At Barnaul, the positive values of  $F_{t,h}$  during winter correspond to the influx of heat into this second Siberian source region of cold. The positive values of  $F_{t,h}$  in December in the region of longitude  $180^{\circ}\text{E}$ , north of latitude  $45^{\circ}\text{N}$ , may be associated with the influx of heat from the northeastern part of the Pacific, where there exists a major source region of heat in winter in the Gulf of Alaska.

In lower latitudes, the negative values of  $F_{t,h}$  during winter in the Pacific Ocean (where there are no local source regions of heat) are conditioned by the general efflux of heat toward the continents. In June  $F_{t,h}$  along longitude  $180^{\circ}\text{E}$  has negative values, which obviously is associated with the efflux of heat toward the source region of cold located in the eastern part of the Pacific in summer.

During the transitional seasons, when the source regions of heat and cold are disintegrated, turbulent fluxes of heat are small and pass through zero values.

The values and signs of the heat fluxes of  $F_{t,h}$  obtained by the heat-balance method do not contradict the qualitative representations about the direction of the turbulent transfer of heat in the atmosphere. This attests to the sufficient reliability of the evaluations of turbulent heat exchange during atmospheric macroprocesses by the heat-balance method.

Let us briefly summarize the contents of this Chapter. It proposes a new method of determining the advective macrotransfer of heat. This method differs from previously used methods in these aspects:

- (1) The proposed method is direct and consequently is more accurate in comparison with an indirect method of determining advection as a residual term of the equation of the heat balance of the atmosphere. The latter, indirect method, provides the general

quantitative characteristics of both the advective and the macroturbulent transfers of heat; that characteristic includes the sum of the errors made in determining all the other components of the heat balance.

(2) The proposed method makes it possible to determine  $A$  for layers in the atmosphere of a finite thickness (which cannot be made by the heat-balance method)

(3) The proposed method makes it possible to compute the components of advection—latitudinal and meridional.

The last circumstance provides the opportunity for a more detailed analysis of the processes of heat release in the atmosphere and for determining not only the in- and outgo characteristics of advective processes  $A$ , but also the quantitative estimate of the contributions of the latitudinal and meridional transfers of air masses, respectively, in the total nonturbulent heat transfer. Up until the present time it has been possible to theorize about the direction of advective fluxes only indirectly [3]. The presently obtained relationships between the components of advection and its total value  $A$  determine completely the prevailing directions of the heat transfer in various regions and in different seasons.

Calculations of the quantitative characteristics of the advective transfer of heat make it possible to investigate more thoroughly the energetic aspect of the processes of general circulation. Research in the energetics of atmospheric processes are still far from being sufficiently developed. There is, however, no doubt that such investigations must be of fundamental importance to the physics of the atmosphere.

The possibility of determining the values of the horizontal macroturbulent heat transfer as a residual term of the equation of heat balance of the atmosphere has been pointed out.

In this way, the advective and the turbulent macro-transfers of heat have been for the first time successfully differentiated from each other. Such a distinct analysis may promote the advancement of knowledge about the heat regime of climate and weather.